



***Low Pressure Turbine efficiency increase
by developing new concept of Outer Air Seal***

by

Kacper Pałkus, M.S.

submitted in partial fulfillment of the requirements for the degree of

Doctor of Philosophy

at the Rzeszow University of Technology

Supervisor: Piotr Strzelczyk, Ph.D., PRz Associate Professor

Advisor: Wojciech Bar, M.S.

Advisor: Karl Engel, Ph.D.

Rzeszów, September 2023

This page intentionally left blank.

Abstract

The doctoral dissertation addresses development and research of new solutions for Outer Air Seals for Low Pressure Turbines. It is realized with an aim of increase in the turbine efficiency, respecting meaningful multidisciplinary limitations for modern turbines.

The understanding about operation of shroud labyrinth seals of Low Pressure Turbines is broadened in the thesis. A thorough identification of flow phenomena associated with the presence of outer seals is elaborated and followed by research of potential areas for improvement of these regions. Specifically in this course is performed dimensional analysis for a typical Outer Air Seal of a Low Pressure Turbine, accompanied by comprehensive parametric studies. From those the most important characteristic quantities are determined, simultaneously allowing identification of primary factors influencing aerodynamic operation of the seals. Based on this, the directions for improvements are determined which further result in development of the new design solutions of Outer Air Seals.

The thesis provides useful guidelines on an approach to multidisciplinary assessment of the new design solutions. The most promising concepts selected for detailed evaluation in the frames of the doctorate are Front Deflector and Vane Bleed Holes. Across the thesis, primary benefits and limitations for their operation are identified.

Both designs are implemented and researched with a numerical model of a modern three-stage Low Pressure Turbine. The concepts are evaluated in detail by means of CFD with respect to the aerodynamic operation and their benefit for the turbine efficiency. The validity of the CFD methods applied for the analyses is confirmed by comparisons with several sets of experimental data. The validation is focused on the turbine efficiency and proper prediction of the flow within the seals and in the shroud areas of the mainstream. The thesis elaborates also on the primary sensitivities and directions for optimization of the new concepts. A thorough research of the aerodynamic operation of the newly developed solutions and effects associated with their integration into the turbomachine is provided.

The ultimate concept poses a combination of both solutions within same seal. It is possible because the first concept is assumed for the front cavity and the second for the rear part. It is found this combination provides the highest improvement in the turbine efficiency.

This page intentionally left blank.

Streszczenie

Przedmiotem rozprawy doktorskiej jest znalezienie oraz przebadanie nowej koncepcji zewnętrznych uszczelnień łopatek turbiny niskiego ciśnienia. Jest to realizowane w celu zwiększenia sprawności turbiny, uwzględniając przy tym niezbędne multidyscyplinarne ograniczenia projektowania nowoczesnych turbin.

Jednym z aspektów pracy doktorskiej było poszerzenie zrozumienia działania zewnętrznych uszczelnień labiryntowych turbin niskiego ciśnienia. W ramach badań zidentyfikowano zjawiska przepływowe związane z obecnością tych obszarów. W szczególności w tym celu przeprowadzono analizę wymiarową typowego zewnętrznego uszczelnienia turbiny niskiego ciśnienia stowarzyszoną z analizami parametrycznymi. Na ich podstawie wyznaczone zostały najistotniejsze wielkości charakterystyczne, pozwalające jednocześnie na określenie podstawowych czynników wpływających na pracę uszczelnień pod kątem aerodynamiki. Dało to możliwość wyznaczania kierunków ulepszeń, a następnie pozwoliło na znalezienie nowych rozwiązań konstrukcyjnych dla zewnętrznych uszczelnień turbin.

Rozprawa zawiera wskazówki dotyczące podejścia do multidyscyplinarnej oceny nowych rozwiązań konstrukcyjnych. Najbardziej obiecujące koncepcje wybrane do szczegółowej oceny w ramach doktoratu to Front Deflector oraz Vane Bleed Holes. W pracy doktorskiej wskazano podstawowe zalety i ograniczenia ich działania.

Obydwa rozwiązania są zaimplementowane i przebadane z użyciem modelu numerycznego nowoczesnej trzystopniowej turbiny niskiego ciśnienia. Koncepcje zostały szczegółowo ocenione z wykorzystaniem CFD pod kątem pracy aerodynamicznej oraz zysku sprawności turbiny, pochodzącego od nich. Poprawność analiz została potwierdzona przez porównanie z danymi eksperymentalnymi z kilku stanowisk badawczych. Walidacja koncentrowała się na trzech aspektach: sprawności turbiny, właściwym przewidywaniu przepływu w uszczelnieniach oraz poprawnym symulowaniu w strumieniu głównym w okolicy uszczelnień. W pracy przebadano także szczegółowo czynniki wpływające na pracę nowo opracowanych koncepcji w celu wskazania kierunków optymalizacji oraz poprawności działania nowo opracowanych rozwiązań od strony aerodynamiki i efektów związanych z ich integracją w maszynie przepływowej.

Ostatecznie proponowana koncepcja stanowi połączenie obu rozwiązań w ramach tego samego uszczelnienia. Jest to możliwe, ponieważ pierwszą koncepcję zakłada się uszczelnienia w przedniej części, a drugą w tylnej. Stwierdzono, że to połączenie zapewnia największą poprawę sprawności turbiny.

This page intentionally left blank.

Acknowledgements

First and foremost, I would like to thank God for countless blessings and never leaving me when I was lost. You gave me strength and wisdom to finish this work. AMDG.

Apart from my efforts, the success of this thesis depended greatly on the encouragement from several other, important for me people.

I would like to express my gratitude to my supervisor Professor Piotr Strzelczyk for all good guidelines and discussions in the course of this work. I would like to also thank my two doctoral fathers, Wojciech Bar and Dr. Karl Engel. Thank you that you always found time for me, thank you for your thoroughness, knowledge that you shared with me and all invaluable hints. It helped me grow as an engineer and a researcher.

I would also like to acknowledge my colleagues, Roman Seiband and Markus Brettschneider for their priceless insight into my work. You were always willing to share your experience and discuss the results.

With all my heart, I want to thank all my family and my close friends for their love and continuous encouragement. Firstly, to Karolina, my love and wife, who has been with me in all important and less important moments, in the good and the bad. Thank you for carrying with me all weights and supporting me in all possible ways. To my Mom and my Dad, Maria and Kazimierz, and my Mom-in-law and Dad-in-law, Małgorzata and Józef for believing that I can achieve everything and for their continuous love and sacrifices for us all. To my siblings, Kajetan, Błażej and Łucja with their second halves for standing by me in hard times and for their whole support. And to all my friends who encouraged me in any possible ways during this long way. I cannot imagine completing this chapter of my life without you all.

Herein thesis is prepared in the frames of the 3rd edition of the Implementation Doctorate program in cooperation between the MTU Aero Engines and Faculty of the Mechanical Engineering and Aviation at the Rzeszow University of Technology. Thus, finally yet importantly, I would like to express my gratitude to those institutions for enabling this work.

This page intentionally left blank.

Contents

| | |
|---|-----|
| Abstract | i |
| Streszczenie | iii |
| Acknowledgements | v |
| Contents..... | 1 |
| Nomenclature | 3 |
| Chapter 1. Introduction | 5 |
| 1.1. Motivation..... | 5 |
| 1.2. Importance of LPT efficiency..... | 6 |
| 1.3. Research objectives | 8 |
| 1.4. Thesis Contributions..... | 9 |
| 1.5. Description of the technical approach | 10 |
| 1.6. Organization of the dissertation..... | 11 |
| Chapter 2. Review of available research with respect to LPT OAS | 13 |
| 2.1. Typical and novel designs of LPT air seals | 13 |
| 2.2. Flow field and characteristics of LPT OAS and their effects on LPT performance.... | 21 |
| 2.2.1. Flow field and characteristics of labyrinth seals | 21 |
| 2.2.2. Flow field of the LPT with Outer Air Seals | 25 |
| 2.2.3. Impact of OAS on performance of LPT | 28 |
| 2.3. Summary of the literature review and formulation of research theses | 32 |
| Chapter 3. Research methodology | 35 |
| 3.1. Methods applied for derivation and multidisciplinary assessment of new design ideas of LPT OAS..... | 35 |
| 3.2. Phenomena similarity and dimensional analysis | 37 |
| 3.3. Numerical CFD modeling..... | 38 |
| 3.3.1. CFD model of reference 3-stage Low Pressure Turbine..... | 38 |
| 3.3.2. CFD modeling of Front Deflector | 43 |
| 3.3.3. CFD modeling of Vane Bleed Holes..... | 44 |
| 3.4. Methods used for assessment of LPT performance improvement..... | 48 |
| Chapter 4. Validation of the applied CFD methods..... | 51 |
| 4.1. Validation of CFD with respect to efficiency of the reference 3-stage LPT | 52 |
| 4.2. Validation of flow in the vicinity of OAS in the cylindrical 1.5-stage LPT | 53 |
| 4.3. Validation of the numerical prediction for OAS in the Rotating Labyrinth Test rig... | 56 |
| 4.3.1. Measurement setup of the RLP | 57 |
| 4.3.2. CFD model of RLP..... | 58 |
| 4.3.3. Validation of the prediction for seals with smooth wall..... | 62 |

| | | |
|----------------------|--|-----|
| 4.3.4. | Validation of the prediction for seal with honeycomb..... | 64 |
| Chapter 5. | New insights into flow phenomena associated with LPT OAS | 67 |
| 5.1. | Primary ways for improvements of the losses associated with LPT OAS..... | 67 |
| 5.2. | Flow through OAS in terms of characteristic quantities | 70 |
| 5.2.1. | Dimensional Analysis of Outer Air Seals | 71 |
| 5.2.2. | Axial Reynolds number for OAS..... | 72 |
| 5.2.3. | Outlet swirl ratio | 74 |
| 5.2.4. | Impact of Windage Heating | 76 |
| 5.2.5. | Summary of findings from Dimensional Analysis of OAS | 78 |
| Chapter 6. | New concepts of LPT OAS and their multidisciplinary evaluation..... | 81 |
| 6.1. | Key multidisciplinary design aspects of LPT Outer Air Seals..... | 82 |
| 6.2. | New LPT OAS concepts and their assessment | 84 |
| 6.2.1. | Baseline geometry | 84 |
| 6.2.2. | Front Deflector..... | 85 |
| 6.2.3. | Vane Bleed Holes..... | 86 |
| 6.3. | The most promising new design concept of LPT OAS..... | 87 |
| Chapter 7. | Evaluation of operation and benefits from the developed solutions..... | 89 |
| 7.1. | Front Deflector concept evaluation | 89 |
| 7.1.1. | Evaluation of performance of Front Deflector without static fin..... | 90 |
| 7.1.2. | Evaluation of performance of the Front Deflector with static fin..... | 93 |
| 7.2. | Evaluation of the Vane Bleed Holes concept..... | 96 |
| 7.2.1. | Basic operation of VBH..... | 97 |
| 7.2.2. | Dimensional analysis for Vane Bleed Holes..... | 98 |
| 7.2.3. | Evaluation of performance and sensitivities with simplified VBH model in 3-stage reference LPT..... | 99 |
| 7.2.4. | Assessment of VBH performance and directions for optimization on detailed 3D model in the 1.5-stage part of the reference LPT..... | 106 |
| 7.3. | Assessment of performance of most promising VBH configuration in 3-stage LPT | 118 |
| 7.4. | Summary of benefits from the developed solutions for improvement of LPT OAS | 121 |
| Chapter 8. | Summary, conclusions and directions for future work | 123 |
| 8.1. | Summary | 123 |
| 8.2. | Main conclusions..... | 126 |
| 8.3. | Recommendations for future work..... | 128 |
| Appendix..... | | 129 |
| A. | Patents | 129 |
| Bibliography..... | | 131 |
| List of figures..... | | 141 |
| List of tables..... | | 145 |

Nomenclature

Symbols:

| | |
|--|-------------------------------------|
| a | Local speed of sound |
| a_1, a_i | any dimensional quantity |
| c_p | Specific heat capacity |
| c | Radial clearance |
| c/R | Relative clearance |
| h | Specific enthalpy |
| k | Ratio of specific heats |
| m | Mainstream mass flow |
| m_{OAS} | Leakage mass flow |
| m_{VBH} | VBH mass flow |
| p | Pressure |
| A | Cross-sectional area |
| C_d | Discharge coefficient |
| $K = \frac{V_\theta}{NR}$ | Swirl ratio |
| Ma | Mach number |
| $M_\theta = \frac{U}{\sqrt{kR_i T_{in}}}$ | Circumferential Mach number |
| N | Rotational speed |
| R | Average radius of fins |
| R_i | Individual gas constant |
| $Re_{ax} = \frac{\rho V_{ax} c}{\mu} = \frac{\dot{m}}{2\pi R \mu}$ | Axial Reynolds number |
| T | Temperature |
| $Ta = \frac{2\omega R c \rho}{\mu} \sqrt{\frac{c}{R}}$ | Taylor number |
| Tu | Turbulence intensity |
| $U = \frac{\pi N}{30} R$ | Rotor fins circumferential velocity |
| V_x | Axial velocity component |
| V_r | Radial velocity component |
| V_θ | Circumferential velocity component |
| y^+ | Dimensionless wall distance |

Nomenclature

| | |
|--|--------------------------------|
| α | Circumferential velocity angle |
| ε | Radial velocity angle |
| $\eta_{is} = \eta = \frac{h_{out} - h_{in}}{h_{out, is} - h_{in}}$ | Isentropic efficiency |
| μ | Dynamic viscosity |
| ρ | Density |
| $\sigma = \frac{2cp(T_{t,out} - T_{t,in})}{U^2}$ | Windage heating |
| $\pi = p_{t,in}/p_{t,out}$ | Total Pressure Ratio |
| Δ | Change in any quantity |
| Π_1, Π_i | any dimensionless quantity |
| y^+ | Dimensionless wall distance |

Subscripts:

| | |
|---------|------------------------|
| t | Total quantities |
| in, out | Inlet, Outlet |
| Ref | Any reference quantity |

Acronyms:

| | |
|---------|--|
| 3D | Three-Dimensional |
| ACC | Active Clearance Control |
| CFD | Computational Fluid Dynamics |
| DA | Dimensional Analysis |
| FD | Front Deflector |
| IAS | Inner Air Seal |
| HPT | High Pressure Turbine |
| OAS | Outer Air Seal |
| LES | Large Eddy Simulations |
| LowRe | Low Reynolds, resolving boundary layer |
| LPT | Low Pressure Turbine(s) |
| PIV | Particle Image Velocimetry |
| RLP | Rotating Labyrinth Test Rig |
| SFC | Specific Fuel Consumption |
| TKE | Turbulent Kinetic Energy |
| (U)RANS | (Unsteady) Reynolds-Averaged Navier-Stokes |
| VBH | Vane Bleed Holes |
| WF | Wall Functions |

Chapter 1. Introduction

1.1. Motivation

Everything what has future develops and improves, it evolves to be the best, the greatest. The same, very general principle is applicable also for aircraft engines – they are subjected to continuous improvement.

Aviation always is in the lead for making possible what might seem impossible or just a dream. An important driver of technological advance is development towards more environmentally friendly and more efficient propulsion, decreasing fuel burn, noise and NO_x emissions. Aviation industry has committed to be carbon-free in production, development and operation by 2050 [21]. It is assumed that it will be achieved by electric or hybrid propulsion for short- and mid-range planes in combination with Sustainable Aviation Fuel. In the past years there have been many efforts in this direction. Historical, current and future trends, gathered in a report from ICAO [37], show increasing long-term goals and trends for reduction in international emissions in aviation industry. The mission of having better, cleaner, more efficient machines is jointly followed by safer, more robust and more profitable designs. This multidimensional situation is a source of challenges in the development of future aircraft engines.

The goals are realized across whole aviation industry amongst different companies and also addressed in big international programs like CLEEN [21]. Technologies developed in the frames of CLEEN are estimated to save aviation industry nearly 40 billion gallons of fuel; to lower CO₂ emissions by about 420 million metric tons; to decrease noise emissions by 14% and to provide further drastic reductions in nitrogen oxide from aircraft operations by 2050 [21]. There are around twenty different projects realized currently in the frames of this program [9]. Exemplary activities are SWITCH [63] or HEAVEN [10], focusing on development and testing of future hybrid-electric and water enhanced propulsion. Simultaneously, also different aircraft engines producers make efforts in development of propulsion systems better than nowadays [81], [87], [63]. It is realized with various innovative technologies. These may be focused either on development of innovative engine cycles or by optimization of existing ones, hence improvements in particular components. There are steps in both directions. As an example, some novel engine cycle concepts, being currently under development are ContraRotative Open Rotor engine [5] or Water Enhanced Turbofan [63]. As visible from the reports and miscellaneous patents, simultaneously, particular components are improved to reach peaks of their performance.

Herein thesis is focused on the latter way for improvements, in particular on new concept for Outer Air Seals for future Low Pressure Turbines.

1.2. Importance of LPT efficiency

Some of the primary features of well-performing engines are coupled. As an example, CO₂ emissions are interconnected with fuel burn, usually related to the specific thrust and denoted as Specific Fuel Consumption (SFC). Thus, it is advantageous to focus on overall fuel burn when aiming for improvements in overall engine performance. It is also one of the basic parameters affecting choice of a specific engine by airlines.

Generally, fuel burn necessary for aircraft operation can be improved in three areas: by reducing engine SFC, its weight and its size. Smaller weight and size result in reduced thrust requirements translating in lower fuel burn for given engine SFC, as elaborated in [50]. Reductions in SFC itself, are primarily achieved by improving engine efficiency. By convenience, usually it is divided on propulsive efficiency and thermal efficiency. Thus, primarily, lower SFC can be reached either by improving thermodynamic cycle or by enhancements in efficiencies of particular components [50], [17], [91]. Improvement of SFC for commercial aviation is mainly driven by increase in propulsive efficiency. A share of improvements in the overall engine efficiency from its components is not equal. The biggest impact on whole engine SFC has Low Pressure Turbine efficiency. It is estimated that 1% improvement in LPT efficiency reduces SFC by around 1% [24], [17]. Thus, importance of efficiently performing Low Pressure Turbines is very high and every activity aiming to improvements in efficiency of the Low Pressure Turbine is crucial for environment, airlines and engine producers.

On the other hand, modern designs assisted with CFD are already considerably loaded and fairly optimized. Application of the high-tech solutions like: low loss airfoils by controlled laminar-turbulent boundary layer transition, ultra-thin trailing edges, optimization of the distribution of work along a machine and endwall contouring in LPT has led to edges of the maximal efficiency of these machines. Due to that, overall isentropic efficiency of the best nowadays designs is already very high. It reaches over 93% [91] for the currently optimized designs. However, there are still few areas which require further development.

Figure 1.1 presents a distribution of relative efficiency along channel height for typical nowadays Low Pressure Turbine. Three plots in the figure reflect different configurations of the LPT: simplified, simplified with purge flows and full geometrical configuration of the turbine. For the simplified LPT case only main gas path is considered, nonetheless friction at endwalls is assumed. This is a source for secondary flows structures developing through the machine and resulting in the decrease of the efficiency at the main channel sides. Second case of the simplified turbine includes purging air at endwalls. This air prevents hot gas injection, but simultaneously interacts with the main flow. The full geometrical configuration of the turbine includes cavities, detailed secondary air purge flows and all other real turbine geometrical features.

As shown in the Figure 1.1, the efficiency in the middle of the channel for all cases is outstanding. Thus, it is not region where considerable improvement can be gained. The biggest potential is still present in regions at the sides of main gas path. Presence of sealing systems in Low Pressure Turbines is indispensable, because they contribute to the proper operation of the engine. Nevertheless, as reported by different researchers [72], [30], presence of air seals in LPT can decrease efficiency of the machine even by 1.6% up to 2.6%, depending on a configuration.

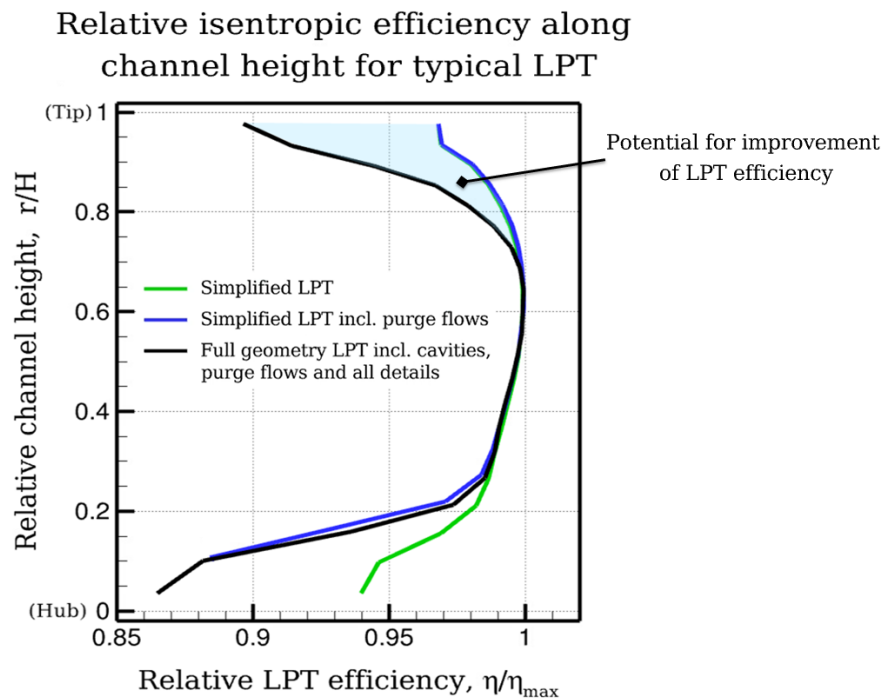


Figure 1.1 Distribution of efficiency along channel height for typical LPT.

As visible in the Figure 1.1, the efficiency potential existing at Outer Air Seals (OAS) is higher than at Inner Air Seals (IAS). Investigations of currently operated LPT have shown that even 0.3% of the efficiency potential still exists in the region of OAS. That is because working fluid going through Outer Air Seals, bypasses blades and directly decreases work extraction from the machine and hence its efficiency generating further losses. At inner part of the main gas path, efficiency is influenced by interactions of the mainstream and purging secondary air. Disks have to be protected from hot gas injection, what is crucial for proper and safe engine operation and cannot be compromised. This significantly reduces potential for improvement in the efficiency by new designs of inner seals. It is well reflected in the Figure 1.1, because in the inner part of the channel, consideration of the inevitable cooling flows already indicates reduced efficiency potential.

Above considerations pose good motivation for research in the direction of improvements in the areas of LPT OAS.

1.3. Research objectives

The thesis is realized with the following objectives:

1. Development of new, improved solution for Outer Air Seals, providing increase in LPT efficiency by minimum 0.1%, respecting meaningful multidisciplinary aspects and limitations
2. Determination of primary sensitivities and directions for optimization of the new concepts with respect to the aerodynamic LPT efficiency
3. Contribution to understanding of operation of Outer Air Seals, in particular to effects associated with the developed solutions

The main objective addressed in the dissertation is development of new concept of Outer Air Seals, in particular, towards its implementation in future Low Pressure Turbines, which design will be launched in the next decade. Specifically, it is aimed to find and investigate solutions providing increase in turbine efficiency by minimum 0.1%. The developed solution should take into account necessary limitations and criteria from different disciplines.

There are also several side goals aimed in the research. First objective is analysis of the new solutions in terms of the multidisciplinary aspects enabling preselection of the ideas and integration of the new solutions into aircraft Low Pressure Turbines. Next goal is identification of crucial factors affecting aerodynamic operation of Outer Air Seals as well as those associated with new solutions. Last, but not least, is detailed aerodynamic evaluation of the most promising solutions. Therefore, it is also necessary to develop methodologies and check applicability of existing modeling for evaluation of the concepts and confirmation of their proper operation. Ultimately, that should allow prediction of the improvement in terms of aerodynamic efficiency resulting from the solutions.

All those goals are aimed in the course of crosschecking of feasibility of the solutions, proving assumed benefits and preparing process their industrialization. This allows obtaining practical - implementation - aspect of the research.

1.4. Thesis Contributions

The main contribution from the thesis is invention and multidisciplinary evaluation of new concepts for Outer Air Seals that bring noticeable efficiency benefits to the LPT. In particular the herein research contributes in:

1. Understanding of operation of shroud labyrinth seals and provides thorough identification of flow phenomena occurring in the LPT environment.
2. Identification and discussion over potential areas for improvements in OAS of LPT
3. Research with respect to multidisciplinary limitations and crucial designs aspects of OAS.
4. Useful guidelines on the approach to multidisciplinary assessment of new design solutions.
5. Development of novel solutions of Outer Air Seals feasible for integration into Low Pressure Turbines and bringing improvement in their efficiency
6. Identification of aerodynamic sensitivities and primary directions for optimization of the new concepts.
7. Understanding of operation of newly developed OAS solutions and effects associated with their integration the LPT.

1.5. Description of the technical approach

To reach the goals assumed in the thesis, in the first stage, the problem is examined in detail. Thus, a review of available knowledge stage is performed. The focus is put on two primary fields – revision of existing design solutions for LPT air seals, their advantages and limitations, and research of aerodynamic effects associated with presence of OAS in LPT. It allows thorough recognition of the issues and identification of gaps in the knowledge state.

Next, determination of key factors influencing aerodynamic operation of OAS is aimed. At this stage, dimensional analysis associated with parametric numerical analyzes is carried out. It allows determination of dependencies between crucial quantities influencing aerodynamic operation of the seals. These findings enable identification of ways of possible improvements in the LPT OAS.

Afterwards, research in the direction of development of new design solutions is carried out. The ideas are collected and preliminarily evaluated in terms of requirements from all meaningful disciplines involved in design of Outer Air Seals. In this way, the concepts are pre-selected in terms of: aerodynamics, structural integrity, manufacturing technology, material capabilities, management of the secondary air and costs. The most promising concepts are secured with patent applications and further evaluated in detail for confirmation of the assumed benefits from their implementation.

In order to validate the numerical models for OAS of LPT, experimental results and post-test numerical analyzes are compared. The validity of the numerical prediction is crosschecked for LPT mainstream, in particular at endwalls in the vicinity of OAS as well as inside the seal. Verified CFD modeling enables numerical research of LPT with new OAS solutions.

Afterwards, thorough analyses of the selected solutions are carried out. Two concepts are evaluated in detail – Front Deflector and Vane Bleed Holes. Both developed designs are analyzed with respect to the aerodynamic operation in LPT and assessed in terms of efficiency benefit for LPT. Multiple geometrical variations that simultaneously account for limitations from other disciplines are researched for both solutions. It results in an extensive sensitivity study of the concepts, identification of directions for their optimization and localization of the most promising configurations.

Finally, the most promising configuration is transferred to the modern 3-stage engine-like turbine model. The LPT efficiency benefit assumed in the doctorate is confirmed with both solutions incorporated into the turbine and simulated with the validated model of the machine. It is followed by indications of directions for further development of the designs.

The applied technical approach summarized in the Figure 1.2.

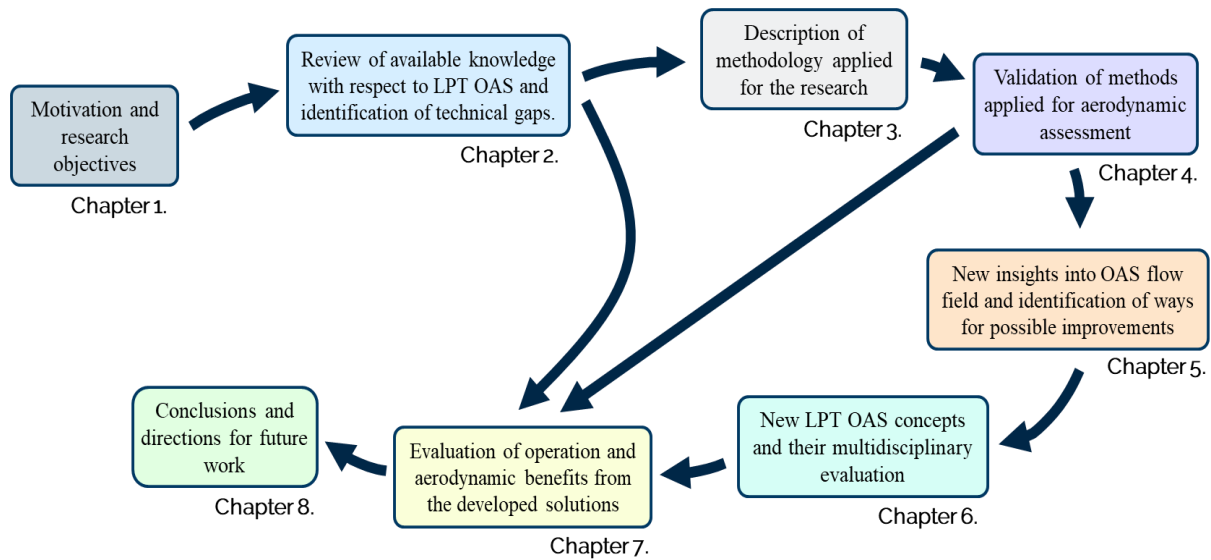


Figure 1.2 Scheme of the dissertation and technical roadmap in a course of development and evaluation of new solutions for LPT OAS

1.6. Organization of the dissertation

The organization of the dissertation corresponds to the technical approach shown in the Figure 1.2.

Chapter 1. introduces into the motivations, objectives and theses behind the research. Chapter 2. provides thorough overview of the available knowledge state in a field LPT OAS. It elaborates two primary topics – state-of-the-art and novel designs of air seals that are available in the literature and across patents and research of the OAS characteristics and effects on the LPT flow field associated with their presence. From this literature review, in a straightforward way, the technical gaps emerge. Thus, also research theses are discussed in this chapter.

Next, Chapter 3. treats about methodology applied for achieving the goals defined for the doctorate. This part is directly connected to Chapter 4. addressing validation of the methods employed for the research. In particular, validity of the numerical prediction is discussed.

Afterwards, the thesis proceeds to the results of the performed research. This part starts with in Chapter 5. where new insights into the OAS flow field and identification of the possible ways for improvements of OAS is described. Subsequently, in Chapter 6. , new concepts for LPT OAS together with their multidisciplinary evaluation are presented and discussed. Next, it proceeds into detail investigations of the two most promising concepts in various configurations, in Chapter 7. , providing sensitivities and final efficiency benefit from the solutions.

A summary of overall benefits and limitations from the developed solutions, the conclusions resulting from the thesis, and suggested directions for future work are provide in Chapter 8.

This page intentionally left blank.

Chapter 2. Review of available research with respect to LPT OAS and gaps in knowledge state

There is a considerable interest in improved performance of the turbomachine sealing system, because it directly transfers to the performance of the whole engine. Efficiency of the turbomachine, its operational life and stability of the whole machine depend on reliable and effective sealing design. Flitney [23], discussing miscellaneous types of seals for different locations for applications in industrial and aircraft engines, highlights the importance of the sealing system. He indicates fifty different locations that require sealing in a typical gas turbine. Simultaneously, as remarked by Hendricks et al. [35], there is no particular sealing configuration that is applicable and satisfactory for general use. Each location where the sealing is required must be assessed independently in terms of its operational requirements for particular environment.

Within LPT main gas path, Inner Air Seals and Outer Air Seals can be differentiated. IAS are located nearby the disk regions, OAS in the vicinity of the casing. Very different conditions are apparent in both regions. There are meaningful differences in pressure gradients, thermal and structural requirements. Significance have also capabilities of materials – not only due to the temperature level, but also with respect to contact at the interface between rotating and nonrotating parts. There is also different role of both seals in the turbomachine.

In herein thesis LPT OAS in the main focus. Nevertheless, some of the common flow features as well as primary differences between OAS and IAS are also addressed.

2.1. Typical and novel designs of LPT air seals

Sealing systems for turbomachinery are under development with continuous advances for decades by now. Chupp et al. [8] provide thorough overview of different types of sealing for aircraft engines. They address state-of-the-art and novel static and dynamic seals intended for use in aeronautical applications. Authors indicate continuous development in the area of sealing in the course of the future more efficient gas turbines. It is clearly visible in the research campaigns over new seals e.g. development of the novel shaft seals [74], [64].

As indicated by Hendricks et al. [35], referring to turbines in general, the sealing requirements are entirely different in the shroud regions at blade tips and in the vicinity of the shaft for sealing

of platform and cavity interfaces. Author indicates different flow fields as well as different functions behind seals in both regions. Those at the inner channel part mainly prevent hot gas ingestion into the cavities to protect the rotating disks and to control blade and disk cooling flows. Improper cooling or hot gas ingress life of critical parts and endangers engine failures [35]. It points to the conclusion that IAS are mainly connected to the engine safety.

A typical state-of-the-art Outer Air Seal of LPT is shown in the Figure 2.1. It is typically two fin configuration with honeycomb structure. OAS are located in the outer channel region directly at the casing. Due to that, they work at twice size of the radius as inner cavities at very high circumferential speeds. Additionally, usually at outer diameter fewer fins are applied. OAS configurations have two [44] or maximally three fins [32]. It is due to the fact that additional mass at such radius is unfavorable for durability of the rotating blade. Furthermore, the relative movements of the parts are incomparably bigger for Outer Air Seals both in radial as well as in axial directions. Because of that it is extremely difficult to maintain relatively small clearances between rotating and nonrotating parts at these regions. A certain difference between inner and outer sealing regions of the LPT is also amount of the cooling flows. OAS experience much less purging and due to that they operate in much higher temperatures, what is limiting for many solutions. Abovementioned points indicate that operating conditions for OAS are very different from all other locations in an engine.

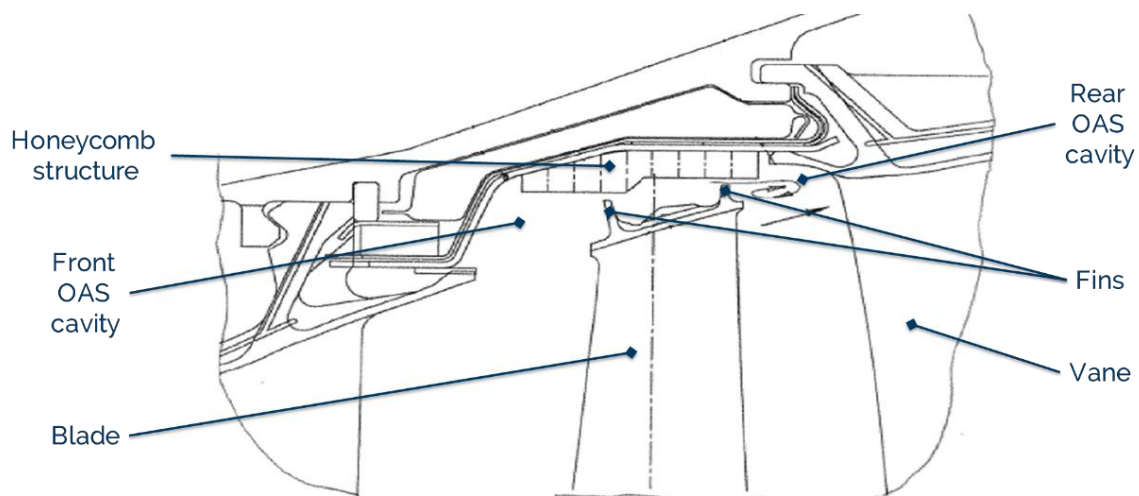


Figure 2.1 Schematic representation of a state-of-the-art Outer Air Seal of LPT [44]

As visible in the Figure 2.1, in LPT the most frequently of the applied seals are labyrinth seals combined with abrasives like honeycombs. Labyrinth seals are effective and reliable. They are already very well-grounded, robust and proven solutions – perfect for aircraft engines as highlighted in [64] or [8]. This sealing solution is able to maintain high requirements and harsh conditions at outer cavities regions. Chupp et al. [8] indicate different issues for the turbomachinery labyrinth seals with abrasives including rubbing of the interfaces, appropriate choice of the materials and proper design of the abrasives for turbomachinery. Authors provide

also overview of several labyrinth seals configurations. Chupp et al. [8] indicate that labyrinth seals are good in restricting flow, but do not respond well to dynamics and may lead to turbomachine instabilities [8].

Alternative for honeycombs are hole pattern seals. They are obtained by drilling holes in a pattern within a metal carrier. With respect to weight and performance, honeycombs have superior performance over the hole pattern seals. As this type of seal, as indicated by Flitney [23], is intended for application in industrial applications, due smaller weight restrictions.

A very promising advance with respect to the sealing is introduced by brush seals. These sealing elements are possible in different configurations, as presented in the Figure 2.2.

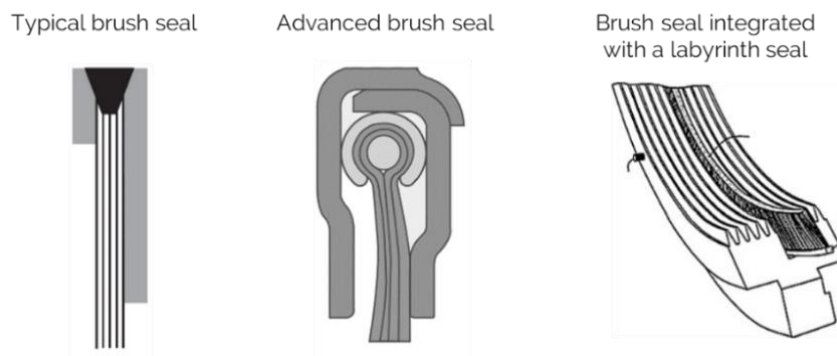


Figure 2.2 Different types of brush seals: typical [23] configuration, advanced design [6], and brush seal integrated within a labyrinth seal [58]

Sealing performance of brush seals is superior over the conventional labyrinth seals. At a certain gap they can decrease the leakage even by 50% [23], up to 80% [8], [6] in comparison to the straight labyrinth seal. Additional advantage of this solution is considerably reduced heat generation in contact with rotating parts [23].

Brush seals are suitable for compressors and nowadays also for inner locations of some turbines, however, they are not applicable to OAS, due to several reasons. Brush seals lose their performance at substantially varying clearances. Chupp et al. [8] report that even a change in the assembly clearance noticeably increases the leakage because of the gap opening. For OAS relative movements are order or even two orders of magnitude bigger than for IAS. Limiting for brush seals are also temperatures. According to Flitney [23] the typical brush seal can be used up to 200°C, with high temperature materials like Haynes 25, or with Kevlar up to 600-650°C [18], [6], but that is not sufficient for sustainable application at outer regions. Another aspect concerns oxidation of wires, thus brush seals deterioration and reliability at high temperatures. Simultaneously, brush seals are limited with respect to the possible diameter. According to the report [6], brush seals are suitable for bearing chamber seals, shaft seals, inter-stage seals and static seals up to diameter of 650mm. All abovementioned limitations exclude application of the brush seals to LPT OAS.

Several modifications of the brush seals, applying different solutions with respect to the sealing elements, are available, as shown in the Figure 2.3. Recent advances include finger seals [64], [8], [73], leaf seals [8], [78], foil seals [64], [8], [86] or brush seals with a pad bearing [41]. The solutions overcome some drawbacks of typical brush seals. Finger seals and leaf seals pose a comparable solution. These alternatives are proven to be more stable than brush seals [23], [73] and even further increase sealing performance in terms of leakage, operability and stability compared to the labyrinth seal and conventional brush seals. That was particularly pronounced in certain ranges of rotational speeds and temperature regimes [74], [64].

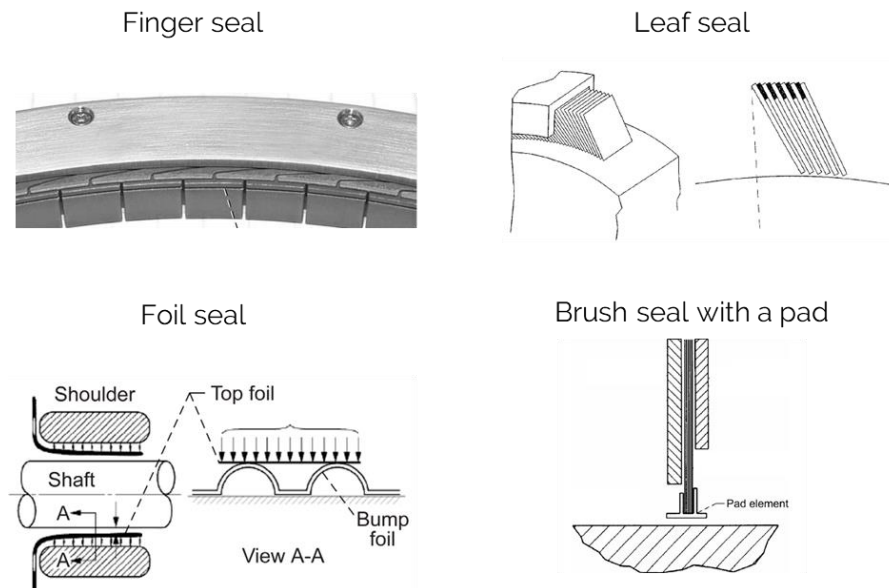


Figure 2.3 Different types of sealing solutions: finger seal [64], leaf seal [78], foil seal [86], brush seal with a pad [41]

Finger and foil seals have been tested by Munson [64] at different axial loads, speeds and pressure ratios and compared with conventional labyrinth and brush seal. It is noted that at very low differential pressures both give similar or even slightly worse performance than brush seals. At higher differential pressures the foil seal has shown clearly superior performance over all other types of the seals. However, as highlighted in by Munson [64], there are only certain engine sealing locations where the foil type seals are best suited e.g. within rotor thrust balance locations or for turbine rim seals. Due to similar limitations as in case of brush seals, even these advanced sealing concepts are not applicable for OAS. Thus, there is a number of solutions for air seals in different regions of the LPT that cannot be used for Outer Air Seals, due to miscellaneous limitations.

With respect to OAS, recent advances [5] indicate application of a separate Active Clearance Control (ACC) to Low Pressure Turbines. This solution typically has been applied to HPT, but also very robustly and effectively increases performance of nowadays LPT. Chupp et al. [8] indicate that clearance control has primary importance for turbomachinery. Authors show a significant effect of clearance control on HPT. It is indicated that over a single mission cycle,

without ACC, running clearances are nearly 3 times larger, due to rub-in. Justak and Doux [42] indicated the clearances in some engines can exceed 1.0mm or sometimes even 1.3mm. In HPT clearances on a level of 1mm radial clearances are responsible for even 4% cost in whole engine SFC. To keep the radial clearances on a very small level ACC becomes state-of-the-art also for nowadays LPT. This system assures increase in performance of LPT on same basis as for HPT.

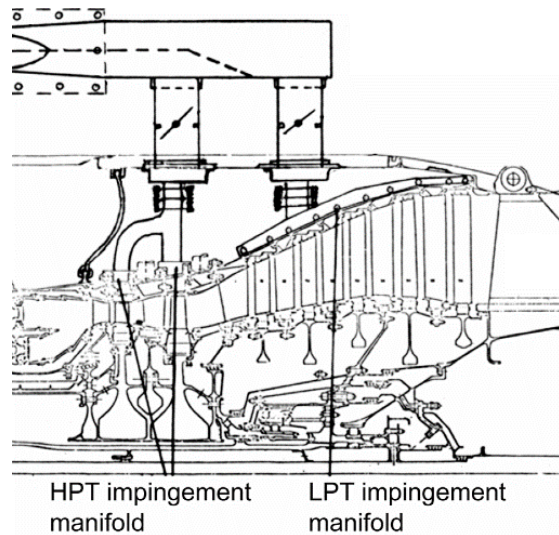


Figure 2.4 Aircraft turbine with two ACC systems dedicated separately to HPT and LPT [8]

Usually, ACC is realized with thermal expansion or contraction of the casing. However, there are also alternative approaches. For instance, Justak and Doux [42] worked out a flexible self-acting clearance control system activated with pressure for shroud sealing of HPT. Authors preliminarily demonstrated possible operation of this solution. Nevertheless, in practice, still thermally adjusted systems are applied.

A number of research goes in a direction of designs improving mixing losses. A typical solution applied for this purpose at chambers in the vicinity of the shaft are swirl reducers [54]. It is a set of flow blocking obstacles [8], resulting in reduction of the swirl. This kind of devices are not applicable at OAS, because, the swirl should be increased after passing the seal, to avoid mixing losses. Due to that, an opposite features called swirlers are more applicable. They provide appropriate circumferential velocity for the flow coming out from the cavities. This principle is researched by Rosic and Denton [83]. Authors investigate concept of turning vanes in a vicinity of the HPT shroud, visualized in the Figure 2.5. Their solution is intended to turn the rotor leakage flow in the direction of the main blade passage flow in order to reduce the aerodynamic mixing losses. Their results prove that it is possible to improve the flow field in the downstream blade row and overall turbine performance by reducing impact of the leakage on the mainstream improving aerodynamic mixing losses in circumferential direction.

Another solution to realize this principle is given by Palmer [71]. He investigated OAS configuration with massively scalloped LPT blade with one fin. In the course of mixing losses reduction, he introduced hybrid blade design with mini bladelets instead of the fin. His investigations show that in this way, mixing losses can be decreased. Despite unclear manufacturability and robustness of the solution, the benefits he noticed are likely to be counterbalanced by increased leakage, due to the considerable opening of the gap. Nonetheless, his investigations highlight great significance of the mixing losses in the LPT performance.

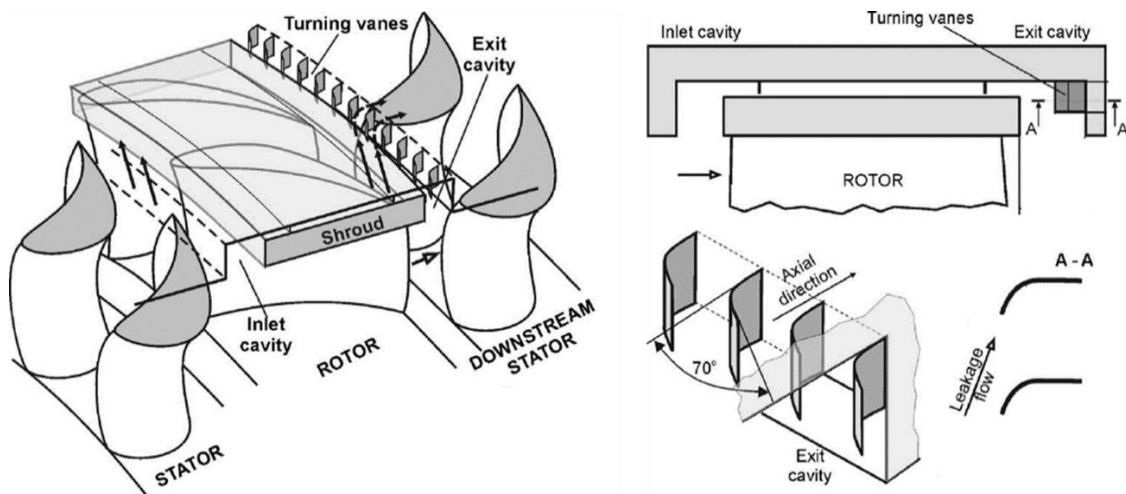


Figure 2.5 Turning devices in the rear OAS cavity of the shrouded steam HPT [83]

Different researchers apply also modifications of the OAS cavities to improve inflow to the mainstream and decrease the leakage. Mahle and Schmierer [57] proposed application of inverse fin configuration to the low-speed aircraft LPT. The concept is visualized in the Figure 2.6. In typical arrangement, fins are usually within a shroud of the blades. The inverse configuration is frequently applied in steam turbines, but such solution is not met in aircraft engines. Authors provide a direct comparison of both configurations. They prove positive effects in the interactions in the leakage and mainstream by better leakage inflow to the main gas path.

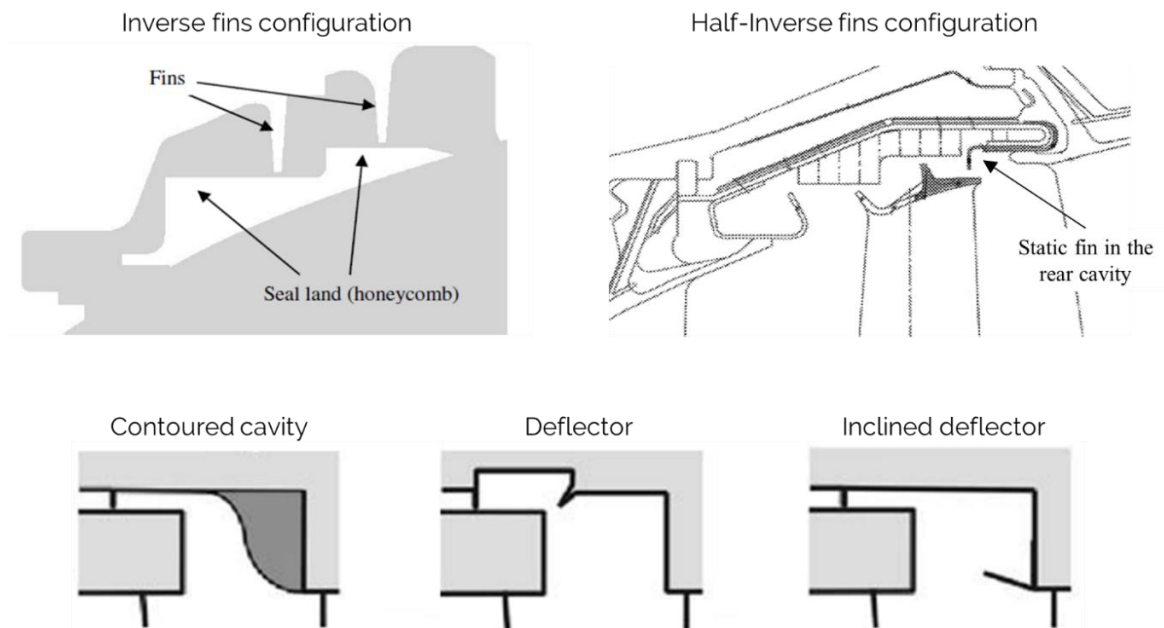


Figure 2.6 Inverse fins configuration [57]. Hybrid solution of conventional fins combined with inverse configuration with additional static fin in a rear cavity [44]. Additional features for improvement of OAS rear cavities [84]

Klingels in his solution [44] suggests combined configuration of conventional and inverse fin design. As shown in the Figure 2.6, beside two conventional fins at the LPT blade shroud, his configuration includes another static fin joined with the casing that points radially downwards.

Features in the rear part of OAS cavity are also researched by Rosic et al. [84]. Authors investigate three different concepts including shaping of the rear part of the exit cavity, axial deflector and a radial deflector in a few geometrical variations. Configurations researched by the authors are also shown in the Figure 2.6. With most of the designs they are able to demonstrate positive impact of the devices in the rear cavity. Nevertheless, application of such devices to LPT OAS is problematic, due to considerable axial movements of the rotor which is limiting for most of such solutions.

Recent concepts, by Nishii and Hamabe [65] or Fujimura et al. [27] respond to this limitation. Their solutions are visualized in the Figure 2.7. Secondary flow suppression structure in the rear part of a cavity [65] is an additional radial opening of the rear cavity. The blade movements are not restricted, but the flow leakage is supposed to be a decreased in a small amount. The second solution, shown in the Figure 2.7, is a particularly shaped subsequent stator leading edge. It is intended to reduce effects from harmful incidence on the leading edge and to keep the leakage in the vicinity of the vane shroud.

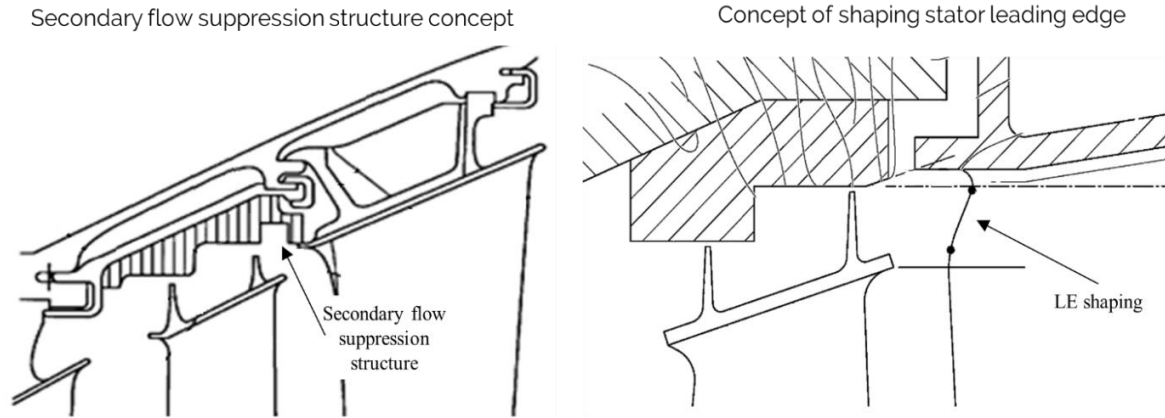


Figure 2.7 Secondary flow suppression structure concept [65]. Shaping of stator leading edge concept [27]

Some solutions for blades with long shrouds are visualized in the Figure 2.8. Jouy et al. in their sealing configuration [40] applied pointing down abradable material adapted to provide additional labyrinth. Interesting solution is also proposed by Fanelli et al. [20]. They suggested small structures with airfoil shape in some locations at the rotating blade shroud.

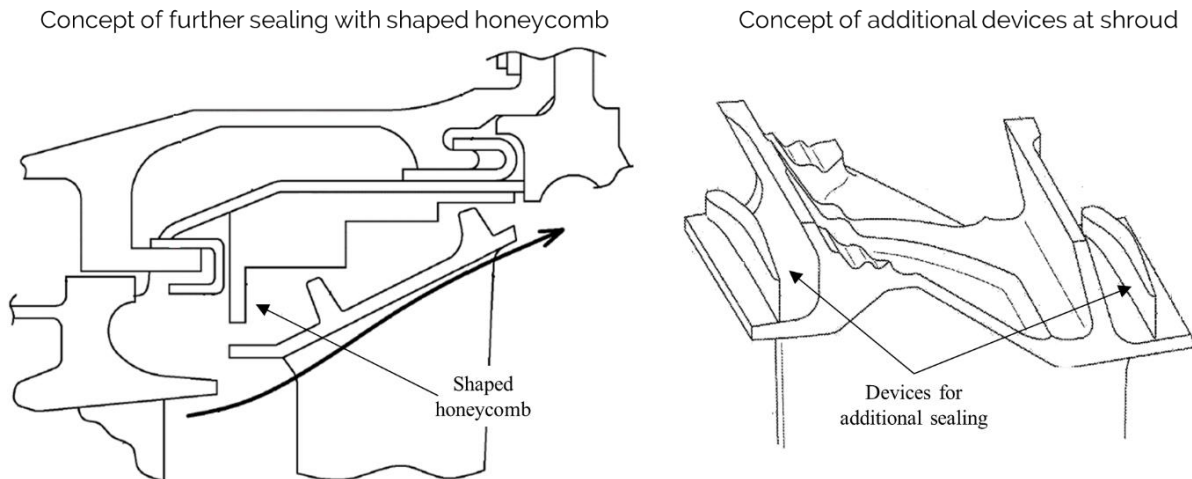


Figure 2.8 Devices for additional sealing between rotor and stator of turbine [40], [20]

The available solutions and also recent development in sealing systems for turbomachinery are under continuous development. There are already known well-performing design solutions for inner gas path. With respect to Outer Air Seals, there are fewer advances yet. Nevertheless, considering limitations for novel Low Pressure Turbines, most of the available solutions are not applicable due to the miscellaneous limitations.

2.2. Flow field and characteristics of LPT Outer Air Seals and their effects on LPT performance

LPT air seals in the shroud regions are typically labyrinth seals with abrasives. LPT OAS have usually two fins and are coupled with honeycombs, as discussed in the Section 2.1. In the course of searching of improvement in a region of outer cavities, it is important to understand the flow field and characteristics of labyrinth seals in general and specifically with respect to LPT OAS. It is also crucial to understand effects from the presence of OAS in the LPT.

2.2.1. Flow field and characteristics of labyrinth seals

Flow through turbomachinery labyrinth seals has been already intensively researched experimentally and numerically. At first, labyrinth seals have been described with correlations based on experimental measurements in numerous configurations. Early research with respect to that is performed by Wittig et al. [105]. Authors provide principal understanding of characteristics of the seals and indicate some driving quantities for operation of the seals. Their research is based on a series of systematic measurements of the straight labyrinths in a non-rotating test stand. It provides baseline dependencies for the discharge and friction factors of the seals with different number of fins at several clearances. Additionally, they investigate effect of the seal scale on seal characteristics. Other baseline benchmark for the labyrinth seals in a straight configuration with several fins is provided by Waschka et al. [99]. They study discharge and heat transfer characteristics for seals rotating at high speeds. Researchers report several principal effects and correlate them with Reynolds number, pressure ratio, and Taylor number.

Willenborg et al. [104] provide detailed measurements with local refinement of a non-rotating stepped labyrinth seal with three fins. They report effects on the losses and heat transfer within the seal, resulting from changes in the seal geometry, pressure ratio and Reynolds numbers. Schramm et al. [89] have extended studies of Willenborg et al. [104] on the same seal geometry by additional research including honeycomb structures. They indicate that presence of honeycombs can lead decreased or increased leakage through the seal, depending on the configuration of effective clearance between the fin and honeycomb. Denecke et al. [14] on the same stationary test stand as the one researched by Willengorg et al. [104] and Schramm et al. [89] perform experimental studies of the impact of the rub-in grooves for a range of possible geometrical variations and for several seals geometries. They demonstrate possible noticeable impact of the grooves on the discharge characteristics. A broad set of developed experimentally correlations is provide by Zimmermann and Wolff [110]. Authors identify labyrinth seals discharge characteristics straight and stepped labyrinths as a function of pressure ratio, clearance size, fins number, honeycomb geometry and several other parameters. Flowingly, Gamal and Vance [28] in a stationary labyrinth seal rig perform investigation of the impact of different

geometrical parameters on a performance of a straight seal. They check additionally that number of fins, their thickness, profile and height affect leakage flow. Additionally, authors indicate that eccentricity contributes to increased flow for most of the studied by them cases.

Flow phenomena within the labyrinth seals are investigated in more detail with advances in numerical modeling. One of the first numerical investigations of labyrinth seals has been carried out by Lee K. et al. [52]. Rhode and Hibbs [77] perform another numerical study for a simple straight seal. They investigate and compare clearance effects in annular and labyrinth seals and correlate them with available measurements showing consistency in the trends.

Denecke et al. [12], with an extensive numerical study and dimensional analysis, crosscheck that the seal characteristics depend on pressure ratio, Reynolds number, circumferential Mach number, swirl ratio, Prandtl number, ratio of heat capacity and geometry of the seal in general. In their analyses authors focused mainly on convergent labyrinth seal, typical for inner seals. Further, Denecke et al. [13] studied experimentally windage heating and exit swirl level of inner cavities. Additionally, they perform Laser Doppler Velocimetry measurements at the seal outlet. It allowed them comparison of outlet velocities with available test data from other researchers and simulations. They report small influence of honeycombs on the axial velocity ratio, but noticeable impact on swirl development and increased windage heating for the configurations with honeycombs. They also observe dependency of the inlet swirl and windage heating. Yan et al. [107] follow their work and carry out further numerical studies of stepped inner air seal. Researchers directly compare cases with smooth walls and honeycombs. They show good agreement of their simulations with the experiments of Denecke et al. [12]. They also provide additional characterization of the seal windage heating and leakage flow. In another study from Kim and Cha [43] numerous straight and stepped labyrinth seals configurations are compared with available experimental characteristics with respect to varying seal topology, clearance size, pressure ratio and number of fins. They indicate that due to numerous parameters of the seals, general correlations for prediction of the discharge behavior might not be applicable, due to considerable differences between numerical prediction and correlations outcomes.

Rapisarda et al. [76] validate their numerical setup with experimental results of Denecke et al. [13] and correlations from Waschka et al. [99]. Afterwards, they perform numerical investigation of impact of the honeycomb and fin rounding at small pressure ratios. They investigate several variants of a seal topology and a range of possible rounding of the fins. They indicate significance of the fin rounding and step position on the discharge coefficient of the seal.

Schramm et al. [88] applying automatic numerical shape optimization of a labyrinth seal with three fins prove that an optimal geometrical configuration for the seal can be identified by varying geometrical parameters. Their study is limited only to position and height of the step, nevertheless, they prove that numerical optimization of the geometry can result in a certain leakage reduction. Another attempt to the optimization of a straight OAS with two fins is

performed by Rulik et al. [85]. Based on the results of the optimization and performed sensitivity studies, authors identify primary geometrical features driving leakage reduction. They find that amongst varied by them parameters, fin width and distance between fin tips have the biggest impact on seal performance.

Recently, Wein et al. [102] compare different solvers and different steady and unsteady setups and investigate different meshing strategies. They perform thorough numerical analyses for a stepped labyrinth seal. Authors analyzed numerical prediction for different setups and codes including stationary, nonstationary and scale adaptive simulations. They demonstrate capabilities and limitations with respect to different setups and different turbulence models. They find general good agreement between different solvers. At some locations, they indicate inaccurate prediction of the swirl development and cavity vortex system by RANS. Nevertheless, simultaneously authors indicate that seal mass flow as well as the outlet velocity profiles are in good agreement between time-averaged solutions achieved with different modeling approaches.

Research of the labyrinth seals discussed so far was more focused on inner seals. Seals investigated by the abovementioned researchers have similar configuration – several fins and small radius. It is due to common application of such seals in engines at several locations, but mainly at inner diameter. They have been researched in the course of baseline understanding of the seals and safe application of the labyrinth seals in engines. As elaborated in the Section 2.1. , Outer Air Seals operate at different conditions and with different purpose.

In recent years, labyrinth seals, particularly in the vicinity of the shroud are also extensively researched. Szymanski et al. [93] perform simulations of typical tip labyrinth seal. They study effects of roughness and rotational speed on the seal characteristics. Authors noted rotational speed can contribute to smaller discharge through the seal. They also check that surface quality noticeably decreases discharge through the seal at high rotational speeds. Later, Szymanski et al. [92] compare experimental data of typical outer air seal from their test stand with available test data for inner air seals configurations from other researchers. Authors compare cases with and without honeycombs and report considerable discrepancies in the trends and values between their test data and data available for inner air seals. They point out considerable sensitivity of general literature-based correlations of labyrinth seals. Researchers indicate that small differences in the geometry or operating parameters can result in significant changes of the overall seal characteristics. They indicate that literature based data cannot serve universally for prediction of labyrinth seal operation or optimization and suggest to confirm expected characteristics experimentally or with extensively validated numerical prediction.

A novel rotating test stand, particularly for research of shrouded outer seals is studied by Kluge et al. [48]. Authors provide a general overview of the test rig and indicate sensitivities and inaccuracies associated with measurements of the labyrinth seals. Later, Kluge et al. [45], for this test rig identify some unsteady pressure fluctuations at the outlet of the rig for in a certain

operation range. Their comparison of numerical and experimental results shows that CFD models are able to capture properly fluctuations modes. Wein et al. [101] analyze in detail the flow in this test stand. Researchers perform detailed measurement campaigns including additional instrumentation of the casing and PIV in addition to conventional measurements of discharge of the seal. Authors compare the experimental results with numerical computations applying several turbulence models and miscellaneous corrections. They aimed finding the best setup for proper prediction of shroud seals. Their measured and predicted flow field behind the seal and distribution of the static pressure along the casing are visualized in the Figure 2.9. With several models authors identify very good fit of measurements and numerical simulations. In particular, they achieve very reasonable prediction with $k-\omega$ model extended for treatment of increased production of turbulent kinetic energy at stagnation points. With this setup they are able to well predict measured discharge coefficient, casing pressure distribution as well as velocities and their fluctuations getting also TKE fields.

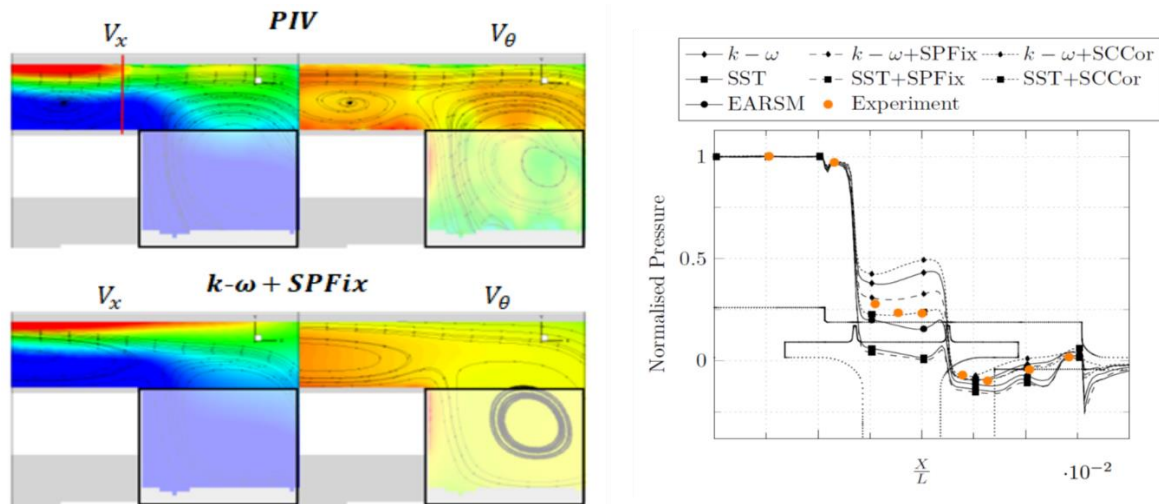


Figure 2.9 Comparison of steady numerical prediction with PIV at rear cavity and static pressure distribution at the casing for shrouded outer air seal test rig [101]

It proves possible application of RANS with proper setup for OAS. However, authors indicate that detailed PIV measurements revealed also that the local flow behavior is not captured accurately in some locations. Due to that, Wein [100] performed LES studies of the straight OAS and compared them with high quality measurements from the test stand. He demonstrates that LES capture most of the effects observed with conventional and advanced measurements techniques. Nevertheless, author indicates that despite some deficits in RANS modeling, they deliver robust and valid prediction of the primary flow features driving phenomena at outer cavities.

Recently, Oettinger et al. [66] in detail investigate aerodynamics of the labyrinth seals with honeycombs and compared with measurements at the same test stand. Authors indicate that overall steady numerical simulations can predict labyrinth seals characteristics and local flow

field in terms of pressure distribution and capture impact of rotational speed for both smooth and honeycomb arrangements. Authors indicate that also properly adjusted correlations, originally obtained for inner air seals can reasonably estimate, with some uncertainty, seal discharge characteristics, despite primary differences between geometries of inner and outer seals such as discontinuous steps in the casing contour.

The numerical investigations performed by independent researchers indicate that due to multiple possible configurations of the labyrinth seals, general correlations provide only preliminary prediction. Thus, reasonable confirmation of the seal performance can be only achieved either by detailed testing of particular seal or numerical simulation of the seal geometry with validated code. Simultaneously, both improperly performed tests and simulations can deliver inaccurate results. Thus, only a careful validation of the numerical prediction based on a high-quality measurements, combined with detailed geometrical study of the tested seal can deliver reasonable prediction of the seal operation.

2.2.2. Flow field of the LPT with Outer Air Seals

Presence of shroud sealing systems in Low Pressure Turbines definitely is indispensable. OAS enables proper operation and enhance performance, but simultaneously influence flow field of the turbomachines. OAS contribute to specific flow structures, phenomena and effects associated with operation of LPT. These have been studied by several researchers.

Anker and Mayer [2], with numerical simulations, investigate influence of the leakage on LPT main stream by variation in a seal clearance size. They indicate that OAS leakage, beside enhancement of mixing losses, can dominate secondary flows. It can induce further severe losses and negative incidence at the subsequent stator. They emphasize that flow from the cavities should be accounted in design and optimization of turbomachinery. Pfau et al. [72] perform detailed experimental and numerical research of a two-stage turbine with inverse fin configuration. Researchers perform comprehensive analysis and high-resolution measurements of the flow field in the front cavity of the shroud seal. They report unsteady interactions in that region. It is indicated by them that part of losses, due to the OAS stems from different circumferential velocities of the mainstream and vortices in the cavity. Giboni et al. [29] provide further highly resolved time-accurate data with different instrumentation including pneumatic five-hole probes and hot-wire probes at several positions in a 1.5-stage turbine. Authors compare test results with steady and unsteady simulations and identify flow structures within the main flow resulting from OAS leakage. Their findings with respect to primary flow features are given in the Figure 2.10. In particular they draw attention to considerable mixing region behind the cavity and highlight that even at small clearances leakage induces flow separations at the subsequent rotor.

Gier et al. [30] investigate three-stage engine-like LPT. Authors validate their numerical prediction at the nominal conditions and geometry with experimental data. Later, they provide comprehensive numerical analyses with respect to varying clearances. They indicate significant interactions between cavity flow and mainstream. Their research confirms change in an incidence to the subsequent stator, intensification of the secondary flows at downstream rows and reveals shift in mass flow distribution. Important contribution is introduced with break-down of the losses resulting from outer cavities provided by them. Lampart [51] investigates mechanisms of formation of the tip leakage in shrouded and unshrouded turbine blades. He indicates several quantities driving principal flow phenomena. He finds leakage mass flow and its direction at the cavity outlet to have the primary importance for shrouded blades. Additionally, author points out that the tip leakage structures dissipate through the subsequent stator only in small part and that these structures can be clearly identified in the flow impinging next rotor. Bohn et al. [4] perform measurements of the flow field of the two-stage LPT equipped with OAS with inverse fin arrangement. They experimentally vary axial and radial clearances. Their findings confirm numerical results of Gier et al. [30] and Lampart [51]. Despite inaccurate numerical prediction at endwalls, they could clearly identify and confirm basic flow phenomena from OAS presence.

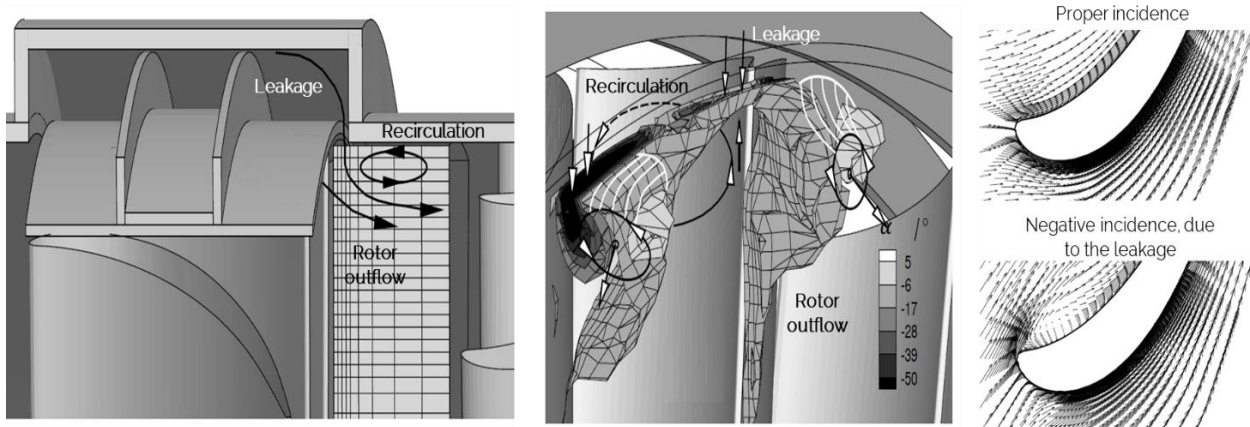


Figure 2.10 Flow structures resulting from the OAS leakage. Negative incidence at shroud of subsequent stator and resulting separation. [29]

Fraczek et al. [25] investigate numerically impact of rub-in of a honeycomb in an OAS. They model part of the turbine mainstream close to the outer diameter together with OAS including the whole honeycomb structure. In their configuration, nominal radial clearance is decreased with rub-in. Authors indicate that the minimum clearance can happen in another location resulting in changes in the seal performance. Researchers do not find bigger differences between turbine with nominal and rubbed-in honeycomb. Wroblewski et al. [106] numerically investigate impact of the geometrical parameters on the straight labyrinth seal including honeycomb performance incorporated into the LPT blade domain. They check several geometrical variants and assess their effect on the leakage mass flow. They vary parameters like fin thickness, its

inclination and position of the fins as well as position of whole honeycomb structure. They confirm that findings for seals with smooth lands also are applicable for honeycombs with respect to fin thickness and its inclination. In addition, they indicate relative position of the fin with respect of honeycomb has small effect. Nevertheless, they identify that the position of the whole honeycomb with respect to the whole seal can affect sealing performance, especially when honeycomb is shifted downstream affects the losses in the mainstream of the machine.

Jameson et al. [39] perform experimental and numerical studies of impact of varying clearance. Detailed measurements allow them particular identification of two separate vortex structures in addition to the regular secondary flow referred as horseshoe vortex usually present in the mainstream. The footprint of these flow features is in agreement with findings of other researchers e.g. [51] who confirm formation of these structures in the mainstream. Jameson et al. [39] identify also origins of these vortices. Their findings are presented in the Figure 2.11. Additionally, authors suggest improved stator design by locally redesigned profile at the shroud. Their improved design allowed them reduction of the incidence from the shroud leakage flow and elimination of separation vortex.

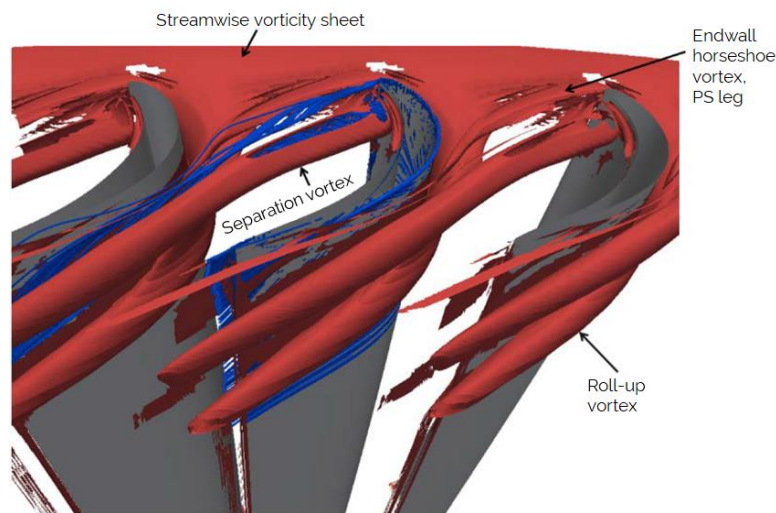


Figure 2.11 Flow structures developing at the stator behind LPT OAS [39]

Wallis et al. [98] in their experimental rig install turning devices directly at the shroud of the rotating blade. Researchers investigate shrouded low aspect ratio HPT, but are able to clearly demonstrate that, the decrease in the harmful effects from the leakage on the circumferential mixing can be reduced with proper turning of the leakage. Following that, Rosic and Denton [83] demonstrate numerically and experimentally that installation of the turning devices in the rear part of the OAS cavity can improve mixing losses at rows downstream the seal. Their results prove that it is possible to improve the flow field in the downstream blade row as well as overall turbine performance by reducing effects of the leakage on the mainstream. They indicate that the effectiveness of the turning vanes depends primarily on their geometry and spacing. Further, Rosic et al. [84] investigated different configurations of the rear part of the OAS. With the

decreased rear cavity, they show increase in the turbine efficiency, confirming it by simulations and tests. Authors report that the beneficial effects are more pronounced if the spacing between devices is tight. They also show with CFD and experiments that also axial deflector can provide increase in efficiency and demonstrate effectiveness of the radial deflector concept for a range of different axial positions. Investigated by them radial deflector has shown reduction in the leakage, but increase of mixing losses in radial direction. In addition, authors study also effect of a chamfer of the rear cavity corner.

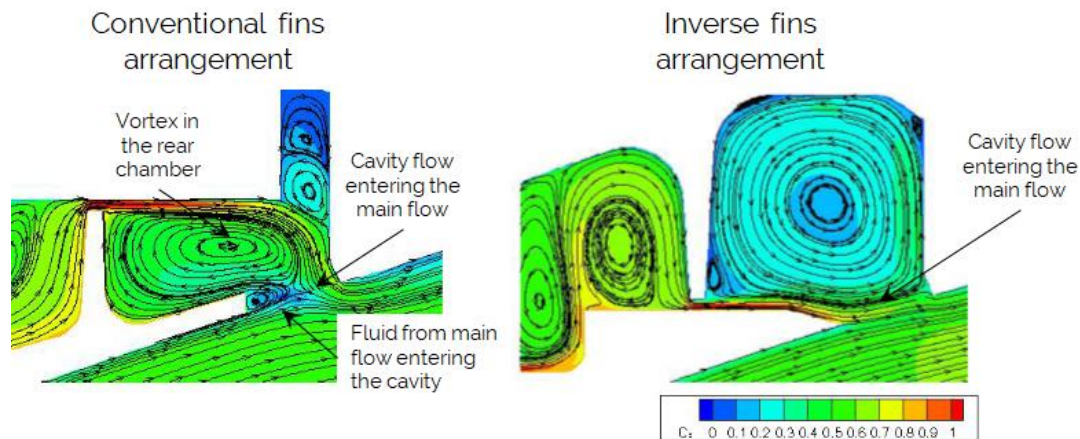


Figure 2.12 Comparison of the primary flow structures between conventional and inverse fins arrangements [57]

Mahle and Schmierer [57] compare conventional and inverse fin configurations applied to three-stage engine-like LPT. They investigate mechanisms of vortices formation in both configurations and study interactions of the leakage with the main stream in both configurations. Some of their findings with respect to the differences in the flow structure are presented in the Figure 2.12. Authors indicate positive effects from the application of the inverse fin solution on the flow structures. Their findings show significant differences in the axial and circumferential velocities of the leakage and the mainstream in both configurations. They indicate that the mixing losses in circumferential direction, being a consequence of differences in velocities, are considerably decreased in the inverse fin configuration. Authors point out that inverse fins are applied typically in steam turbines, but they are not applied in aircraft LPT.

2.2.3. Impact of OAS on performance of LPT

In the direction of search for improved solution of the outer air seals regions, it is necessary to understand possible impact from their presence on the performance of LPT. It is found useful to identify quantification of particular solutions or direction for the improvements.

Depending on the researched machine, seals configurations, and operating conditions, different researchers indicate considerably varying impact of OAS on performance of turbomachine. Rosic and Denton [83] investigate 1.5-stage shrouded low aspect ratio steam HPT with flow

coefficient 0.384 and stage loading close to 1.0 based on the exit velocity. They note overall drop in efficiency from OAS cavity up to 2.6%. Comparable decrease for a similar shrouded HPT report also Liu et al. [55]. Pfau et al. [72] research low-speed, two-stage LPT, operating at pressure ratio 1.32, with inverse fins arrangement at OAS. Authors indicate possible decrease of 1.6% in the machine efficiency, due to OAS. Gier et al. [30] report efficiency drop in a range from 2.2% up to 2.6%, resulting from all IAS and OAS cavities in the three-stage LPT.

Outer Air Seals are associated with several types of losses. Witte [34] reviewed all possible sources and that they can be divided into four main groups: bypass losses, mixing losses, dissipation losses (frequently called step losses) and losses associated with impact on subsequent downstream rows. His findings are summarized in the Figure 2.13. Particular sources of losses meaningful in herein thesis are treated in more detail in the Chapter 5.

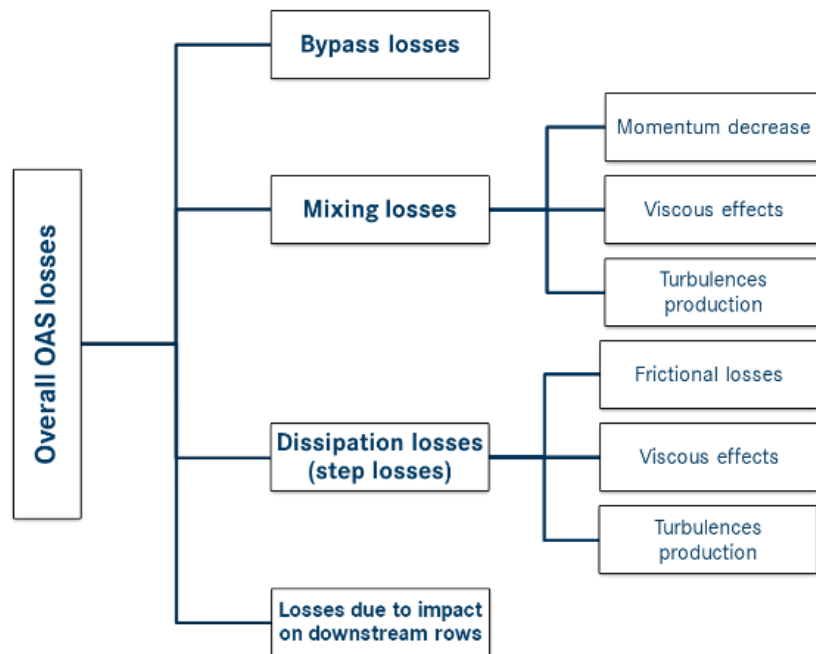


Figure 2.13 Sources of losses for LPT associated with OAS presence

Rosic and Denton [83], identify loss mechanisms from shroud leakage and provide loss breakdown for 1.5-stage low aspect ratio steam HPT. They differentiate losses due to front and rear cavities, windage losses, mixing losses at reentry and bypass losses. Gier et al. [30] also provide loss breakdown for conventional 3-stage LPT. Similarly to Witte [34], authors differentiate bypass losses, mixing losses, step losses and incidence losses, simultaneously indicating negligible windage losses.

These findings point to the conclusion that Outer Air Seals can be enhanced by improvements in the fields of particular sources of losses. Nevertheless, magnitude of these differ depending on sealing configuration and turbine design. Particularly strongly it is associated with running

clearance size, as indicated by Yaras and Sjolander [109]. Qualitative share of the different losses at different tip gap sizes for tip sealing, obtained by the authors by means of the special cascade testing, is visualized below in the Figure 2.14.

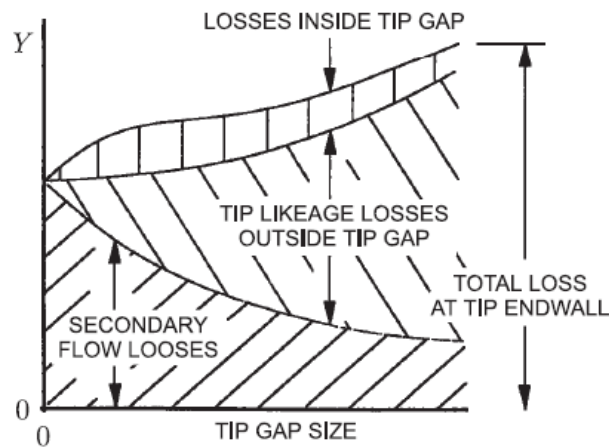


Figure 2.14 Fraction of losses due to shroud sealing at different gaps obtained with cascade testing acc. Yaras and Sjolander [109]

It is considered that a corresponding variation of fractions of different sources of losses is also recognizable for LPT. The figure suggests that particular solutions might be more appropriate at certain clearance levels. It is one of the reasons for different shares of the losses obtained by different researchers. Rosic and Denton [83], indicate that presence of inlet and outlet cavities stands for nearly 20% of total losses. Similar portion of around 15% results from mixing at the reentry. The rest, thus around 65%, they assign to the bypass of the leakage. Gier et al. [30] estimate fractions of particular losses at several clearances levels with the LPT which they investigate. The biggest share, 30-50% of all losses, pose mixing losses. In their configuration, the bypass losses are responsible for 10-20% of total loss due to cavities depending on the clearance. Step and windage losses, referenced as losses due to dissipation reach 20-30% of all losses. The remaining part of 10-20%, authors assign as subsequent row. Their research confirms that the shares of different losses depend on the clearance size.

With respect to the bypass losses, Witte [34] demonstrates that they are purely associated with the leakage mass flow. This mass flow does not contribute in the generating work at the rotor. The dependencies of the seal leakage are elaborated in the Section 2.2. Mainly, it is associated with radial clearance, pressure ratio, geometry of the seal in general and few secondary order effects.

Denton [15] indicates that the mixing losses tend to be smaller for smaller reinjected mass flow, also for smaller difference in velocity angles, their magnitudes and temperatures. They are less enhanced if the reintroduction occurs at lower Mach number of the mainstream. Step losses depend strongly on the geometrical seal configuration in particular axial clearances. Traupel [97] suggests that they also depend on the velocities in the mainstream and their angles. Treatment of

losses due to influence on the subsequent loss is not straightforward. OAS leakage definitely contributes to enhanced secondary flows and improper incidence of following blades as reported e.g. by Jameson et al. [39]. From the Figure 2.15 it is clearly visible that the entropy production due to presence of OAS is transported downstream the machine as confirmed by Biester et al. [3] or Lampart [51].

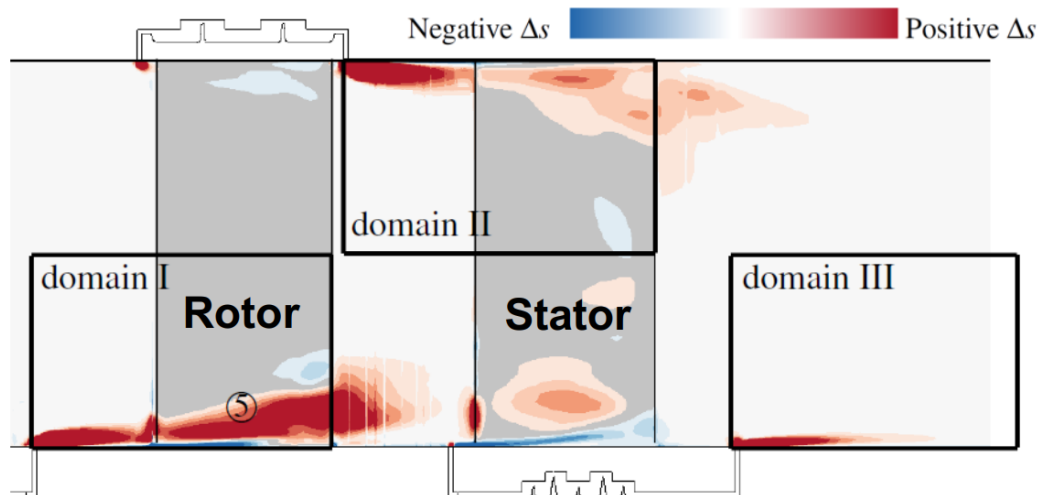


Figure 2.15 Entropy production due to LPT air seals and their impact on next stator [3]

Reviewing available literature, there are no reasonable analytical formulas for assessment of these effects. The influence of the secondary flow and the incidence of following blades is omitted in the model of Witte [34]. Gier et al. [30] determine those losses indirectly, subtracting from all other losses. Their quantification could be attempted by estimation of losses due to incidence with correlations. From data collected by Moustapha H. et al. [62], it is visible that the profile losses due to the incidence are the smallest for the values close to the design value. Thus, any incidence results in increased losses. Nevertheless, the available correlations based on the data obtained in the cascades are not valid for the incidence range resulting from OAS. In addition, the approach is not meaningful, due to the data come from cascade testing, and correlations do not include interaction of airfoil and endwalls. Thus, it is not possible to reliably apply them. Therefore, they the only available option is to account for them applying numerical simulations. Validated CFD can greatly contribute to the understanding of the flow features very difficult for accounting analytically or empirically.

All abovementioned researchers prove LPT performance can be improved with respect to OAS in addressing particular sources of losses associated with their presence: bypass losses, mixing losses, dissipation losses and losses due to impact on subsequent rows downstream the machine.

2.3. Summary of the literature review and formulation of research theses

The following conclusions are drawn from the review of available research in the field of Outer Air Seals of Low Pressure Turbines.

LPT OAS allow proper operation of the turbomachine and enhance its performance, but simultaneously influence the flow field. A continuous interest in improved operation of the sealing system of LPT is observed, because it directly transfers to the performance of the whole engine.

There is no particular sealing configuration that is applicable and satisfactory for general use. Meaningful differences in operating conditions between IAS and OAS apparent. It implies that solutions applicable for inner air seals cannot be directly transferred to the outer ones.

The most frequent configuration of LPT OAS is labyrinth seal with two fins combined with honeycomb structure. It is proven that geometry of the labyrinth can be optimized, thus, it is assumed that geometry of the labyrinth seals is already optimal, under LPT design conditions. Several solutions improving OAS operation are available, but they are not applied in aircraft LPT, due to multidisciplinary limitations. Recent advance in LPT is introduction of separate Active Clearance Control system for decrease of running clearance across whole mission cycle. Researchers and engine manufacturers still invest effort in searching for better solutions in LPT OAS. Thus, it is concluded that such solution is not found yet.

Flow through turbomachinery labyrinth seals has been already intensively researched experimentally and numerically. A considerable sensitivity of general literature-based correlations of labyrinth seals is noted. Literature based data cannot serve universally for prediction of labyrinth seal operation or their optimization. Phenomena within labyrinth seals can be investigated in more detail applying numerical modeling. Despite small inaccuracies in the local flow field with steady numerical prediction, different researchers indicate that steady numerical simulations with appropriate setup can well predict overall labyrinth seals characteristics, effects associated with particular seal operation and local flow field for labyrinth seals with smooth walls as well as with honeycombs. It indicates with properly adjusted CFD setup, new design solutions in the region of OAS can be researched applying steady numerical modeling.

As reported by different researchers, inevitable presence of outer cavities in LPT decreases its efficiency in a range of about 1.6% up to 2.6%, depending on the configuration. The decrease cannot be completely avoided, but some fraction can be recovered by mitigation of particular sources of losses. OAS induce specific flow structures in the LPT flow field, resulting in bypass

losses, mixing losses, dissipation losses (step losses) and losses associated with impact on downstream rows. Magnitude of particular sources of losses can differ depending on configuration and running clearance size.

Based on the literature review and available knowledge state, the herein dissertation is prepared with theses that:

1. There exists an improved solution for LPT Outer Air Seals which:
 - a) can fulfill multidisciplinary requirements,
 - b) improves LPT efficiency in the required amount of at least 0.1%,
 - c) is not found and not researched yet
2. There is a solution for LPT OAS that either:
 - a) decreases leakage mass flow through the seal or
 - b) reduces mixing losses, dissipation losses, due to cavity geometry or losses due to impact on the downstream rows or
 - c) improves any other aspect of the seal performance that results in required increase in LPT efficiency

This page intentionally left blank.

Chapter 3. Research methodology

3.1. Methods applied for derivation and multidisciplinary assessment of new design ideas of LPT OAS

The main subject addressed in the herein dissertation is development of new solution for Outer Air Seals of Low Pressure Turbines providing requested increase in aerodynamic efficiency and possible for application in the multidisciplinary environment of LPT.

After a review of available solutions, knowledge state, research and patents for the investigated region, the new ideas are collected. In a next step, in the process of defining improved design solutions, the ideas are gathered in a specifically prepared matrix of the concepts. For every design idea a unique number and name are assigned, together with a description of essential design features, expected improvements and a picture. Subsequently, these ideas are preliminarily evaluated in the light of miscellaneous criteria from particular disciplines and likelihood of fulfilling assumed goals.

In multidisciplinary areas, it is especially crucial to confront the solutions against criteria from all meaningful disciplines. It is crucial to understand assumptions and limitations under particular solutions. The concepts are verified and checked in the multidisciplinary project team. It is valuable to discuss the ideas with experts from different fields. It frequently brings another perspective to the solution and leads to significantly improved concepts. In case of LPT Outer Air Seals requirements from: aerodynamics, design, manufacturing technology, materials technology, secondary air management, thermal engineering, structural integration and costs have to be fulfilled.

Frequent situation in such multidisciplinary cases is that the enhancement of operation in terms of one discipline, results in stretching or violation of other disciplines. Thus, it is preliminarily revised, if the compromise can be reached or the introduced deficit at some discipline be mitigated with another technology. If it is impossible to allow the modification, meaning the solution significantly and inalterably violates criteria from some discipline, the solution is not further considered. Second matter is with respect to likeliness for the solution to reach assumed goals in terms the expected benefits. It is also preliminarily evaluated if the solution in further development is likely to bring expected benefits. If the design solution is possible to work, not violating criteria from any discipline and it is likely to reach project goals, it is further developed, detailed and thoroughly analyzed. A scheme for preselection of the ideas is pictured in the Figure 3.1. Early assessment of the multidisciplinary criteria simultaneously narrows the area of searching and eliminates low-rated ideas.

Next, the preselected ideas are evaluated based on the available predesign tools, expert knowledge, available tests and experiences or preliminary models. It is also carried out in the multidisciplinary team, involving experts from the fields. At this stage of evaluation, preliminary designs are prepared, but detailed designs for the solutions are not available yet. In the technology development is attempted to perform reasonable trading if some criteria from one for the fields are violated. To avoid situations that the developed solution worsens the overall profits from the whole machine. It is also performed in a form of matrix, where the results of this evaluation are rated. The structure of the matrix is also shown in the Figure 3.1.

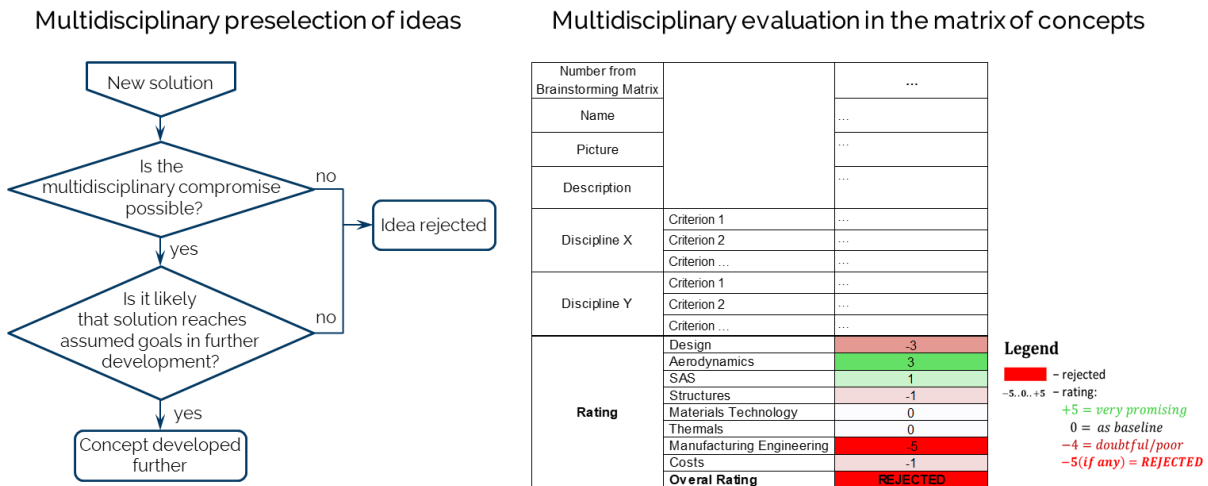


Figure 3.1 Scheme of preselection of the ideas and matrix of concepts for multidisciplinary evaluation of the solutions

The approach in the assessment is to evaluate the preselected solutions in terms of all the meaningful criteria from the disciplines – quantitatively and if possible, with predesign tools also qualitatively. The results are reflected in the multidisciplinary rating. It is attempted that from all disciplines a legitimate rating is assigned. The exemplary rating is shown in the Figure 3.1. The neutral zero refers to the situation without any change with respect to the reference. The positive rating indicates certain benefits for a discipline. The negative means worsening situation in terms of a discipline. By an agreement, rating of “-5” indicates that the criteria are violated greatly and solution is not considered further. In this phase of the assessment, from all disciplines possible risks are also identified and collected. It is important to have a clear differentiation between a showstopper and a risk. In case of the first option, the solution cannot be further considered. The risks, are important to be indicated, because with the further development of the solution, they are mitigated with appropriate treatment or additional technology.

This approach enables also consideration of the benefits at several fields. The final rating can be arithmetic or weighed average of the particular ratings. That is a fair attempt, because proper operation from every discipline’s perspective is crucial for well-performing solution. The most promising ideas in terms of the rating and fulfilling assumed goals are chosen and evaluated in detail with numerical models validated with experiments to confirm the expected benefit in terms of LPT efficiency.

3.2. Phenomena similarity and dimensional analysis

Proper operation of the developed solutions needs to be assured. Outer Air Seals of LPT are driven by aerodynamic phenomena. The similarity of phenomena is one of the most important things in describing and modeling of the nature. Similarity theory includes definition of dimensionless similarity numbers that describe and characterize the phenomenon. In practice, if the characteristic numbers are the same, two phenomena are similar. These numbers are commonly used in engineering because they simplify considerably calculations, allow scaling of the device for testing or another application and are very convenient way of comparing different solutions. The similarity enables also studies on a model and later transfer of the results to the real system. It allows performing tests on a smaller scale or at different conditions e.g. at lower temperatures and pressures, as indicated by Taylor [95].

The similarity theory can be applied to any device. Qing [75] states that the phenomena in the nature and also engineering problems can be described by a set of physical quantities that the physical laws governing those phenomena and problems can be understood. Such characteristic numbers for instance are applied for turbines in general indicated by Dixon et al. [19]. However, the approach can be also applied for particular components when attempting their analysis.

Thus, there are two primary benefits from application of the similarity theory – firstly, it enables proper modeling and comparison to reality and secondly it facilitates understanding of the laws governing the phenomena.

In practice research of similarity is realized applying Dimensional Analysis. It is a formal procedure that allows representation of the group of variables describing some physical situation and reduction to a smaller number of dimensionless numbers. It is based on a mathematically proven theorem by Buckingham. The principal theorem states that, if N variables a_1, a_2, \dots, a_N describe some physical phenomenon, as given by eq. 3-1

$$f(a_1, a_2, \dots, a_N) = 0 \quad \text{eq. 3-1}$$

and include l dependent variables and $N-l$ independent variables, an implicit general formulation in a form of the function can express a physical law governing the phenomenon. Without losing generality, it is possible to indicate k quantities a_1, a_2, \dots, a_k referred as fundamental quantities. The rest, i.e. $N-k$, quantities are termed derived quantities. In practice, k fundamental quantities are unit system quantities. By application of the power law method, the above equation can be reduced to the relation of $N-k$ dimensionless Π characteristic numbers, as in the eq. 3-2:

$$f(\mathbf{1}, \mathbf{1}, \dots, \mathbf{1}; \Pi_1, \Pi_2, \dots, \Pi_{N-k}) = 0 \quad \text{or} \quad f(\Pi_1, \Pi_2, \dots, \Pi_{N-k}) = 0 \quad \text{eq. 3-2}$$

In the herein thesis, the approach described by Qing [75] is applied including guidelines from Taylor [95]. The complete procedure applied for LPT OAS is described by Palkus and Strzelczyk [70]. In herein thesis, only a short summary is provided.

While reviewing a physical phenomenon that is supposed to be described, first of all the quantities that essentially influence the phenomenon are determined. Next, each dependent quantity is evaluated in terms of independent variables, applying Buckingham theorem and power law. Simultaneously, the dimensional analysis facilitates reduction of parameters to minimum and their formulation in a form of essential characteristic dimensionless numbers.

The dimensional analysis facilitates localization of the relations between variables with the great economy of effort. Certain dependencies between parameters, resulting from dimensional analysis are provided for generally for OAS and particularly for the new solutions. The dimensional analysis applied for OAS allowed the identification of the primary parameters meaningful for the flow through the seal.

3.3. Numerical CFD modeling

For assessment of the aerodynamic efficiency benefit from the newly developed solutions of LPT Outer Air Seals, they are simulated employing Computational Fluid Dynamics. A majority of the three-dimensional detailed numerical analyses is performed with a model of 3-stage Low Pressure Turbine rig. The machine is researched at Institute of Aircraft Propulsion Systems (ILA) in Stuttgart. The LPT is investigated in reference configuration with baseline OAS as well as with developed solutions.

3.3.1. CFD model of reference 3-stage Low Pressure Turbine

Geometry

The CFD model of the turbine reflects a full geometrical configuration of the aerodynamic rig. The view on the geometry of the researched machine is given in the Figure 3.2.

Properly reflected geometry has primary importance for the numerical prediction. Due to that, in the mainstream airfoils including all meaningful geometrical details e.g. fillets are thoroughly modeled. In addition to the main gas path, cavities at inner and outer endwalls regions are included. Modeling of those, as demonstrated by Gier et al. [30], has significant importance for reliable prediction of the LPT flow field and its characteristics, including efficiency. Authors indicate that the models with cavities are considerably closer to the measurements than those only reflecting ideal main gas path. Similar conclusions have also Giboni et al. [29] and Henke et al. [36].

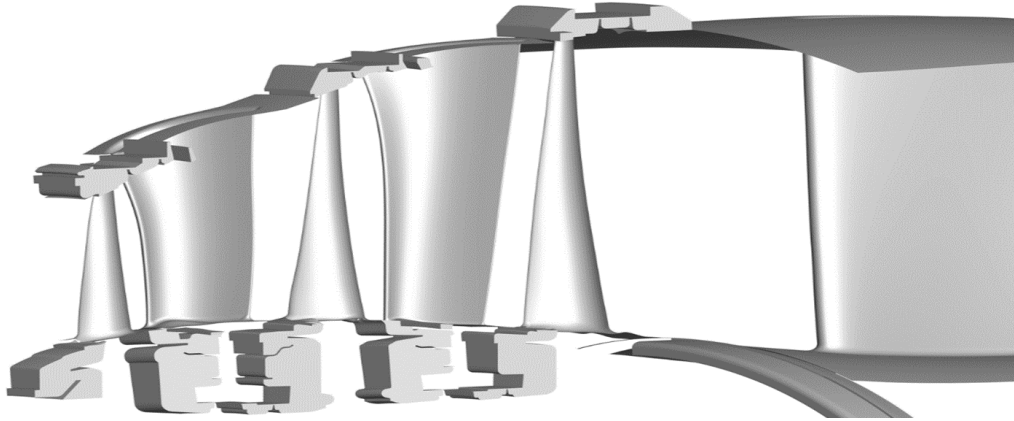


Figure 3.2 Geometry of the main gas path with connected inner and outer cavities of the baseline 3-stage LPT

Due to importance of abovementioned, as visible in the Figure 3.2 the model of the researched turbine includes all meaningful geometrical feature, reflecting in considerable detail the tested rig. Figure 3.3 provides additional side view on the geometry of the outer cavities, being subject of research in herein thesis.

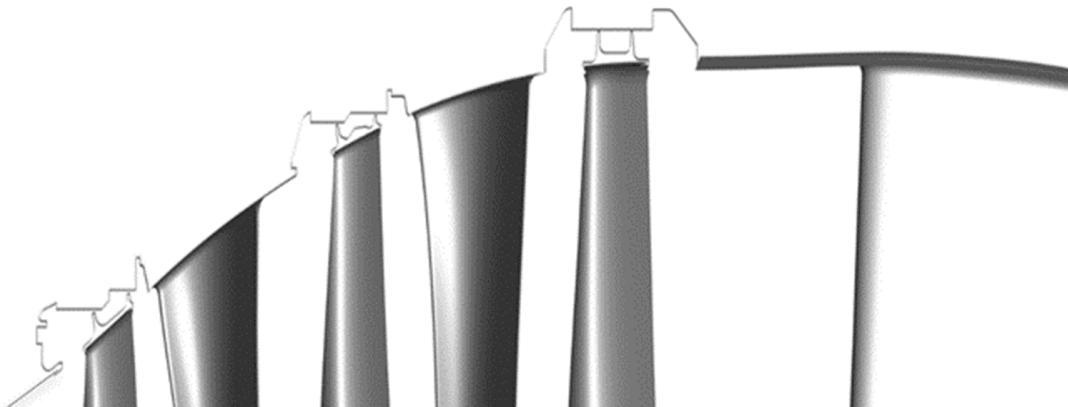


Figure 3.3 Geometry of the channel and outer cavities of the baseline three-stage LPT

The aspect ratio of all airfoils is larger than 3. As discussed by Moustapha et al. [61], such design allows limitation of secondary flows generation, due to smaller boundary layers. The larger the aspect ratio, the closer to the endwalls are kept secondary flow structures. It is important for the herein research, because it allows modification of the Outer Air Seals without significant impact on the mainstream and unchanged machine operating point.

Domains discretization

Connection of all abovementioned geometrical details is nontrivial. The approach for the machine discretization corresponds to the procedure applied by Gier et al. [30] and Mahle [56]. It assumes separate meshing of the mainstream and cavities and their further connection. In this way, high quality meshes are obtained. The grids generated for the machine are shown in the Figure 3.4. Structured, hexahedral meshes are generated for both main gas path and cavities.

This type of meshes is proven to be more robust, involve less computational resources and provide better quality results. Nevertheless, they also require considerably more time for their preparation. Application of the sophisticated mesh generator AutoGrid from Numeca, designed particularly for turbomachinery, provides high quality grids. Every row is meshed separately. Particular rows are further connected. Geometrical features like fillets are also meshed, as visible in the Figure 3.4. The meshes of the cavities are generated applying ANSYS ICEM. The cavities are axisymmetric. Due to that, it is possible to prepare two-dimensional cavity meshes and extrude them to the required circumferential extension. Exemplary grid for the cavity is also shown in the Figure 3.4.

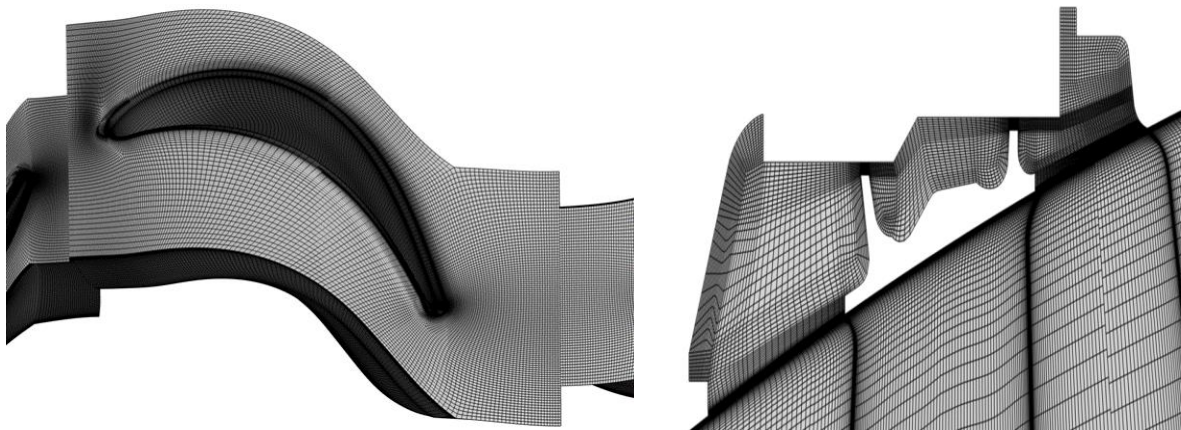


Figure 3.4 Baseline LPT mainstream and cavity meshes

The same meshes are applied across all simulations in herein thesis. The mesh of whole machine in total consists of around 24 million cells, including 6 million representing cavities. The grids are refined at the walls and in the regions with high gradients, e.g. at the fins of the labyrinth seals. At walls in the mainstream, at airfoils as well as at endwalls, averaged dimensionless wall distance y^+ is around 1. It allows proper resolution of boundary layers. In the cavities, resolution at walls is coarser and Wall Functions are applied. It is considered that boundary layers are not of primary importance in these regions. It is also justified and confirmed later in the Chapter 4. , when revising validity of the prediction in OAS.

The quality of the meshes is considered very good, fulfilling best practices for both applied CFD solvers. Exemplary criteria checked for meshes in the OAS regions are: elements grow ratios smaller than 1.4, minimum angle always above 25 degrees and determinant above 0.5. It complies with suggested criteria given for ANSYS ICEM [38]. The mainstream mesh sensitivity study is not performed. It has been performed by other researchers and is not addressed in herein thesis. The proper prediction with respect to machine efficiency and in particular at endwall and cavities regions is proven by validation with test data in the Chapter 4.

Numerical setup and solvers

For the efficiency assessment, numerical steady state Reynolds-Averaged Navier-Stokes simulations are performed. Two different flow solvers are used in herein thesis – TRACE, a solver specialized in turbomachinery applications and CFX, a commercial solver. The first one is a density-based code, developed by the German Aerospace Center (DLR) and MTU Aero Engines [96]. The software enables very accurate prediction of turbomachines. It is applied for full-geometry simulations of the reference LPT. The second solver, CFX is pressure-based unstructured code. This software is applied for detailed parametric sensitivity studies of the VBH concept. It is due to its capability of handling complicated geometries with unstructured meshes. TRACE uses predictor-corrector solution strategy. ANSYS CFX is a coupled solver – equations are solved within a single algorithm. It allows fully implicit discretization of the equations at given time step. In both solvers higher resolution spatial discretization schemes are used. For TRACE, it is second order accurate Fromm scheme [26], together with a special van Albada limiter [1] to stabilize solving process. In CFX it is high resolution upwind scheme embedded in the solver for advection terms is used [7]. For time integration implicit procedures are used until a steady state is reached in both solvers.

Turbulence and Transition modeling

In both solvers different eddy viscosity turbulence models are used. In TRACE, the two-equation Wilcox $k-\omega$ turbulence model [103] is chosen. It provides reliable representation of turbulence in the boundary layers for a range of Reynolds numbers typical for aircraft engines. As confirmed by Gier et al. [30] and Henke et al. [36] it provides reliable prediction with respect to Low Pressure Turbines including cavities. The setup includes also few other extensions, in particular, the turbulence model is extended with correction from Kato and Launder [61] to account for turbulent kinetic energy production at the stagnation points. In CFX, due to the solver is used for parametric studies only, the Shear Stress Transport turbulence model [59] is applied as suggested by Szymanski et al. [94].

Low Reynolds approach with proper models for transition modeling are applied on the airfoil walls. Accurate prediction of transition is essential for the proper prediction of LPT performance. Since the flow in a Low Pressure Turbines is significantly influenced by laminar to turbulent transition, the multi-mode transition model by Kozulovic [49] is applied. In the cavities a fully turbulent flow regime is expected, thus, transition is neglected there. In CFX, the $\gamma-Re_{\theta}$ transition model is applied [7].

Boundary conditions

The researched Low Pressure Turbine is simulated at its design point. At the inlet of the CFD model of the turbine, boundary conditions measured in the test rig are specified. Radial distributions of total pressure, total temperature, turbulence quantities as well as velocity angles

are specified there. At the outlet static pressure is set and radial equilibrium is assumed. Both inlet and outlet are non-reflecting. Boundary conditions imposed at walls are shown in the Figure 3.5. All walls are assumed adiabatic.

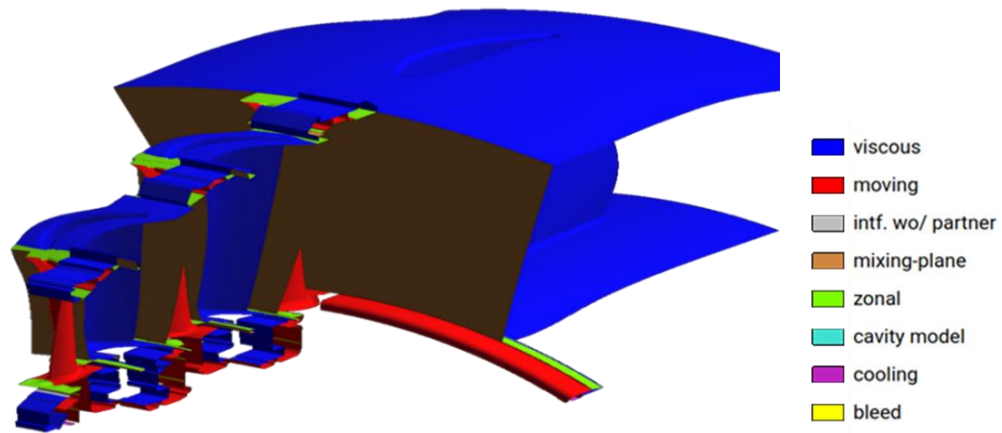


Figure 3.5 CFD model and TRACE Boundary Conditions of the reference LPT

For steady simulations, particular rows in the mainstream are connected in the typical way applied for turbomachinery i.e. with mixing planes. This way enables connection of vanes and blades with different speeds and pitches defined in the flow domains. Where necessary, also in the cavities, mixing planes between stationary and rotating domains are specified. Special zonal interfaces, described by Yang [109], are applied and used for connection of the cavities and the mainstream. The approach is visible in the Figure 3.7. The interfaces transfer numerical information at both sides, modeling inflow or outflow. To provide proper connection of both, at the interfaces, grids are adjusted to provide a very similar resolution at both sides.

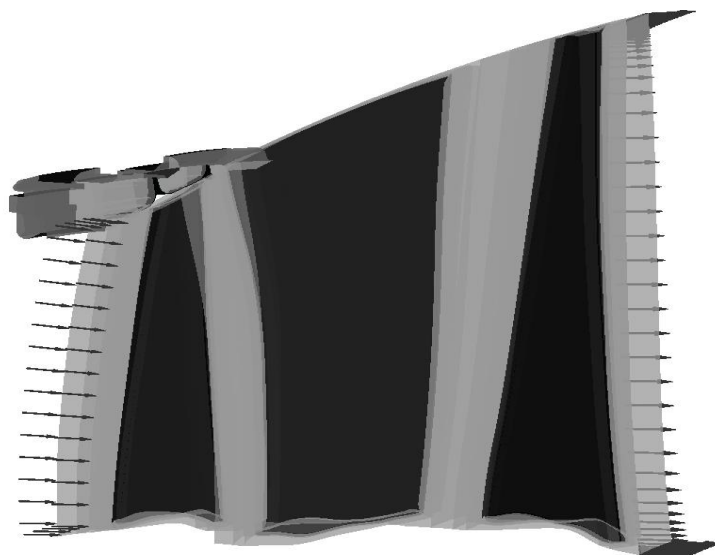


Figure 3.6 CFD model of 1.5-stage part of the baseline LPT in CFX

CFX is used only for parametric sensitivity studies. Due to that, only a 1.5-stage part of the researched turbine is analyzed. The 1.5-stage configuration consists of rotor, subsequent vane

and next rotor. This approach allows simulation of the cavity leakage and its impact on the subsequent rows. The subsequent rotor is modeled to enable uninhibited formation of the flow structures at the vane. The described computational domain is presented in the Figure 3.6. At inlet and outlet are imposed radial profiles extracted from the full turbine simulations. The boundary conditions at walls correspond to the one used in TRACE, shown in the Figure 3.5.

In both solvers, the working fluid is modeled as an ideal gas with Prandtl number of 0.72. The dynamic viscosity is modeled according to the Sutherland's law with temperature dependency.

Convergence

The simulations are accepted as converged under several conditions. In both solvers, for steady-state analyses, mass flow, pressure ratio and efficiency are monitored for the whole system as well as for individual rows at a certain interval. Additionally, the behavior of averaged flow quantities at all interfaces is monitored, to confirm that the solution is stable. The global and maximal residuals are monitored as well. The global residuals are accepted below $1e-5$. The simulations are stopped if all above criteria are fulfilled.

3.3.2. CFD modeling of Front Deflector

Front Deflector is one of the solutions for improvement of LPT OAS, developed in the frames of herein doctoral research. A detailed description of the concept is a subject of Chapter 6. The modification is applied in Outer Air Seals at all stages of the reference LPT. The solution in several configurations is modeled and analyzed applying CFD. The modeling approach is presented in the Figure 3.7. The fluid control domain of the cavity including surrounding the feature and the OAS cavity walls is modeled and appended to the main gas path with zonal interfaces. The setup applied for the modified cases is corresponding to this used in the reference turbine.

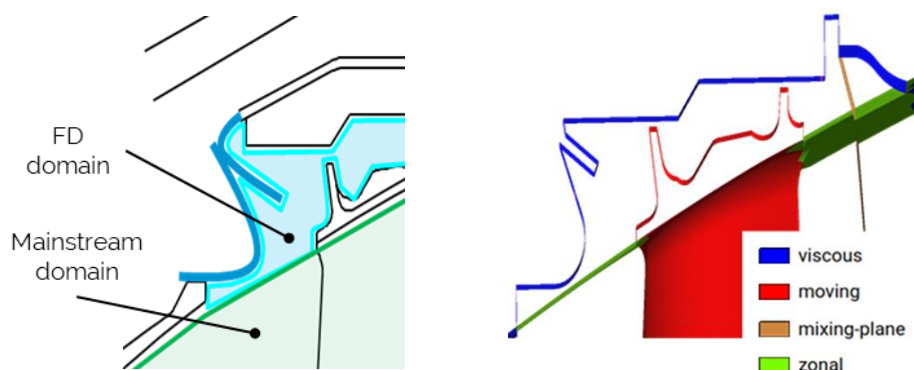


Figure 3.7 CFD modeling of the Front Deflector

Figure 3.8. presents meshes for different configurations of the Front Deflector. The grids reflect baseline cavity, reduction of the front cavity volume without static fin and Front Deflector with

the static fin. The changes to the mesh are kept at the minimum level – only front part of the cavity is modified. In particular, number of cells at the interface is the same for all configurations and a region in a vicinity of the blade fin is already unchanged. Small refinement is necessary in the vicinity of the static fin, but it is considered acceptable. Mesh criteria for the modifications are also considered acceptable.

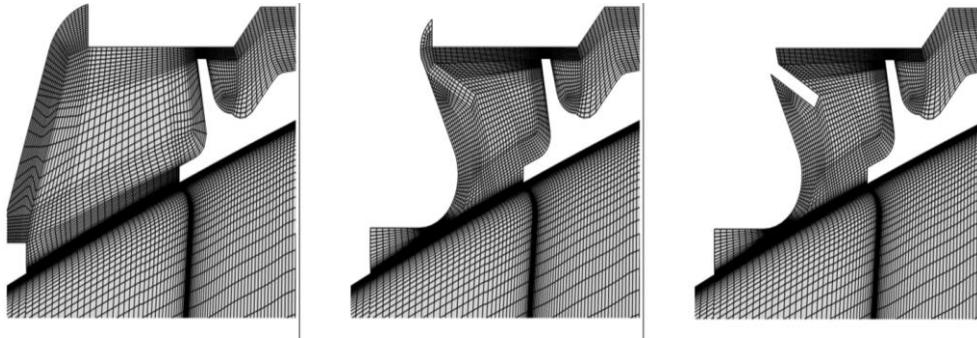


Figure 3.8 Comparison of the meshes for different Front Deflector configurations. From the left: reference cavity, Front Deflector without static fin and Front Deflector with static fin.

The setup applied for Front Deflector cases is the same as for the reference turbine. Boundary conditions particularly for the modification are visualized in the Figure 3.7.

3.3.3. CFD modeling of Vane Bleed Holes

Vane Bleed Holes is the second concept developed in the frames of the herein doctorate. It is also modification of Outer Air Seal, but applied in the rear part of the cavity. A detailed description of the concept is a subject of Chapter 6.

The VBH solution can be applied in two out of three Outer Air Seals of the reference 3-stage LPT. Application of this modification in the OAS of last blade does not bring any benefit to the LPT performance. It is because the outflow from the last cavity is already beyond the turbine rotor; further downstream is only exhaust, where work extraction does not take place, hence application of VBH there is redundant.

VBH geometry

Multiple geometrical configurations of the solution are researched and modeled using CFD. The variations of the VBH researched in the herein thesis are pictured in the Figure 3.9. The geometrical parametric study addresses variations in VBH inlet and outlet, extension of the feature in axial and radial directions as well as its inclination in circumferential and radial directions. For simplicity, for the parametric studies, fillets at the corners are skipped.

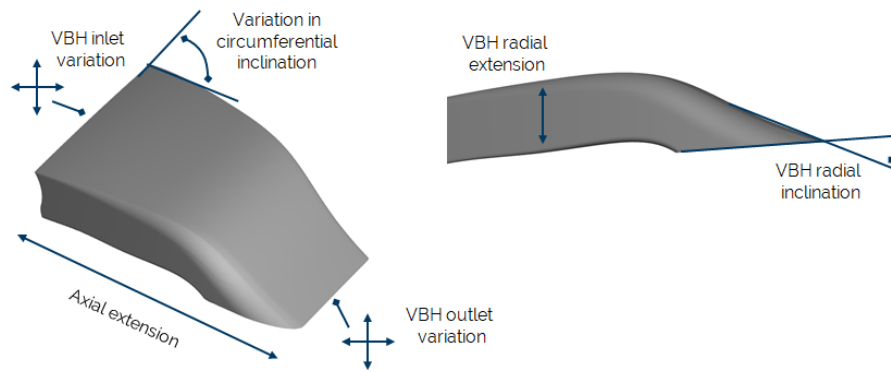


Figure 3.9 VBH channel geometry and its researched variations

VBH domain discretization

VBH channel is meshed separately and appended to the researched LPT domain with the same procedure as applied in case of the cavities. Several kinds of the VBH grids are used for investigations, depending on the purpose. Both, hexahedral and tetrahedral meshes, are used. Hexahedral meshes are proven to be more robust, involve less computational resources and provide better quality results, simultaneously requiring considerably more preparation time. Tetrahedral meshes, on the other hand, can be generated very quickly on the sake of solution quality. Due to this reason, tetrahedral meshes are applied in the parametric study for different geometrical variations of the VBH channel. With increased effort in grid preparation, hexahedral meshes are used for determining final efficiency benefit from the solution. Different applied grids are visualized in the Figure 3.10.

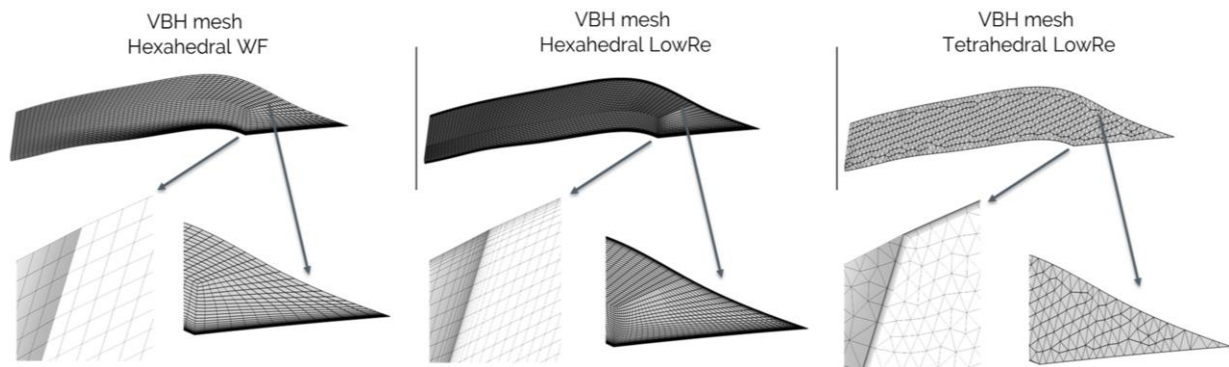


Figure 3.10 Different types of VBH channel meshes used for analyses

Hexahedral meshes are prepared for resolving boundary layer with LowRe approach as well as with coarser resolution at walls for application of Wall Functions. The most reliable results for the flow through VBH are considered to be obtained with hexahedral mesh and LowRe resolution at walls, thus it is considered reference. In case of tetrahedral grids, boundary layer is also resolved. It is modeled with prism layer of 11 layers, being a result of the mesh sensitivity study. For the cases with LowRe approach, averaged dimensionless wall distance y^+ is around 1, allowing proper resolution of the boundary layers. In cases of Wall Functions typically it is

around 30. To provide proper connection of the grids at the interfaces, providing very similar grid resolution at both sides of the connection. Grids applying LowRe resolution consist of around 400,000 nodes, in case of hexahedral mesh with Wall Functions, it is around 80,000 nodes. Tetrahedral meshes of the VBH channel have typically around 550,000 nodes. The quality of the meshes is considered acceptable, following mesh criteria suggested in [38].

The VBH is simulated with all mentioned grids on a 1.5-stage part of the reference turbine. As visible in the Figure 3.11, a sensitivity to different mesh type is small. The variation in the VBH mass flow on the significantly coarser mesh applying Wall Functions is less than 2%. Very small impact is also visible on the efficiency gain for the whole analyzed 1.5-stage part of the LPT, between configurations it is less than 0.01%. It indicates that grids applying Wall Functions as well as tetrahedral meshes can be used with only minor modeling error. It is also considered that the parametric study for different geometrical variations can be performed with tetrahedral grids.

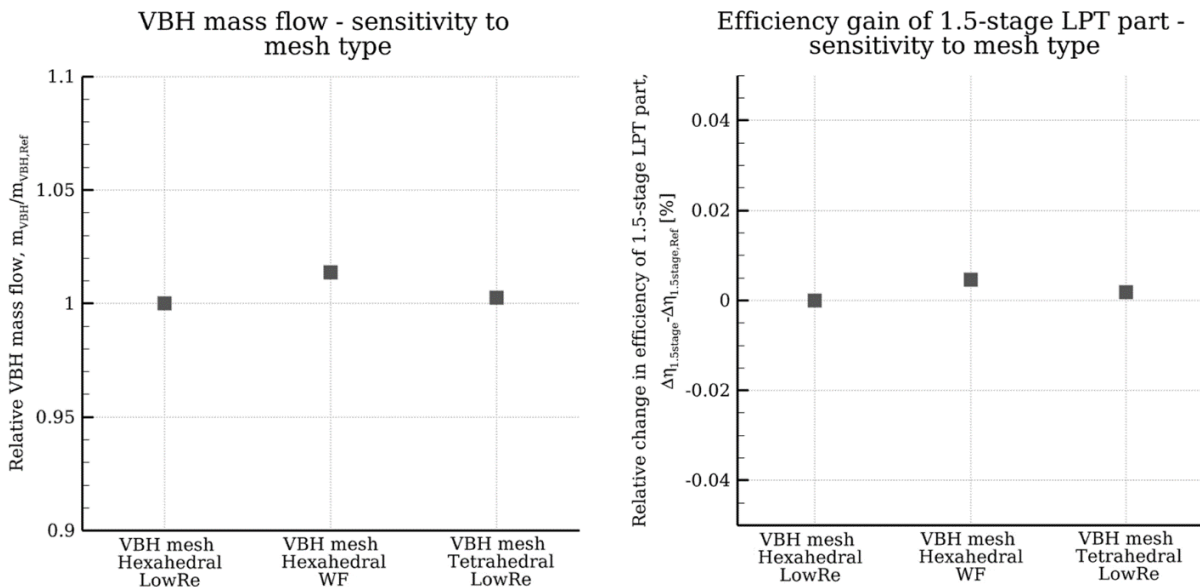


Figure 3.11 Impact of different VBH mesh types on mass flow and efficiency gain of 1.5-stage LPT part

In addition, an extensive mesh sensitivity studies in both solvers have been carried out. These analyses also confirm that the VBH is not sensitive to the mesh changes. That is due to a fact that VBH is a channel flow. The OAS leakage flow transferred through VBH is considerably turbulent. Due to that, the boundary layer stays mainly fully turbulent and it can be fairly modeled with all types of investigated meshes.

VBH modeling

Several modeling approaches are applied for simulating VBH. For preliminary analyses, a simplified VBH model is set up. The approach assumes modeling of VBH only by mass outlet (VBH inlet) and mass inlet (VBH outlet) boundary conditions as shown in the Figure 3.12. It

needs to be highlighted that there is no loss model implemented between both boundary conditions. There are several advantages of such modeling. Primarily, the feature is not meshed what saves time, effort and computational resources. Simultaneously, it allows isolation of particular factors influencing VBH performance.

These kinds of boundary conditions allow variations with respect several quantities. Mass flow inlet condition presumes mass flow, circumferential and radial velocity angles, total temperature, turbulence quantities as well as variation the panel area. Mass flow outlet boundary condition requires only definition of the outflowing mass flow and panel area. All those quantities can be specifically imposed as the boundary conditions for the solver. This is beneficial in gathering trends even in conditions that are uneasy to be modeled with actual geometry. In addition, if the simplified model is well correlated with the detailed one, it can successfully represent the feature without detailed 3D modeling in the machine.

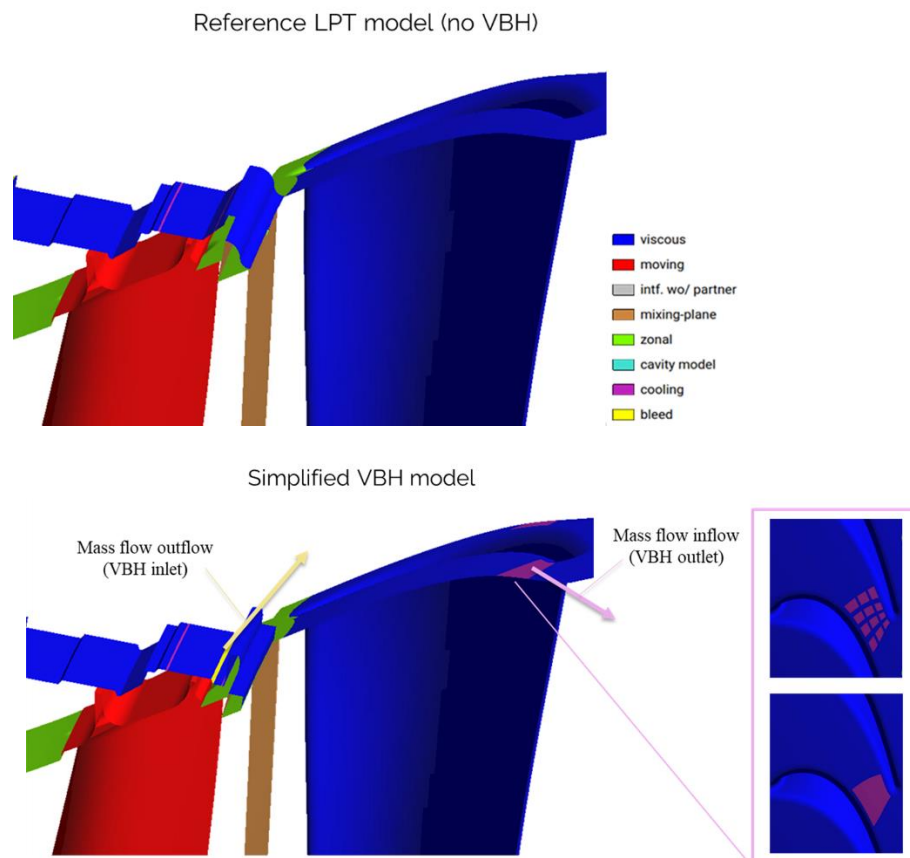


Figure 3.12 Simplified modeling of VBH with mass outlet and mass intake.

The VBH configuration can be arranged with single mass outflow boundary condition panel or several smaller panels, imitating case with several holes. It is visualized in the Figure 3.12. The investigations show no primary difference between two approaches, provided that the total area is the same. It is because the model is not able to capture differences between the configurations. Due to that, for efficient modeling and simplicity, the mass outflow boundary condition is modeled only by single panel with particularly defined conditions throughout all studies.

The simplified VBH model incorporates certain assumptions (e.g. does not include loss model between VBH inlet and outlet) that impact assessment of the VBH performance and considerably influence efficiency benefit. This implicates need for detailed 3D modeling of the channel. The detailed VBH model is applied on full 3-stage researched LPT model as well as on the 1.5-stage part of this machine, shown in the Figure 3.13.

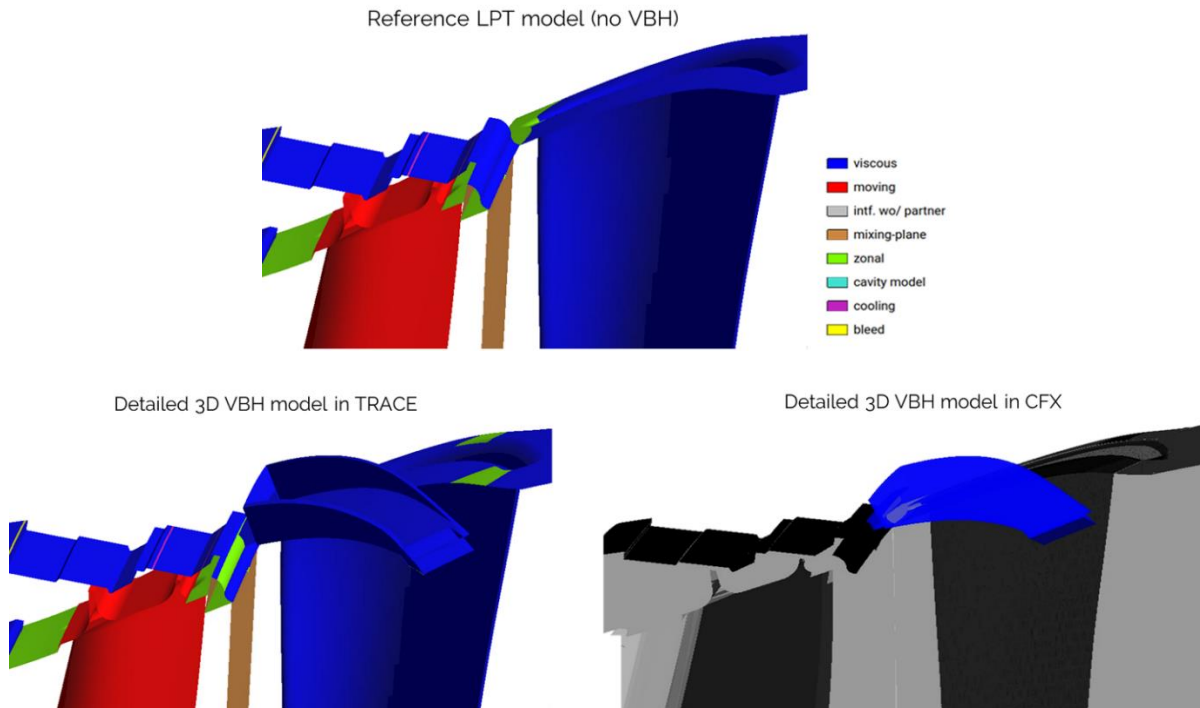


Figure 3.13 Detailed modeling of VBH in TRACE and CFX.

In case of modeling of actual VBH channel geometry, the VBH fluid domain is modeled in three-dimensions. Subsequently, it is appended to the mainstream with the interfaces, similarly as the cavities in the reference turbine model. In this way, the flow through the VBH channel as well as its impact on the LPT are resolved.

3.4. Methods used for assessment of LPT performance improvement

One way to improve the efficiency of turbomachinery is to reduce aerodynamic losses. The term loss is commonly used in turbomachinery applications. Fundamentally, it characterizes how much fluid energy exchange is affected by irreversibility, i.e. creation of entropy. There are several metrics for evaluation of losses. In the context of turbomachines, often a reduction in stagnation pressure is referred, because this quantity is measurable. There are also other definitions based on the enthalpy or kinetic energy of the fluid [15]. Nevertheless, the reduction in the losses is reflected anyhow in the efficiency of the machine. It is a very convenient way of

determination improvement in the machine performance, because it covers complete improvement in terms of the energy exchange. A typical definition of efficiency e.g. cited in [61] is used in herein dissertation. It is given by the eq. 3-3.

$$\eta = \eta_{is} = \frac{h_{out} - h_{in}}{h_{out,is} - h_{in}} \quad \text{eq. 3-3}$$

The isentropic efficiency is defined with a difference in specific enthalpy h at the inlet and outlet of the control volume of the considered thermodynamic cycle and referred to the enthalpy difference of the isentropic cycle.

CFD modeling enables also other ways of quantification of the loss generation. Main contributors of the loss generation processes are mean viscous dissipation and turbulence dissipation, referred frequently as Turbulent Kinetic Energy (TKE) production as indicated e.g. by Leggett et al. [53]. Dissipation of the viscous strain depends on the time mean flow, TKE production depends on instantaneous fluctuating velocity. In herein thesis, analyzing the improvements introduced by the developed modifications of the Outer Air Seals, due to convenient availability, TKE is found a useful indicator for the losses generation. Nevertheless, the overall improvement is judged by the increase of the LPT efficiency.

This page intentionally left blank.

Chapter 4. Validation of the applied CFD methods

Proper aerodynamic operation and benefits from the developed OAS solutions are determined with use of CFD. One of the main benefits of CFD is that it enables design by means of numerical experiments and analyses and gives good insight into the flow phenomena occurring in the machine. Nevertheless, CFD stays only a model of reality and it includes certain simplifications. As indicated by Denton [16], the importance of the experiment in fluid mechanics cannot be underestimated. Thus, it is crucial to verify the reliability of the applied modeling with the test data in order to crosscheck if it correctly predicts phenomena of interest, trends and absolute values. Due to that, the applied CFD is compared and validated with the experimental data. An approach to validation of the CFD methods applied in herein thesis and confirmation of the proper prediction of performance of the new OAS concepts is given in the Figure 4.1.

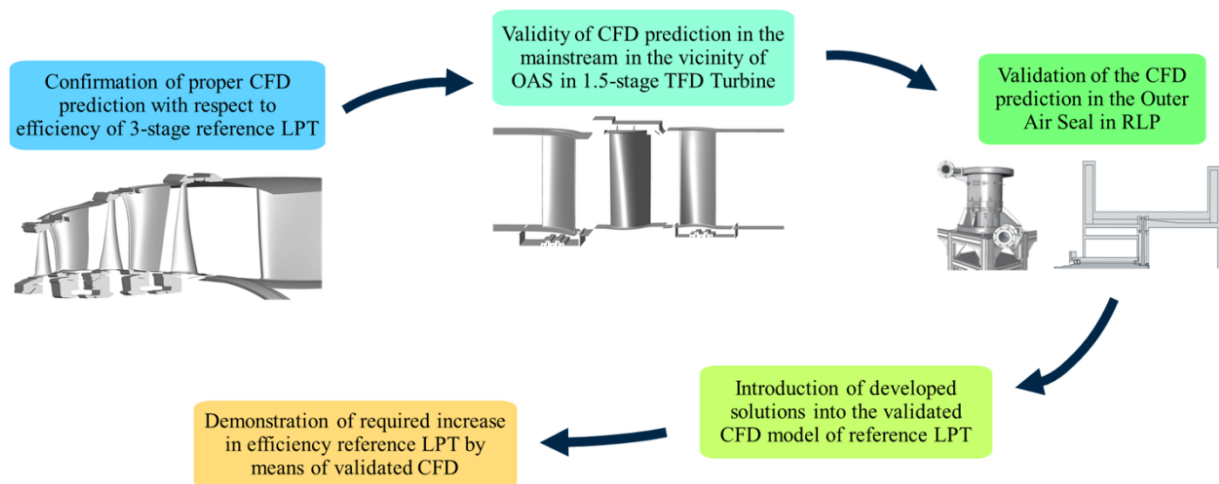


Figure 4.1 Approach for confirming increase in efficiency from developed solutions by validated CFD analyses of the reference LPT

Validation of the CFD prediction is nontrivial. Considerable level of complexity, difficulties in high quality measurements in multistage machines, accessibility of the instrumentation and its possible impact on the flow and the measurement results, to name a few, introduce additional uncertainties and impact direct comparison. These reasons imply validation of the particular regions and phenomena in smaller, dedicated test stands.

In herein thesis, validity of the applied CFD models is confirmed by:

1. Proper prediction of the LPT mainstream flow, in particular in the vicinity of the shroud
2. Reliable simulation of Outer Air Seals providing design capabilities for analyses of new solutions

The prediction of the efficiency level in the mainstream for the reference LPT is verified with the experimental data from the reference turbine testing at Stuttgart University. Next, appropriate simulation of the mainstream in the vicinity of the shroud and Outer Air Seal is additionally validated with 1.5-stage cylindrical LPT operated at Leibniz University Hannover. Flow through Outer Air Seals and setup reliability is confirmed by detailed measurements obtained with Rotating Labyrinth Test Rig (RLP), also operated at Leibniz University Hannover.

With abovementioned, it is assumed, the applied CFD method is valid for design and prediction of the flow in OAS and its impact on the LPT performance. Thus, on the delta basis, the efficiency benefit for the developed solutions can be demonstrated.

4.1. Validation of CFD prediction with respect to efficiency of the reference 3-stage LPT

Primary importance in the prediction of the performance of turbomachines has main gas path. The CFD setup applied for analyses of the reference LPT in herein dissertation is already validated for the prediction of the LPT in mainstream. The machine has been researched and measured at a high altitude test facility at Stuttgart University. The high quality measurements of total pressure, total temperature have been taken with probe traverses in front and behind turbine. It allowed calculation of the efficiency distribution over the turbine channel height, shown in the Figure 4.2.

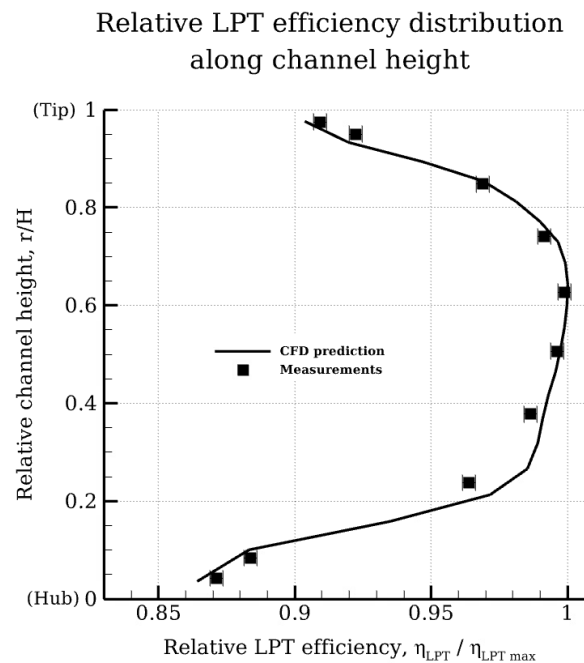


Figure 4.2 CFD prediction in comparison to experimental data of relative efficiency of the reference 3-stage LPT over relative channel height

As visible in the figure, CFD model of the researched turbine captures very well turbine efficiency with respect to the distribution as well as the values at particular locations. Even after passing all 3-stages, the flow in the LPT between its inlet and outlet is predicted fairly well. In majority of the locations, the efficiency is captured well within measurement uncertainty. In particular this is visible for the core stream and in the vicinity of the outer shroud, being crucial for research in the herein thesis. There is only one measurement location around 20% of the span where the prediction could be improved. Nonetheless, for the high aspect ratio airfoils, the flow in the inner region does not impact midstream and flow in the outer region, as confirmed e.g. by Moustapha et al. [61] or Henke et al. [36]. Due to that the region in the vicinity of the inner part of the channel is considered acceptable for purposes of research in herein thesis.

4.2. Validation of the flow in the vicinity of Outer Air Seal in the cylindrical 1.5-stage LPT

The measurements inside of highly complicated multistage engine-like turbomachines are very difficult. It is troublesome to obtain reliable data for the validation of the prediction, due to interactions between instrumentation and the flow. Thus, for reliable measurements, there is a need for research of simpler configurations in the dedicated test rigs, with better measurements capabilities. One of such LPT test stands is operated at TFD at Leibniz University Hannover. It is a cylindrical 1.5-stage LPT. Due to its design, the turbine has possibility of measurements even between the rows and in the cavities, providing very good insight into the flow field.

The turbine has been designed and researched thoroughly by Henke et al. [36]. Recently, it was applied for the validation for flows within and behind the Outer Air Seal [47]. The test stand is equipped with a selection of time-average and time-accurate instrumentation. The measuring equipment is designed with purpose of high quality measurements of turbomachinery. As Henke et al. [36] report, upstream and downstream of every airfoil, flow field quantities incl. total temperature, total pressure, Mach number and velocity angles are taken with five-hole probes. The probes are able to traverse in radial and circumferential directions. It is realized by simultaneous rotation of the vane rings, thanks to a special design of the rig. In this way, detailed measurements of the flow field over the passage up to full ring can be taken with very good resolution. The blading is equipped with steady and unsteady wall taps at several span locations especially in the vicinity of the shroud. The sensors measure airfoil loading of both stators and provide information about time-averaged and time-accurate static pressure. The flow behind the Outer Air Seal can be researched with miniaturized pneumatic four-hole probe, designed specifically for measurements in the vicinity of the shroud. Thanks to very small dimensions, it does not influence the flow significantly, as reported by Kluge et al. [46]. The traversing of the

probe is realized in the same way as in case of the probes at the inlet and outlet of the machine. An additional modification of the test stand allows monitoring of the radial clearances and PIV measurements in the front and rear parts of the outer cavity. Overall, the test stand is very well instrumented and gives good possibilities for detailed investigations of the flow field and validation of the CFD codes.

Figure 4.3 shows results obtained behind the rotating blade by Kluge et al. [47] for validation of the CFD prediction for Outer Air Seals. Researchers put focus only on the outer part of the channel, inner one was not instrumented in detail, thus the prediction there is not well researched. Additionally, the gray region in the direct vicinity of the endwalls, shown in the Figure 4.3, indicates region highly is associated with severe inaccuracies of the measurements due to the interactions with walls. In the Figure 4.3, it is clearly visible that CFD is in fairly good agreement with the measurements. The prediction for both total pressure and circumferential velocity angle follows the measured distribution correctly and is nearly within the measurement uncertainty. In particular measurements with miniaturized probe are closer to CFD prediction without instrumentation modeled. It indicates that the expected effect of interaction of the instrumentation is smaller and the measurements and CFD get closer.

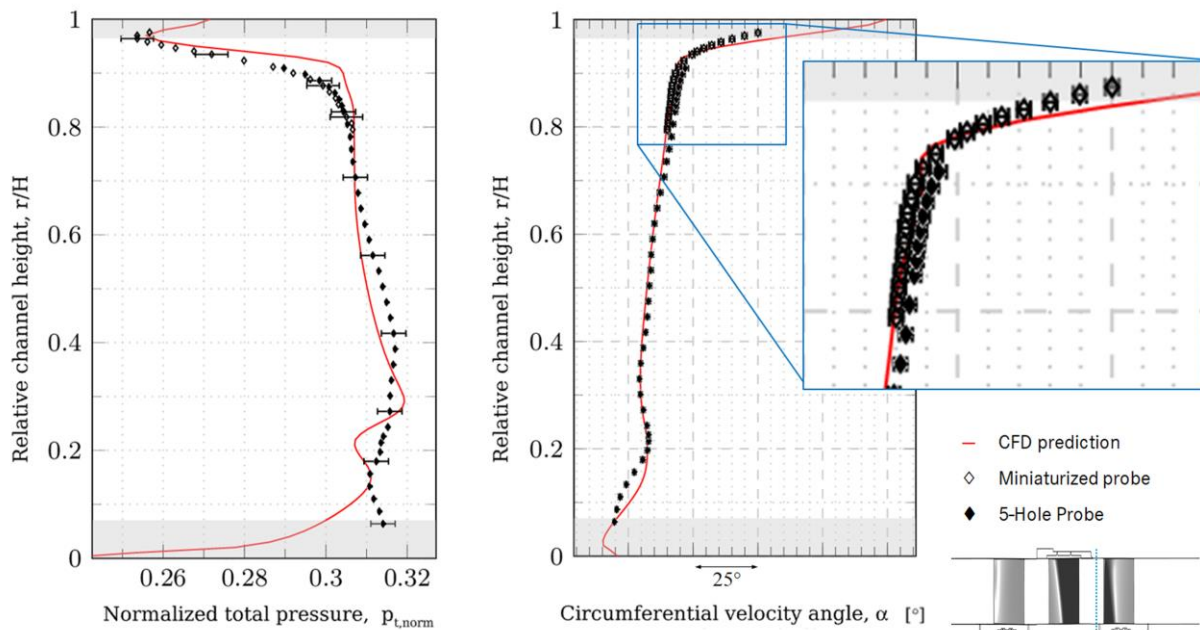


Figure 4.3 Circumferentially averaged profiles of normalized total pressure and circumferential velocity angle behind rotating blade and Outer Air Seal [47]

Proper numerical prediction of the flow at the casing is additionally confirmed with measurements of the second stator loading, presented in the Figure 4.4. The measurements are taken in several locations over the span in the outer shroud region. The results show very good matching within measurement uncertainty of the experimental data and numerical prediction including air seals. As shown in the Figure 4.4, the region close to the shroud is strongly influenced by the secondary flows including effects due to the OAS leakage. It is especially

visible comparing CFD prediction with and without cavities. The effect of the negative incidence from the OAS flow is noticeable across the airfoil span in the vicinity of the outer seal. This gets stronger towards the casing, where bigger deviations between both predictions are present. The measured static pressure profiles fit well to the prediction including OAS at nearly all locations. In particular, as reflected by the distributions at the leading edge, the changed incidence, due to the OAS leakage is captured accurately.

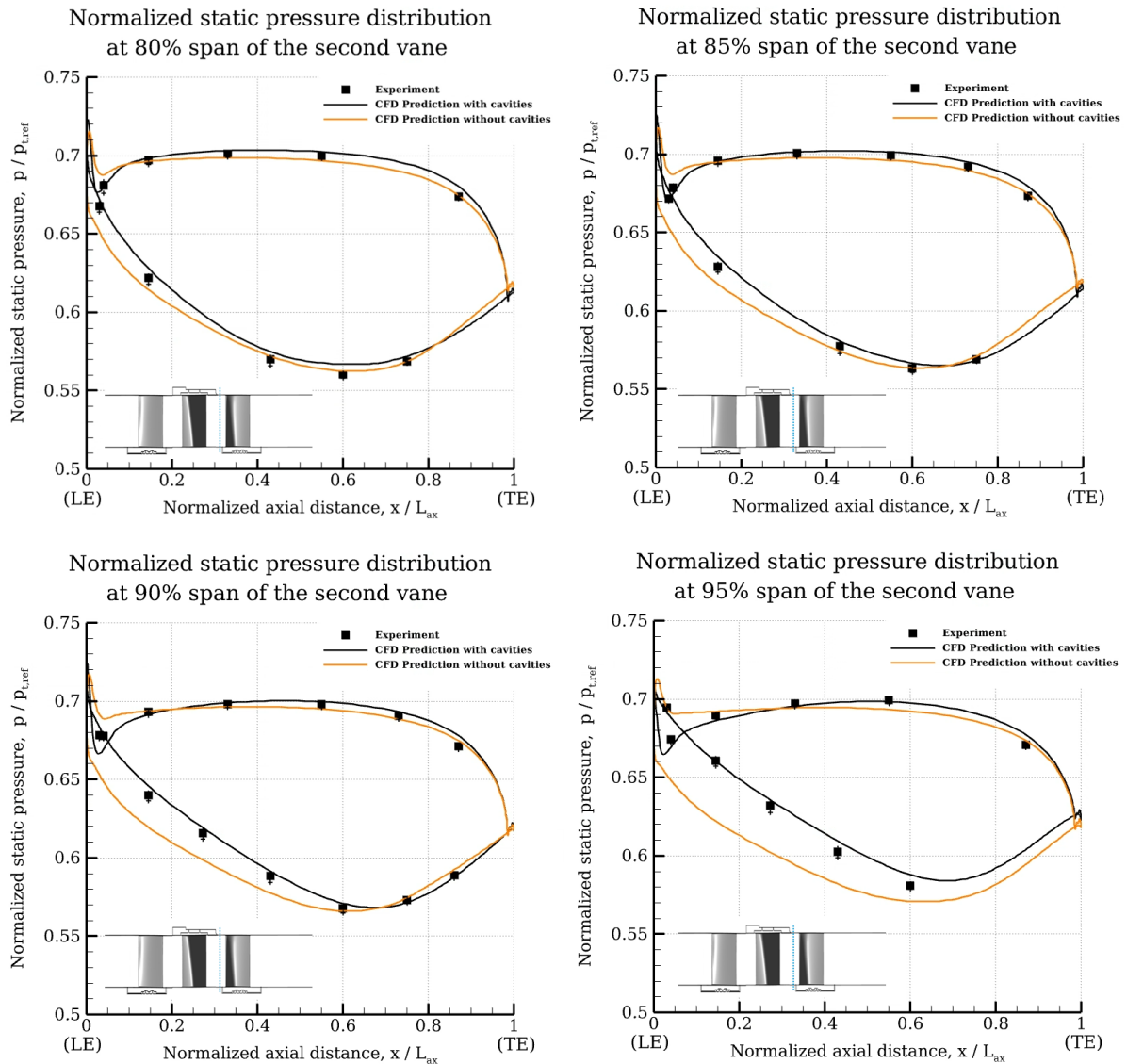


Figure 4.4 Airfoil loading at 80%, 85%, 90% and 95% span of the downstream stator [46]

Figure 4.5 shows circumferentially averaged profiles of the normalized total pressure and circumferential velocity angle downstream the LPT. The radial distributions confirm good agreement between test data and CFD prediction including cavities. Unsteady CFD simulations show marginally better prediction. Especially at mid-span, lower radial gradients are noticeable. It results from resolving in time domain without mixing planes. The prediction without cavities is visibly outstanding in the tip region with respect to both revised quantities.

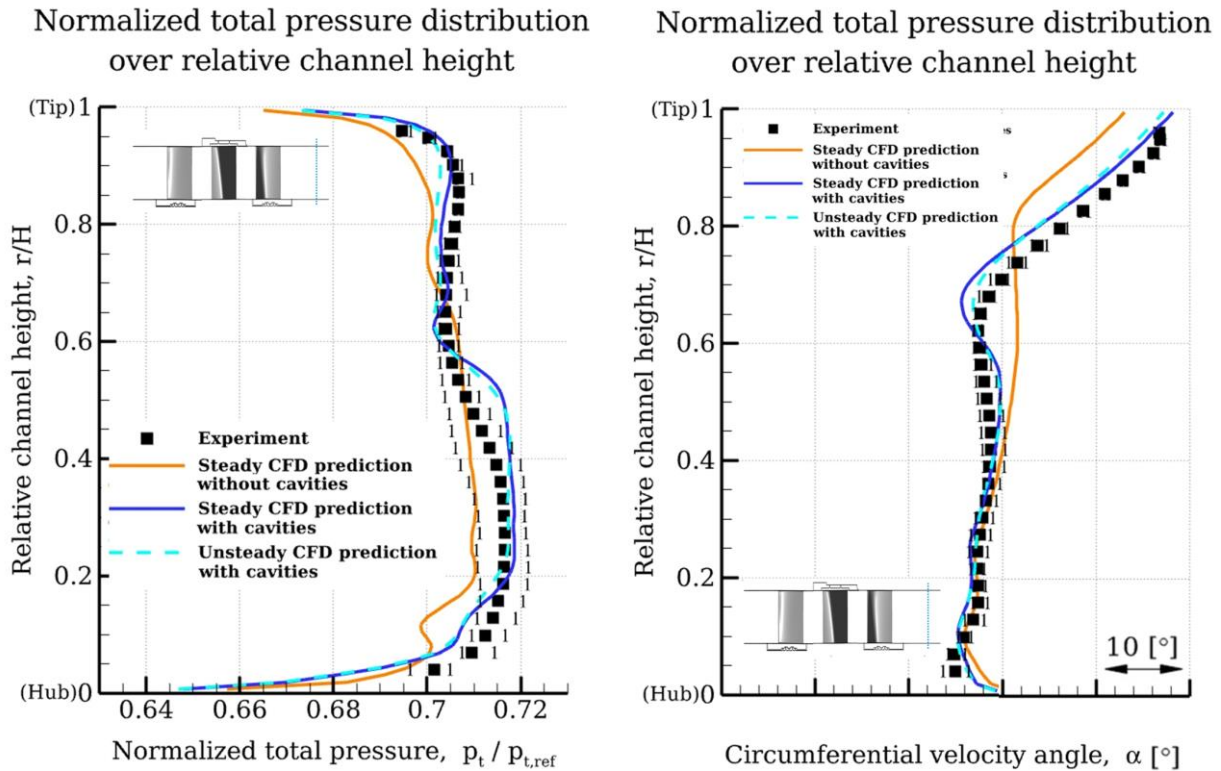


Figure 4.5 Normalized total pressure and circumferential velocity angle at LPT outlet [46]

Kluge et al. [46] indicate that there are some deviations visible only in two locations with respect to the distributions. The radial gradients in the central section are over-predicted and circumferential velocity angle in the region of outer diameter is radially shifted. Nevertheless, such small deviations are acceptable for purposes of herein thesis, due to the change in the machine performance is judged on the delta basis. Thus, it is considered that the prediction capabilities of the applied CFD setup are valid and provide proper prediction of the flow field inside LPT including OAS cavities.

4.3. Validation of the numerical prediction for Outer Air Seals in the Rotating Labyrinth Test rig

The validation of the numerical prediction with respect to the flow in the Outer Air Seals is carried out with special Rotating Labyrinth Seal rig (RLP). RLP is a specially designed rotating rig imitating only labyrinth seal without the mainstream. As indicated by Kluge et al. [48], the rig is particularly designed to allow experimental validation of numerical codes. The test campaigns have been performed at Leibniz University Hannover [46].

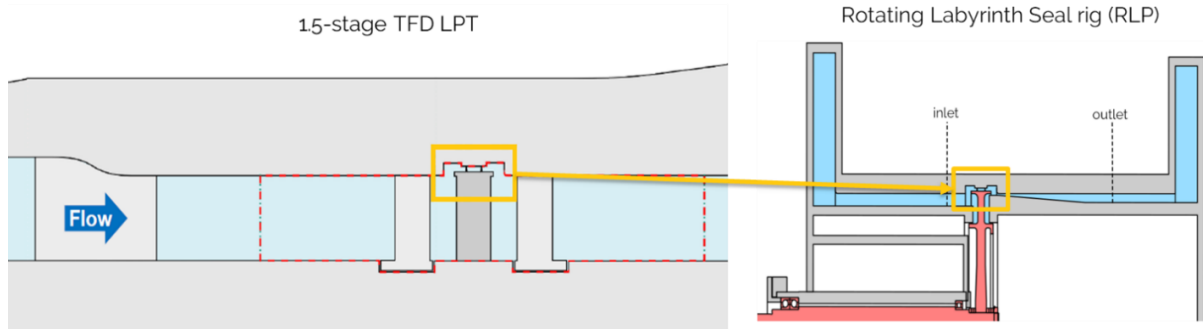


Figure 4.6 Transfer of Outer Air Seal geometry from 1.5-stage TFD turbine to the RLP [48]

The aerodynamic design of the RLP, shown in the Figure 4.6, is based on the 1.5-stage LPT researched by Henke et al. [36]. The geometry and flow conditions reflect those from the turbine. With the blade replaced by the rotating disc with the cavity. This procedure ensures that the conclusions can be transferred to the real engines with simultaneous separation of the cavity flow from the mainstream.

RLP composes of a channel and a straight-through labyrinth seal with two fins. It is one of the typically configurations used in all aircraft engines. The fins are mounted on a rotor as shown in the Figure 4.7. The CFD prediction capabilities are crosschecked with respect to two seal geometries met in practice – for labyrinth seal with the smooth wall and with the honeycomb structure. Both configurations are met in practice. Smooth walls e.g. in the cold engine rigs; honeycombs typically in the engine applications.

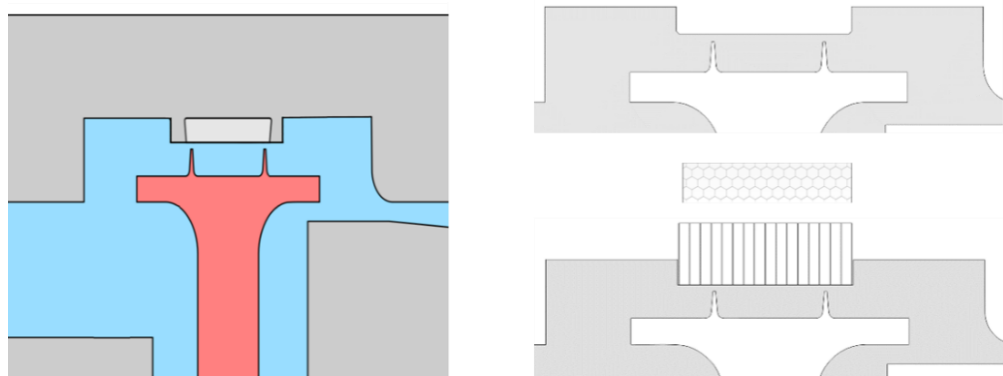


Figure 4.7 Seal geometries with smooth wall and honeycomb researched in RLP

4.3.1. Measurement setup of the RLP

High quality measurements and detailed insight into the flow field of the Outer Air Seals are possible with the RLP. In good detail, the instrumentation available at RLP is described by Kluge et al. [48]. Both geometrical configurations used for validation in herein thesis are measured with steady and unsteady instrumentation, in the configuration shown in the Figure 4.8. During

testing, integral quantities including mass flow, ambient conditions and rotational speed are gathered. Mass flow is measured both upstream and downstream of the test rig with thermal mass flow meter and calibrated Venturi nozzle. At the inlet and the outlet, total pressure, total temperature and velocity circumferential angles are measured with probes. Also turbulence intensity is obtained with constant temperature anemometry measurements. The measurements at the inlet and the outlet are taken in several radial positions at six equally distributed circumferential positions.

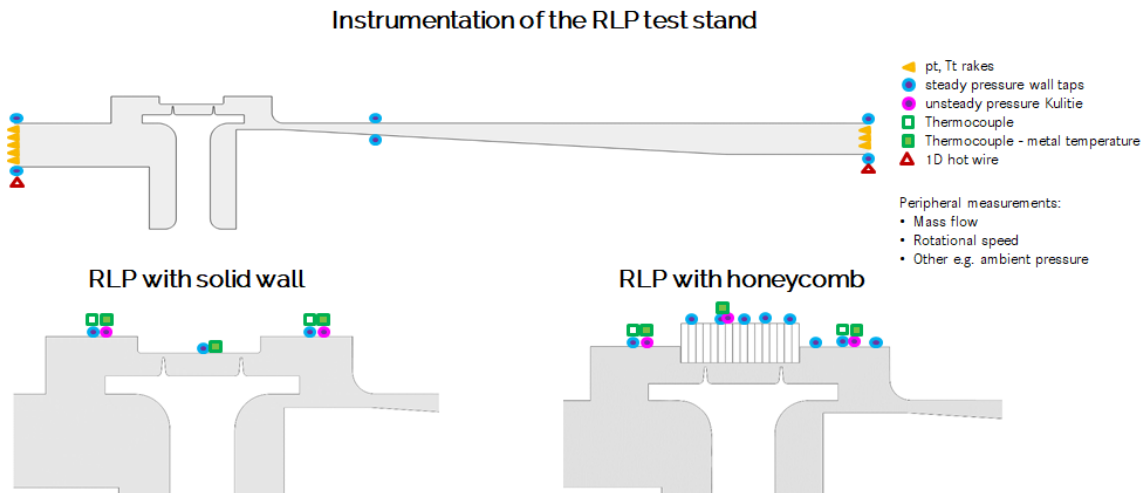


Figure 4.8 Primary instrumentation available at RLP

The casing is well instrumented with steady and unsteady static pressure and static temperature sensors. The number of sensors differs between configurations. It is six up to twelve axial positions. At every axial position the quantities are measured at six circumferential locations. In addition, advanced measurement techniques like stereoscopic particle image velocimetry (PIV) are available at RLP. More information about the design, instrumentation, sensitivities of the test stand and previous measurement campaigns are given by Kluge et al. [48], Oettinger et al. [66] and Wein [100] who researched RLP.

4.3.2. CFD model of RLP

For the validation of the CFD prediction for both geometrical configurations of Outer Air Seals, steady-state simulations of the rig are conducted. The applied setup is the same as the one used in the cavities simulated within LPT, described in the Chapter 3. At the inlet measured radial distributions of total pressure, total temperature, turbulent quantities and velocity angles are specified. At the outlet, static pressure measured at the walls is imposed. Boundary conditions at walls are shown in the Figure 4.9. For connecting honeycomb, a zonal interface is used.

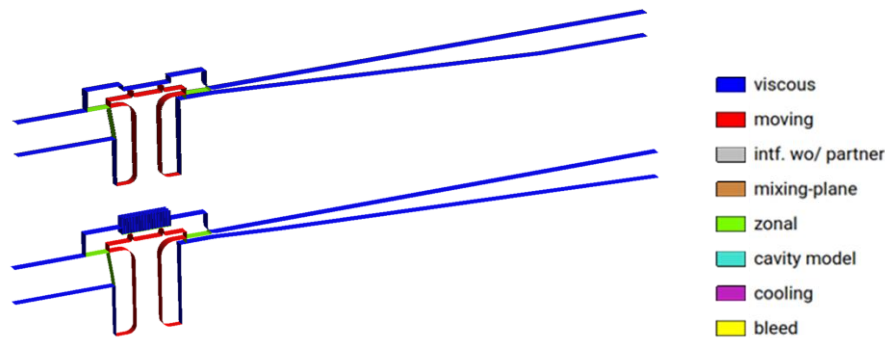


Figure 4.9 Boundary conditions applied to RLP with the smooth wall and the honeycomb

Several operating points are researched. The seal is tested and simulated at pressure ratios of 1.280, 1.152, 1.044 and rotational speeds 7000RPM, 3500RPM and 700RPM. The complete map for RLP is given by Kluge et al. [48]. The chosen cases are considered to be representative for research of the major flow phenomena.

Sensitivity of the cavity flow to the sector size

Kluge et al. [48], who designed and provided baseline research of the RLP, indicate uniform time-averaged flow at the inlet and the outlet of the rig. Researchers point out that a quasi-three-dimensional steady simulations of the rig already provide reliable prediction. To confirm that, three different RLP domain extensions in circumferential direction are compared: 1.5deg-sector, 60deg-sector and full 360deg ring. As visible in the Figure 4.10, indeed, the same mass flow through the seal is received with all. It confirms that the flow in the RLP is periodic. In addition, influence of unsteady phenomena on mass flow through the seal is compared and plotted in the Figure 4.10. As shown, the unsteadiness also does not impact the predicted mass flow. That is also confirmed in the experiments for both geometry cases, revising unsteady pressure measurements. Due to negligible sensitivity to the sector size and to the unsteady effects, the 1.5deg sector is used for further RLP analyses.

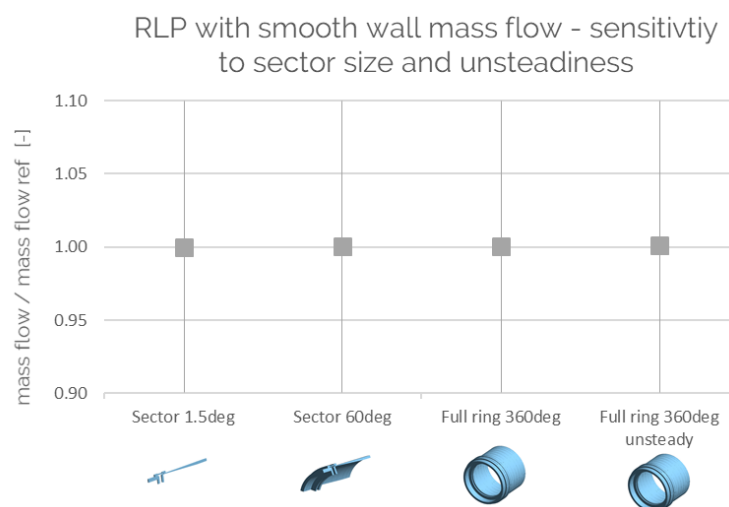


Figure 4.10 RLP with smooth wall – sensitivity to sector size and unsteadiness

Sensitivity of the cavity flow to mesh resolution

The mesh sensitivity studies for both researched RLP cases are carried out to investigate impact of the seal discretization on the prediction. In particular, two mesh types are investigated, one applying Wall Functions (WF) and second resolving boundary layer with Low Reynolds (LowRe) approach. Meshes for both geometrical configurations are pictured in the Figure 4.11. In particular, as presented, the honeycomb is meshed, to resolve flow there.

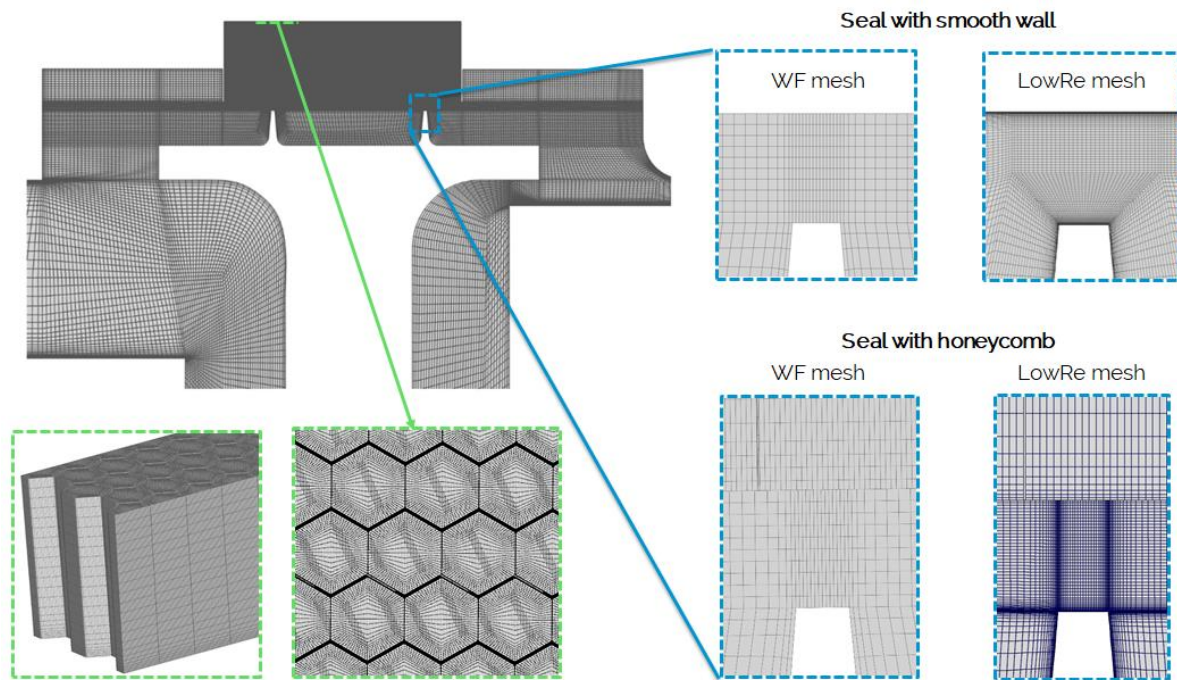


Figure 4.11 Different meshes applied for numerical analyses of RLP with smooth wall and honeycomb

For assessing the sensitivity to the mesh changes, it is isentropically refined several times in all directions. Also, LowRe mesh is prepared and compared with all other meshes. The prediction on LowRe grid is considered reference. The primarily monitored quantity is the mass flow through the seal. As described in the Chapter 2, it is a first order quantity that impacts the flow in seals. As visible in the Figure 4.12 and in the Figure 4.13 there is only small sensitivity to the mesh for the seal. For smooth wall configuration, mass flow predicted on the coarsest mesh with Wall Functions differs only by 2.3% from the reference mesh and only slightly more from the finest mesh with around 120 million cells. In addition, a well recognizable logarithmic trend with an increase in cells number is noticeable. The sensitivity to the mesh is even smaller in case of the seal with the honeycomb structure, plotted in the Figure 4.13. When the honeycomb mesh is considerably refined, the predicted mass flow differs only by 1.7% with respect to the reference mesh. A reason is seen in aeroacoustic phenomena in the honeycomb, because the honeycomb can act as a resonator. However, these phenomena are considered to be improperly resolved within the steady-state simulations that are carried out. Due to that, the baseline refinement of the honeycomb is kept throughout investigations.

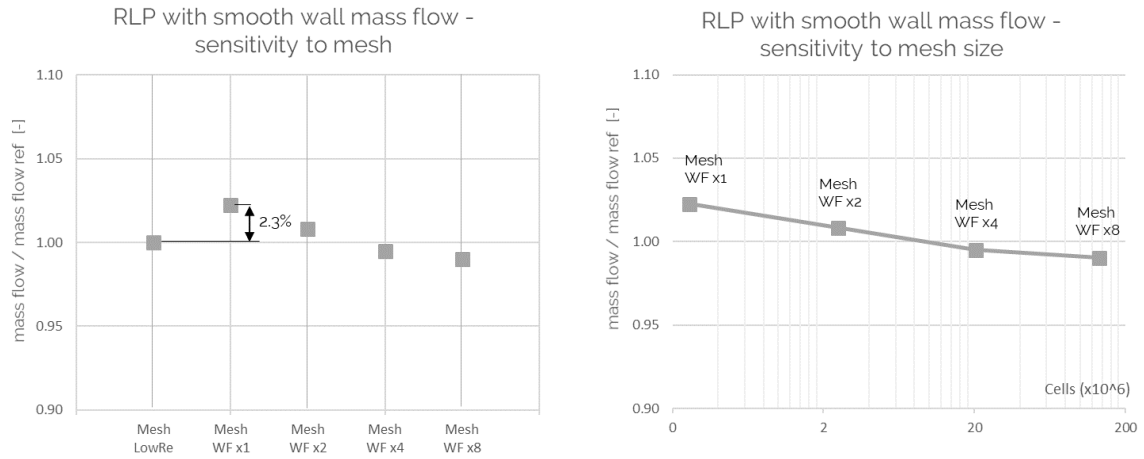


Figure 4.12 Sensitivity of the mass flow to the mesh of RLP with smooth wall

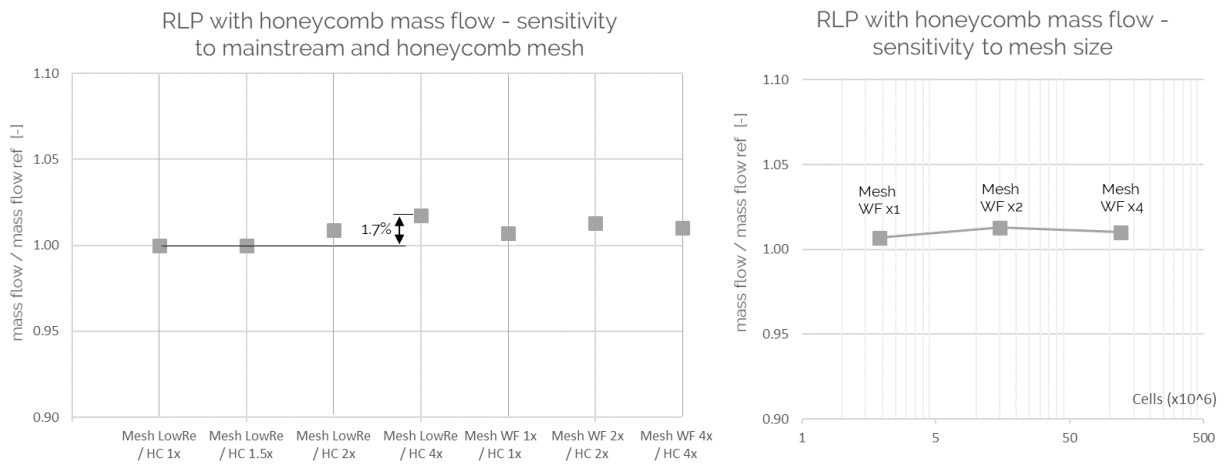


Figure 4.13 Sensitivity of the mass flow to the mesh of RLP with honeycomb

Figure 4.14 shows that overall, the leakage jet is predicted similarly with all meshes. Additionally, it indicates that the dependency on the mesh in the air seals is rather small. The mass flow through the labyrinth seal is mainly defined by a region above the fins. In this region the smallest cross-sectional area occurs. At the fins usually a separation bubble forms. As visible in the Figure 4.14, the smallest area, is decreased by the presence of the bubble. The effect is especially noticeable if the fins are sharp. For rounded fins a significance of the phenomenon decreases, as pointed by Rapisarda et al. [76], is smaller. The separation bubble is not resolved properly for the coarse resolution applying Wall Functions. In all other cases, the bubble is visible. Nevertheless, despite considerable refinement in the mesh, the mass flow stays on a very similar level. It has even much smaller meaning for the cases with the honeycomb, due to a fact that the region over the fins is open. The leakage penetrates honeycomb cells and the limiting, smallest area, occurs in another location. Due to that resolving of the separation bubble has smaller significance.

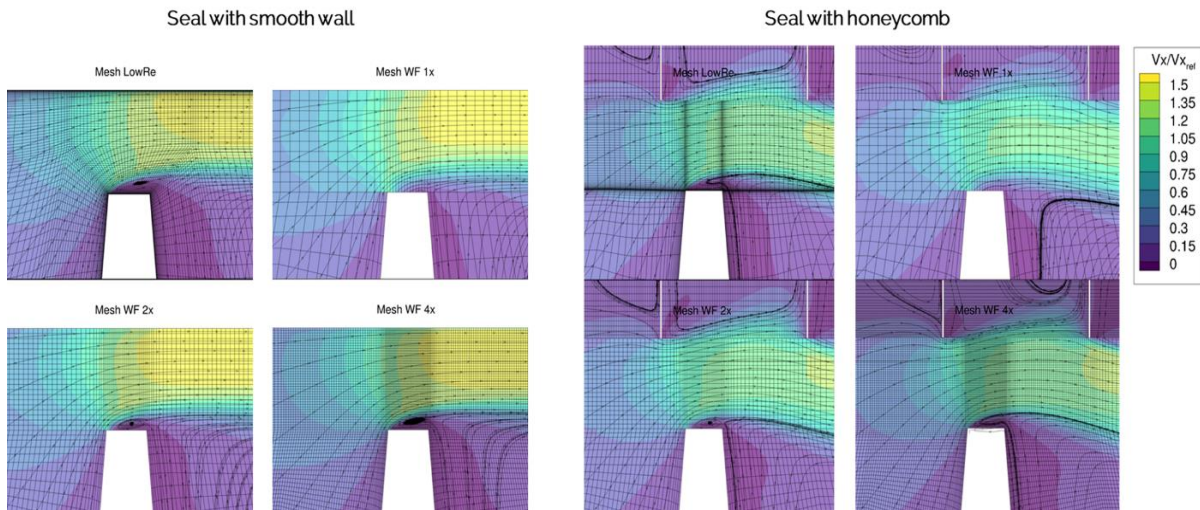


Figure 4.14 Cross-sectional view to the axial flow velocity at the first fin of RLP with smooth wall and honeycomb for different mesh refinements

The small mesh dependency in the labyrinth seals with honeycombs and with smooth walls is demonstrated by Kluge et al. [48] and Wein [100] who studied RLP. Authors additionally performed Grid Convergence Index studies proposed by Roache [79], indicating the same behavior.

4.3.3. Validation of the prediction for seals with smooth wall

Firstly, measurements taken in RLP are compared with the CFD prediction for the geometrical configuration with the smooth wall above the fins. Figure 4.15 provides comparison of the relative mass flow measured in RLP and resulting from the numerical analyses. As well visible in the figure, CFD well captures mass flow through the seal. For all operating points mass flow is predicted nearly within the measurement uncertainty. When resolving boundary layer, with LowRe mesh, the predicted mass flow is the closest to the measured values. However, also the mesh with Wall Function shows fairly good agreement with the test data. It confirms very good performance of the applied numerical setup for predicting flow through the OAS with solid wall above the fins. It is considered, that the labyrinth seals can be well predicted on both types of grids. Nevertheless, further results are analyzed only on the LowRe mesh.

Analyzing further Figure 4.15, it is apparent, that the mass flow with increasing pressure ratio also increases. This trend is well recognizable. It is in agreement with the reports of several researchers pointed out in the Chapter 2. e.g. by Denecke et al. [13]. The Figure 4.15 shows additionally the impact of the rotational speed on the mass flow through the seal for one of the pressure ratios. With the rotational speed increase, relative mass flow also slightly increases. This is in agreement of the trends investigated by Oettinger et al. [66]. It is confirmed, that the applied CFD setup captures these effects in terms of trends and absolute values.

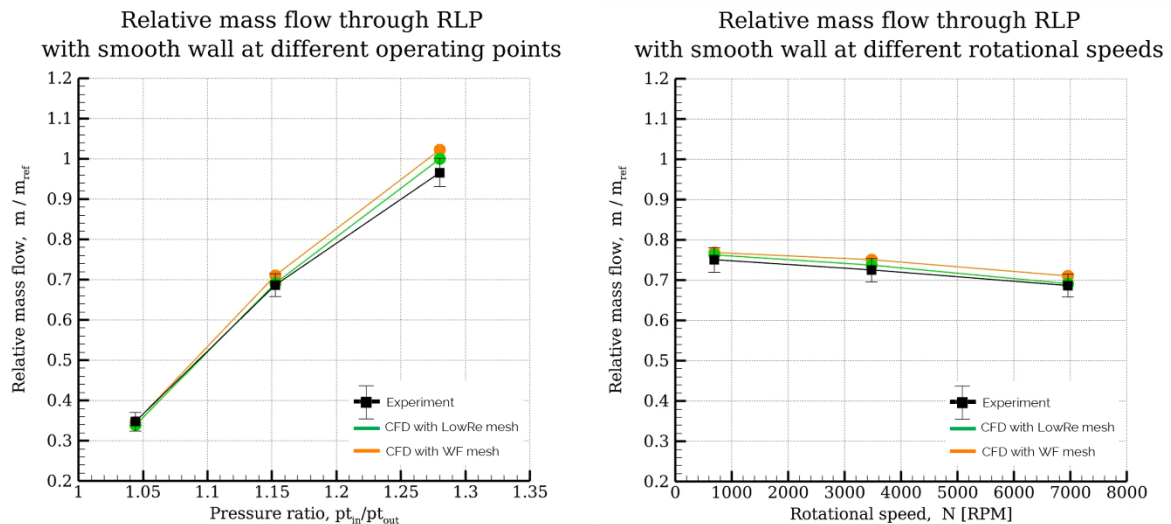


Figure 4.15 Relative mass flow with variation of pressure ratio and rotational speed in RLP with smooth wall above the fins

The maximum discrepancy between measured and predicted value is around 5% for the mesh with Wall Functions. It is nearly within uncertainty of the experimental data. Even this over-prediction is considered acceptable from the practical perspective of LPT applications. Other researchers of labyrinth seals indicated uncertainties on similar or even higher level e.g. [13], [92], [104].

In addition, the static pressure measured at the casing is compared between CFD and experiment. The distribution of this quantity along the RLP is shown in the Figure 4.16. As visible in the Figure 4.16, for all operating points, static pressure is very reliably predicted by CFD at all locations. Small differences appear only for the operating point with the smallest pressure ratio in the location between the fins and in the rear chamber. This could arise from imprecisely reflected radial clearances e.g. due to imbalance and other factors, as pointed out by Wein [100]. Nevertheless, the differences are considered marginal for the practical applications. Static pressure distribution in the Figure 4.16 provides also an insight into the impact of the rotational speed. With speed increase, at the first fin the pressure drop is smaller. On the other hand, with pressure ratio increase, visible is bigger contribution of the first fin to the sealing. Lastly, the circumferentially averaged profiles at the outlet are revised. As well visible in the Figure 4.16, the profiles are also captured very well. Both, trends and absolute values at all locations are very well reflected within the measurement uncertainty.

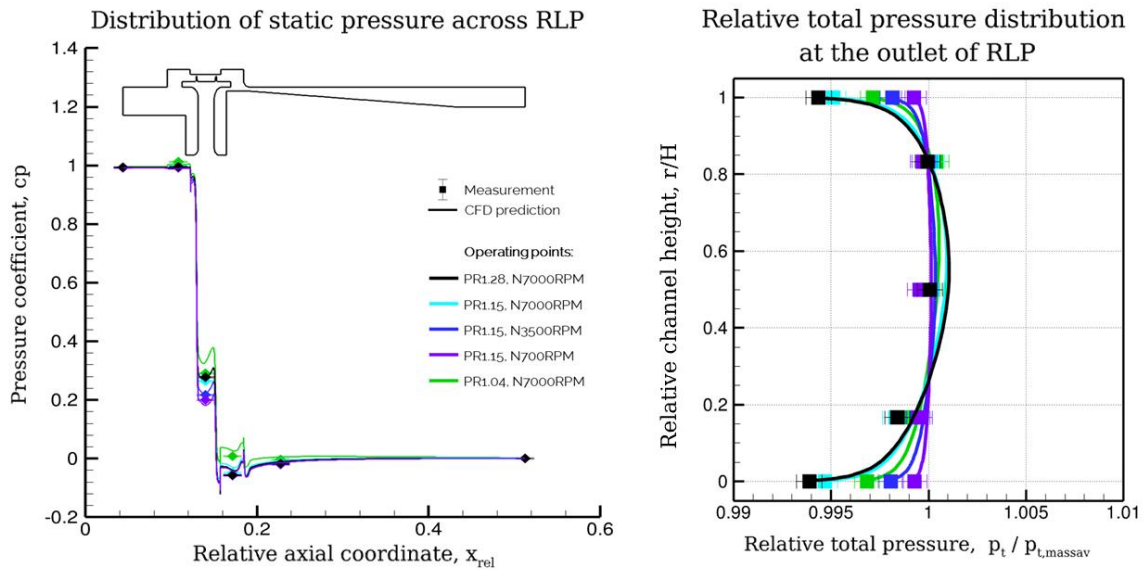


Figure 4.16 Distribution of the static pressure along and total pressure at the outlet of RLP with smooth wall above the fins

Summing up all findings for the configuration of the seals with the smooth wall, it is concluded that the applied CFD method is capable of predicting changes in the performance of OAS, providing design capabilities of these regions.

4.3.4. Validation of the prediction for seal with honeycomb

Similarly, the second OAS geometry case with the honeycomb is investigated. In a similar way, the results the tests with honeycomb above fins are analyzed and put together with CFD. Figure 4.17 depicts comparison of the relative mass flow measured and predicted for RLP. For the case with the honeycomb, the mass flow is predicted even closer to the experimentally gathered values. In the contrary to the previous geometry, the results obtained on both meshes are nearly the same. The reason is already discussed in the previous section, analyzing sensitivity to the mesh. It is that the smallest cross-section limiting the mass flow through the seal, appears in another location than directly over the fin, due to the presence of honeycomb.

Similarly to the smooth wall configurations, as visible in the Figure 4.17, the mass flow increases with increasing pressure ratio. It is considered, that the labyrinth seals including honeycombs are predicted well with both types of grids. For better clarity of the pictures, only the results received with LowRe mesh are presented in the further figures.

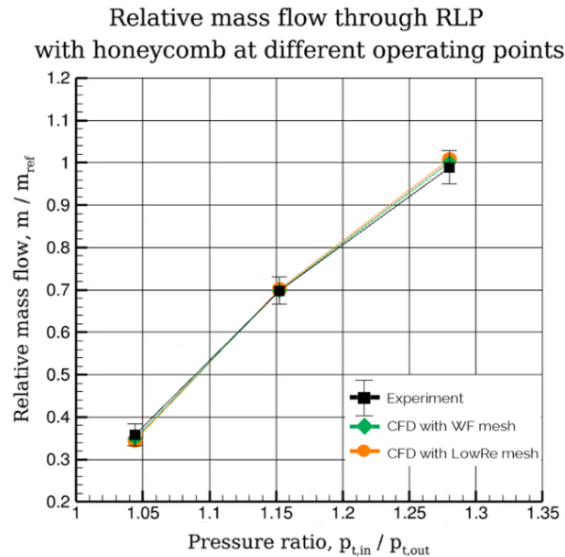


Figure 4.17 Relative mass flow with variation of pressure ratio and rotational speed in RLP with honeycomb above the fins

Subsequently, the static pressure measured at the casing along RLP is shown in the Figure 4.18. As visible, for all operating points static pressure is captured perfectly with the measurement uncertainty at all locations. It is also true for the circumferentially averaged profiles at the outlet. The total pressure is in very good agreement with the test data. Both trends and absolute levels at all locations are very well reflected.

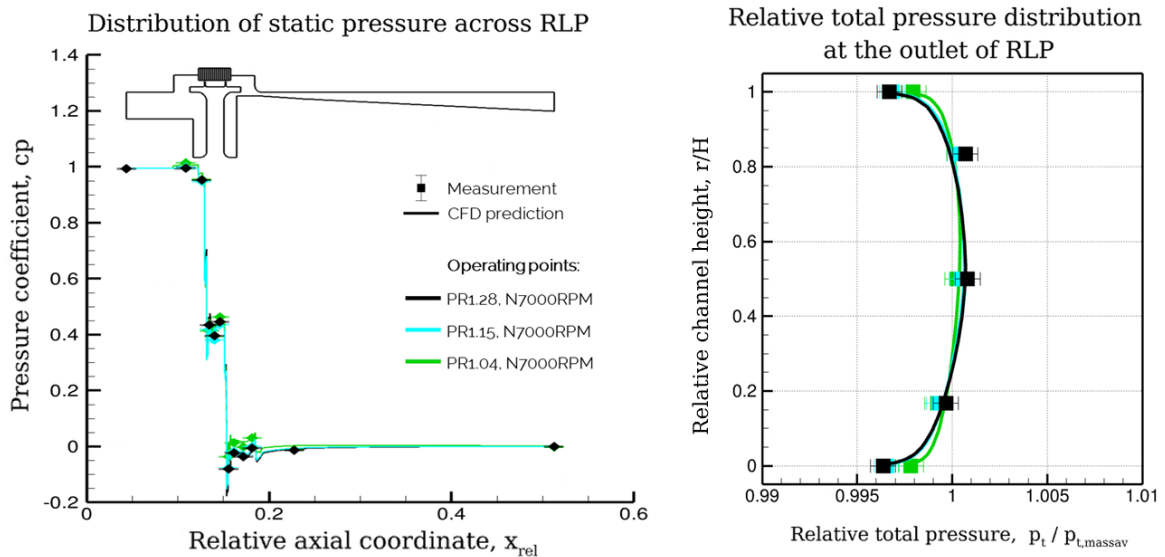


Figure 4.18 Distribution of the static pressure along and total pressure at the outlet of RLP with honeycomb above the fins

This confirms very good prediction for OAS with the applied numerical setup. It is considered that it is possible to quantify changes in the investigated turbine performance by means of efficiency introduced by modifications of the OAS having impact on the mainstream.

This page intentionally left blank.

Chapter 5. New insights into flow phenomena associated with LPT OAS

5.1. Primary ways for improvements of the losses associated with LPT OAS

Prime importance for operation and performance of the Outer Air Seal has leakage mass flow. The leakage bypasses the blade not contributing to the work extraction. Thus, it is an immediate loss for the performance of a turbine. The leakage is inevitable consequence of the gap existing between rotating and non-rotating parts of the machine and pressure ratio across the blade. The aerodynamic design of LPT is not focused on minimization of the pressure ratio – it is actually opposite. Thus, it is not a way for reduction of the OAS leakage. For given operating parameters of a turbine, in this consideration meaning a given total pressure level and its ratio across the seal, the leakage can be reduced primarily by reduction of the minimum cross-sectional area. Usually, it occurs in the vicinity of a blade fin and an abradable material.

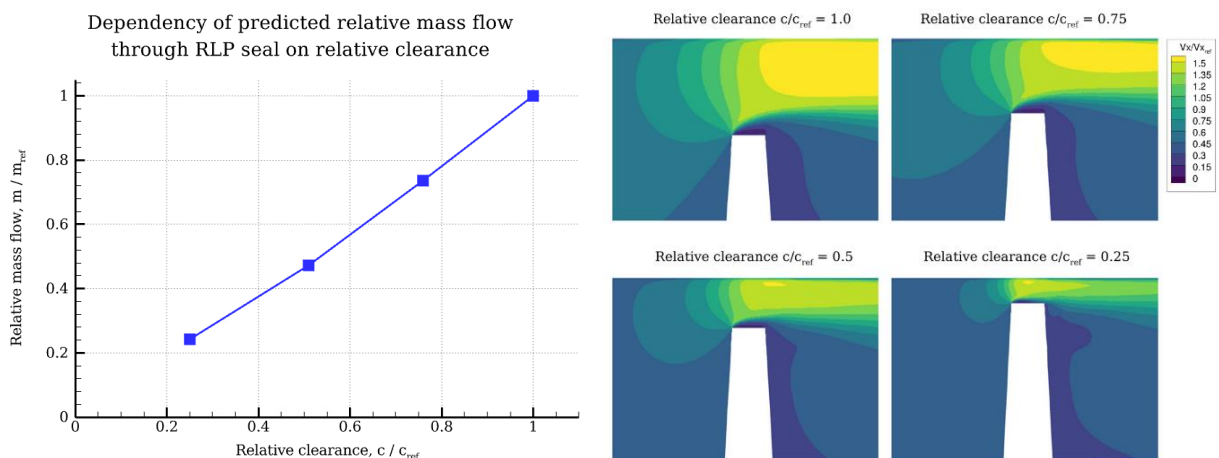


Figure 5.1 Dependency of relative mass flow and relative axial velocity on radial clearance at OAS

A change in the leakage amount together with the flow field at the fin are presented in the Figure 5.1. The figure shows linear trend of leakage mass flow decrease with decrease of the radial clearance, what is directly significant for LPT performance. Due to that, one of developments in Low Pressure Turbines is integration of ACC systems into the LPT design. The primary idea behind is to actively decrease clearance during the steady-state engine operation at the design point of the machine. Taking into account the actual variation in the clearance, it appears very convenient to actively change the running clearance, during engine operation. Due to that this

system, keeping radial at very small level, needs be accounted as state-of-the-art for nowadays and future LPT.

The leakage can be also additionally reduced by higher pressure losses across the air seal. All kinds of stagnation points or additional labyrinths, creating an obstacle for the flow, reduce the leakage and thus enhance sealing performance.

Nevertheless, even for highly effective ACC systems, there must be a gap between rotating and non-rotating parts of the turbine. Thus, the OAS leakage is inevitable. Beside bypass effect, presence of the leakage is associated with secondary phenomena, in particular with mixing behind the seal. The mixing losses are smaller, if reintroduced leakage mass flow gets smaller. Thus, reduction of the leakage mass flow has primary importance, because simultaneously bypass and mixing losses are improved. Mixing losses are also smaller if velocities and temperatures of both flows are similar. The latter cannot be influence. With respect to the first quantities, a typical flow situation in the vicinity of the OAS is visualized in the Figure 5.2 and Figure 5.3.

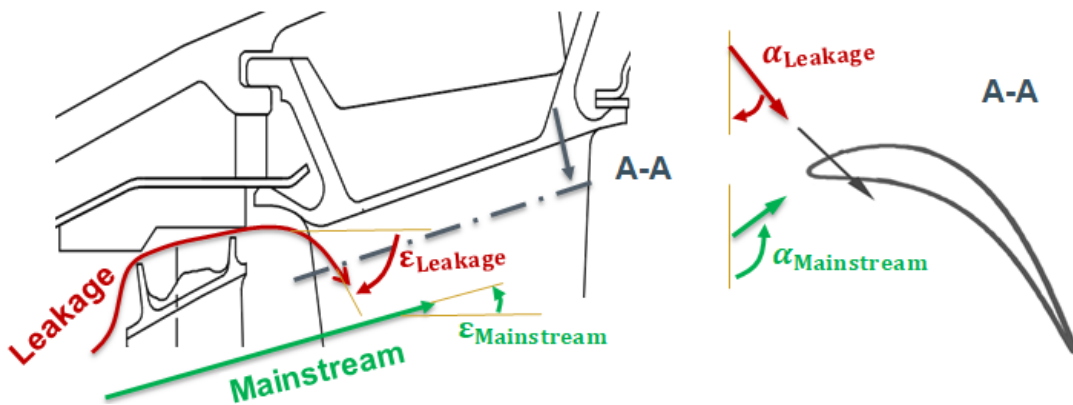


Figure 5.2 Schematic visualization of the flow at outer channel of LPT.

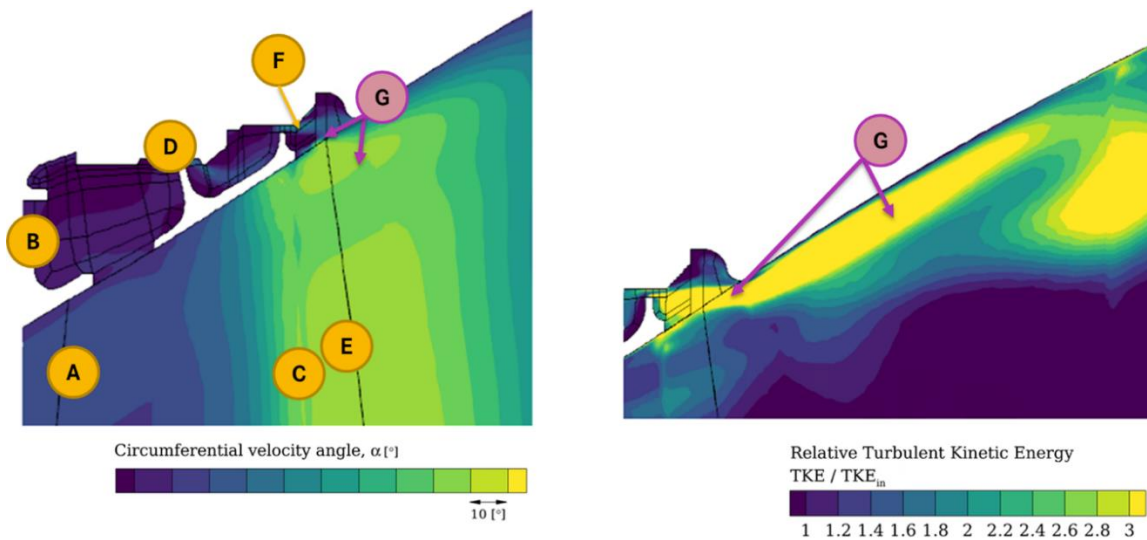


Figure 5.3 Mixing in the vicinity of LPT OAS with marked flow features described in the Table 5-1

The OAS leakage is reintroduced to the mainstream behind the seal. As visible in the Figure 5.2, velocity angles of the LPT mainstream and OAS leakage are very different. The differences in both radial and circumferential directions are significant and may reach even above 100°, depending on geometrical constraints, flow situation and leakage amount. Primarily, that is because the mainstream flow experiences turning at the blade in contrary to the leakage bypassing the rotor. A detailed description of this mechanism is given in the Table 5-1 and pictured in the Figure 5.3.

Table 5-1 Flow situation and sources of mixing losses at LPT OAS. Letter markings as in the Figure 5.3.

| Main stream | | OAS cavity | |
|--|--|-------------------|---|
| A | The mainstream flow is guided by foregoing vane, providing proper inflow to the rotor | B | In the front part of OAS cavity flow angle in circumferential direction is similar to mainstream |
| C | On the rotor flow experiences turning | D | OAS leakage is turned only in little amount at the fins by viscous forces |
| E | Behind the blade the circumferential velocity angle in absolute frame is considerably high | F | In the rear part of OAS cavity, leakage has similar direction as in the front chamber of the seal |
| G Significant difference between OAS and mainstream flows leads to high mixing losses | | | |

Another source of losses due to OAS presence are interactions between cavity geometry and mainstream. These losses need to be differentiated from the losses inside the air seal, between the fins. The cavity internal losses between the fins contribute to smaller leakage, thus higher sealing performance. The vortices in the front and rear parts of the OAS cavity are source of disturbances of the mainstream, negatively influencing turbine performance. Figure 5.4 shows different cases of reductions in the volume of OAS cavity. Decreasing front chamber, a considerable reduction of the vortex circulating there is possible. As reflected in the contours in the Figure 5.4, it is positive for turbine performance. However, reduction of the rear chamber to minimum has reverse effect, due to steeper inflow of the leakage into the mainstream. This leads to separations at the shroud and increased losses. Due to that, the rear cavity should be rather properly shaped, than decreased to very minimum, as visible in the last case, presented in the Figure 5.4.

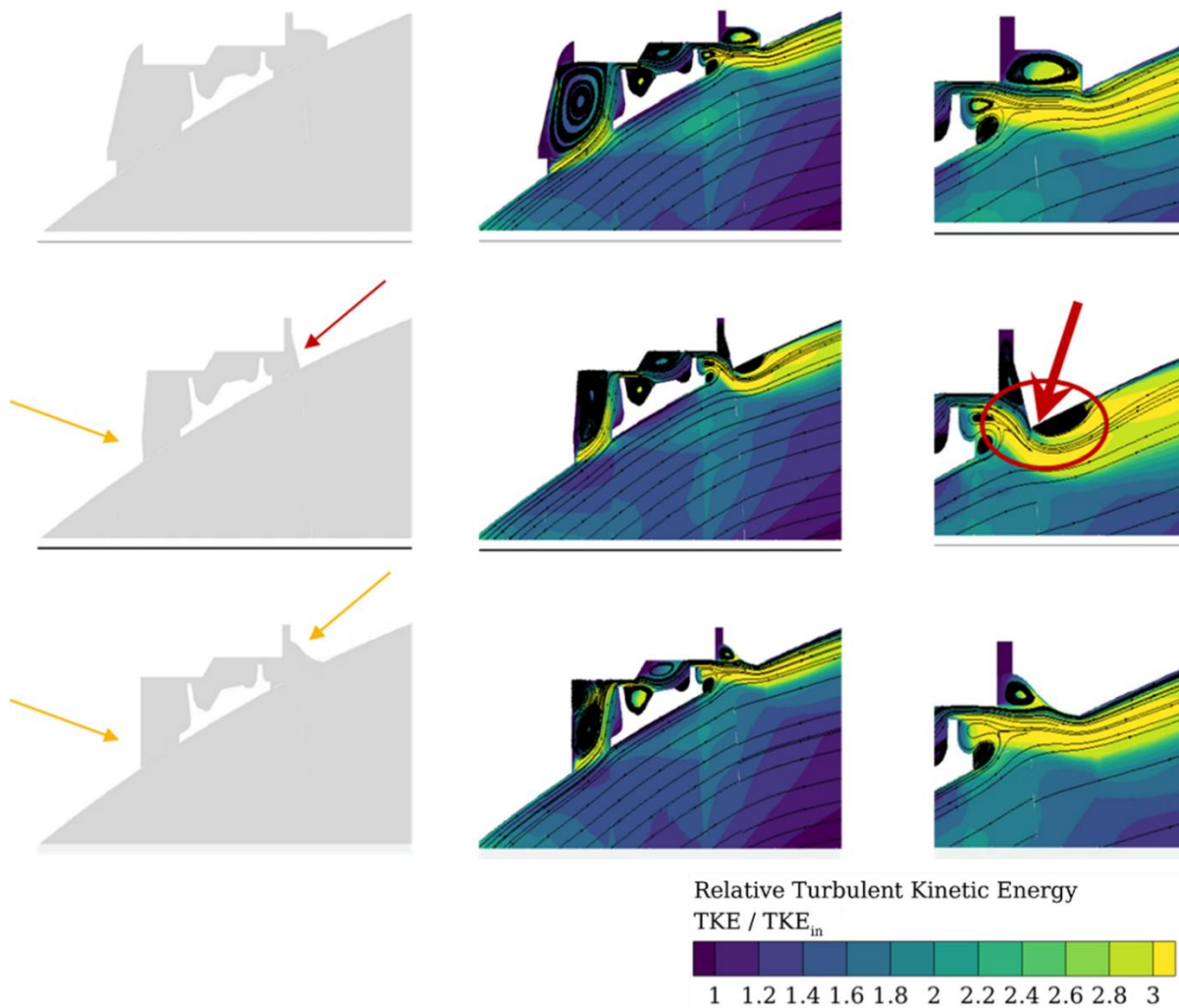


Figure 5.4 Impact of interactions between mainstream and front and rear parts of OAS cavity

To conclude, any possible reductions in the leakage that are positive for LPT performance. The improvements in this field should be focused on increasing pressure losses across the seal by additional labyrinths or stagnation points, because state-of-the-art ACC for LPT provide already very tight running clearances. The mixing behind the OAS poses the second field for improvements. The improvements in this field should be focused on aligning OAS leakage and mainstream flows. It is beneficial to decrease front cavity volume to minimum and advised to avoid steep reintroduction at the rear cavity part.

5.2. Flow through OAS in terms of characteristic quantities

The flow within Outer Air Seals, can be described in terms of the characteristic, similarity numbers. As elaborated in the Chapter 3. there are several benefits from application of the

similarity theory - it allows proper modeling, comparison to reality and facilitates understanding of the laws governing the flow phenomena. To study the dependencies between characteristic numbers and their impact on OAS flow characteristics, an independent CFD study on standalone seal is carried out. The parametric analyses are carried out on a model of typical stepped LPT Outer Air Seal with smooth wall. It is confirmed by Zimmermann and Wolff [110] and Yan et al. [107], that the influence of honeycomb can be superimposed to the general behavior of the seal. Thus, the honeycomb itself is not modeled, to keep the model simple. The complete description of the test cases and applied setup is described by Palkus and Strzelczyk [70].

5.2.1. Dimensional Analysis of Outer Air Seals

While reviewing a physical phenomenon with Dimensional Analysis, firstly quantities essentially influencing phenomena are determined. Quantities identified meaningful for Outer Air Seals are pictured in the Figure 5.5 and listed in the Table 5-2. Next, every dependent parameter is evaluated in terms of unit system variables, referred as independent quantities. It is performed applying Buckingham theorem and power law, as described in the Chapter 3. Complete procedure is elaborated by Palkus and Strzelczyk [70].

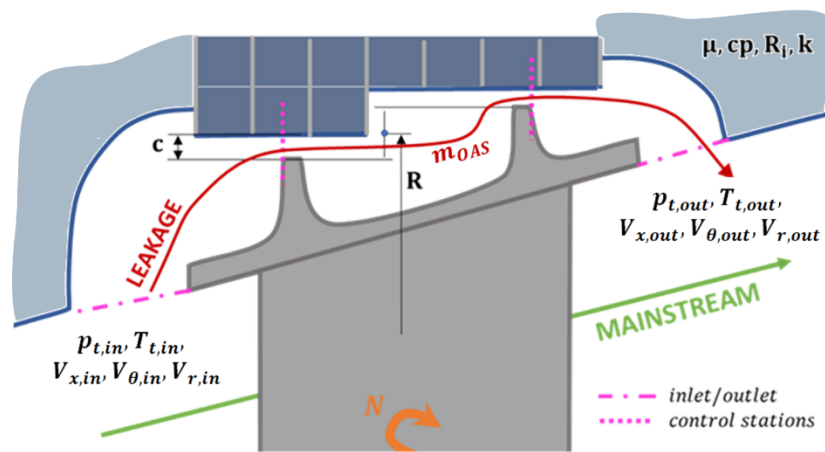


Figure 5.5 Quantities meaningful for flow through Outer Air Seals [70]

Table 5-2 Selection of the quantities applied for Dimensional Analysis of OAS

| | |
|--|--|
| Quantities considered meaningful for OAS | $c, R, N, a, R_i, \mu, p_{t,in}, p_{t,out}, T_{t,in}, T_{t,out}, m_{OAS}, V_{\theta,in}, V_{\theta,out}, V_{r,in}, V_{r,out}, V_{x,in}, V_{x,out}$ |
| Base units | [s], [m], [kg], [K] |
| Chosen independent variables | $R, N, \mu, T_{t,in} \sim [m], [s^{-1}], [kg \cdot m^{-1} \cdot s^{-1}], [K]$ |
| Dependent variables | $c, a, R_i, p_{t,in}, p_{t,out}, T_{t,out}, m_{OAS}, V_{\theta,in}, V_{\theta,out}, V_{r,in}, V_{r,out}, V_{x,in}, V_{x,out}$ |

The procedure applied in terms of the Dimensional Analysis facilitates reduction of the parameters to a very minimum and simultaneously formulation of the characteristic numbers.

The complete analysis performed for OAS reveals that for the chosen independent variables, the most significant dimensionless numbers are: axial Reynolds number, describing mass flow through the seal; outlet swirl ratio, corresponding to the exit flow angle crucial for mixing; and windage heating, related to the internal losses. The relations between the similarity numbers, in a general form, are given by the eq. 5-1, as:

$$Re_{ax}, K_{out}, \sigma = f\left(\frac{c}{R}, M_{\theta}, \frac{p_{t,in}}{N\mu}, \pi, K_{in}\right) \quad \text{eq. 5-1}$$

As visible, application of the dimensional analysis considerably reduces number of analyzed variables. The identified parameters are further analyzed in the parametric study, aiming determination of the dependencies between the herein defined quantities. The range in which the variables are varied is considerably broad to cover vast number of possible scenarios and to capture the trends. However, within the chapter are also indications about the reasonable range of the quantities for modern LPT.

5.2.2. Axial Reynolds number for OAS

The first crucial quantity acc. to eq. 5-1 is the axial Reynolds number, calculated as shown with the eq. 5-2.

$$Re_{ax} = \frac{\rho V_{ax} c}{\mu} = \frac{\dot{m}}{2\pi R \mu} \quad \text{eq. 5-2}$$

By the definition, it expresses ratio of mass to viscous forces. Thus, with respect to flow through OAS, axial Reynolds number incorporates information about the mass flow. From the definition of the quantity results that the bigger the leakage mass, the higher the axial Reynolds number. Plots presented in the Figure 5.6, indicate that the Re_{ax} is considerably dependent on the pressure ratio and relative clearance size. Prime importance for the air seal has the smallest cross-section area – usually determined by the clearance size or in terms of characteristic quantities – the relative clearance size. It influences axial Reynolds magnitude drastically. It is obvious that with increasing cross-sectional area, the mass flow and correspondingly Re_{ax} . As visible in the figure, both quantities are nearly linearly proportional.

With respect to the pressure ratio, in the Figure 5.6, a recognizable trend is visible. It is worth noticing that from a certain value of the pressure ratio around 1.5 ÷ 1.7, the change in the axial Reynolds number is small. It is because choking originates at fins. Current Low Pressure Turbines operate on considerably higher PR in the vicinity of outer diameter than in the past decades. Nowadays, depending on the overall pressure ratio of the machine and number of stages, usual values of the pressure ratio are in a region of 1.5, or even higher. In contrary, Outer Air Seals of legacy LPT, regularly operate in a regime of around 1.3. Thus, OAS designs in modern turbines, due to higher operating pressure ratios are subjected to relatively 20 ÷ 30% more OAS leakage. Due to that it is even more important to investigate advances in the OAS regions.

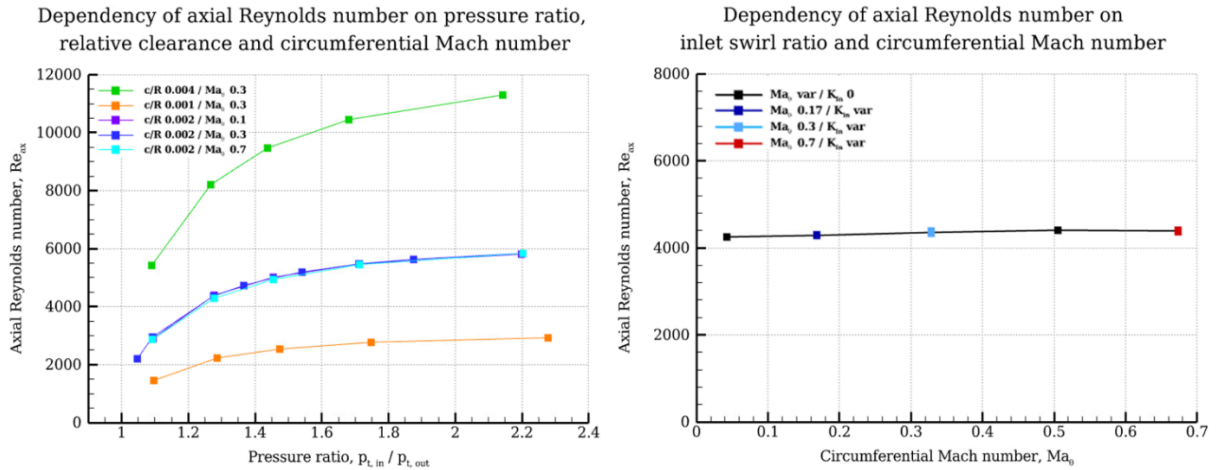


Figure 5.6 Dependency of axial Reynolds number on pressure ratio, relative clearance, circumferential Mach number and inlet swirl ratio

Revising further Figure 5.6, it becomes clear that the axial Reynolds number is independent from the rotational speed given in terms of circumferential Mach number. For practical cases of outer seals, located at considerable radius, it becomes clear that the rotation does not influence the mass flow. It can be connected to the effects in a certain range of Couette flows [100]. Another conclusion from the Figure 5.6 is that the axial Reynolds number is independent from the inlet swirl ratio over the whole spectrum the possible values investigated in the parametric study. In addition, it is checked that the ratio of specific heats has no influence on the axial Reynolds number. It is also not possible to influence this parameter looking for improved designs of Outer Air Seals, because it is one of the characteristics of the fluid itself for a given case.

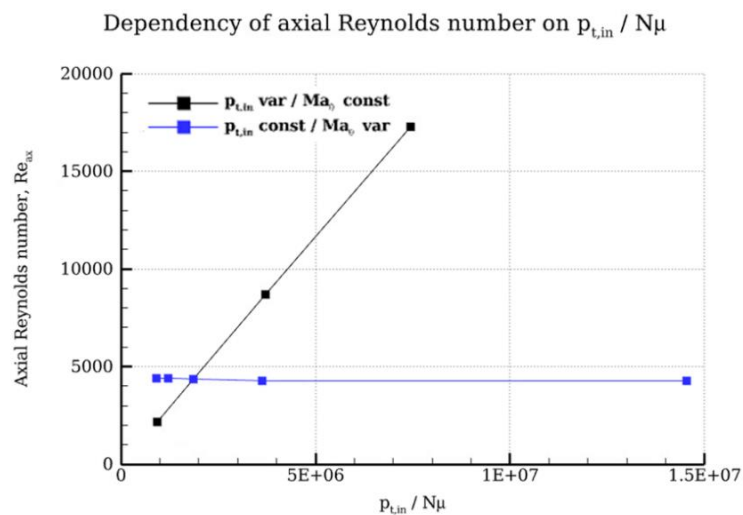


Figure 5.7 Influence of the ratio $p_{t,in} / N\mu$ on axial Reynolds number

The last quantity from the list in the eq. 5-1 is the ratio $p_{t,in} / N\mu$. It can be varied with respect to the total pressure at the inlet and rotational speed. Impact on this parameter on the axial Reynolds number is presented in the Figure 5.7. There are visible two different trends when

varying the quantity. It has been already shown that the axial Reynolds number is not influenced by the circumferential Mach number, also incorporating rotational speed. On the other hand, with increased total pressure at the inlet, the density, thus also the mass flow is proportionally increased. Thus, this effect needs to be accounted when for looking for dependencies of OAS axial Reynolds number.

5.2.3. Outlet swirl ratio

The swirl ratio refers to the inclination of the flow velocity vector. The quantity is calculated as given with the eq. 5-3.

$$K = \frac{V_{\theta}}{NR} \quad \text{eq. 5-3}$$

This parameter indicates magnitude of the circumferential velocity of the leakage flow with respect to the circumferential velocity of the rotor. The outlet swirl is contributor of the mixing between OAS leakage and the mainstream.

In the Figure 5.8 are presented meaningful dependencies between outlet swirl ratio and other OAS dimensionless quantities. As visible in the figure, with an increase in the rotational speed and with a decrease of the relative gap size, the dependency on pressure ratio is marginally higher. From the Figure 5.8, it is well visible that exit swirl ratio is clearly dependent on the axial Reynolds number of OAS. Thus, it becomes clear that the leakage flow amount, reflected in the axial Reynolds number is a primary driver for most of the losses due to the presence of Outer Air Seals, including bypass losses, due to the leakage not contributing to the work over the rotor and mixing losses, due to the leakage reintroduction into the mainstream. It is logical, because, for theoretical seal without the leakage, the whole working fluid would do the work and it would not generate additional losses behind the seal.

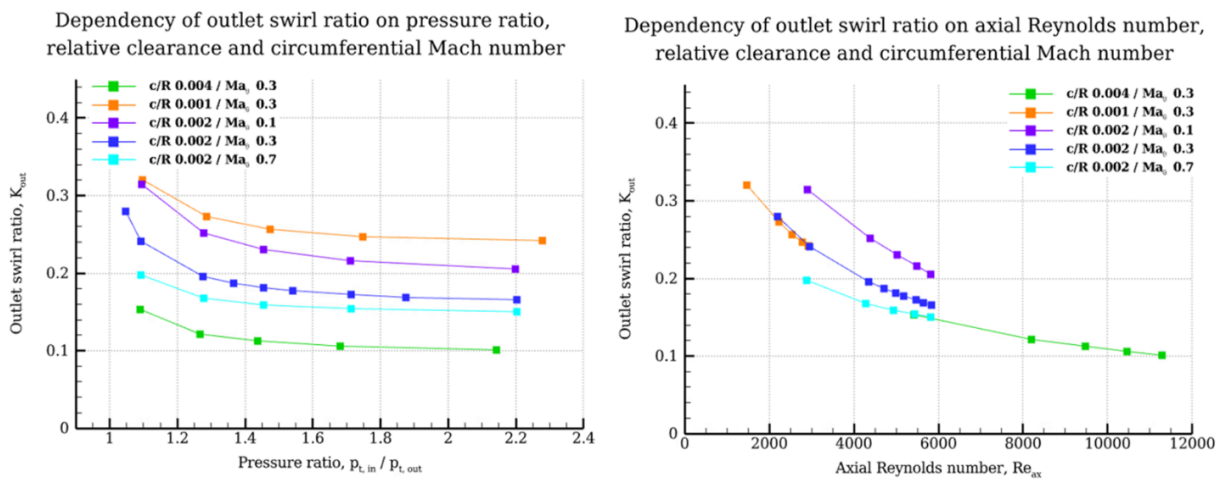


Figure 5.8 Dependency of outlet swirl ratio on pressure ratio, relative clearance and circumferential Mach number

Furthermore, from the Figure 5.8, it is deduced that with an increase of the relative gap size and circumferential Mach decrease, the outlet swirl ratio tends to experience less dragging by the viscous forces at the fins. Hence, the bigger the clearance and the smaller the rotational speed of the blade, the more flow passes through the OAS without any turning at the rotating surfaces. The turning of the flow results from the viscous forces especially acting at the casing and at the fins. For smaller clearances the shear layer dominates in the smallest cross-sectional area, in the vicinity of the fins. In other words, very little flow is free from the influence of the boundary layer. The leakage is subjected then to viscous effects. Since the rotor is turning, the flow, because of the viscous effects, is also turned. Thus, it well correlates with the meaning of the Reynolds number, expressing ratio of the mass to the viscosity forces. For small Reynolds numbers, viscosity forces dominate and it results in higher outlet swirl ratio.

Looking on the pressure ratio impact, it is seen that from a certain value around 1.4, the outlet swirl ratio is further independent from this quantity. It is observed at all configurations of the parameters like relative clearance and circumferential Mach numbers. Thus, for modern OAS, operating in the regime above 1.4, pressure ratio is of small importance for the outlet swirl ratio and mixing at rear part of the cavity.

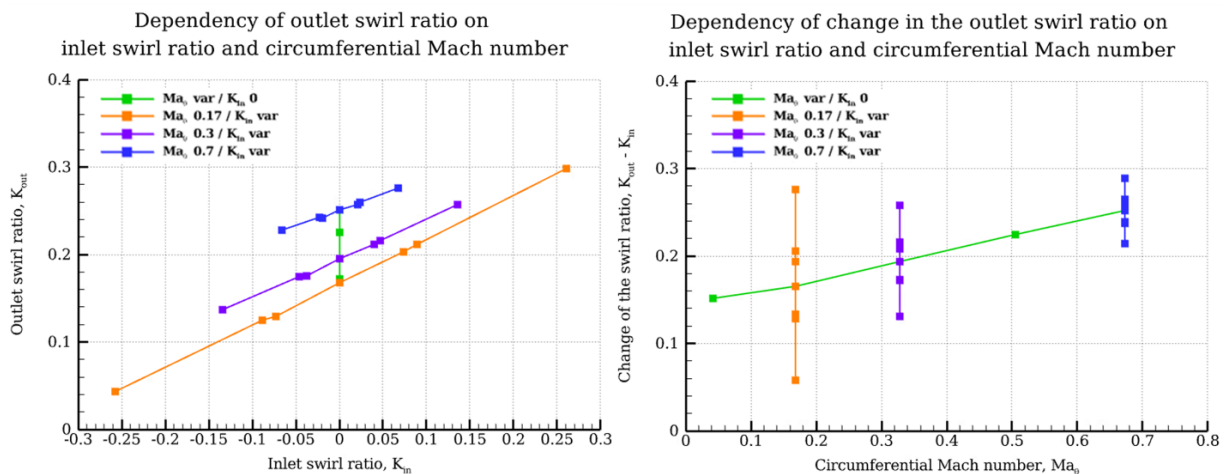


Figure 5.9 Dependency of outlet swirl ratio on circumferential Mach number and inlet swirl

Figure 5.9, reveals that the outlet swirl ratio is linearly dependent on both circumferential Mach number and inlet swirl ratio. It is clear that if the swirl at the inlet of the seal is bigger, proportionally, the outlet swirl is increased. Interestingly, the gradient of the plots at different circumferential Mach numbers is the same, even if the inlet swirl is against the rotational speed. On the other hand, increase of circumferential Mach number results in proportional increase of the outlet swirl ratio in direction of blade rotation. It is due to the viscous forces, as already mentioned earlier.

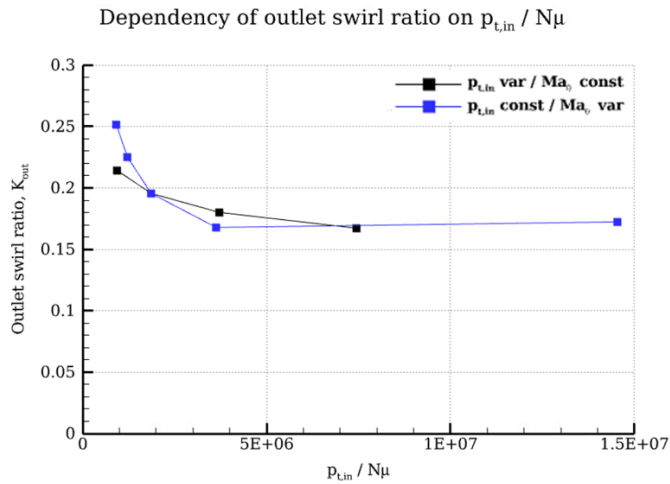


Figure 5.10 Influence of the ratio $p_{t,in} / N\mu$ on outlet swirl ratio

With respect to the $p_{t,in} / N\mu$ ratio, shown in Figure 5.10, with changes in the quantities, characteristics follow the same trend. A considerable gradient for smaller values is also noticeable. The dependencies are further discussed in the next section, combined with the outcomes of investigations regarding windage heating.

5.2.4. Impact of Windage Heating

Windage heating corresponds to the power losses across the seal due to internal losses e.g. resulting from vortices or friction it is defined as given with the eq. 5-4.

$$\sigma = \frac{2cp(T_{t,out} - T_{t,in})}{U^2} \quad \text{eq. 5-4}$$

The temperature at the outlet of the seal is slightly increased due to those and due to work input by the rotating blade through viscous forces. It is assumed that there is no heat transfer at walls. Figure 5.11 and Figure 5.12 presented relations between windage heating and other characteristic numbers identified with Dimensional Analysis.

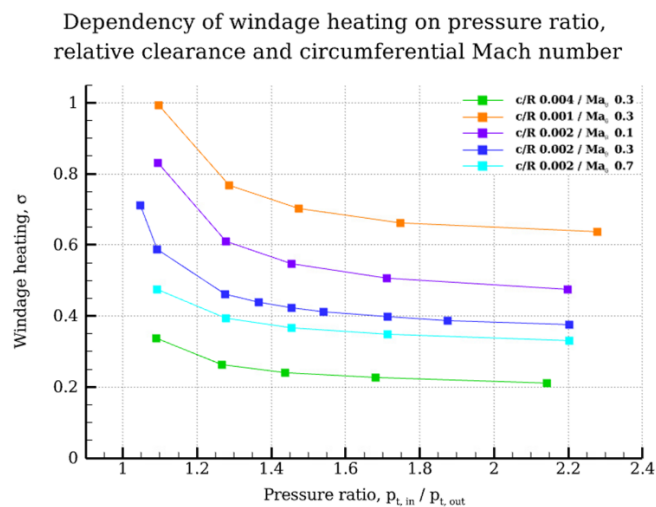


Figure 5.11 Dependency of σ on axial Reynolds, pressure ratio and relative clearance

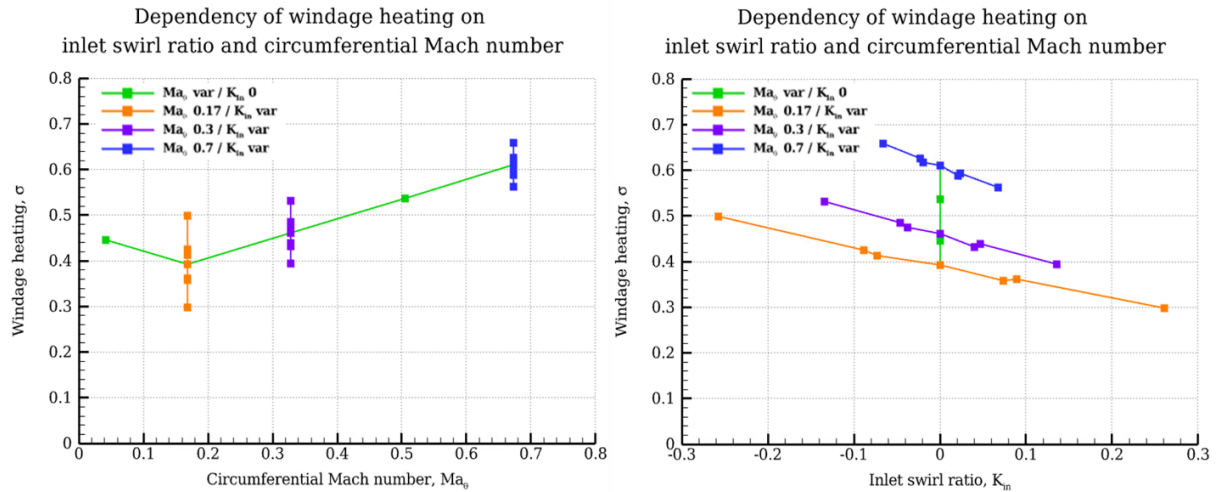


Figure 5.12 Dependency of windage heating circumferential Mach number and inlet swirl

In the Figure 5.11, it is visible that the windage heating is higher at smaller pressure ratios. Recalling findings from the Figure 5.6, it corresponds to the smaller axial Reynolds numbers, thus also bigger viscous forces imprint and enhancement of internal losses. Also with increase of circumferential Mach number, windage losses increase proportionally. It is because vortices within the seal cavity are augmented by the rotational speed of the turbine, resulting in higher windage losses.

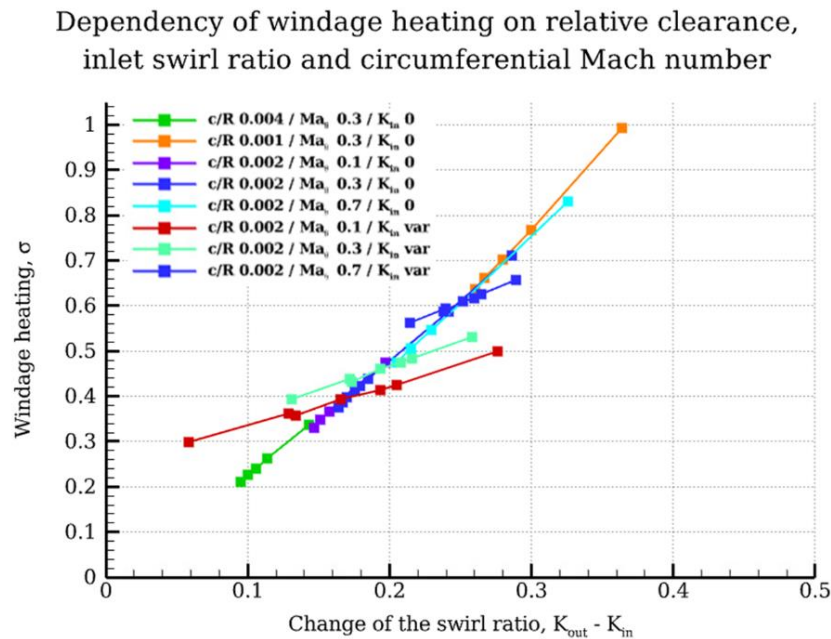


Figure 5.13 Dependency of windage heating on the change in the swirl ratio across the seal at different circumferential Mach numbers and inlet swirl ratios

The dependency on the swirl level is similar as in case of the outlet swirl ratio. It is also linear, but the gradient is opposite. Negative values of the inlet swirl mean that flow is against blade rotation. It indicates that if the leakage flow acts against the rotation, more interaction of the flow with the vortices are induced by the rotation, resulting in more losses. Revising Figure 5.9 and

Figure 5.12, it is clear that the windage heating has very similar behavior as outlet swirl ratio. It indicates, that both quantities should be also dependent, as presented in the Figure 5.13. To compare cases with different inlet swirl ratio, the windage heating is plotted with respect to a change in the swirl ratio between outlet and inlet of the seal.

The Figure 5.13 confirms that physical drivers for both windage heating and outlet swirl ratio are the same with respect to relative clearance, axial Reynolds number and circumferential Mach number. Only inlet swirl ratio results in changes in windage heating beyond the main trend.

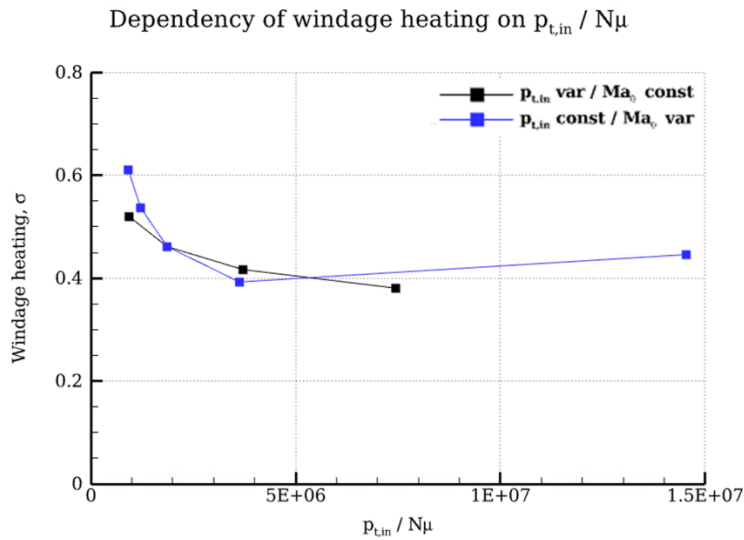


Figure 5.14 Influence of the ratio $p_{t,in} / N\mu$ on windage heating

The trends of both quantities are also corresponding to each other when revising ratio of $p_{t,in} / N\mu$, as visible comparing Figure 5.10 and Figure 5.14. Charts show that regardless variation of the pressure ratio or rotational speed, characteristics are corresponding. Both outlet swirl ratio and windage heating with respect to the $p_{t,in} / N\mu$ ratio tend to a limit at a certain value. A considerable gradient for smaller values is also noticeable. It refers to the situation when inlet total pressure is small and rotational speed high. Thus, for these cases outlet swirl ratio and windage losses are higher. Applying the conclusion to the situation in a turbine e.g. with total pressure decreasing downstream the machine, flow at the outlet of the seals is expected to experience higher swirl ratio at the seal outlet and higher internal windage losses.

5.2.5. Summary of findings from Dimensional Analysis of OAS

For the flow similarity of the Outer Air Seals particular characteristic numbers need to be kept. Investigating effects connected to seal leakage mass flow, axial Reynolds number is crucial. Outlet swirl ratio is very important for the latter mixing with mainstream at the reintroduction and windage heating is most refers to the internal losses.

The parametric study reveals that there are also further dependencies between the non-dimensional quantities. The investigations have been performed in a range of the quantities reflecting operating conditions of state-of-the-art LPT. In this range, it is found that axial Reynolds number is independent from the circumferential Mach number, thus rotational speed and the inlet swirl ratio, but strongly depended on the relative gap size, the pressure ratio and the ratio $pt_{in}/N\mu$. Axial Reynolds number is found to be the most important quantity for the seal, because its impact significantly impacts the seal and other characteristic quantities. Beside axial Reynolds number, the outlet swirl ratio is found to be dependent also on the circumferential Mach number and inlet swirl. Both, outlet swirl ratio and windage heating indicate similar behavior, what indicates that they are driven by similar phenomena. The only difference between the quantities is in the opposite impact of the inlet swirl ratio. These findings indicate useful directions for possible improvements in the Outer Air Seals operation.

This page intentionally left blank.

Chapter 6. New concepts of LPT OAS and their multidisciplinary evaluation

The main subject of the project is development of a new solution for LPT Outer Air Seals. According to the methodology, described in Chapter 3. , in the first place, new ideas aiming improvements of these regions are identified. The ideas are further preselected to narrow the area of searches and to focus on the most meaningful proposals. Solutions with good potential for improvement of the reference turbine efficiency in assumed amount and simultaneously possible for multidisciplinary compromise are considered. After the preselection, the multidisciplinary evaluation is attempted. These ideas, subsequently, are evaluated in detail in the light of miscellaneous criteria from particular disciplines including: design, manufacturing technology, materials technology, aerodynamics, secondary air management, thermal engineering, structural integrity and costs. In this way, the most promising ideas are chosen. It is aimed that only two, the most promising concepts are further developed and analyzed in detail in order to confirm the final efficiency benefit. The final solution is supposed to improve overall LPT efficiency by minimum 0.1%, as defined in the project goals, and it has to obey multidisciplinary requirements enabling application of the solution in the engine environment.

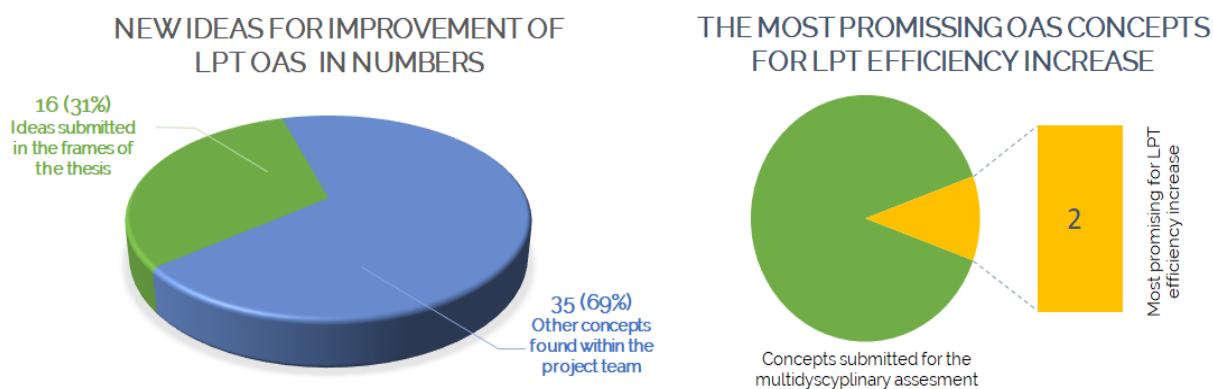


Figure 6.1 Summary of new ideas developed for improvement of LPT OAS

As visualized in the Figure 6.1, in the frames of works over the doctorate, in total 16 ideas for improvement of Outer Air Seals ideas is found. After preselection and preliminary evaluation 8 out of those are indicated for further evaluation. These ideas are assessed in sense of criteria from different disciplines. This allows choice of the most promising concepts.

6.1. Key multidisciplinary design aspects of LPT Outer Air Seals

The newly developed solution for improvement of LPT Outer Air Seals should fulfill a set of criteria from all disciplines meaningful for proper operation of OAS. There are multiple criteria from aerodynamics, design, manufacturing technology, materials technology, secondary air management, thermal engineering, structural integration and costs that have to be fulfilled. Frequent situation in such cases is that enhancement of operation in terms of one discipline, results in stretching or violation of other disciplines. The only possibility for improving of such regions is reaching a multidisciplinary compromise.

All disciplines have certain requirements. Some of the requirements cannot be compromised, other need to be traded to reach the compromise. From the point of view of Design, the solution has to be first of all feasible and realizable. It should not add too much weight, what is always negative in aviation industry. Next, new solutions should be manageable in terms of the maintenance. If the blade is modified, its center of gravity should stay unchanged. The running clearance should be maintained and definitely it cannot be worsened, because it directly transfers into poorer performance, issues in the fields of aerodynamics and secondary air management. There also should be enough design space available. Particular axial and radial movements of the blade within the cavity, so called “keep-out-zones”, have to be respected. Simultaneously, the assembly has to be possible. The solution should be also robust and able to work under continuously changing conditions in different operation of the turbine and for over whole required engine mission scenarios. Lastly, the overall consequence on an engine design has to be considered. It is not reasonable to change the whole engine design only to enable small modifications in some area. Nevertheless, it might be worth, if the benefits are very significant.

With respect to Aerodynamics, the most important criteria for Outer Air Seals are gain in the efficiency of the machine and robust aerodynamic operation. It has been elaborated in detailed in previous Chapter 5. Only to mention, the primary drivers are amount of the leakage through the seal, the mixing losses and consequences of interactions of the cavity regions with the mainstream. Beside the assumed efficiency benefit at the design point, a robust of the modification has to be assured. The solution should operate well in off-design operation of the machine, not introducing considerable aerodynamic losses.

Directly connected to this is the Secondary Air System. It is another important aspect of the sealing. In the light of this, the criteria crosschecked under this discipline include sealing effectiveness, and secondary air consumption. The sealing performance transfers to the leakage through the seal and its robustness over the lifecycle of the machine, including deterioration of its performance and the wear of the seal with time. With respect to consumption of the secondary air, LPT are usually not very highly pressurized and cooled with the secondary air in OAS regions. The secondary air is kept at minimum, because it is costly. It needs to be brought to the certain pressure in compressor, later transported, experiencing losses through the turbomachine and then actually introduced into the mainstream in a way that it is not harmful, but beneficial for the whole system. Thus, if it is used, it directly decreases the overall benefit.

From the perspective of Materials Engineering, it is important to assure that the materials used for realization of the solutions are available and technology for their production is available. The materials have to withstand temperatures that occur in these regions, thus the applicability of the material to this particular location in the turbine has to be possible. Another aspect is the rub-in procedure and materials wear behavior. In addition, possibility, availability and application of the coatings has to be considered. Because it might be necessary for some solutions.

From the Thermal Engineering perspective, the temperature level and gradients are important. Both cannot be too high, because it is a source of thermo-mechanical fatigue. The applied solution cannot result in unexpected additional heating of the parts e.g. due to the continuous contact of the rotating and nonrotating parts, thus interconnected is also rub-in behavior.

The temperatures are one of key inputs for further structural resilience. The most important to assure appropriate life of all parts. All, static stresses, high- and low-cycle fatigue cannot lead to damage of the parts over the assumed period. So the overall robustness of the whole system and particular parts has to be assured. If cracking appears, it also needs to be evaluated if it does not propagate considerably, assuring safe operation.

From the perspective of manufacturing engineering, the solution should be realizable and producible with known methods. Together with the material itself, it is also strongly connected with the overall cost of the modification. And this should be kept on similar level as the baseline.

Last, but not least, during the assessment, from all disciplines possible risks are identified and collected. It is important to have a very clear line, that the indicated issue is a showstopper or a risk. If it is the first, then the solution cannot be further considered. The risks, are mitigated with the further development of the solution.

6.2. New LPT OAS concepts and their assessment

6.2.1. Baseline geometry

All solutions developed in herein doctoral work are intended for improving LPT operation in area of Outer Air Seals. The OAS design shown in the Figure 6.2, is chosen as a baseline. It is a labyrinth seal with two fins and abradable honeycomb structure. The functional principle of this sealing system is that the fins and the honeycomb pose a labyrinth for the leakage, resulting in significant decrease of the leakage mass flow over the blade, thus overall reducing losses and increasing machine performance. The leakage goes through the fins and further inflows into the mainstream before the subsequent vane.

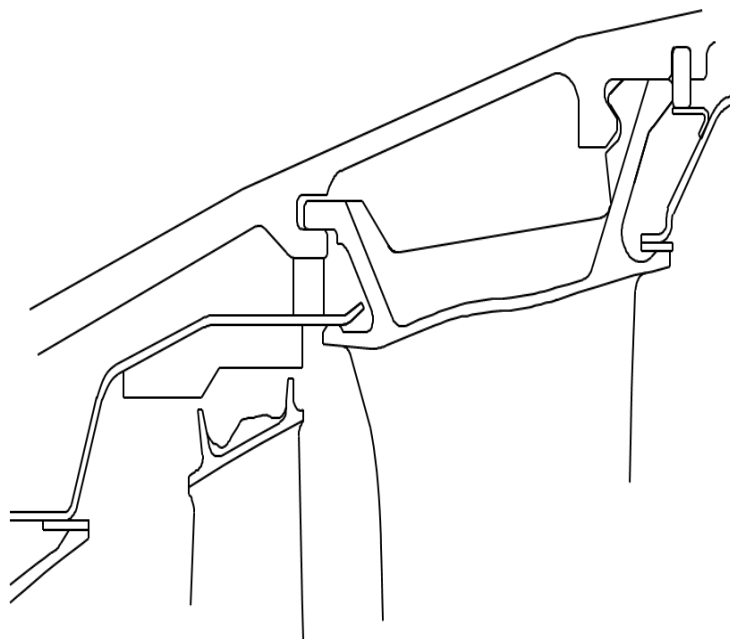


Figure 6.2 Schematic representation of a state-of-the-art Outer Air Seal of LPT EP3561228B1 [44]

The blade moves relative to the non-rotating parts, over the engine mission, due to thermal and structural displacements. This movement varies over in different operating points. Thus, there the space where the blade moves must be avoided. The interaction of the blade and the honeycomb structure is allowed. In regular operation, the fins rub into the honeycomb structure. In addition, it needs to be also accounted that the LPT may be equipped with the ACC system, providing tight running clearances over the whole mission.

The discussed OAS design is the most common realization of OAS that is proven to operate robustly over the whole LPT life cycle.

6.2.2. Front Deflector

The first concept developed for improvement of the LPT is Front Deflector (FD). It is schematically pictured in the Figure 6.3. The solution is a modification of the front part of the OAS cavity. The principle behind the concept is to provide additional labyrinth for the leakage and to reduce the front volume to minimum. The solution is secured under the patent EP19209602A1 [68].

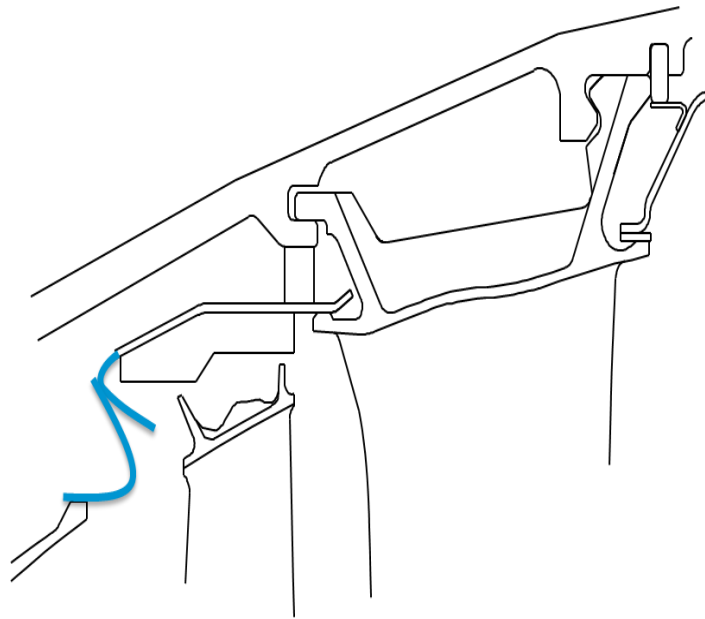


Figure 6.3 Schematic representation of the Front Deflector concept. Reference patent EP19209602A1 [68]

The front volume of the cavity is decreased to minimum. In this way the gas path contour is closer to the ideal flow path and interactions between the OAS cavity and the mainstream are reduced. The additional labyrinth is created between the static fin and the rotating blade. The labyrinth is intended to contribute to a decrease in the leakage across the seal. It is expected that the solution improves the performance even more in off-design operation when the blade moves close to the deflector. Additionally, the front fin can be modified to provide improved overlapping.

| Front Deflector | | |
|-----------------|---------------------------|----|
| Rating | Design | -1 |
| | Aerodynamics | 2 |
| | Secondary Air System | 0 |
| | Structures | 0 |
| | Materials Technology | 0 |
| | Thermal Engineering | 1 |
| | Manufacturing Engineering | 0 |
| | Costs | 0 |
| | Overall Rating | 2 |

Legend

■ - rejected

-5..+5 - rating:

+5 = very promising

0 = as baseline

-4 = doubtful/poor

-5(if any) = REJECTED

Figure 6.4 Preliminary multidisciplinary rating of the Front Deflector concept

The preliminary multidisciplinary evaluation for the concept is shown in the Figure 6.4. The feature can be realized in various ways e.g. it can be integrated within the cavity liner, brazed to the liner or fixed in any other way. The feature is assessed feasible and straightforward for implementation. The static fin length depends on the blade keep-out-zones. The contact between the deflector and rotating blade should be excluded.

6.2.3. Vane Bleed Holes

The second solution developed in herein thesis for improving LPT OAS is Vane Bleed Holes (VBH), shown in the Figure 6.5. The main principle behind the solution is that the leakage flow from the rear cavity chamber is guided over the subsequent vane. The solution is intended to decrease harmful mixing and disturbances of the main flow resulting from the OAS leakage. The solution is secured under the patent EP4123124A1 [69].

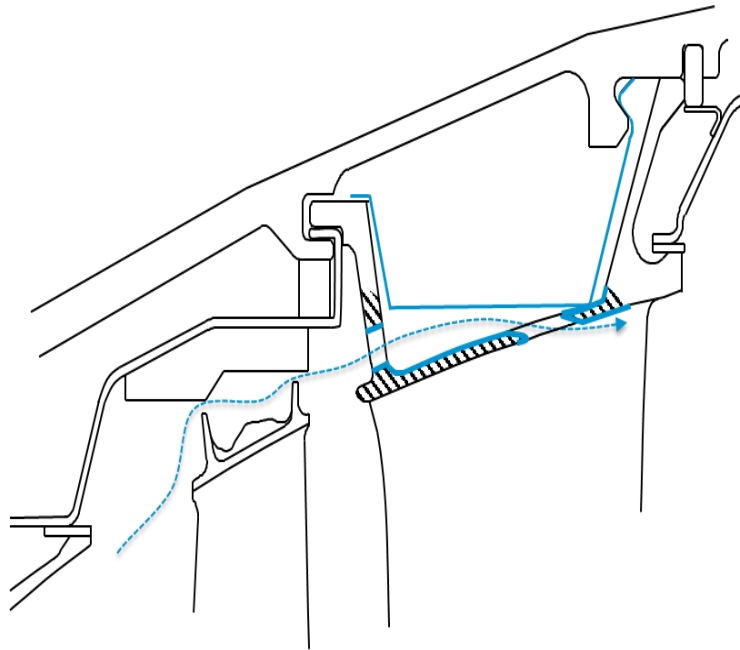


Figure 6.5 Schematic representation of the Vane Bleed Holes concept. Reference patent EP4123124A1 [69]

The rear cavity is shaped in a way to enable the leakage flow to go through the vane hook. The leakage in the rear part of the flow path has higher specific enthalpy compared to the mainstream, even if it experiences pressure losses through the seal, because the work has not been extracted at the rotor from this portion of the fluid. Due to that, between inlet and exit of the solution exists pressure difference, enabling transfer of the leakage over the vane. Flow directions of the mainstream and the OAS leakage are considerably different, as elaborated in the Section 5.1. With VBH, the leakage flow is guided improving leakage flow direction and thus mixing. The leakage is reintroduced to the mainstream preferably tangentially to the vane shroud. The

circumferential component is achieved by turning the flow with additional geometrical features e.g. particularly shaped ribs between vane hooks. The features can additionally reinforce the hook. The flow angles can be further improved with particular inclination of the outlet holes or slots.

| Vane Bleed Holes | | |
|------------------|---------------------------|----|
| Rating | Design | -1 |
| | Aerodynamics | 5 |
| | Secondary Air System | 0 |
| | Structures | -2 |
| | Materials Technology | 0 |
| | Thermal Engineering | -1 |
| | Manufacturing Engineering | 0 |
| | Costs | -1 |
| | Overall Rating | |

Legend

■ - rejected

-5..+5 - rating:

+5 = very promising

0 = as baseline

-4 = doubtful/poor

-5 (if any) = REJECTED

Figure 6.6 Preliminary multidisciplinary rating of the Vane Bleed Holes concept

The preliminary multidisciplinary evaluation of the concept is shown in the Figure 6.6. As visible, the solution is very promising for aerodynamics in terms of efficiency benefit. The main contributor are improvements in the mixing of the leakage and mainstream. The guidance of the leakage reduces also separations at vane leading edge caused by the leakage what improves overall flow at the airfoil. In addition, the leakage reintroduced with particular momentum can further decrease secondary flows building up along the vane passage. The design and manufacturing of the feature are more complicated, but assessed feasible. It is reflected also in the additional costs of the solution. Manufacturing of the holes in the vane may be realized in several ways, depending on the possibilities. Different guidance of the leakage can influence also temperature gradients in the vane. In combination with the additional holes, the vane structure can be weakened. It is not straightforward if the impact is positive or negative, because it depends on particular part and its operation. Nevertheless, it is assessed that it with proper location of inlet and outlet holes and additional reinforcement of the hooks with the ribs, the solution is realizable and possible for implementation.

6.3. The most promising new design concept of LPT OAS

Both described concepts – Front Deflector and Vane Bleed Holes are found realizable in the light of criteria from meaningful disciplines and promising in providing required efficiency benefit. Because FD is intended for improvement of the OAS front part and VBH for the rear area, both solutions can be applied simultaneously. The combined solutions are visualized in the Figure 6.7.

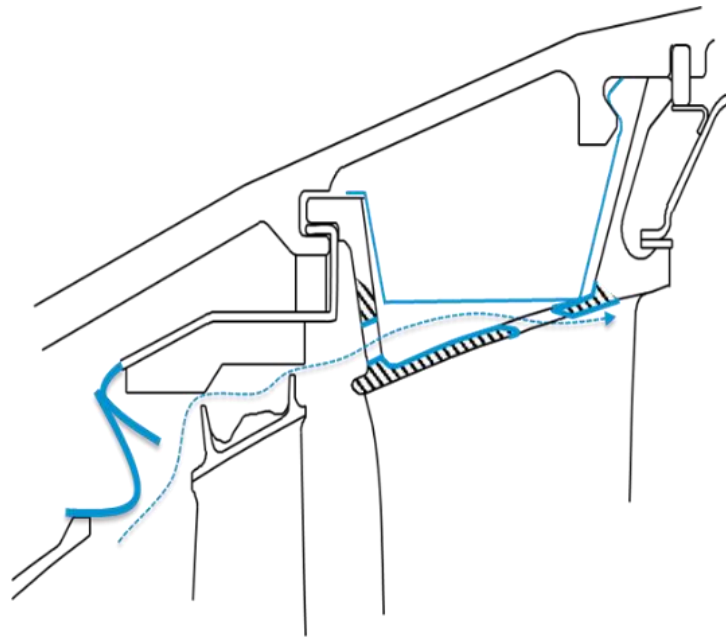


Figure 6.7 Schematic representation of the most promising solution of LPT OAS – Front Deflector combined with Vane Bleed Holes. Reference patents – EP19209602A1 [69], EP4123124A1 [68]

The FD concept is simpler and straightforward for implementation. Nevertheless, efficiency benefits expected from this solution are moderate. Whereas, the VBH concept is more complicated, but simultaneously associated with higher efficiency gain. Combined concepts provide the highest overall improvement of the OAS regions.

In the next chapter, performance and sensitivities for both concepts are addressed, followed by the assessment of the predicted efficiency benefit resulting from their implementation.

Chapter 7. Evaluation of operation and aerodynamic benefits from the developed solutions

7.1. Front Deflector concept evaluation

The initial multidisciplinary assessment of the Front Deflector concept indicates that it is a relatively simple and beneficial idea for enhancement of the front part of OAS. The improvements that are introduced by the solution are twofold – it is creation of the additional labyrinth and reduction of the interactions between mainstream and big vortices present in the cavities.

There are various ways for realization of the Front Deflector concept, but the aerodynamic benefit is expected to be the same provided that the main geometrical features of the concept are preserved. The deflector is expected to be beneficial in the LPT aerodynamic design point and even more in such off-design operation when the blade moves closer to the deflector, because of the axial movement of the rotor relative to the casing. In such operation additional improvement in the sealing is expected. It is summarized in the Figure 7.1.

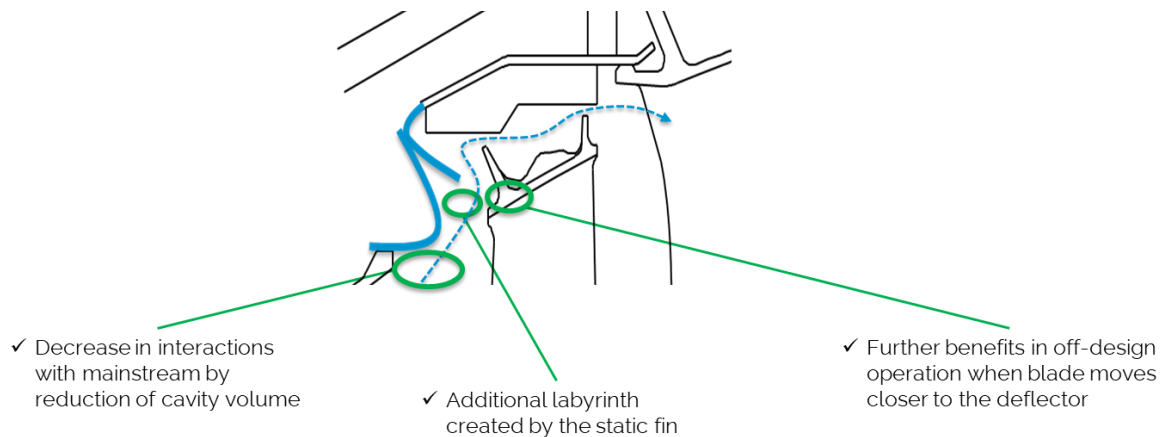


Figure 7.1 Main aerodynamic benefits from Front Deflector

This chapter addresses evaluation of the Front Deflector performance and main sensitivities important for its operation. In order to evaluate benefits from Front Deflector application, it is designed for all stages of the reference 3-staged LPT. Next, the feature is modeled in several configurations and further analyzed applying validated CFD, as discussed in the Chapter 4. The modeling approach for FD is described in the Chapter 6.

7.1.1. Evaluation of performance of Front Deflector without static fin

At first, aerodynamic operation and benefits from reduction of the front OAS cavity with Front Deflector without static fin are assessed. Two configurations, shown in the Figure 7.2, are analyzed and compared with the baseline case. The first modification represents geometry of the feature with two bends, the second is realized with single bend. The solution with two bends requires slightly more manufacturing effort, but allows for reduction of the step and very close reproduction of the ideal flow path. In this way, it is assumed that step losses can be further reduced. The significance of the step losses increases if the leakage through the seal is at low level, being a case of nowadays turbines, due to the advanced systems for running clearance reduction. Thus, looking for the further fractions of efficiency, it is also worth checking this direction of improvement.

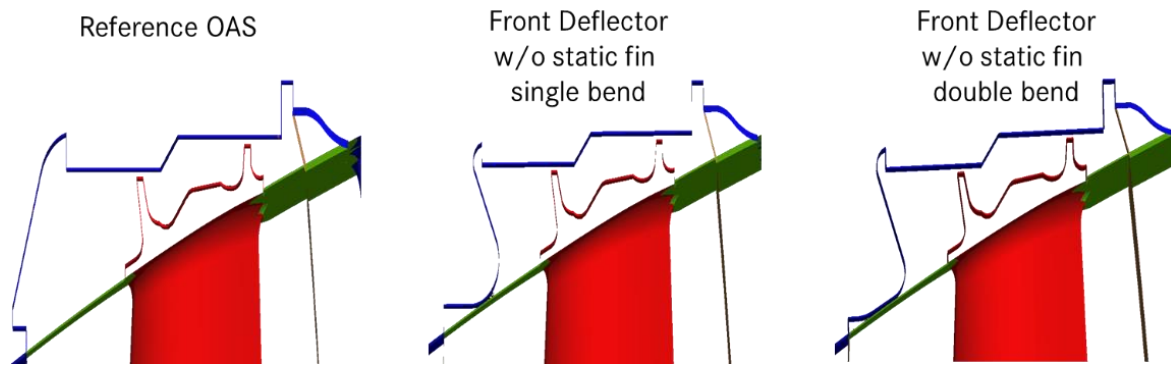


Figure 7.2 Investigated designs cases of front cavity reduction with Front Deflector without static fin

Detailed CFD simulations of all configurations are performed with solutions at all three stages of reference LPT. The analyses of the variants, presented in the Figure 7.3 show that both solutions perform almost equally well. The solution with two bends is negligibly better, but it also requires slightly more manufacturing effort, thus it is considered that the overall benefit is comparable. It indicates that such additional small step in the flow patch, being a source of additional perturbation for the fluid, has relatively small impact on the overall improvement.

Figure 7.4 and Figure 7.5 present flow field of the investigated cases. As visible in the figures, big vortices present in the front cavity are considerably reduced when the cavity volume is decreased. These vortex structures are not standing, they move over circumference, what is visible looking on the relative circumferential velocity in the Figure 7.4. The figure reveals also that the decrease of front volume, besides contributing to the reduction of the vortex itself, simultaneously reduces circumferential velocity.

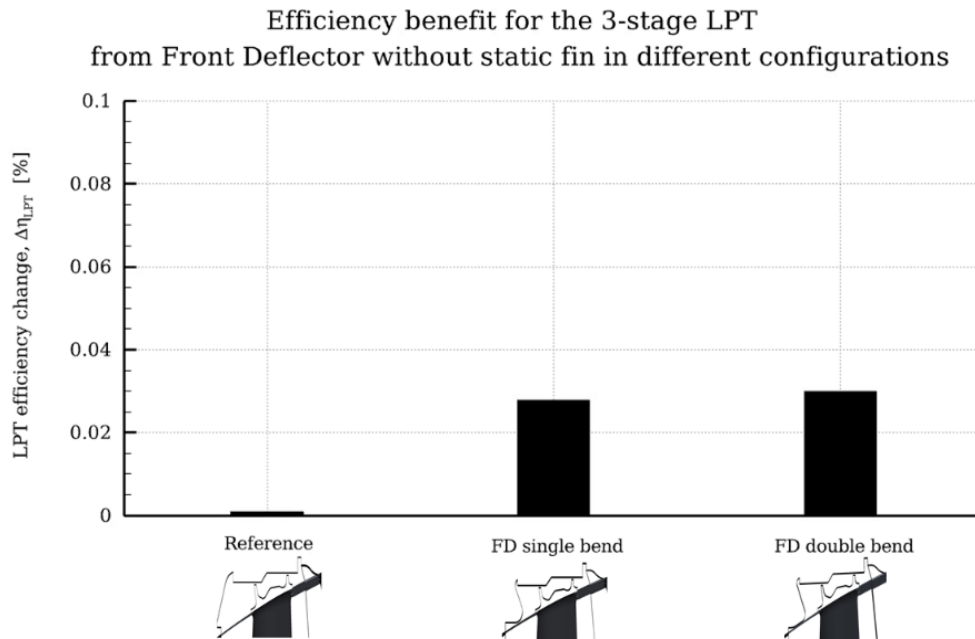


Figure 7.3 LPT Efficiency benefit from front cavity reduction with Front Deflector without static fin

The magnitude of this velocity in the cavity is different than in the mainstream. It is shown in the Figure 7.5 that the interactions between the cavity and the mainstream are reduced. Nevertheless, as also visible in the Figure 7.4 and Figure 7.5, the main leakage path, is actually not influenced by the presence of the front deflector without static fin. This is also reflected in the primary dimensionless numbers, given for one of the seals in different variants in the Figure 7.6.

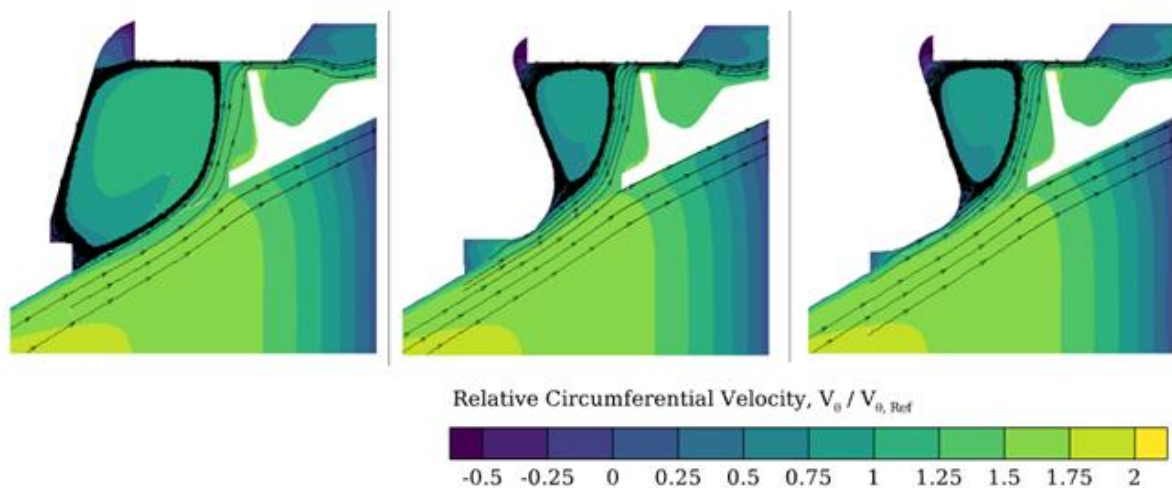


Figure 7.4 Relative Circumferential Velocity and streamlines for investigated cases of Front Deflector without static fin in different configurations

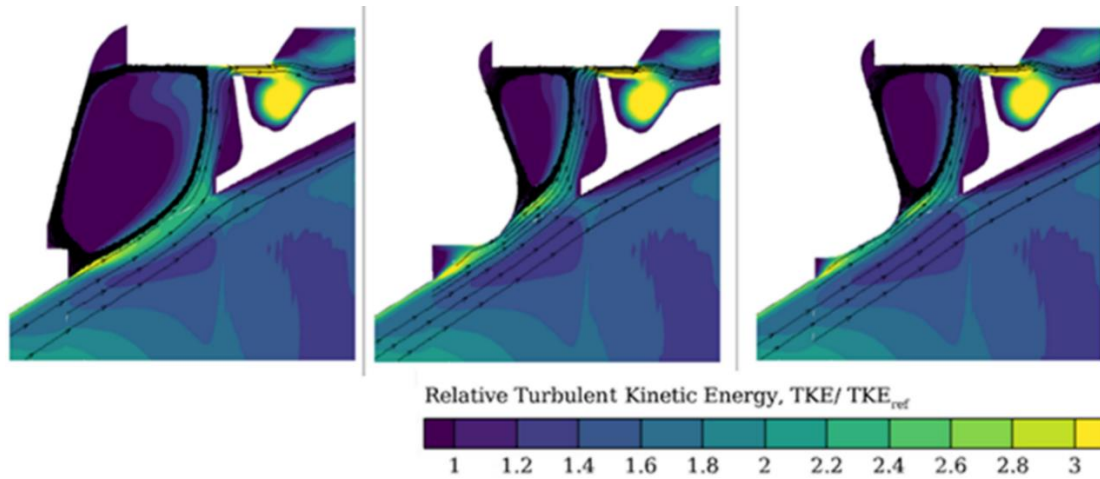


Figure 7.5 Relative Turbulent Kinetic Energy and streamlines for investigated cases of Front Deflector without static fin in different configurations

As visible in the Figure 7.6, for all variants, the characteristic numbers are nearly the same. It indicates, that the general operation of the seal is unchanged with the investigated designs of Front Deflector without static fin. In particular, the axial Reynolds number, indicating about leakage behavior, is on the same level. It is concluded that the reduction of the front cavity volume does not influence the OAS leakage itself. Thus, it is not the reason for the observed benefit.

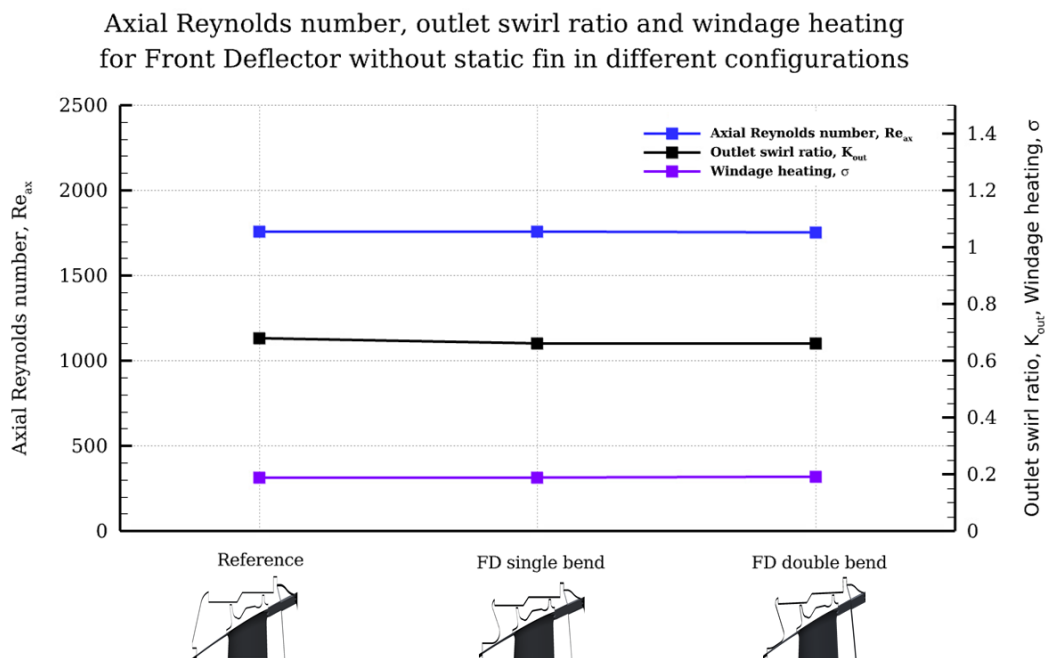


Figure 7.6 Comparison of characteristic numbers for OAS with Front Deflector without static fin in different configurations for one of the OAS.

The main benefit is found to result from decreased interaction of the mainstream and big vortices present in the front cavity and decrease of the step losses. Particular benefits due to both factors are shown in the breakdown of efficiency benefit shown in the Figure 7.7. The breakdown is prepared by following methodology applied by Gier et al. [30]. To separate benefit coming from

improvement in the step losses, simulations without any leakage through the seal for the reference case and the case with the single bend variant are researched. They are prepared in a way that the radial clearance is closed completely, resulting in reduction of the leakage mass flow to zero.

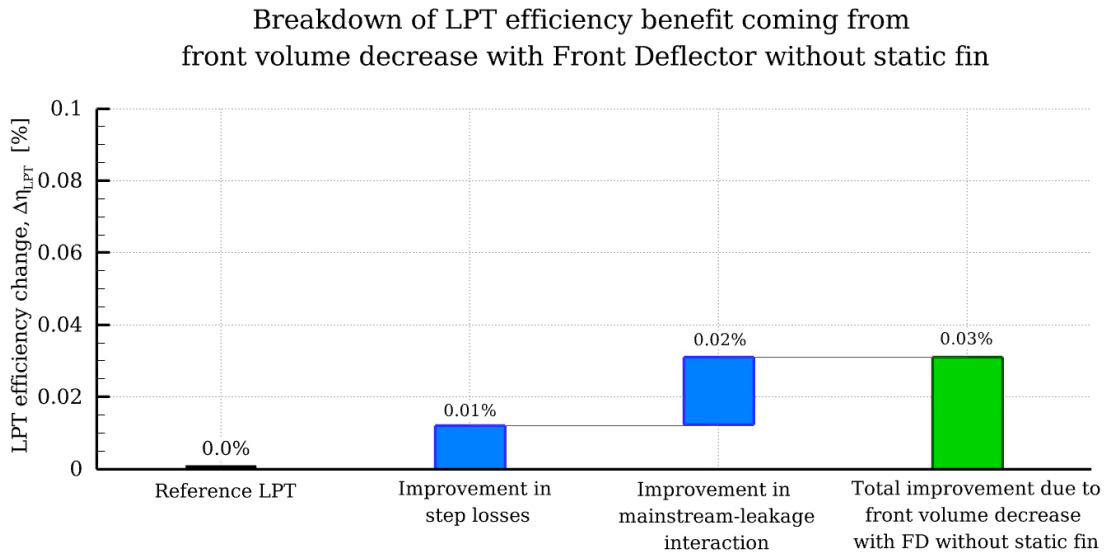


Figure 7.7 Breakdown of LPT efficiency benefit due to front volume reduction

As visible from the Figure 7.7, the improvement in the step losses due to OAS cavity presence, but excluding influence of the leakage stands for around one third of total benefit coming from implementation of the front cavity reduction. Two thirds of the total benefit, is due to the reduced interactions in the leakage and mainstream.

7.1.2. Evaluation of performance of the Front Deflector with static fin

The static fin creates the additional labyrinth for the OAS leakage and in this way leads to its reduction. Two cases of the static fin are considered – short and long, to investigate sensitivity of the concept to the length of the feature. The variants are compared with the reference OAS design and with the Front Deflector case without static fin. The investigated configurations are presented in the Figure 7.8.

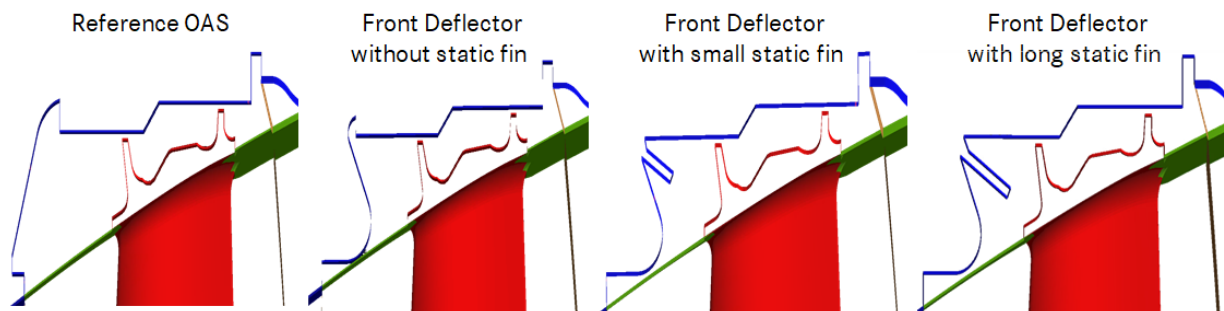


Figure 7.8 Investigated designs cases of front cavity reduction with Front Deflector with static fin

Revising the flow field in the Figure 7.9, it is noticeable that the big vortex present in the cavity is further reduced with application of the static fin. Nevertheless, looking on the benefit in LPT efficiency in the Figure 7.11, it is visible that the short static fin does not provide any further improvement compared to the Front Deflector case without the static fin. It can be concluded, that decrease of the vortices in the front cavity has meaningful impact only, if it involves reduction in interaction of these structures with the mainstream. It is also reflected in the Figure 7.9, comparing both cases. Thus, the short fin does not operate as intended, because the main assumption behind presence of the static fin is formation of additional labyrinth for the leakage. It is well visible in the Figure 7.10 comparing axial Reynolds number, reflecting the leakage for both configurations. Additionally, streamlines visible in the Figure 7.9 confirm that for the Front Deflector with short static fin, the leakage path is not influenced.

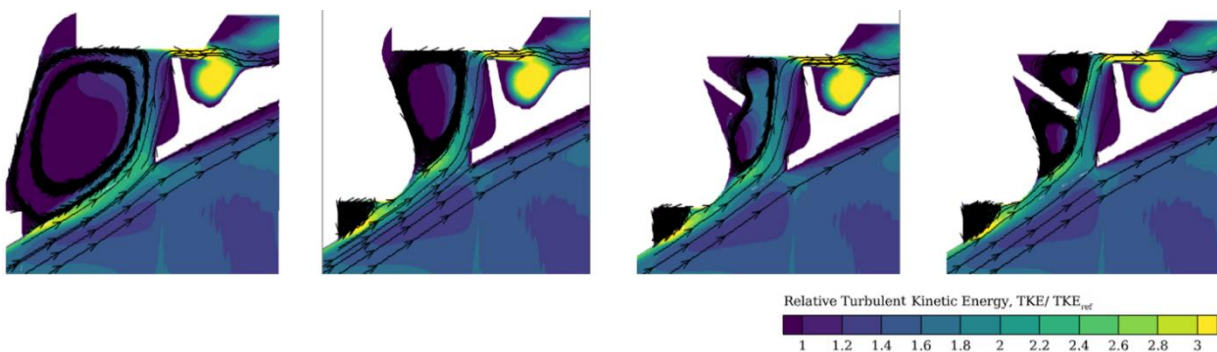


Figure 7.9 Relative Turbulent Kinetic Energy and streamlines for investigated cases of Front Deflector with static fin in different configurations

It points to the conclusion that the fin length is crucial for the overall benefit from the solution. It is clear that when the clearance between the blade and the static fin decreases, the leakage experiences more blockage and thus is reduced. Nevertheless, it needs to be considered that the blade cannot contact with the fin to avoid its damage. Respecting this limitation, the case with longer fin is investigated.

As noticeable in the Figure 7.10, the analyses show that the Front Deflector with longer static fin visibly reduces axial Reynolds number through the seal. It indicates that the longer fin contributes to leakage reduction by around 6% compared to the reference case. This reflects positively in the efficiency gain, given in the Figure 7.11.

Figure 7.10 reveals also that outlet swirl ratio and windage heating are not visibly influenced with application of the Front Deflector. Only for the long static fin configuration, a very small change in the outlet swirl can be noted. Thus, it is concluded, that the mixing behind the cavity as well as internal losses are not noticeably changed with application of the Front Deflector. This is also confirmed revising plots in the Figure 7.9, because already in the vicinity of the first fin, there are no visible differences between configurations.

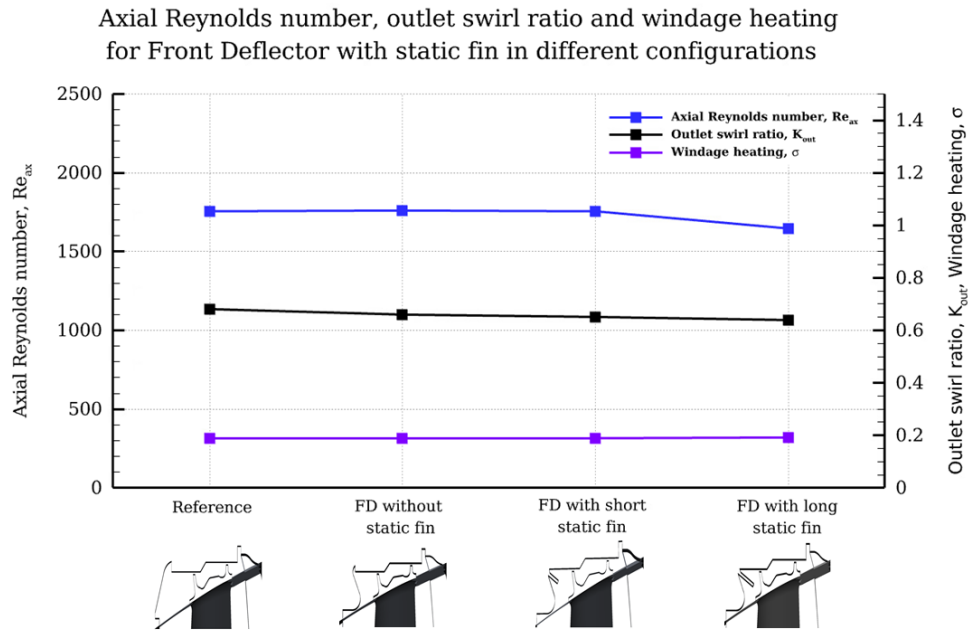


Figure 7.10 Comparison of characteristic numbers for OAS with Front Deflector with static fin in different configurations

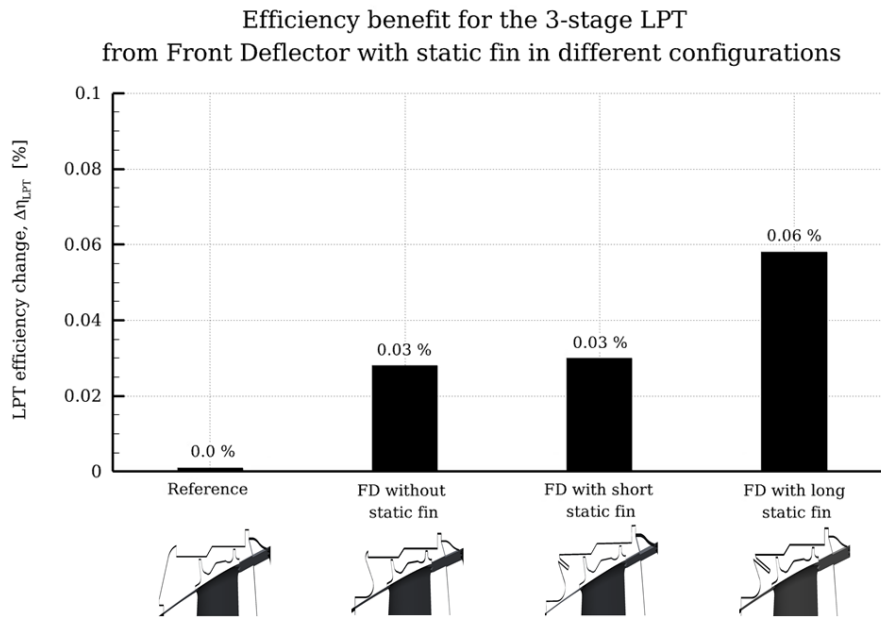


Figure 7.11 LPT Efficiency benefit from front cavity reduction mounted on all stages.

The overall efficiency potential from the Front Deflector concept is thus assessed between 0.03% – 0.06%, depending on the length of the static fin. As pointed out, the configuration with short static fin is close to the variant without static fin. Thus, it might be applicable to skip the static fin for the turbines with operation limiting noticeably length of the fin, due to the keep-out-zones.

7.2. Evaluation of the Vane Bleed Holes concept

The second concept developed for improvement of LPT in OAS regions is Vane Bleed Holes. This modification is introduced in the rear part of OAS cavities on following vanes, as described in the Chapter 6. The working principle behind VBH is that the OAS leakage from the rear cavity is guided over the subsequent vane and next, it is reinjected into the main gas path at the vane shroud in a controlled way.

The initial multidisciplinary assessment of the VBH concept revealed that the solution is more difficult, but also having higher potential for increases of LPT efficiency. Improvements coming from the solution are trilateral, they are summarized in the Figure 7.12.

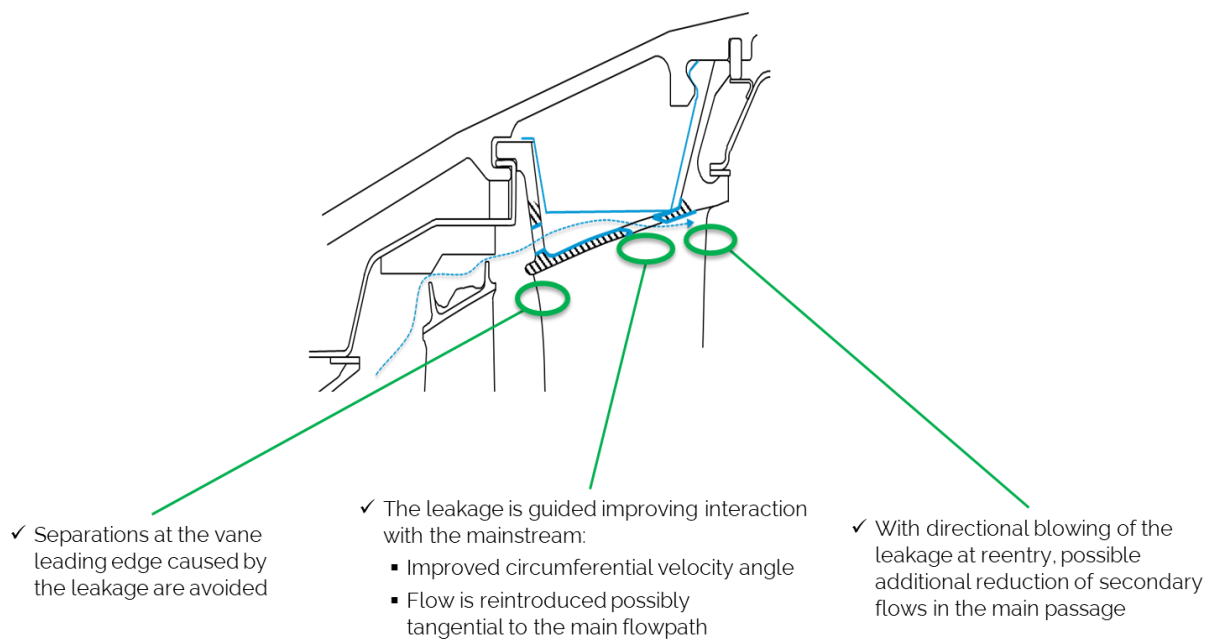


Figure 7.12 Main benefits resulting from Vane Bleed Holes

The primary gain due to application of the solution results from decreased interactions between the leakage and mainstream in the rear part of the Outer Air Seal. Secondary benefits from the solution are associated with reduction in separations at the leading edge of the vane and with additional reduction of secondary flows in the passage achieved with particular directional blowing from VBH at the reentry.

In this chapter, performance and sensitivities of VBH concept in different variants and under different conditions are investigated. Firstly, the solution is researched on a simplified model, described in the Chapter 3. Next, complete parametric study on a detailed three-dimensional model of VBH with 1.5-stage partial model of the reference LPT is carried out. Finally, all learners are transferred to the validated full geometrical model of 3-stage reference LPT, discussed in the Chapter 4., for prediction of the overall efficiency gain from the solution.

7.2.1. Basic operation of VBH

The operation of VBH is visualized in the Figure 7.13. With application of the solution, the OAS leakage does not interact with the mainstream at the rear part of the cavity (marked with **A**, in the Figure 7.13). Due to that the mixed mainstream-leakage flow in the vicinity of the vane shroud (marked with **B**, in the Figure 7.13) does not develop through the vane. This unaligned, turbulated flow, is usually amplified along the vane passage (marked with **C**, in the Figure 7.13), resulting in the so-called passage vortex. The secondary flows, which are indispensably generated in the passage, with application of VBH get smaller (marked with **C**, in the Figure 7.13).

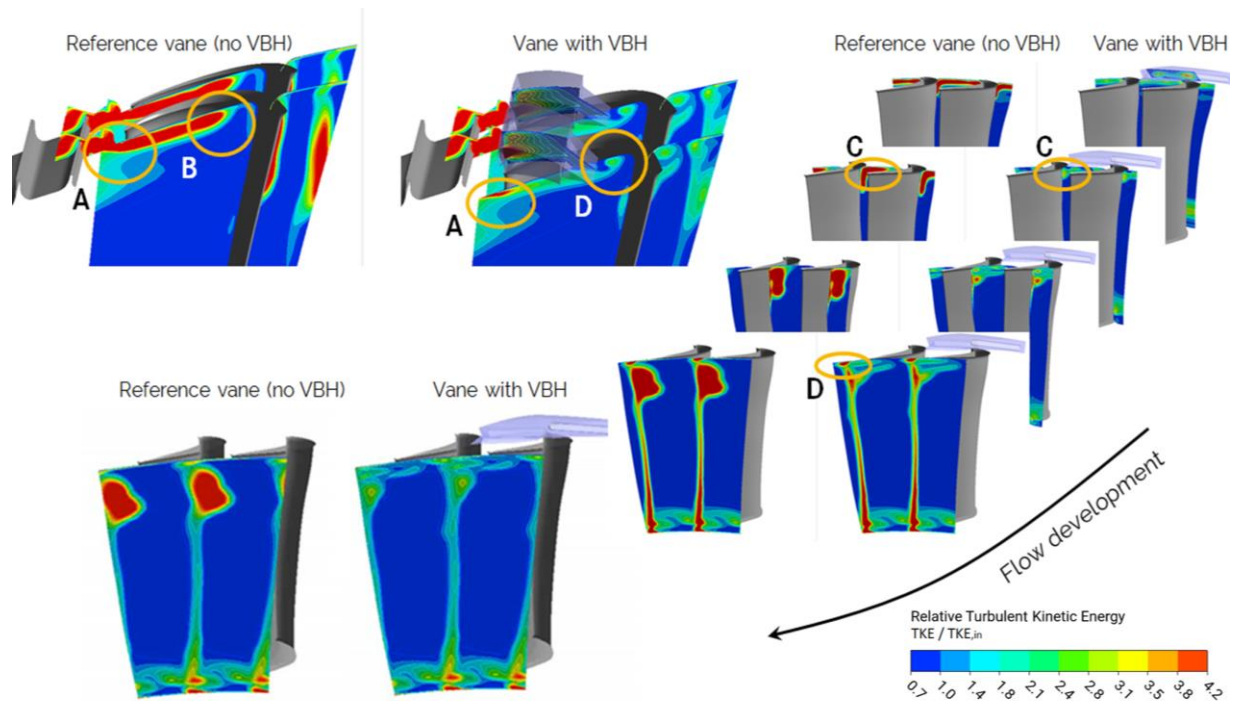


Figure 7.13 Flow field and development of the secondary flows for the Reference vane and vane equipped with VBH. Main flow features are marked with letters.

The flow is guided in the VBH channel in particular way, to achieve required circumferential and radial velocity angles. The better both flows are aligned in all directions, the less mixing occurs. However, the reintroduction of the VBH flow into the mainstream is associated with inevitable mixing losses (marked with **D**, in the Figure 7.13). It is difficult to avoid this completely, because both flows would require identical velocity vectors and temperatures, as indicated by Denton [15]. Nevertheless, the flow from VBH is noticeably better aligned with the mainstream and the mixing is also significantly reduced compared to the original situation.

7.2.2. Dimensional analysis for Vane Bleed Holes

In terms of flow similarity, Vane Bleed Holes cannot be treated with characteristic numbers identified for LPT OAS. It is because both flows are principally different. Flow through OAS is associated with blocking leakage with rotating labyrinth seal and VBH is a channel flow with latter blowing at the vane shroud.

Flow through VBH can be considered to be similar to blowing at the trailing edge of the compressor vane or to cooling of HPT. For those phenomena some characteristic quantities can be found at Fischer et al. [22] or Han et al. [33]. However, particularly for VBH, the similarity quantities can be obtained with dimensional analysis, applying procedure described in the Chapter 3. for determination of characteristic numbers for OAS. The quantities considered meaningful for flow through VBH are visualized in the Figure 7.14 and summarized in Table 7-3.

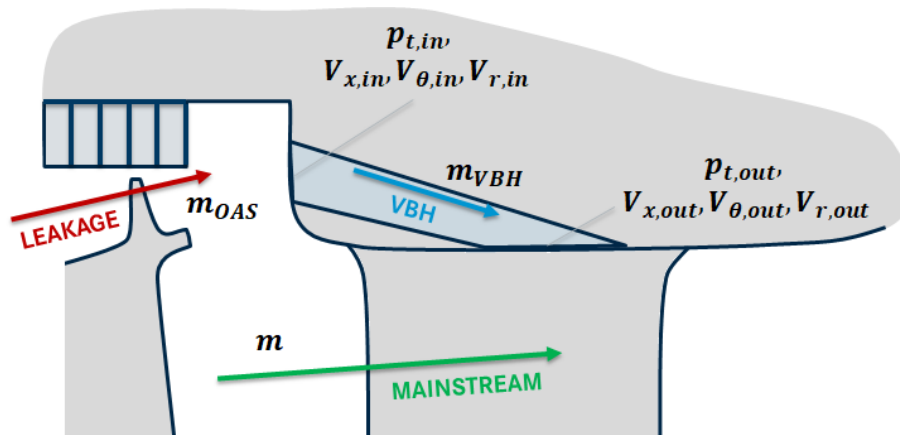


Figure 7.14 Quantities meaningful for flow through VBH

Table 7-3 Selection of quantities applied for Dimensional Analysis of VBH

| | |
|--|---|
| Quantities considered meaningful for VBH | $m_{VBH}, m, m_{OAS}, p_{t,VBH,in}, p_{t,VBH,out}, V_{x,VBH,in}, V_{x,VBH,out}, V_{\theta,VBH,in}, V_{\theta,VBH,out}, V_{r,VBH,in}, V_{r,VBH,out}, \alpha$ |
| Base units | [s], [m], [kg] |
| Chosen independent variables | $V_{x,VBH,out}, m_{VBH}, p_{t,VBH,in} \sim [m \cdot s^{-1}], [kg \cdot s^{-1}], [kg \cdot m^{-1} \cdot s^{-2}]$ |
| Dependent variables | $m, m_{OAS}, p_{t,VBH,out}, V_{x,VBH,in}, V_{\theta,VBH,in}, V_{\theta,VBH,out}, V_{r,VBH,in}, V_{r,VBH,out}, \alpha$ |

A result of the analysis is a set of meaningful characteristic parameters enabling comparisons between different cases and crosschecks in terms of flows similarity. In practice, it is very difficult to reach similarity with respect to all possible dimensionless numbers and flow phenomena. Due to that dimensional analysis assumes determination of the most meaningful quantities for particularly considered situation. Thus, the choice of the similarity parameters strongly depends on the researched phenomena and researched case.

For VBH flow, in particular it is considered that the characteristic numbers have to reflect transport of mass through the VBH channel and its reintroduction into the main gas path. The dependencies between the numbers resulting from dimensional analysis for VBH in general form are given in the eq. 7-1.

$$\frac{m_{VBH}}{m_{OAS}}, \frac{p_{t,VBH,in}}{p_{t,VBH,out}}, \alpha_{VBH,out}, \epsilon_{VBH,out} = f\left(\frac{m_{VBH}}{m}, \frac{V_{x,VBH,in}}{V_{x,VBH,out}}, \alpha_{VBH,in}, \epsilon_{VBH,in}, Ma_{VBH,out}\right) \quad \text{eq. 7-1}$$

The similarity numbers that are considered the most meaningful for describing VBH flow are fraction of OAS leakage transferred through VBH, pressure ratio and velocity angles. Other quantities are assumed to have smaller importance.

7.2.3. Evaluation of performance and sensitivities with simplified VBH model in 3-stage reference LPT

For the preliminary studies, a simplified VBH model is prepared and applied. The approach is described in the Chapter 3. It assumes modeling of VBH only by mass outlet and mass inlet boundary conditions, as shown in the Figure 3.12. Simplified modeling, complementarily to the dimensional analysis also helps in identifying parameters that are crucial for the performance of the feature.

The sensitivity studies are carried out by changing only one particular factor at the time. Other parameters are kept unchanged. It allows isolation of the influencing factors. For all studies with the simplified model one case three-dimensional VBH case modeled in detail in is given for reference.

Sensitivity to Mach number at VBH outlet

One of the drawbacks of the simplified model occurs to be considerable sensitivity to the VBH outlet Mach number. It is due to forcing of the assumed mass flow through the panel with area that may be arbitrary. In the analyses with the simplified modeling, for most of the test cases, it is assumed that the whole OAS leakage is transferred. Summary of assumptions in the simplified model parameters for this study is given in Table 7-4.

Table 7-4 Parameters of the simplified model for studies over Mach number

| Parameter | VBH outlet / inlet mass flow | VBH outlet circumferential angle | VBH outlet radial angle | VBH outlet Mach number | Other settings |
|-----------|------------------------------|----------------------------------|---------------------------------|------------------------|----------------|
| Variation | Constant | Constant | Constant | Variable (by area) | Constant |
| Setting | 100% leakage | Approx. mainstream angle | Const. inclination to flow path | 0.2 ÷ 1.2 | - |

As shown in the Figure 7.15, the efficiency benefit is nearly linear with the Mach number. Nevertheless, in this case this is only artificial gain. Actually, Mach number is defined by the pressure ratio between inlet and outlet. As visible in the Figure 7.15, imposing particular area for the VBH outlet, can result even in Mach number values around unity. In practical cases of OAS, the effective pressure ratio is not able to approach critical flow, especially if some energy is lost due to the internal losses inside the VBH channel. Thus, the right part of the trend is considered implausible.

This artificial increase in Mach number, thus also in efficiency, is caused by a definition of the mass outlet boundary condition. Particular mass flow is prescribed at the panel with flexibly assumed area, which is not known at this point. From these predefined quantities results velocity, thus also Mach number. Even if the area is too small to transfer the mass flow in realistic case, due to the definition of this boundary condition, it is imposed at the panel, causing high Mach at the outlet. The efficiency benefit comes then from artificially added flow with high kinetic energy that results in improvement in the machine performance. On the other hand, if Mach number at the panel is too small, a decrease in efficiency appears, as visible from the data in the Figure 7.15. This refers to the situation when VBH flow is reintroduced with low velocities resulting in increased mixing losses, due to considerable difference between the flow and the mainstream.

LPT efficiency gain with respect to Mach number
at VBH outlet in simplified model

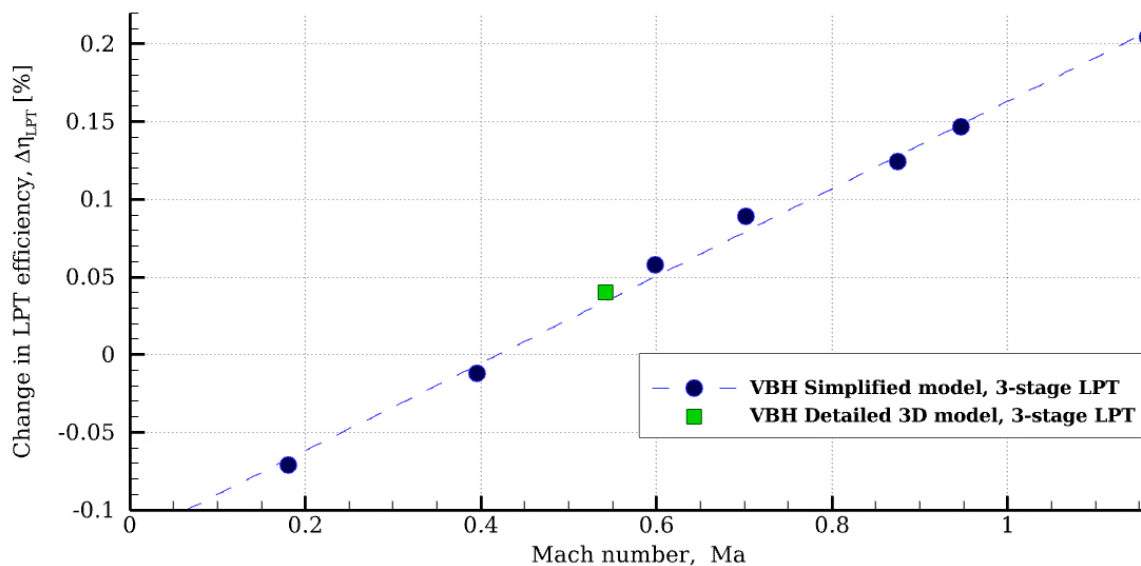


Figure 7.15 Sensitivity to Mach number at VBH outlet. Results obtained with simplified modeling

The performed study indicates the fact that the efficiency benefit predicted with simplified VBH model strongly depends on the Ma at the VBH outlet. The simplified modeling allows also for unphysical conditions at the outlet, due to undefined outlet area. To eliminate this sensitivity, in

all subsequent analyses, Mach number at the VBH outlet is kept constant. Based on the pressure conditions calculated at both boundaries approximating VBH inlet and outlet, Mach number is calculated for a level around 0.6. This reflects real situation that Mach number is actually fixed between two pressures at inlet and outlet of the channel. The estimated value is reasonable, because, as visualized in the Figure 7.15, it is close to the Mach number resulting from preliminary 3D detailed model of VBH.

Sensitivity to VBH mass flow

Another factor strongly impacting benefit from the solution occurs to be mass flow through the VBH channel. It is found convenient to consider the VBH mass flow as a fraction of the OAS leakage mass flow, because the leakage determines primarily flow field directly at the shroud. Summary of assumptions in the simplified model parameters for this study is given in the Table 7-5.

Table 7-5 Parameters of the simplified model for studies over VBH mass flow fraction

| Parameter | VBH outlet / inlet mass flow | VBH outlet circumferential angle | VBH outlet radial angle | VBH outlet Mach number | Other settings |
|------------------|-------------------------------------|---|---------------------------------------|-------------------------------|-----------------------|
| Variation | Variable | Constant | Constant | Constant (by varying area) | Constant |
| Setting | 25% ÷ 150% leakage | Approx. mainstream angle | Const. inclination to flow path | 0.6 | - |

As visible in the figure, the solution is ineffective, if less than 50% of the leakage from OAS enters the VBH channel. In such case even if the flow inside VBH channel is guided and later it is reintroduced with proper velocity angles, at the reentry it does not mix with the mainstream, but rather with the remaining leakage flow, which is kept close to the casing. That is explained and visualized better by the Figure 7.21 and Figure 7.22, during analysis of the results from the detailed model of the VBH.

It is also concluded from the plot in the Figure 7.16 that the most beneficial is to transfer considerable portions of the flow through VBH – preferably entire the entire leakage and slightly more. In addition, for reference, in the Figure 7.16 the preliminary 3D detailed VBH model is shown. It indicates realistic amounts the mass flow possible to be transferred through the channel.

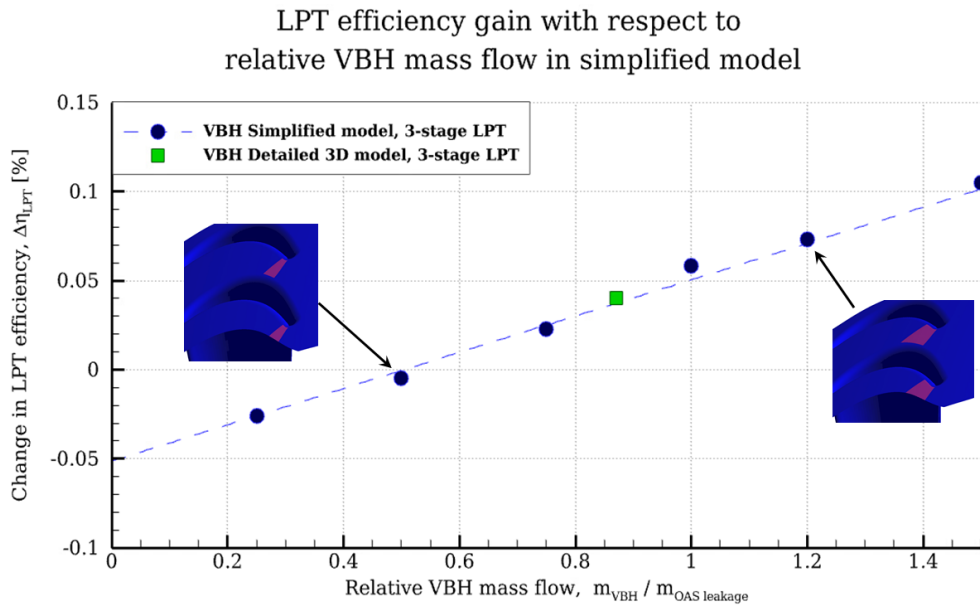


Figure 7.16 Sensitivity to fraction of the OAS leakage mass flow. Results obtained with simplified modeling

Sensitivity to VBH outlet location

Pressure ratio is one of the similarity parameters identified in the Dimensional Analysis of VBH. With simplified model, impact of the pressure ratio cannot be investigated straightforwardly, due to the limitations of this approach. Nevertheless, the position of the VBH outlet is connected to the overall pressure ratio that is achieved between VBH inlet and outlet. The closer the VBH outlet is located with respect to the leading edge of the vane, the smaller pressure ratio is obtained. On the other hand, the more it is located downstream and closer to the throat, the more pressure ratio increases. Higher pressure ratio drives higher mass flow through VBH. Greater VBH mass flow is beneficial as discussed in the previous section. Summary of assumptions in the simplified model parameters for this study is given in the Table 7-6.

Table 7-6 Parameters of the simplified model for studies over VBH outlet location

| Parameter | VBH outlet / inlet mass flow | VBH outlet circumferential angle | VBH outlet radial angle | VBH outlet Mach number | VBH outlet position | Other settings |
|------------------|------------------------------|----------------------------------|---------------------------------|------------------------|---------------------|----------------|
| Variation | Constant | Variable | Constant | Variable (by area) | Variable | Constant |
| Setting | 100% leakage | Approx. mainstream angle | Const. inclination to flow path | 0.2 ÷ 1.2 | As in Figure 7.17 | - |

For the investigations of the outlet location with simplified model, mass flow that is imposed is kept constant for consistency. At different locations, different pressure ratio implicates different Mach numbers at the VBH outlet. Due to that, it is convenient to plot different locations against Mach number at the VBH in the Figure 7.17.

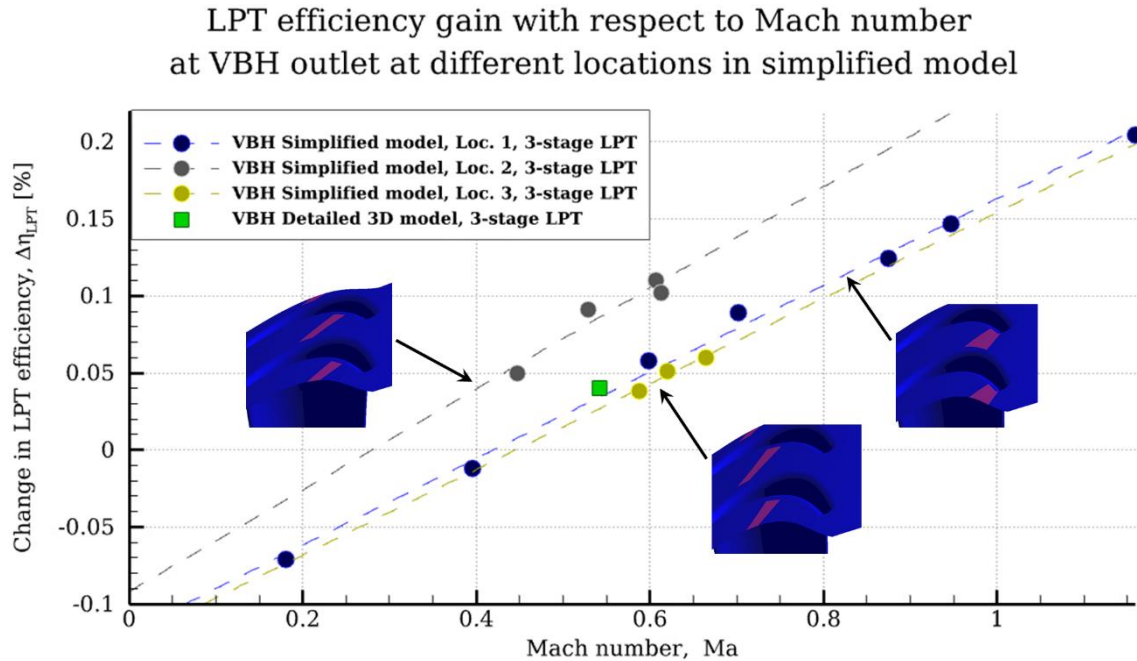


Figure 7.17 Sensitivity to VBH outlet location. Results obtained with simplified modeling

The figure reveals that upstream placement of the VBH outlet in some cases may lead to further benefits. This corresponds to the literature findings [15] that losses are less enhanced if the mixing occurs at smaller velocities. As visible in Figure 7.17, trend of one of the investigated upstream locations, across Mach number range, gives higher benefits than those located directly at the throat. Nevertheless, it needs to be accounted that the upstream location of the VBH outlet in the simplified model is associated also with smaller Mach number, reflecting decrease in the pressure ratio. These results from the studies over the VBH outlet location show that with simplified modeling, indication of the proper direction with respect to the outlet placement is not straightforward. Due to that, the investigation is followed closely with detailed 3D VBH modeling.

Sensitivity to circumferential velocity angle at the VBH outlet

Decrease of secondary flows at vane shroud, as indicated in Figure 7.12, can be achieved with reintroduction of the VBH flow at certain angle with respect to the flow in the vane passage. The directional blowing as researched in the literature, e.g. by Fisher et al. [22], can either strengthen or weaken the passage vortex. Summary of assumptions in the simplified model parameters for this study is given in Table 7-7.

Table 7-7 Parameters of the simplified model for studies over VBH mass flow fraction

| Parameter | VBH outlet / inlet mass flow | VBH outlet circumferential angle | VBH outlet radial angle | VBH outlet Mach number | Other settings |
|-----------|------------------------------|---|---------------------------------|----------------------------|----------------|
| Variation | Constant | Variable | Constant | Constant (by varying area) | Constant |
| Setting | 100% leakage | Approx. mainstream angle $\pm 30^\circ$ | Const. inclination to flow path | 0.6 | - |

With particular blowing at VBH outlet, further benefits are expected if the passage vortex developing at the vane shroud is weakened. Due to that it is approached to analyze variation in circumferential velocity angle at few axial locations upstream of the throat, according to the findings from the previous section. All cases are adjusted with respect to particularly calculated Mach number at outlet at a resulting pressure ratio, each time adjusting area. Beside variation in the circumferential velocity angle, all other parameters in simplified model are unchanged. The results are presented in the Figure 7.18.

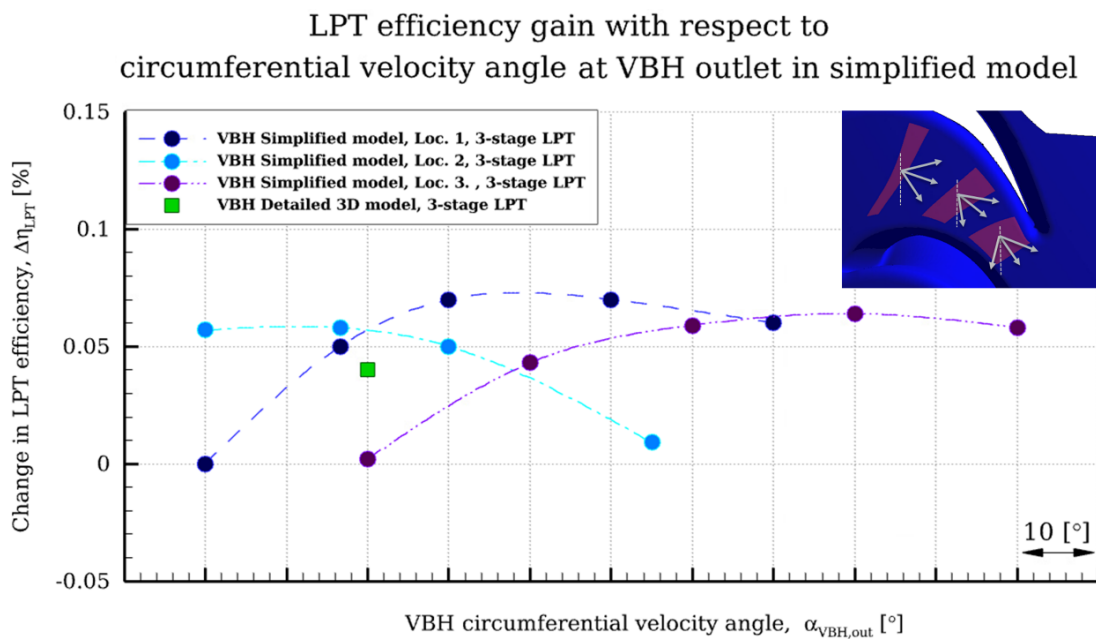


Figure 7.18 VBH sensitivity to circumferential velocity angle at the VBH outlet

The benefit and the trends are similar for all investigated locations. For these parameters, trends are not linear. At each axial location, a maximum efficiency gain appears for the outflow circumferential velocity angle corresponding to a local circumferential velocity angle in the mains gas path. A sensitivity to the circumferential velocity angle is not that considerable. The gain is similar in a range of ± 20 deg of the circumferential velocity angle at the VBH outlet. Nevertheless, choice of improper outflow angle at the VBH outlet can lead to nearly complete reduction in the benefit, thus these parameters also need to be carefully considered.

Sensitivity to VBH radial velocity angle at the VBH outlet

Simplified modeling allows also flexibility in adjustment of the velocity angle at the VBH outlet. It is possible to investigate outflows that are introduced very steeply into the mainstream as well as nearly tangentially to the vane shroud. Figure 7.19 pictures the dependency of the benefit from VBH with respect to the variation in radial velocity angle at the VBH outlet. Summary of assumptions in the simplified model parameters for this study is given in Table 7-8.

Table 7-8 Parameters of the simplified model for studies over VBH mass flow fraction

| Parameter | VBH outlet / inlet mass flow | VBH outlet circumferential angle | VBH outlet radial angle | VBH outlet Mach number | Other settings |
|-----------|------------------------------|----------------------------------|---|----------------------------|----------------|
| Variation | Constant | Constant | Variable | Constant (by varying area) | Constant |
| Setting | 100% leakage | Approx. mainstream angle | Varied $\pm 10^\circ$ with respect to flow path inclination | 0.6 | - |

As visible in the figure, the more the flow from VBH outlet is tangential to the main flow path, the better for machine performance. It is also in agreement with the literature findings, e.g. Denton [15] indicated that the difference in the velocity directions of two flows that join, results in the losses. The VBH solution intends to reduce the mixing losses. Due to that reintroducing flow back to the mainstream steeply is detrimental for the machine performance and reduces the benefit. The trend in the Figure 7.19 is again very linear. The biggest gain is observed when the flow from VBH outlet tends to be the most aligned with the main channel.

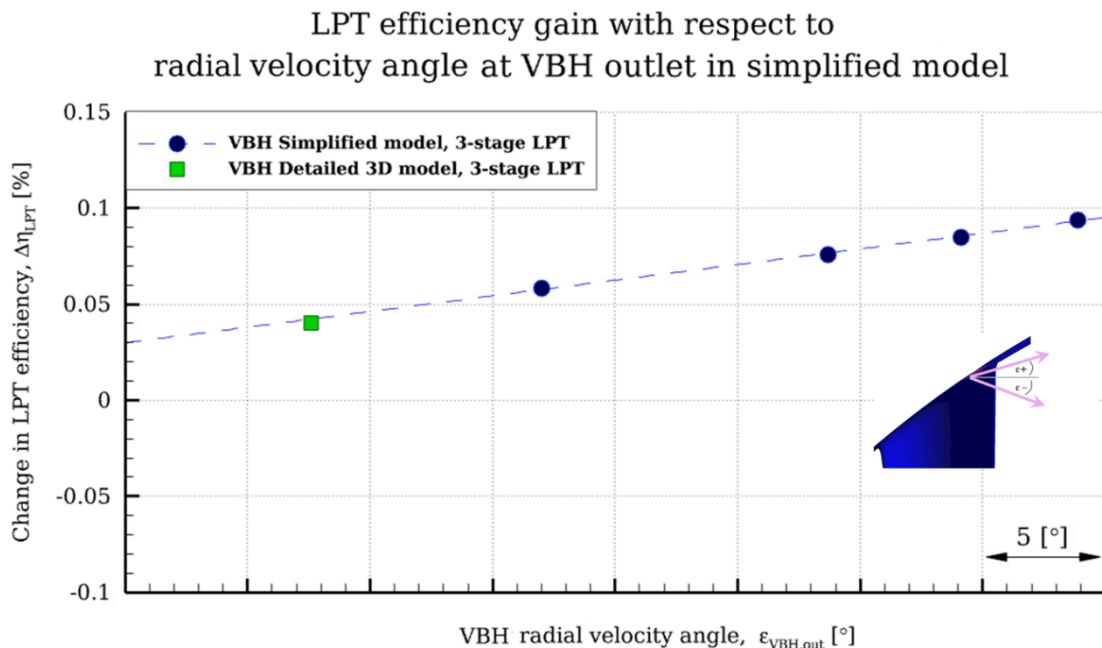


Figure 7.19 Sensitivity to radial velocity angle at the VBH outlet. Results obtained with simplified modeling

For reference, also the preliminary detailed 3D VBH model is plotted in the figure. The detailed model lies within the trend line of the simplified one. Nevertheless, the detailed modeling of the VBH channel geometry reveals that achieving small radial velocity angle at the reintroduction is difficult in practice. As visible in the Figure 7.19, the flow resulting from 3D geometry modeling in the preliminary case results in a steep inflow into the mainstream. This points to the possible design challenges with respect to radial angle at the VBH outlet for the practical applications.

Conclusions from the sensitivity study on the simplified VBH model

The study on the simplified model indicates possible directions for further studies. Due to some limitations of the simplified modeling approach e.g. considerable sensitivity to Mach number at the VBH outlet or no loss model between VBH mass outflow and inflow, further research needs to be carried out with the detailed 3D VBH models.

Results received with the simplified model, point that with respect to the absolute efficiency benefit and its trend, the greatest importance has amount of mass flow transferred through the VBH channel. It is concluded that it is most beneficial to transfer considerable portions of the flow through VBH – preferably entire leakage or even slightly more. Second greatest importance has radial velocity angle. The biggest gain is observed when the flow at the VBH outlet tends to be the most aligned with the main channel. Further importance has also circumferential velocity angle. That should be aligned with the flow direction of the mainstream at the reintroduction. Based on the simplified model, it is not straightforward however, where to place the VBH outlet. However, upstream placement of the VBH outlet in some cases may lead to further benefits from the solution.

7.2.4. Assessment of VBH performance and directions for optimization on detailed 3D model in the 1.5-stage part of the reference LPT

In the previous section, the main sensitivities for VBH performance are determined. Simplified model, beside many advantages, in particular numerical robustness, simplicity and flexibility in variation of the parameters has also certain limitations and involves several assumptions. Due to that, research of the primary factors impacting VBH performance is carried out with the detailed 3D VBH modeling. Isolation of the influencing factors is more difficult on the feature modelled in three-dimensional space. Nevertheless, also the trends resulting from the analyses are more reliable prerequisiting the validated 3D CFD model.

Detailed modeling provides further insights into the operation of VBH and crosschecks trends resulting from the simplified model. The investigations are carried out on the 1.5-stage part of the reference LPT, according to the methodology described in the Chapter 3. It is aimed to carry out complete study on the most important VBH parameters impacting its performance. It is supposed to indicate directions for determining the most promising configuration of the VBH

solution. The learnings with respect to the configuration are later transferred to the full model of the reference LPT in order to evaluate final benefit expected from the solution.

Impact of the VBH flow amount

Foregoing studies, indicate that the ratio of mass flow through VBH and OAS leakage has primary importance for performance of the solution. With detailed model it is also aimed to investigate the efficiency benefit for a range of mass flows through VBH. The variation in mass flow is realized with a decrease in a cross-sectional area of the channel in the vicinity of the outlet. Summary of variations in the geometrical parameters of VBH for this study shown in the Figure 7.20 is given in Table 7-9.

Table 7-9 Geometrical variations of VBH for flow amount study

| Parameter | VBH inlet | VBH mid channel | VBH outlet | Smallest cross-sectional area | Other |
|-----------------------|-----------|-----------------|------------|-------------------------------|----------|
| Geometrical variation | Constant | Constant | Constant | Variable | Constant |

Figure 7.20 presents change in the efficiency benefit for different VBH mass flows. It is convenient to plot the efficiency gain against the VBH mass flow as a fraction of the OAS leakage flow, because the leakage determines flow field directly at the shroud.

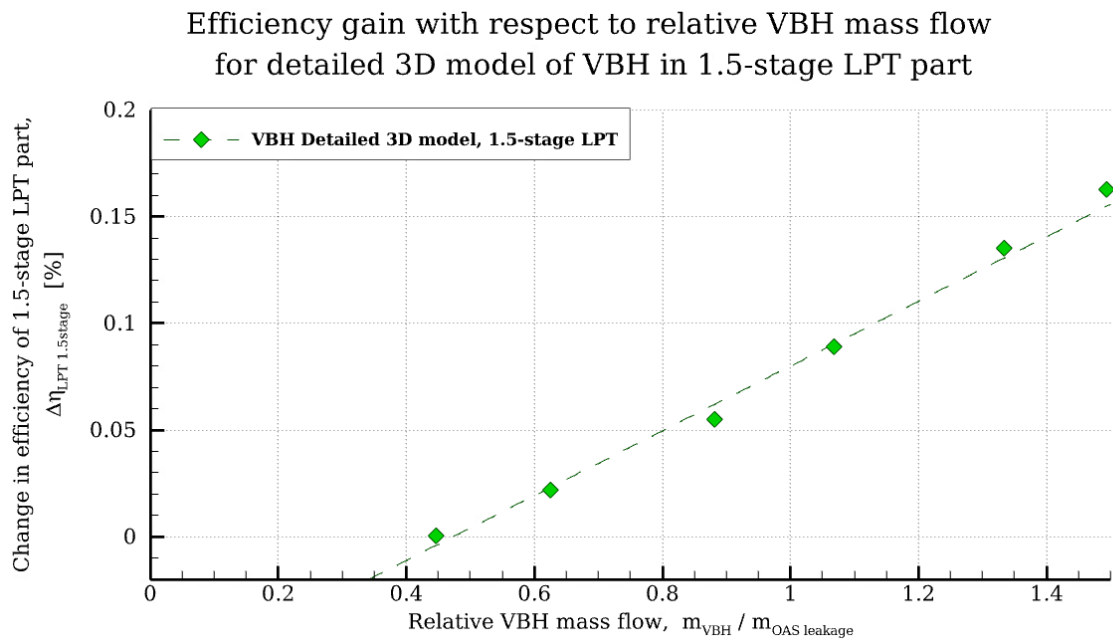


Figure 7.20 Efficiency benefit resulting from VBH with respect to leakage mass flow fraction obtained with detailed 3D model of VBH on a 1.5-stage part of reference LPT

As visualized in the Figure 7.20, detailed modeling confirms previous observations that the higher the mass flow through the VBH, the higher overall efficiency gain. The overall trend well corresponds to the one obtained with the simplified modeling. The absolute level of the

efficiency benefit is not on the same level as in case of the whole turbine. However, the gradient, similarly to the simplified model, is also linear and increasing with increasing OAS leakage and VBH flow ratio.

The leftmost part of the trend presented in the Figure 7.20 indicates that VBH may also decrease machine performance. Correspondingly to conclusions from earlier sections, the solution does not bring any benefit, if less than 50% of the leakage from OAS enters the VBH channel. In such case even if the flow inside VBH channel is properly guided and reintroduced with appropriate velocity angles, at the reentry, it does not mix with the mainstream, but with the remaining leakage flow that is kept close to the casing. Hence, even more mixing loss is induced at the reentry. It is visualized in the Figure 7.21 and Figure 7.22. Such situation is unfavorable. Thus, VBH channels shall be designed in a way that the amount of the VBH flow is kept appreciably above the level of 50% of the OAS leakage flow.

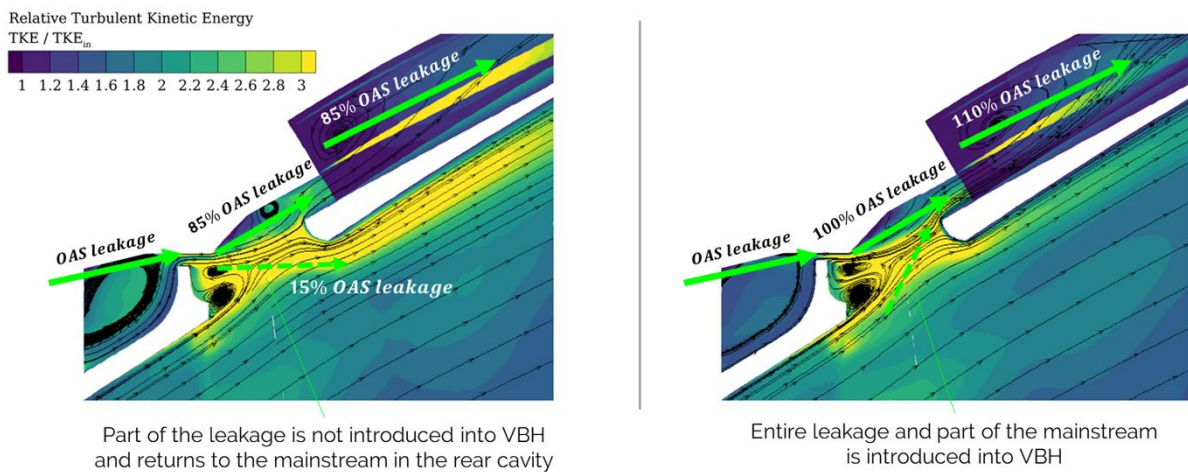


Figure 7.21 Visualization of exemplary scenarios for two different VBH flows as a fraction of the OAS leakage obtained with detailed model of VBH

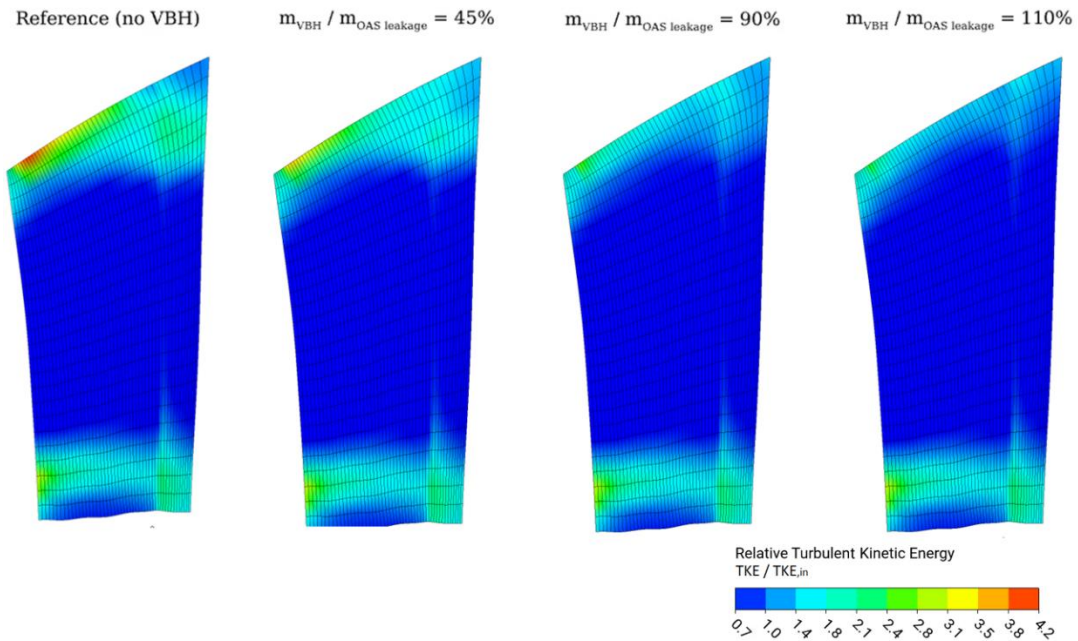


Figure 7.22 Circumferentially averaged relative Turbulent Kinetic Energy for different ratios of OAS leakage and flow through VBH flow.

Detailed modeling of the VBH reveals however, that it is also possible to introduce into VBH channel even slightly more than OAS leakage flow. This corresponds to the second situation pictured in the Figure 7.21. It is also visualized in the Figure 7.22. In such case, also small portion of the mainstream flowing down from the foregoing blade shroud goes through the VBH. In this way, with application of the solution, it is possible to considerably reduce secondary flows that would inevitably arise across the vane. It is confirmed by the results presented in the Figure 7.20 and the Figure 7.23 that even higher benefit from the solution is expected, if VBH transfers more than 100% of the OAS leakage.

Summary of variations in the geometrical parameters of VBH for this study shown in the Figure 7.23 is given in Table 7-10.

Table 7-10 Geometrical variations of VBH for inlet configuration study

| Parameter | VBH inlet | Cross-sectional area at the inlet | VBH mid channel | VBH outlet | Other |
|-----------------------|-----------|-----------------------------------|-----------------|------------|----------|
| Geometrical variation | Variable | Variable | Constant | Constant | Constant |

The Figure 7.23 visualizes efficiency benefit and the VBH mass flow for miscellaneous configurations of the VBH inlet. Multiple configurations including variations in the inlet geometry are investigated. As visible in the figure, proper inlet configuration can further enhance the benefit. Investigations prove that the inlet is also important for the overall mass transferred through the VBH channel.

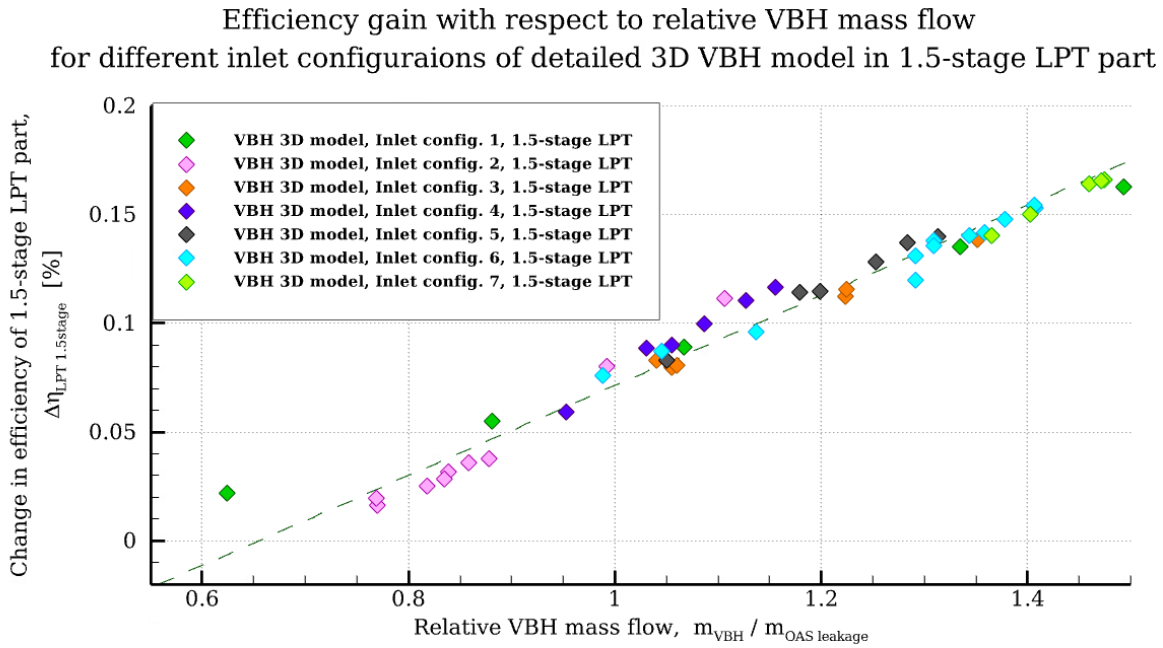


Figure 7.23 Efficiency benefit from VBH with respect to mass flow transferred through VBH for different inlet configurations. Results obtained with detailed 3D model of VBH on a 1.5-stage part of the reference LPT

The analyses confirm that it is possible to find configurations of VBH that enable transfer of the considerable mass flow through the channel. In addition, these analyses still confirm the identified linear trend and increasing efficiency benefits with the increasing flow through VBH. Nevertheless, in practice, due to design constraints and other limitations e.g. in existing pressure ratio, it is difficult to transfer significant mass flows through the VBH channel what leads to reduced benefits.

Impact of VBH radial velocity angle at outlet

The sensitivity study on the simplified model revealed that radial velocity angle is another important factor driving efficiency benefit from the solution. That is also corresponding to the findings from Dimensional Analysis of VBH. To further evaluate these findings, the radial angle at the VBH outlet is investigated on the detailed VBH model in the 1.5-stage part of the reference machine. To receive isolated impact of only radial velocity angle, the outlet part of the VBH is redesigned. In this way only the change in the rear part of the channel, near the reentry region, is obtained. Simultaneously other fragments of the channel are intentionally unchanged. In particular, efforts are made to keep the same cross-sectional area, to settle the mass flow. Summary of variations in the geometrical parameters of VBH for this study is given in Table 7-11.

Table 7-11 Geometrical variations of VBH for studies over radial angle at the VBH outlet

| Parameter | VBH inlet | VBH mid channel | VBH outlet radial inclination | Smallest cross-sectional area | Other |
|-----------------------|-----------|-----------------|-------------------------------|-------------------------------|----------|
| Geometrical variation | Constant | Constant | Variable | Constant | Constant |

The results obtained with the detailed 3D VBH model are presented in the Figure 7.24. As visible from the chart, the radial velocity angle influences considerably benefit from VBH. The absolute level of the efficiency benefits is not exact, due to modeling on the 1.5-stage part of the reference LPT. The trend is nearly linearly increasing with increasing radial velocity angle. It well corresponds to the trend received with the simplified model.

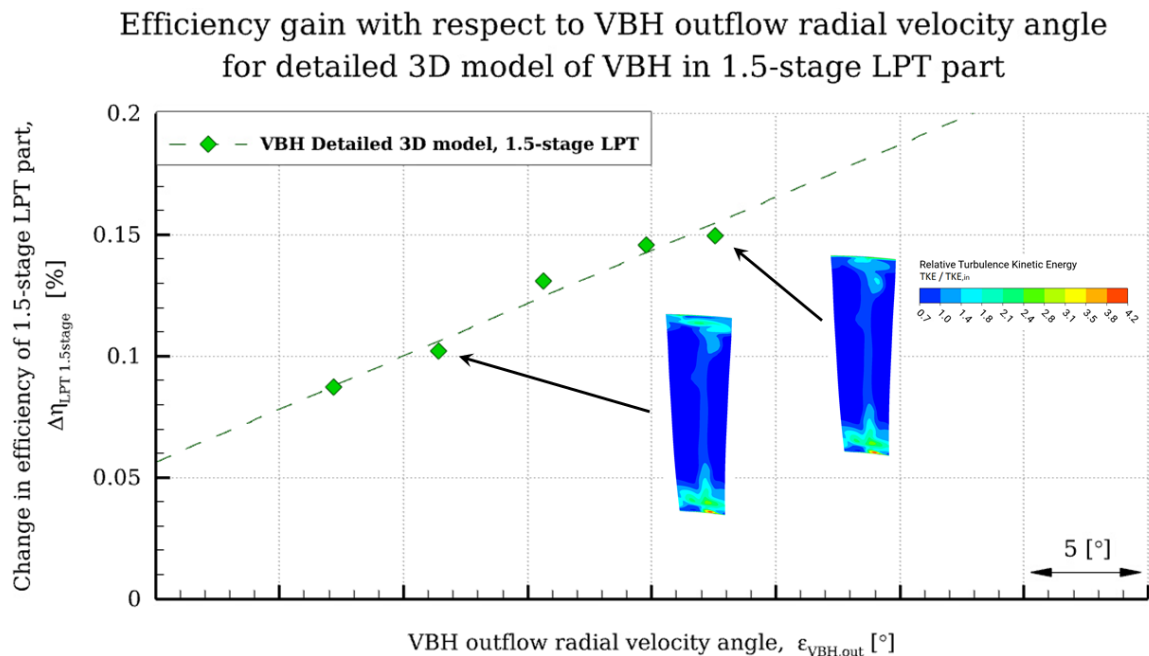


Figure 7.24 Efficiency benefit resulting from VBH with respect to leakage mass flow fraction obtained with detailed 3D model of VBH on a 1.5-stage part of reference LPT

Additionally, for better visualization of the impact of the VBH radial velocity angle at the VBH outlet, in the Figure 7.24 are presented contours of TKE at the outlet of the vane. Two cases with different radial velocity angle are shown. They clearly visualize the region influenced by the steep outflow from the VBH. Later on this flow goes to a subsequent rotor, reducing its performance.

As a conclusion from these investigations, the VBH outflow at its outlet should be kept as tangential as possible to the main flow path. The better the flow is aligned with the angle of the main channel, the better for the machine performance. It is also in agreement with general

understanding of the reduction in mixing losses, e.g. provide by Denton [15]. Reintroducing the flow back into the main flow steeply is detrimental for the flow, because it results in enhanced mixing losses.

Impact of VBH outlet inclination

Analyses carried out on the detailed model of the VBH indicate that there is also one more important aspect of the VBH design. It is inclination of the outlet of VBH with respect to the airfoil in the main gas path. The flow situation in the passage is complicated due to the shape of the airfoils. It is illustrated in the Figure 7.25. Both static pressure as well as the flow direction vary along the vane passage. For the VBH important are both – pressure ratio existing between its inlet and outlet as well as the flow direction, due to the mixing losses. As discussed in the previous section, pressure ratio is one of the important factors that drive mass flow through the channel. Circumferential velocity angle has consequences with respect to the mixing of the VBH flow and the mainstream. Reviewing plots in the Figure 7.25, it is visible that isolines of both quantities have different direction and their inclination is not the same in any place.

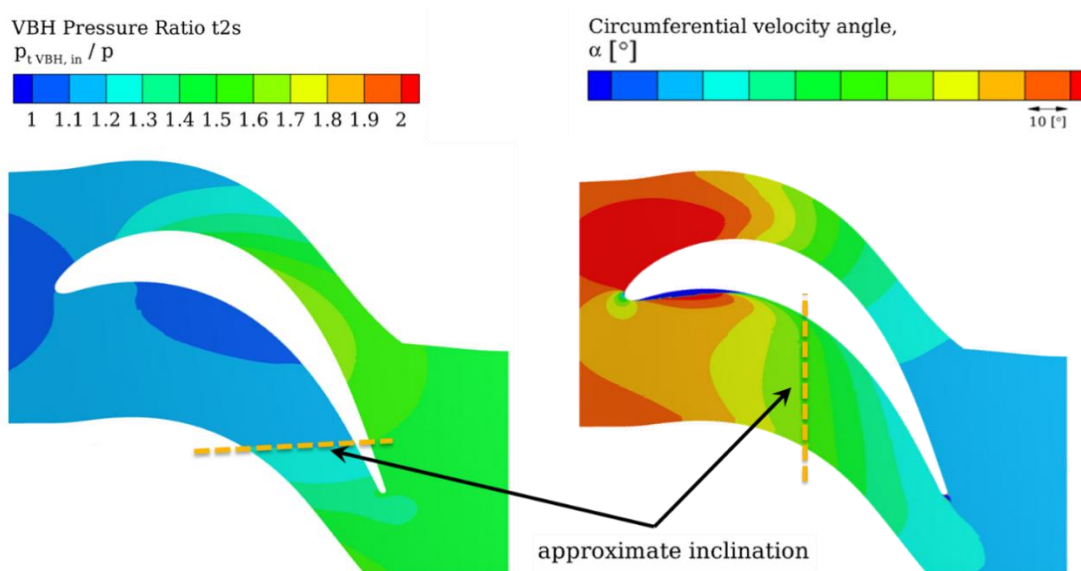


Figure 7.25 Contours of pressure ratio between inlet and outlet of VBH and circumferential velocity angle in the vicinity of the vane shroud

Because both factors can influence overall performance of the VBH and because VBH outlet can be positioned in different ways in the passage, the most beneficial configuration of the outlet with respect to the inclination to the vane is researched.

The outlet geometry is rotated with respect to its center of gravity, changing its staggering to the airfoil. The efforts are made to isolate only this influencing factor. In the study complete geometry of the VBH channel beside the outlet are kept the same. In particular, the outlet area and cross-sectional areas are fixed to differentiate variation in the mass flow caused by the change in the pressure ratio from the area changes. Several cases are researched covering

complete range of outlet configurations, realizable from a design perspective. The resulting efficiency benefit together with the relative VBH mass flow are presented in the Figure 7.26. Summary of variations in the geometrical parameters of VBH for this study is given in Table 7-12.

Table 7-12 Geometrical variations of VBH for studies over outlet inclination

| Parameter | VBH inlet | VBH mid channel | VBH outlet inclination | Smallest cross-sectional area | Other |
|-----------------------|-----------|-----------------|------------------------|-------------------------------|----------|
| Geometrical variation | Constant | Constant | Variable | Constant | Constant |

It is visible, that the efficiency pick occurs for the outlet aligned in the direction of the isolines of circumferential velocity angle. On the other hand, the relative mass flow pick appears, as expected, for the geometry with the outlet inclination following pressure ratio isolines from the Figure 7.25. For better visualization of this effect, in addition, in the Figure 7.26, the contours of the relative mass flow with plotted isolines of the pressure ratio are shown for two extreme outlet configurations. It is clear, that in both cases actually mass flow is driven to the locations with the smallest static pressure, thus with the highest pressure ratio. It confirms expectations that due to the maximal driving force, the mass flow for these cases is also maximal.

Efficiency gain and relative mass flow with respect to VBH outlet configuration of detailed 3D model of VBH in 1.5-stage LPT part

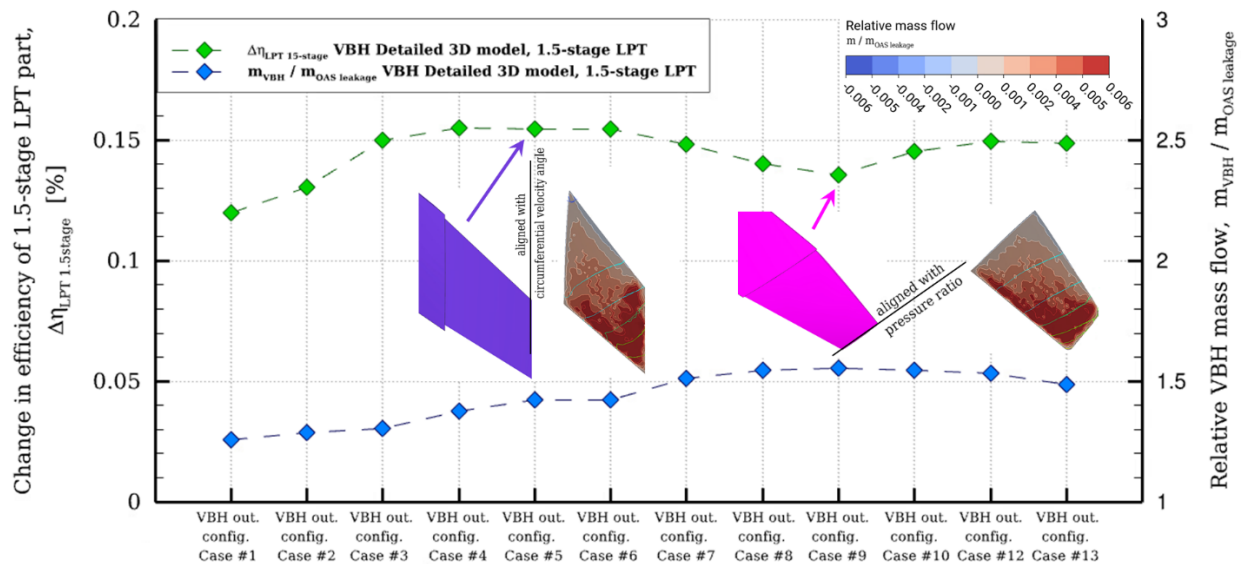


Figure 7.26 Efficiency benefit resulting from VBH with respect to outlet configuration obtained with detailed 3D model of VBH on a 1.5-stage part of reference LPT

As visible from the plot in the Figure 7.26, inclination in the direction of the pressure ratio results in approximately 20% more mass flow through VBH. Previous studies indicate that the increase in the VBH mass flow should result in bigger benefits from the solution. Referring to the Figure 7.20, the overall benefit should be increased by several hundredths, due to the mass flow

increase. However, as visible in the Figure 7.26, for the location with the highest mass flow, occurs the smallest efficiency out of all investigated cases. It is because by varying outlet staggering, the mixing losses are also influenced, due to changed direction of the outflow from the VBH outlet. It confirms that the decrease in the mixing losses at the reentry has importance for the final efficiency benefit from the solution. The study shows that the benefit resulting from the increased mass flow can be counterbalanced by the enhanced mixing losses. Nevertheless, it is considered, the efficiency curve with respect to the outlet staggering is rather flat. It indicates that the solution is robust with respect to the outlet inclination, allowing some flexibility. Also, the difference in the efficiency benefit is not primarily significant – in the order of few hundredths, nevertheless it indicates that both investigated factors have opposite impact on the VBH performance. Hence, pointing to the conclusion that the definition of the most promising VBH configuration is an optimization task.

Impact of VBH outlet position and circumferential angle at the VBH outlet

Previous studies with respect to the outlet position along the vane passage revealed that the choice of the VBH outlet configuration is no straightforward and it has to be followed in the detailed 3D model of VBH.

As visible in the Figure 7.25, the curvature of the airfoil, implies changes of the flow direction in the main gas channel. Due to these facts, research in the variation in the VBH outlet position has to be coupled with the simultaneous change in the circumferential velocity angle at VBH outlet. If the velocity angle is kept the same, it will result in enhanced mixing losses as described in the previous section. Due to that, at every investigated location it is attempted to vary circumferential velocity angle in a considerable range of several dozen. The change is realized by particular shaping of the VBH channel. Simultaneously, to isolate the investigated factors all other VBH features, e.g. the radial velocity angle, are unchanged. The Figure 7.27 shows impact of location as well as the impact of the circumferential velocity angle on the efficiency gain and on the mass flow through VBH. Summary of variations in the geometrical parameters of VBH for this study is given in Table 7-13.

Table 7-13 Geometrical variations of VBH for studies over outlet position and circumferential velocity angle

| Parameter | VBH inlet position | VBH mid channel | VBH outlet position | Smallest cross-sectional area | Other |
|------------------------------|---------------------------|------------------------|----------------------------|--------------------------------------|--------------|
| Geometrical variation | Variable | Variable | Variable | Constant | Constant |

Similarly, to the cases investigated in the previous sections, there are several factors influencing the benefit from the solution. According to the literature findings [15], there are several aspects impacting mixing losses. The entropy production increases when: the remixing occurs in the region of high Mach number, reinjected mass flow is considerable, difference in the temperatures is high and both flows are considerably different with respect to the velocity vectors directions and magnitudes.

Two separate trends are visible in the Figure 7.27. The first apparent tendency in the chart is with respect to the location. The highest benefit appears in the vicinity of the biggest curvature of the airfoil. Towards the throat as well as towards the leading edge, the benefit declines.

Efficiency gain and relative mass flow with respect to VBH outlet location and outflow circumferential angle of detailed 3D VBH model in 1.5-stage LPT part

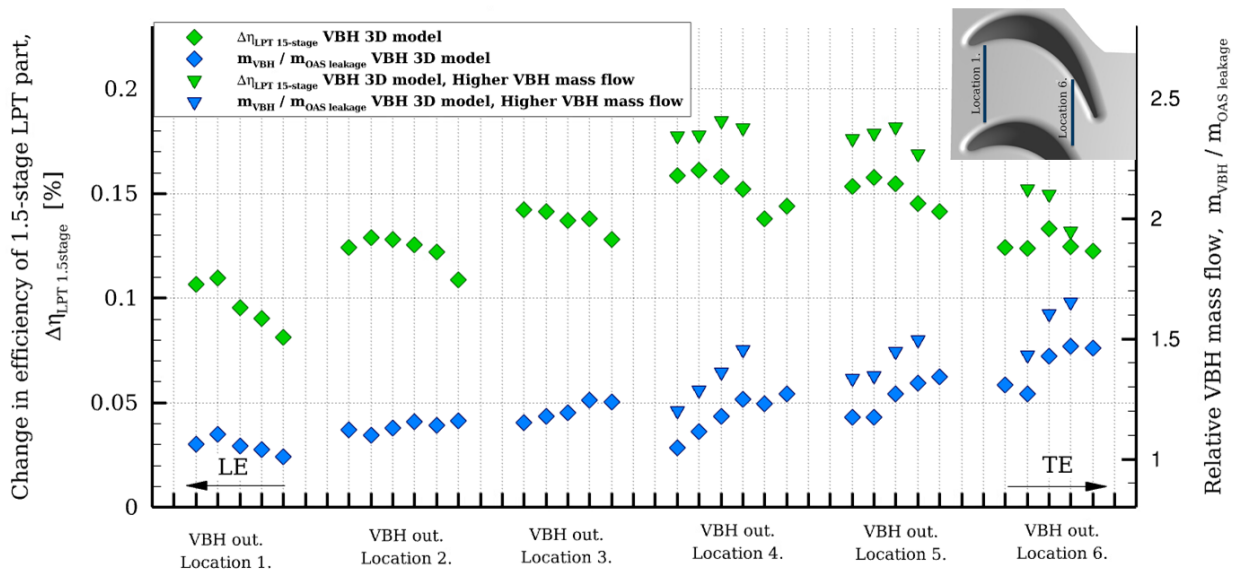


Figure 7.27 Efficiency benefit resulting from VBH with respect to outlet position obtained with detailed 3D model of VBH on a 1.5-stage part of reference LPT

In the direct vicinity of the throat, the highest location Mach number region exists. Reentry at this region, magnifies mixing losses. In consequence that reduces the benefit. On the other side, there are two factors causing that reintroducing very close to the leading edge – in a small Mach number region – is also not optimal. VBH outlet location close to the leading, enforces VBH channel to be short. It does not allow leakage flow to be well aligned inside the VBH channel. Second aspect is also that early reintroduction of the flow favors induction of the secondary flows what also decreases benefits.

Another trend visible in the Figure 7.27 is with respect to the circumferential velocity angle. This trend is well in line with the Figure 7.18 and the results obtained with the isolated factors in the simplified model. The peak of the efficiency benefit appears also at the reintroduction angle that

is the closest to the flow direction in the passage. It again confirms that further benefits result from small mixing losses if the velocities are aligned at the VBH reentry.

Nevertheless, results presented in the Figure 7.27 indicate that some of the influencing factors are contradictory to the previously investigated main trends for the VBH benefits. Especially in respect to the mass flow transferred through the channel. As discussed, based on the Figure 7.20, the benefits from VBH increase with increased fraction of OAS leakage. Observing the trend in the Figure 7.27, the VBH mass flow increases, towards the throat. With this mass flow increase, the efficiency benefit is in fact decreased. The reasoning is similar as the one discussed in the previous section, analyzing outlet inclination in the Figure 7.26.

As mentioned above, the literature research indicate that the bigger mass flow is reinjected in the high Mach number region and the bigger the difference in the velocity angles, the higher are mixing losses. That in consequence reduces benefits from VBH. It is well visible in trend towards the throat of the efficiency benefit in the Figure 7.27. To further investigate these findings, two locations are investigated in detail. Figure 7.28 and Figure 7.29 visualize additionally circumferentially averaged plots of the relative entropy in the vane passage. Figure 7.28 provides these plots for all circumferential angles being investigated in the Location 4. in the vicinity of the inflection point at the suction side of the airfoil and the Figure 7.29 pictures all investigated cases at the Location 6 in the vicinity of the throat.

The Figure 7.28 reveals that in comparison with the reference case, a considerable part of the mainstream is much less influenced by the losses from the leakage. The flow is improved up to around 70% of the channel height. Only in the closest vicinity of the shroud the entropy is produced due to mixing losses at the reentry of the VBH flow. However, this flow is kept directly at the shroud not impacting the core stream significantly. Similar behavior can be noted in the Figure 7.29. But in addition, the figure confirms that despite proper alignment of the flow directions, reintroduction in the high Mach number region leads to higher mixing losses. It indicates that the previous conclusions with respect to the mass flow are still applicable and that the decrease in the VBH performance with respect to location is indeed caused by the enhanced mixing losses.

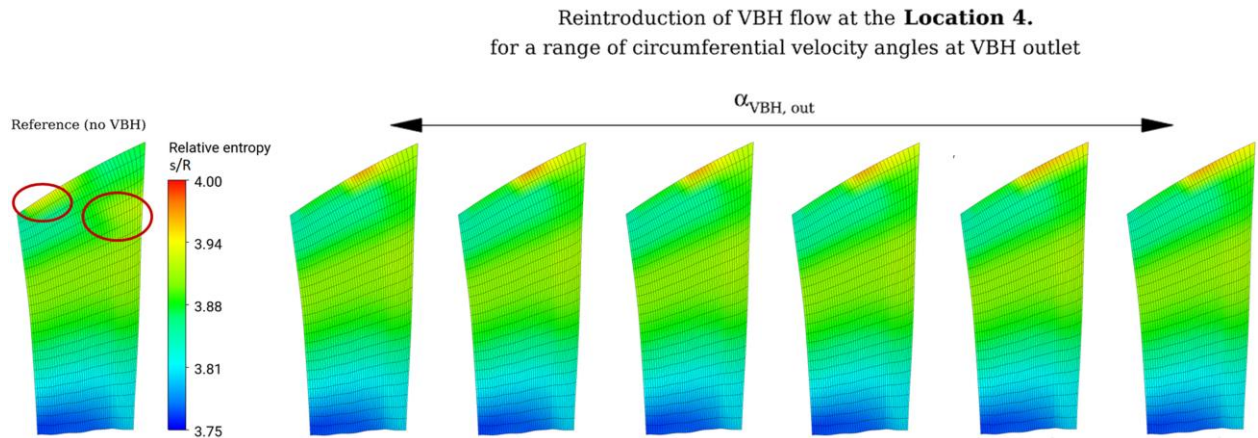


Figure 7.28 Circumferentially averaged relative entropy plots of the vane domain when reintroducing VBH flow with different circumferential velocity angle at the most promising investigated VBH outlet position. Results obtained with detailed 3D model of VBH on a 1.5-stage part of reference LPT

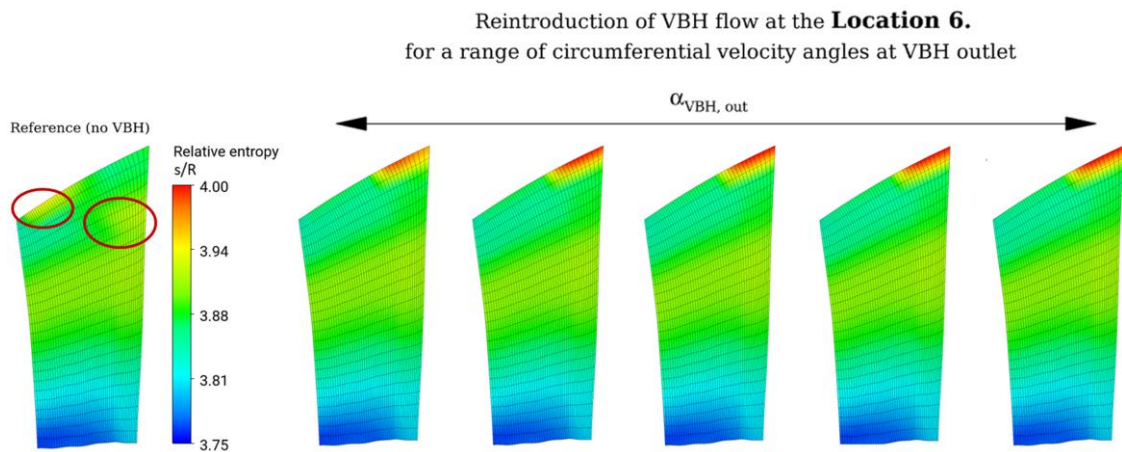


Figure 7.29 Circumferentially averaged relative entropy plots of the vane domain when reintroducing VBH flow with different circumferential velocity angle at the most downstream investigated VBH outlet position. Results obtained with detailed 3D model of VBH on a 1.5-stage part of reference LPT

A proper choice of both location and circumferential angle can lead to the further benefits from VBH solution. However, it is considered that small misalignment of the flows or inaccuracies in the location choice, do not reduce completely the benefit from VBH. It indicates that the solution is robust, as also reflected in the Figure 7.27 by the relatively flat curves and small gradients in the plots.

The investigations concerning outlet inclination and the studies with respect to the outlet position along the vane passage reveal that the choice of the VBH outlet configuration is no straightforward. The discussed aspects point to the conclusion that choice of the proper VBH configuration is an optimization task, due to several influencing parameters with opposite trends.

7.3. Assessment of the performance of the most promising VBH configuration in the 3-stage LPT

In the last step, all learners for VBH concept are transferred to the full geometrical model of 3-stage reference LPT, which is validated in the direction of turbine efficiency prediction as well as for the flow in the regions of Outer Air Seals, as discussed in the Chapter 4.

Taking into consideration all identified factors influencing VBH performance the most promising configuration is defined. For this configuration it is preferred that the highest possible mass flows through the VBH channel is transferred. The flow from the VBH at its outlet should be the most tangential to the flow path in radial direction and the most aligned with the flow in the passage in the main stream in the circumferential direction. The outlet should be also inclined in the direction of the mainstream at the reentry, thus in the direction of the circumferential velocity angle in the main flow at the shroud. The reintroduction should take place at the location in between the leading edge and the throat in the vicinity of the inflection point at the suction side of the airfoil. These requirements with respect to the optimal VBH configuration are transferred to the full geometrical model of the reference 3-stage LPT.

As pointed out earlier, several factors influencing VBH performance have opposite trends. Due to that, finding optimal solution is an optimization task for particular machine and conditions and also respecting limitations from other disciplines. For any future machine where the VBH solution would be applied, to find the configuration with the highest benefit, it is suggested to turn to the numerical optimization. This optimization is not performed in the frames of the herein doctorate. The most promising configuration is identified based on the results of the performed analyses. The finally investigated solution is based on the abovementioned guidelines resulting from the main sensitivities and directions for optimization.

For the final assessment of the benefit from the solution applied to the researched LPT, the VBH is modeled at both stages of the machine. Modeling at the last stage is redundant, as described in the previous chapters. The turbine equipped with VBH in comparison to the reference LPT is visualized in the Figure 7.30. In the first step, the most promising configurations of VBH are investigated. Next, also configuration respecting meaningful multidisciplinary limitations is analyzed.

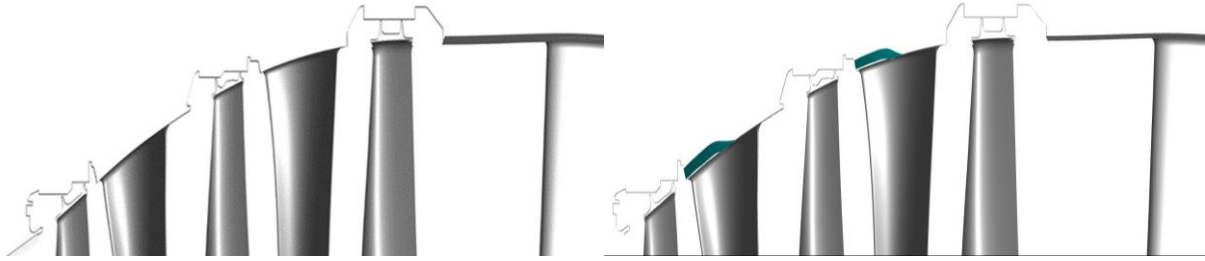


Figure 7.30 Reference 3-stage LPT with and without implemented VBH

The resulting efficiency gain, for the whole turbine together with the radial distribution of the efficiency for the most promising VBH configuration, are pictured in the Figure 7.31. As visible in the figure, a considerable improvement of +0.21% in the isentropic efficiency of the reference LPT is achieved with VBH applied at both stages. As also visible in the chart, the benefits from implementation of the VBH at particular vanes almost sum up. This indicates only small interaction between them. In conclusion, the beneficial presence of the VBH can be superimposed at particular vanes.

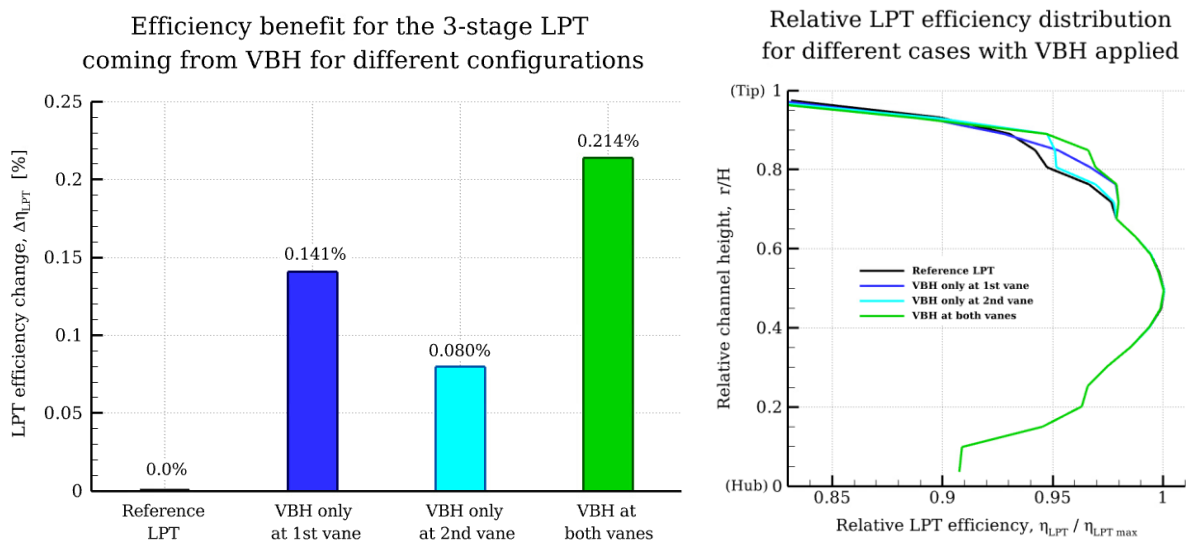


Figure 7.31 Final improvement in efficiency resulting from application of the most promising aerodynamically VBH design. Results obtained with detailed 3D model of VBH on a full geometry model of researched 3-stage LPT.

In addition, Figure 7.31 also shows that efficiency is significantly improved in the shroud region up to 70% of the channel height. It corresponds to the findings from the previous Section 7.2. and discussed at the Figure 7.28. It also well fits into the designs space that considered in the Chapter 1. as visible in the Figure 1.1. Radial distributions also confirm that effects from both VBH channels can be summed up. The Figure 7.31 confirms also that VBH modification does not influence the part of the machine below 70% of the channel height. Thus, it can be separately treated from the core stream as well as from the inner channel region.

The most promising VBH case shows considerable improvement already for the first vane with the solution implemented. Figure 7.32 indicates that the benefits from the VBH on the first vane are bigger, due to a fact that the flow at the first vane is subjected to more losses in the shroud region. VBH robustly improves this area. In the Figure 7.32 is also well visible that the highly turbulated region with high TKE is kept considerably closer to the shroud region.

For the case of the VBH only at the first vane, it might be noticed, a marginally higher production of the TKE at the shroud region in the subsequent rows. The biggest improvement in the losses reduction is observed for the case with both vanes equipped with the VBH solution. It is noticeable that the losses in the core stream are considerably – almost completely reduced at the shroud. It confirms earlier conclusion that the solution operates as intended, resulting in improved mainstream up to around 70% of the channel height.

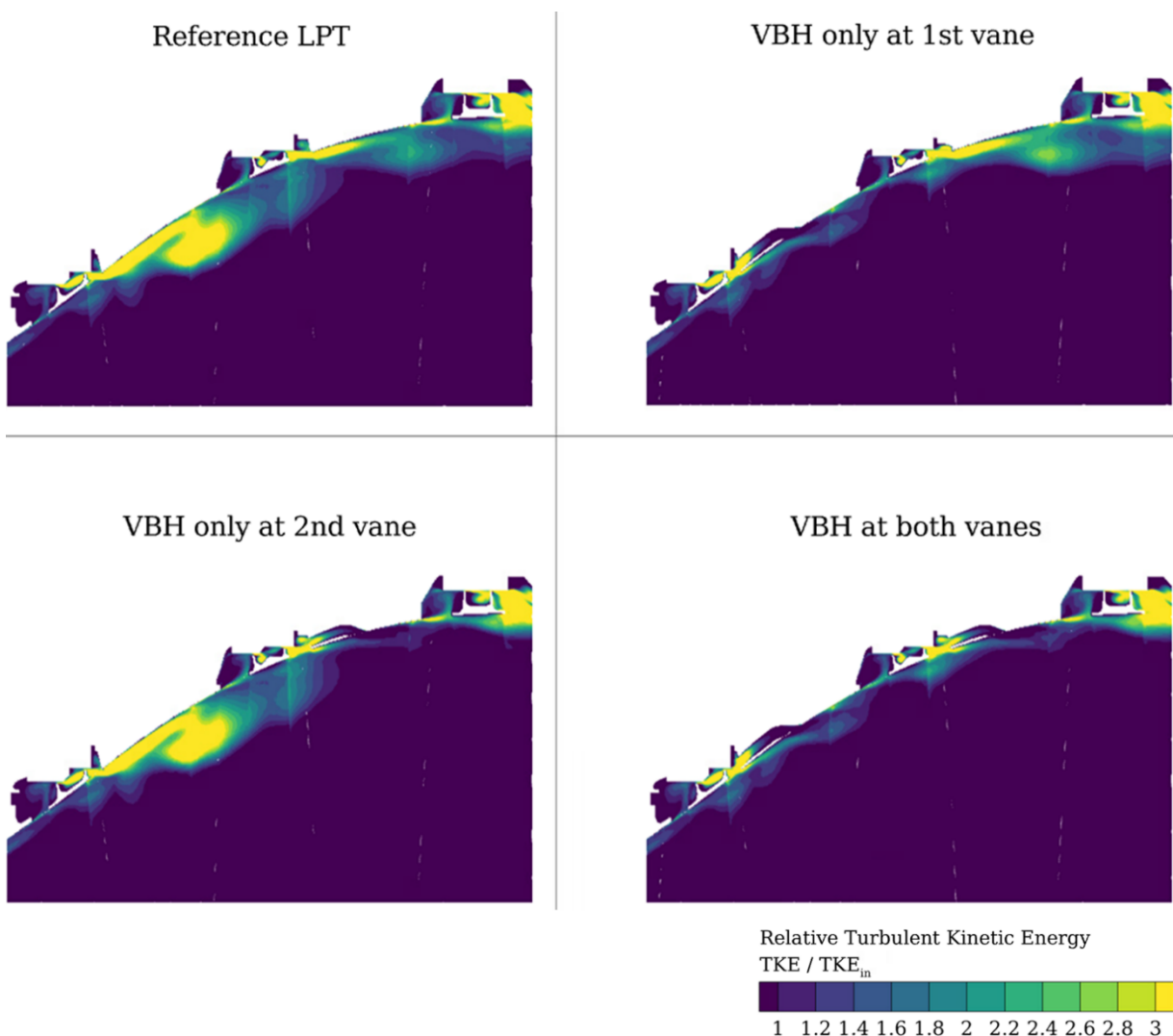


Figure 7.32 Relative TKE circumferentially averaged with and without VBH. Results obtained with detailed 3D model of VBH on a full geometry model of researched 3-stage LPT

All studies show, the VBH brings benefits to the overall performance of the LPT. Nevertheless, there are also other design limitations that have to be considered. This requirements with respect to the design space, manufacturing, thermal stresses and structural integration may decrease the overall benefit from the VBH, depending on the configuration and particular design case. In addition, interactions between the developed concept and endwall contouring at the vane shroud, becoming state-of-the-art for modern LPT, is not investigated. Interaction between both features could be either positive or negative, but it would require further additional investigations beyond herein thesis.

Considering those limitations, it is attempted to evaluate efficiency benefit for the VBH constrained with the limitations from other disciplines. It is considered as the worst case for the VBH performance. Evaluating this, the benefit from the solution is considerably reduced. The efficiency gain for the whole LPT is +0.13% what is nearly 40% lowered with respect to the most promising configuration. Nevertheless, some of those requirements are essential for the implementation of the solution in the real environment for the sake of robustness, manufacturability, costs or weight. It again indicates that Outer Air Seals are highly multidisciplinary area and particular disciplines cannot be omitted in the design process of the properly operating OAS.

7.4. Summary of the benefits from the developed solutions for improvement of LPT Outer Air Seals

In the frames of the herein dissertation new design concepts for improvement of the LPT Outer Air Seals are researched. The most promising concepts that were developed are Front Deflector and Vane Bleed Holes. Both solutions are investigated in detail, in particular with respect to the aerodynamic efficiency gain. The assumed improvement in LPT efficiency benefit aimed in the doctorate is 0.1%. The detailed CFD analyzes enabled prediction of the LPT flow field after implementation of the solutions and allowed prediction of the main sensitivities, directions for optimization and the overall improvement of in the performance of the machine.

The solutions are also considered with respect to the limitations resulting from requirements from other design fields that are important for operation of the solutions in the LPT environment. The impact of those limitations on the overall performance of the developed solutions is also evaluated. In the Figure 7.33 are visualized the least and the most promising design cases of the researched solutions.

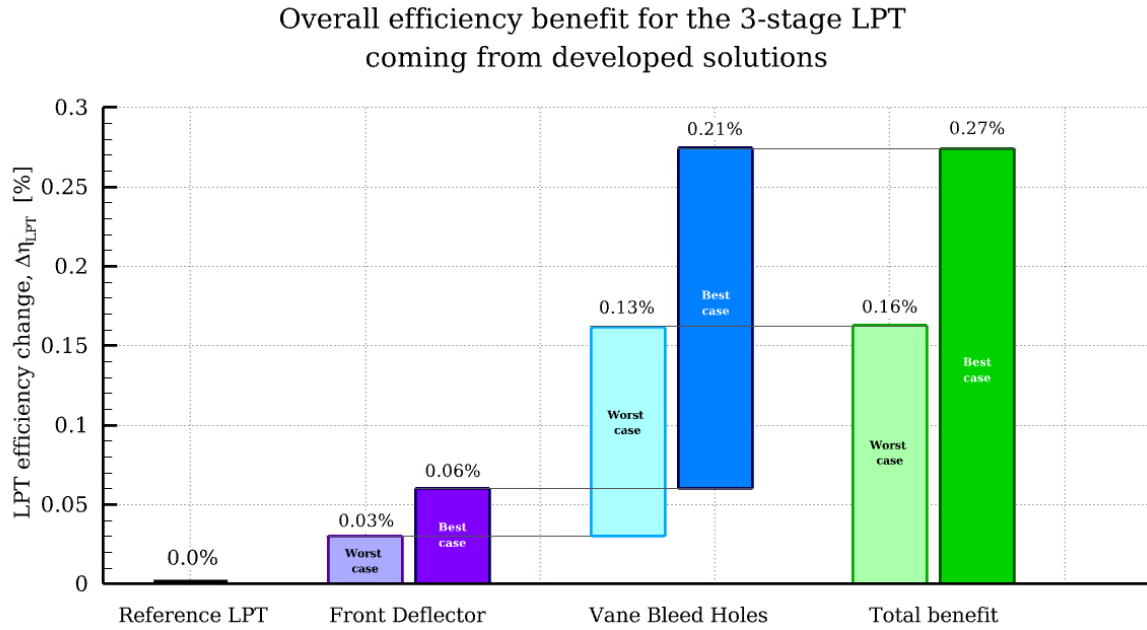


Figure 7.33 Overall benefit from the Front Deflector and Vane Bleed Holes solutions to the 3-stage high speed LPT

The worst-case benefit results from the design cases that reflect certain design limitations. In those configurations the solutions are considered to obey all meaningful requirements with the cost of reduced efficiency. The highest benefit reflects the best aerodynamically identified configurations.

Front Deflector, as indicated in the previous chapters, is simpler and more straightforward for implementation solution, but simultaneously associated with smaller benefit. On the other hand, Vane Bleed Holes, settling more difficult and more complicated solution results in a considerably higher efficiency gain. Both concepts can be combined in the same seal, thus the total maximal efficiency benefit from the concepts developed in the frames of PhD is between 0.16% and 0.27%. The final benefit strongly depends on the LPT configuration and assumed requirements for the solution. As visible in the figure, already the least promising configuration of the developed solutions results in a meaningful gain in the LPT efficiency being above of the goal for the increase in efficiency aimed in the herein research. Worth mentioning is that already benefits from the VBH implementation fulfills targeted value. Due to that, it is considered that main objectives posed in the doctorate are reached.

Chapter 8. Summary, conclusions and directions for future work

8.1. Summary

Herein thesis addressed development and research of new concepts for Outer Air Seals for future Low Pressure Turbines, providing increase of in their efficiency. Two most promising solutions that have been developed and evaluated in detail are Front Deflector and Vane Bleed Holes.

Research of the actual knowledge state and dimensional analysis performed specifically for LPT OAS, accompanied by comprehensive parametric study, allowed identification of the primary factors influencing aerodynamic operation of OAS. The most important characteristic quantities for that have been found are: axial Reynolds number – incorporating changes in the mass flow, outlet swirl ratio – corresponding to the exit flow angle, important for mixing and windage heating – related to internal losses.

Based on this research, knowing possible directions for improvements, new concepts of Outer Air Seals have been researched. In total 16 ideas for improvement in OAS regions was found within the works over doctorate. These concepts have been evaluated with respect to criteria from the different fields including: aerodynamics, secondary air system management, thermal engineering, material engineering, design, manufacturing, structural integrity and costs. In this way, the most promising concepts have been identified. The preliminary evaluation has shown that the Front Deflector and Vane Bleed Holes solutions have biggest potential for improvement of the LPT efficiency, simultaneously respecting meaningful limitations from the disciplines. Patents for the solutions have been obtained what proves novelty of the concepts.

The solutions have been further investigated in detail with respect to the aerodynamic LPT efficiency benefit, at the minimum level of plus 0.1%. Models with different scope and size have been applied to identify sensitivities of the designs, physical drives for the improvements and directions for optimization of the features. Multiple configurations of the solutions have been investigated analytically with CFD. The validity of the numerical prediction has been confirmed with experimental data with respect to efficiency in the mainstream and proper prediction of the flow in the vicinity of the outer channel as well as within Outer Air Seals. This enabled evaluation of the new designs by means of numerical simulations.

Front Deflector has found to be simpler solution and more straightforward for implementation. Nevertheless, simultaneously associated with smaller overall benefit. The device improves OAS performance in two ways, by additional labyrinth for the leakage and by reduction of the

interactions between mainstream and cavities, due to reduced front volume. Concept has been investigated in two primary configurations – with and without static fin at the front. The efficiency gain for the case without additional static fin results from decreased interactions of the mainstream and vortices in the front cavity. The reduction of the front cavity volume does not influence the leakage itself. It has been found that the static fin contributes to the leakage reduction, by creation of additional labyrinth only if the static fin is long enough, what strongly depends on particular turbine design. The overall improvement of the LPT efficiency from the Front Deflector implemented in all three OAS is between 0.03% and 0.06%, depending on a possible application.

Vane Bleed Holes concept is intended for the rear part of OAS. The principle behind VBH is that the leakage from the OAS cavity is guided over the subsequent vane and further is reinjected into the main gas path at the vane shroud in appropriate velocity angles. The primary benefit from VBH is decrease in mixing losses, due to smaller interactions between the leakage and the mainstream. Secondary benefits have been associated with reduction in separations at the leading edge of the vane and additional reduction of secondary flows in the vane passage.

In terms of flow similarity, Vane Bleed Holes could not be treated with characteristic numbers identified for LPT OAS, because both types of flows have been associated with different phenomena. Due to that dimensional analysis was also performed specifically for VBH. It has been identified that the most important for flow through VBH is fraction of OAS leakage transported through VBH channel, pressure ratio between inlet and outlet of VBH and velocity angles at the outlet of the feature in the location of reintroduction into the mainstream. In the preliminary studies with simplified VBH model main sensitivities for VBH performance have been determined. Results obtained with the simplified model, indicate that the greatest importance for the VBH performance has fraction of the VBH mass flow with respect to the OAS leakage. The highest benefits observed with simplified model have been found for the VBH flow at its outlet most aligned with the mainstream in radial in circumferential directions.

The study on the simplified model indicated possible directions for further studies, however due to some limitations and assumptions behind the method, further research has been carried out with the detailed three-dimensional models of VBH. These investigations have been carried out on the partial 1.5-stage model of reference LPT, to increase robustness and decrease computational effort. Detailed analyses confirmed trends identified with previous studies. In particular, increasing efficiency benefit with bigger fraction of the flow through VBH has been reported. With higher mass flows, it was additionally possible to reduce secondary flows in the vane passage. The simulations revealed that the decrease in the mixing losses at the reentry has importance for the final efficiency benefit from the solution. Proper choice of both location and circumferential angle can lead to the further benefits from VBH. The highest benefit appears in

the vicinity of the inflection point at the suction side of airfoil. Towards the throat as well as towards the leading edge, the benefit declines, due to the enhanced mixing losses.

The most promising configuration of the solution has been transferred to the full geometrical model of the reference LPT in order to evaluate overall benefit expected from the solution. A visible improvement in the isentropic efficiency of the reference LPT has been achieved with VBH applied at both vanes. The flow is significantly improved in the shroud region up to 70% of the channel height. It has been noticed that the losses due to the leakage and secondary flows in the core stream have been almost completely reduced. The requirements with respect to the design space, manufacturing, thermal stresses and structural integration can decrease the overall benefit. The analyses of the different scenarios of the VBH indicated that the overall benefit from the solution is between 0.13% and 0.21%, depending on realizable configuration and particular turbine design.

Both solutions can be combined within same seal because FD has been assumed for the front OAS cavity and VBH for the rear part. This combination provided the highest improvement in the turbine efficiency. The predicted benefit for the LPT efficiency has been found between 0.16% and 0.27%, respectively for the worst and best case. The final benefit strongly depends on the LPT configuration and requirements for the solution.

8.2. Main conclusions

1. Improvements of Outer Air Seals can be achieved primarily by leakage decrease, reduction of mixing losses and reduction in interactions between mainstream and OAS cavities.
2. Proper multidisciplinary design of OAS requires taking into account aerodynamics, secondary air system management, thermal engineering, material engineering, design, manufacturing, structural integrity and costs.
3. The initial multidisciplinary assessment and early preselection of the new concepts allows focusing on the most important solutions. It effectively reduces number of investigated cases facilitating selection of the most promising solutions.
4. Front part of the OAS cavity can be improved with implementation of Front Deflector. Main benefits from this solution result from additional labyrinth and reduced interactions between mainstream and cavities:
 - a. For the cases without static fin, improvements come from decreased interaction of the mainstream and big vortices in the front cavity.
 - b. Long static fin provides additional labyrinth for the OAS leakage and in this way contributes to the leakage reduction.
 - c. If relative movements of parts within OAS cavity allow only application of short fin, then the fin does not contribute to the leakage reduction and it can be skipped
 - d. The overall improvement of the LPT efficiency from the Front Deflector implemented at all OAS is between 0.03% and 0.06%, depending on the possible length of the static fin.
5. The rear part of OAS can be improved with application of Vane Bleed Holes. The primary benefit from VBH is associated with reduced mixing losses in the rear part of the cavity. Secondary benefits are due to smaller separations at the leading edge of the vane and due to additional reduction of secondary flows in the passage.
6. VBH performance is primarily associated with the VBH mass flow as a fraction of OAS leakage, pressure ratio between VBH inlet and outlet, and velocity angles at the reentry.
 - a. The biggest importance for the VBH performance has amount of mass flow transferred through the VBH channel. The most beneficial is transferring of considerable portions of the flow through the feature – preferably entire leakage or more.

- b. Further significance also has radial velocity angle at the VBH outlet which should be aligned preferably tangentially to the flow path.
 - c. Choice of the outlet location and circumferential angle at the VBH outlet can lead to the additional benefits from the solution. The highest benefit appears for the outlet located in the vicinity of the inflection point at the suction side of airfoil for the outflow from VBH aligned with the mainstream
 - d. The outlet should be preferably inclined in the direction of the circumferential velocity in the mainstream for reduction of the missing losses.
 - e. Definition of the optimal VBH configuration is an optimization task for particular turbine design
7. With VBH efficiency is visibly improved. The losses in the upper part of the mainstream stream are almost completely reduced at the shroud up to 70% of the channel height
8. The requirements with respect to the design space, manufacturing, thermal stresses and structural integration can decrease overall benefit. The overall improvement of LPT efficiency coming from Vane Bleed Holes is between 0.13% and 0.21%, depending on realizable configuration and particular design case.
9. Both Front Deflector and VBH concepts can be combined within same seal. The predicted benefit in LPT efficiency for this combination is between 0.16% and 0.27%, respectively for the worst and best case, depending on the LPT configuration and requirements for the solution.

8.3. Recommendations for future work

A list of future work and recommendations is provided in a priority order below.

1. Experimental validation of CFD prediction with respect to the mixing process at the VBH flow reentry
2. Numerical optimization of the VBH solution for particular design of LPT
3. Experimental validation of the proper operation of the solution and its impact on the mainstream for the particular LPT design
4. Research of interactions between the VBH concept and endwall contouring at the vane shroud including possibilities combination of both features
5. Analytical description of the VBH process with correlations with intention of reflecting effects from VBH in predesign tools

Appendix

A. Patents

A.1 Patent No. EP3822461A1: Axial turbomachine sealing system. [68]



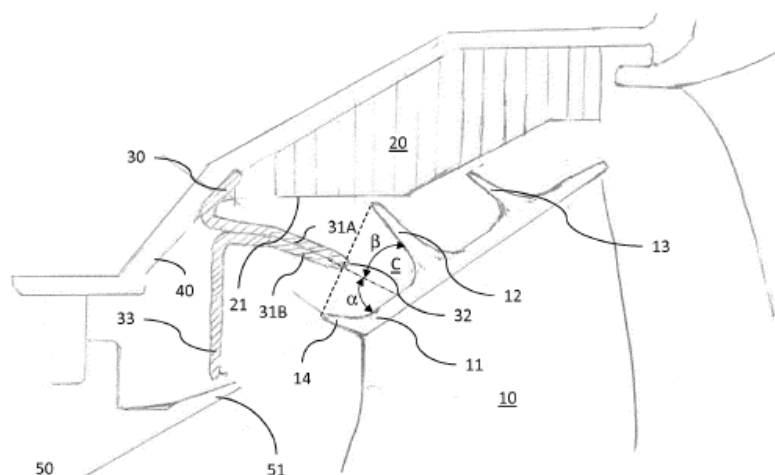
| | |
|---|---|
| (19)  Europäisches Patentamt European Patent Office Office européen des brevets |  |
| (11) EP 3 822 461 A1 | |
| (12) EUROPEAN PATENT APPLICATION | |
| (43) Date of publication: 19.05.2021 Bulletin 2021/20 | (51) Int Cl.: F01D 11/02 (2006.01) F01D 5/22 (2006.01) F01D 11/12 (2006.01) F01D 11/08 (2006.01) |
| (21) Application number: 19209602.2 | |
| (22) Date of filing: 15.11.2019 | |
| (84) Designated Contracting States: AL AT BE BG CH CY CZ DE DK EE ES FI FR GB GR HR HU IE IS IT LI LT LU LV MC MK MT NL NO PL PT RO RS SE SI SK SM TR Designated Extension States: BA ME Designated Validation States: KH MA MD TN | (71) Applicant: MTU Aero Engines AG 80995 München (DE) (72) Inventors: • Palkus, Kacper 36-002 Jasionka (PL) • Lauer, Christoph 80995 München (DE) • Schmierer, Roman 80995 München (DE) |
| (54) AXIAL TURBOMACHINE SEALING SYSTEM | |
| (57) A sealing system for an axial turbomachine comprises: - a circle of blades (10) with an outer shroud (11) and a first sealing fin (12; 13) projecting away from said outer shroud; - a seal surface (21) opposite to said first sealing fin; and | - an, in particular grooved, static fin (30; 60) with at least one fin flange (31A, 31B; 61) for restricting flow between the seal surface (21) and the outer shroud (11), wherein the static fin (30; 60) is stationary with respect to the seal surface (21). |

Fig. 1



EP 3 822 461 A1

Printed by Jouve, 75001 PARIS (FR)

A.2 Patent No. EP4123124A1: Turbine module for a turbomachine and use of this module. [69]

(19)  (11)  **EP 4 123 124 A1**

(12) **EUROPEAN PATENT APPLICATION**

(43) Date of publication: **25.01.2023 Bulletin 2023/04** (51) International Patent Classification (IPC): **F01D 9/04^(2006.01)**

(21) Application number: **21187063.9** (52) Cooperative Patent Classification (CPC): **F01D 9/04; F05D 2240/121; F05D 2240/122; F05D 2240/126**

(22) Date of filing: **21.07.2021**

(84) Designated Contracting States: **AL AT BE BG CH CY CZ DE DK EE ES FI FR GB GR HR HU IE IS IT LI LT LU LV MC MK MT NL NO PL PT RO RS SE SI SK SM TR**
 Designated Extension States: **BA ME**
 Designated Validation States: **KH MA MD TN**

(71) Applicant: **MTU Aero Engines AG 80995 München (DE)**

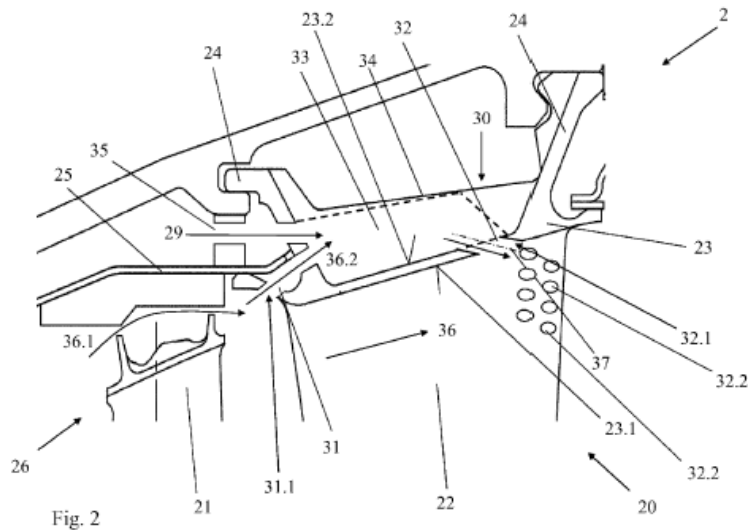
(72) Inventors:
 • **Palkus, Kacper 36-002 Jaslonka (PL)**
 • **Schmierer, Roman 80995 München (DE)**
 • **Klingels, Hermann 80995 München (DE)**

(54) **A TURBINE MODULE FOR A TURBOMACHINE AND USE OF THIS MODULE**

(57) A turbine module (2) for a turbomachine (1), the turbine module (2) comprises, a main channel (26) to guide a main flow (36) through the turbine module (2), a rotor blade (21) and a stator vane (22), the stator vane (22) comprising a stator airfoil (22) and a platform (23), with the stator airfoil (22) arranged downstream of the rotor blade (21) in the main channel (26), and a cavity

(30) comprising an inlet (31) for injecting a part (36.2) of the main flow (36) into the cavity (30), an outlet (32) for a reinjection of the part (36.2) of the main flow (36) from the cavity (30) into the main channel (26), wherein the cavity (30) is arranged at an axial position of the stator vane (20) and is radially offset from the stator airfoil (22).

EP 4 123 124 A1



Processed by Luminess, 75001 PARIS (FR)

Bibliography

- [1] Albada, van, G. D., Leer, van, B. and Roberts, W. W. (1982), A comparative study of computational methods in cosmic gas dynamics, *Astron Astrophys* 108, pp. 76–84.
- [2] Anker, J. E, Mayer, J. F. (2022, June 3–6). Simulation of the interaction of labyrinth seal leakage flow and main flow in an axial turbine. Proceedings of the ASME 2022 Turbo Expo. Amsterdam, Netherlands. pp. 217-224. ASME. <https://doi.org/10.1115/GT2002-30348>
- [3] Biester, M. H., Wiegmann, F., Guendogdu, Y., & Seume, J. R. (2013, June 3–7) Time-resolved numerical study of axial gap effects on labyrinth seal leakage and secondary flow in a LP Turbine. Proceedings of the ASME 2013 Turbo Expo. Vol. 6A. San Antonio, Texas, USA. ASME. <https://doi.org/10.1115/GT2013-95628>
- [4] Bohn, D., Krewinkel, R., Tummers, C., Sell, M. (2006, May 8-11). Influence of the radial and axial gap of the shroud cavities on the flow field in a 2-stage turbine. Proceedings of the 2006 ASME Turbo Expo. Barcelona, Spain. pp. 821-830. ASME. <https://doi.org/10.1115/GT2006-90857>
- [5] Brouckaert, J. F. (2022, November 21-23). Clean aviation: Towards climate neutrality in 2050 – Research needs for next gen aero engines [Paper presentation, speech video recording]. VKI online Workshop on Next Generation High-Speed Low Pressure Turbines. Von Karman Institute Lecture Series and Events
- [6] Brush seals: World-class sealing technology. (2014). MTU Aero Engines. EN10/20/MUC/00500/AD/RI/D https://power.mtu.de/fileadmin/DE/MTU_Power/Engineering_and_Manufacturing/Engineering_Service/MTU-20-010_Broschu_re_Bu_rstendichtung_GB_low.pdf (Accessed: 2023, September)
- [7] CFX-Solver Theory Guide. (2022). Release 2022 R1. ANSYS Inc. and ANSYS Europe Ltd.
- [8] Chupp, R. E., Hendricks, R. C., Lattime, S. B., Steinetz B. M. (2006). Sealing in Turbomachinery, NASA, Glenn Research Center, Cleveland, Ohio, USA, NASA/TM-2006-214341. <https://ntrs.nasa.gov/api/citations/20060051674/downloads/20060051674.pdf>
- [9] Clean Aviation Joint Undertaking. (2022, September). Clean Aviation’s daring new projects. https://clean-aviation.eu/sites/default/files/2022-09/CleanAviation-daring-new-projects-List_en.pdf (Accessed: 2023, September)

- [10] CORDIS. (2022, December). Hydrogen engine architecture virtually engineered novelly. Publications Office of the European Union. <https://cordis.europa.eu/project/id/101102004>, (Accessed: 2023, September)
- [11] Darwish, M. (1993). New high-resolution scheme based on the normalized variable formulation. *Numerical Heat Transfer, Part B: Fundamentals* 24(3), pp. 353–371. <https://doi.org/10.1080/10407799308955898>.
- [12] Denecke J.; Farber J.; Dullenkopf F.; Bauer H. J. (2005, June 6–9) Dimensional analysis and scaling of rotating seals. *Proceedings of the ASME 2005 Turbo Expo. Reno, Nevada, USA.* pp. 1149-1160. ASME. <https://doi.org/10.1115/GT2005-68676>
- [13] Denecke, J., Dullenkopf, K, Wittig, S, Bauer, H. (2005, June 6–9). Experimental investigation of the total temperature increase and swirl development in rotating labyrinth seals. *Proceedings of the ASME 2005 Turbo Expo. Reno, Nevada, USA.* pp. 1161-1171. ASME. <https://doi.org/10.1115/GT2005-68677>
- [14] Denecke, J., Schramm, V., Kim, S., Wittig, S. (2003). Influence of rub-grooves on labyrinth seal leakage. *ASME. Journal of Turbomachinery.* Vol. 125(2). pp. 387–393. <https://doi.org/10.1115/1.1539516>
- [15] Denton, J. D. (1993, May 24-27). Loss mechanisms in turbomachines. *Proceedings of the ASME 1993 International Gas Turbine and Aeroengine Congress and Exposition. Cincinnati, Ohio, USA.* ASME. <https://doi.org/10.1115/93-GT-435>
- [16] Denton, J. D. (2010, June 14-18). Some limitations of turbomachinery CFD. *Proceedings of the ASME 2010 Turbo Expo. Glasgow, UK.* pp. 735-745. ASME. <https://doi.org/10.1115/GT2010-22540>.
- [17] Dewanji, D., Gangoli Rao, A., van Buijtenen, J. P. (2010). Conceptual study of future aero-engine concepts. *International Journal of Turbo and Jet Engines.* Vol. 26(4). pp. 263-276.
- [18] Dinc, S., Demiroglu, M., Turnquist, N., Mortzheim, J., Goetze, G., Maupin, J., Hopkins, J., Wolfe, C., Florin, M. (2002). Fundamental design issues of brush seals for industrial applications. *ASME. Journal of Turbomachinery.* Vol. 124(2). pp. 293–300. <https://doi.org/10.1115/1.1451847>
- [19] Dixon, S. L., Hall, C. A. (2010). *Fluid mechanics and thermodynamics of turbomachinery* (pp. 29-51). Ed. 6th. Butterworth-Heinemann, 2010, <https://doi.org/10.1016/C2009-0-20205-4>
- [20] Fanelli, J. J. A., Bassery, J. J. A., Dupeyre, R. J. P., Francois, E. L. (2020). Aube mobile pour une roue d'une turbomachine. Applicant: Safran Aircraft Engines. Patent No. FR3092864A1

- [21] Federal Aviation Administration Press Office. (2021, September). Continuous Lower Energy, Emissions, and Noise (CLEEN) program. <https://www.faa.gov/newsroom/continuous-lower-energy-emissions-and-noise-cleen-program> (Accessed: 2023, September)
- [22] Fischer, S., Mueller, L., Saathoff, H., Kozulovic, D. (2012, June 11–15). Three-dimensional flow through a compressor cascade with circulation control. Proceedings of the ASME 2012 Turbo Expo. Copenhagen, Denmark. pp. 147-158. ASME. <https://doi.org/10.1115/GT2012-68593>.
- [23] Flitney R. K. (2007). Seals and sealing handbook (pp. 1-288). Ed 6th. Butterworth-Heinemann. <https://doi.org/10.1016/B978-0-08-099416-1.00002-4>
- [24] Fowler, T. W. (1989). Jet Engines and Propulsion Systems For Engineers (pp. 1.1-30), Human Resource Development GE Aircraft Engines.
- [25] Frączek, D., Wróblewski, W., and Bochon, K. (2016). Influence of Honeycomb Rubbing on the Labyrinth Seal Performance. ASME. Journal of Engineering for Gas Turbines and Power. Vol. 139(1): 012502. <https://doi.org/10.1115/1.4034183>
- [26] Franke, M., Kugeler, E., Nurnberger, D. (2005, September 26-29), Das DLR-Verfahren TRACE: Moderne Simulationstechniken für Turbomaschinenströmungen [Paper presentation]. DGLR-Jahrbuch. Deutscher Luft- und Raumfahrtkongress 2005.
- [27] Fujimura, D., Watanabe, H., Hanada, T., Hase, T. (2022). Gas turbine for aircraft. Applicant: Mitsubishi Heavy Ind Aero Engines. Patent No. EP3779125B1
- [28] Gamal, A. J. M., and Vance, J. M. (2008). Labyrinth seal leakage tests: Tooth profile, tooth thickness, and eccentricity effects. ASME. Journal of Engineering for Gas Turbines and Power. Vol. 130(1): 012510. <https://doi.org/10.1115/1.2771571>
- [29] Giboni, A.; Wolter, K.; Menter, J.R.; Pfof, H. (2004, June 14-17). Experimental and numerical investigation into the unsteady interaction of labyrinth seal leakage flow and main flow in a 1.5-stage axial turbine. Proceedings of the ASME 2004 Turbo Expo. Vienna, Austria. pp. 983–992. <https://doi.org/10.1115/GT2004-53024>
- [30] Gier, J., Stubert, B., Brouillet, B., de Vito, L. (2003). Interaction of shroud leakage flow and main flow in a three-stage low pressure turbine. ASME. J. Turbomach. Vol. 127(4). pp. 649–658. <https://doi.org/10.1115/1.2006667>
- [31] Girardeau J. (2004). Turbine comportant un espace secondaire interne équipé d'ailettes de correction de giration d'un flux d'air. Applicant: Safran Aircraft Engines. Patent No. FR3107298B1

- [32] Gonzalez, P., Lantero, M., Olabarria, V. (2006, May 8-11) Low Pressure Turbine Design for Rolls-Royce Trent 900 Turbofan. Proceedings of the ASME 2006 Turbo Expo. Barcelona, Spain. pp. 875-881. ASME. <https://doi.org/10.1115/GT2006-90997>
- [33] Han, J. C., Dutta, S., Ekkad, S. (2013). Gas Turbine Heat Transfer and Cooling Technology (pp. 1-328). Ed. 2nd. CRC Press. <https://doi.org/10.1201/b13616>.
- [34] Hauke, W. (2020). Einfluss des Betriebspunktes auf rotorspaltinduzierte Verluste in modernen Niederdruckturbinen. [Master thesis, Leibniz University Hannover]
- [35] Hendricks, R. C., Chupp, R. E., Lattime, S. B., Steinetz B. M. (2005). Turbomachine interface sealing, NASA, Glenn Research Center, Cleveland, Ohio, USA, NASA/TM—2005-213633. <https://ntrs.nasa.gov/api/citations/20050175891/downloads/20050175891.pdf>
- [36] Henke, M, Wein, L, Kluge, T, Guendogdu, Y, Biester, MH, Seume, J. R. (2016, June 13-17). Experimental and numerical verification of the core-flow in a new low-pressure turbine. Proceedings of the ASME 2016 Turbo Expo. Seoul, South Korea. ASME. <https://doi.org/10.1115/GT2016-57101>
- [37] ICAO. (2022, September). Environmental Report: Innovation for a Green Transition. <https://www.icao.int/environmental-protection/Documents/EnvironmentalReports/2022/ICAO%20ENV%20Report%202022%20F4.pdf> (Accessed: 2023, September)
- [38] ICEM CFD User's Manual. (2022). Release 2022 R1. ANSYS Inc. and ANSYS Europe Ltd.
- [39] Jameson, H. K, Longley, J. P. (2020, September 21–25) New multi-stage turbine stator design for improved performance retention. Proceedings of the ASME 2020 Turbo Expo 2020. Virtual, Online. ASME. <https://doi.org/10.1115/GT2020-14407>
- [40] Jouy, B. M. A. P., Sicard, J. L. F., Verdier, M. C. J., Villard, L. F. F. (2022). Device for sealing between a rotor and a stator of a turbine engine. Applicant: Safran Aircraft Engines. Patent No. EP3615774B1
- [41] Justak, J. F. (2001). Hydrodynamic brush seal. Applicant: Justak, J. F. Patent No. US6428009B2
- [42] Justak, J. F., Doux, C. (2009, June 8–12). Self-Acting Clearance Control for Turbine Blade Outer Air Seals. Proceedings of the ASME 2009 Turbo Expo. Orlando, Florida, USA. pp. 1229-1237. ASME. <https://doi.org/10.1115/GT2009-59683>
- [43] Kim, T.S., Cha, K.S. (2009). Comparative analysis of the influence of labyrinth seal configuration on leakage behavior. Springer. Journal of Mechanical Science and Technology. Vol. 23. pp. 2830-2838. <https://doi.org/10.1007/S12206-009-0733-5>

- [44] Klingels, H. (2021). Sealing system for a turbomachine and axial flow turbomachine. Applicant: MTU Aero Engines AG. Patent No. EP3324002B1
- [45] Kluge, T., Lettmann, I. S., Oettinger, M., Wein, L., Seume, J. R. (2021). Unsteady flow phenomena in turbine shroud cavities. *Journal of the Global Power and Propulsion Society*. Vol. 5. pp. 177-190. <https://doi.org/10.33737/jgpps/141211>
- [46] Kluge, T., Wein L., Seume, J. R., Hartung, A., Schmierer, R., Herbst, F., (2021, December 13-14) Optimaler Deckbandrückschnitt bei Turbinenlaufschaufeln. Teilverbundprojekt: 17. Statusseminar der AG Turbo Verbundprojekt COOREFLEX-turbo: TVP Expansion Vorhabengruppe: 4.2 Gasturbinen-Schaufelentwicklung: COOREFLEX-turbo 4.2.5. Koln, Germany. pp. 227-295. DLR. https://www.dlr.de/at/PortalData/20/Resources/dokumente/agturbo/2022_AG_Turbo_Statusseminar_Statusband.pdf
- [47] Kluge, T., Wein L., Seume, J. R., Hartung, A., Schmierer, R., Herbst, F., (2021, December 7-8) Abschlussvortrag COOREFLEX-turbo 4.2.5: Optimaler Deckbandrückschnitt bei Turbinenlaufschaufe [Paper presentation]. AG Turbo AKS Expansion 2020 Videokonferenz.
- [48] Kluge, T., Wein, L. Schmierer, R., Seume, J. R. (2019, April 8-12). Sensitivity analysis, design, instrumentation, and experimental validation of a novel labyrinth seal rig, *Proceedings of 13th European Conference on Turbomachinery Fluid dynamics & Thermodynamics*. Lausanne, Switzerland. <https://doi.org/10.29008/ETC2019-078>
- [49] Kozulovic, D., Rober, T., Nurnberger, D., (2007). Application of a multimode transition model to turbomachinery flows. *Proceedings of 7th European Turbomachinery Conference*, pp. 1369-1378, Athens, Greece
- [50] Kyprianidis, K. (2011) Future aero engine designs: An evolving vision. *Advances in Gas Turbine Technology* (pp. 3-24). Rijeka, Croatia. <https://doi.org/10.5772/19689>.
- [51] Lampart, P. (2006). Tip leakage flows in turbines. *Task Quarterly*. Vol. 10. pp. 139-175.
- [52] Lee, K. W., Lee, S. U., Kim, C. H., Song, T. H. (1990). Numerical analysis in the flow field of a labyrinth seal. *International Compressor Engineering Conference*. Paper 778. <https://docs.lib.purdue.edu/icec/778>
- [53] Leggett, J., Zhao, Y., Richardson, E.S., Sandberg, R. D. (2021, June 7–11). Turbomachinery loss analysis: The relationship between mechanical work potential and entropy analyses. *Proceedings of the ASME 2021 Turbo Expo*. Virtual, Online. ASME. <https://doi.org/10.1115/GT2021-59436>
- [54] Li, J., de Choudhury, P. (2004). Swirl-reversal abradable labyrinth seal. Applicant: ELLIOTT CO. Patent No. WO2004113770A2

- [55] Liu H, An Y, Zou Z. (2016). Aerodynamic impact of hub and shroud leakage flow on an axial turbine stage. *Journal of Mechanical Engineering Science*. Vol. 230(14), pp. 2483-2495. <https://doi.org/10.1177/0954406215597711>
- [56] Mahle, I. (2010, June 14–18). Improving the interaction between leakage flows and main flow in a low pressure turbine. *Proceedings of the ASME 2010 Turbo Expo*. Glasgow, UK. pp. 1177-1186. ASME. <https://doi.org/10.1115/GT2010-22448>
- [57] Mahle, I., Schmierer, R. (2011, June 6–10). Inverse fin arrangement in a low pressure turbine to improve the interaction between shroud leakage flows and main flow. *Proceedings of ASME 2011 Turbo Expo*. Vancouver, British Columbia, Canada. pp.559-568. ASME. <https://doi.org/10.1115/GT2011-45250>
- [58] Menendes, R. P., King H. (2004). Leaf seal manufacturing process. Applicant: Perkinelmer Inc. Patent No. WO2004023008A1
- [59] Menter, F. R. (2009). Review of the Shear-Stress Transport turbulence model experience from an industrial perspective. *International Journal of Computational Fluid Dynamics*. Vol. 23(4), pp. 305–316.
- [60] Menter, F., Kuntz, M., Langtry, R. B. (2003). Ten years of industrial experience with the SST turbulence model. *Heat and Mass Transfer*. Vol. 4(1). pp. 625-632.
- [61] Moustapha, H., Zelesky, M. F., Baines, N. C., Japiske D. (2003). *Axial and radial turbines* (pp. 1-138). ISBN: 978-0933283121. Concepts NERC.
- [62] Moustapha, S. H., Kacker, S. C., and Tremblay, B. (1990). An improved incidence losses prediction method for turbine airfoils. ASME. *Journal of Turbomachinery*. Vol. 112(2), pp. 267–276. <https://doi.org/10.1115/1.2927647>
- [63] MTU Aero Engines AG. (2022, February). Clean aviation SWITCH project to advance hybrid-electric and water-enhanced turbofan technologies. <https://www.mtu.de/newsroom/press/press-archive/press-archive-detail/clean-aviation-switch-project-to-advance-hybrid-electric-and-water-enhanced-turbofan-technologies> (Accessed: 2023, September)
- [64] NASA (2008). *Proceedings of conference Seal/Secondary Air System Workshop*. NASA/CP-2009-215677 pp. 131-193. <https://ntrs.nasa.gov/api/citations/20090041726/downloads/20090041726.pdf>.
- [65] Nishii D., Hamabe, M., (2004). Secondary Flow Suppression Structure. Applicant: IHI CORP. Patent No. WO2021199718A1

- [66] Oettinger, M., Kluge, T., Seume, J. (2022). Influence of honeycomb structures on labyrinth seal aerodynamics. *Journal of the Global Power and Propulsion Society*. Vol. 6, pp. 290-303. <https://doi.org/10.33737/jgpps/152697>
- [67] Oettinger, M., Mimic, D., Henke, M., Schmunk, O., Seume, J. R. (2021). Loss assessment of the axial-gap size effect in a low-pressure turbine. *Journal of the Global Power and Propulsion Society*. Vol. 5, pp. 1-14. <https://doi.org/10.33737/jgpps/127834>
- [68] Pałkus, K., Lauer, C., Schmierer, R. (2021). Axial turbomachine sealing system. Applicant: MTU Aero Engines AG. Patent No. EP3822461A1
- [69] Pałkus, K., Schmierer, R., Klingels, H., (2023) A turbine module for a turbomachine and use of this module. Applicant: MTU Aero Engines AG. Patent No. EP4123124A1
- [70] Pałkus, K., Strzelczyk, P. M. (2021). Dimensionless numbers relationships for outer air seal of low pressure turbine. *International Journal of Turbomachinery, Propulsion and Power*. <https://doi.org/10.3390/ijtp6030033>
- [71] Palmer T. R. (2015). Effects of axial turbine tip shroud cavity flow on performance and durability. [Doctoral dissertation, Massachusetts Institute of Technology]. <https://dspace.mit.edu/handle/1721.1/97771>
- [72] Pfau, A., Schlienger, J., Rusch, D., Kalfas, A. I., Abhari, R. S. (2003). Unsteady flow interactions within the inlet cavity of a turbine rotor tip labyrinth seal. *ASME. Journal of Turbomachinery*. Vol. 127(4). pp. 679–688. <https://doi.org/10.1115/1.2008973>
- [73] Proctor, M. P., Kumar, A., and Delgado, I. R. (2004). High-speed, high-temperature finger seal test results. *Journal of Propulsion and Power*. Vol. 20(2). pp. 312-318. <https://doi.org/10.2514/1.9256>
- [74] Proctor, M., Delgado, I. (2003). Compliant foil seal investigations, NASA, Glenn Research Center, Cleveland, Ohio, USA. NASA/CP-2004-212963/VOL1. <https://ntrs.nasa.gov/api/citations/20040182398/downloads/20040182398.pdf>
- [75] Qing, M. T. (2011). Dimensional analysis (pp. 1-47). Springer Berlin, Heidelberg. <https://doi.org/10.1007/978-3-642-19234-0>
- [76] Rapisarda, A., Desando, A., Campagnoli, E., Taurino, R. (2016). Rounded fin edge and step position effects on discharge coefficient in rotating labyrinth seals. *ASME. Turbomach.* January Vol. 138(1)11005. <https://doi.org/10.1115/1.4031748>.
- [77] Rhode, D. L., Hibbs, R. I. (1993). Clearance effects on corresponding annular and labyrinth seal flow leakage characteristics. *ASME. Journal of Tribology*. Vol.115(4). pp. 699–704. <https://doi.org/10.1115/1.2921696>

- [78] Rhodes, N. (2005). Leaf seal manufacturing process. Applicant: Alstom Technology Ltd. Patent No. WO2005103535A1
- [79] Roache, P. J. (1994). Perspective: A method for uniform reporting of grid refinement studies. ASME. J. Fluids Engineering. Vol. 116(3), pp. 405–413. <https://doi.org/10.1115/1.2910291>.
- [80] Roe, P., (1997). Approximate Riemann solvers, parameter vectors, and difference schemes. Journal of Computational Physics. Vol. 135(2), pp. 250–258. [https://doi.org/10.1016/0021-9991\(81\)90128-5](https://doi.org/10.1016/0021-9991(81)90128-5).
- [81] Rolls-Royce plc. (2019, November). Pioneering intelligent innovation for our customers. <https://www.rolls-royce.com/products-and-services/civil-aerospace/future-products.aspx#/> (Accessed: 2023, September)
- [82] Rosic, B, Denton, J. D., Pullan, G. (2005, June 6–9). The importance of shroud leakage modelling in multistage turbine flow calculations. Proceedings of the ASME 2005 Turbo Expo. Reno, Nevada, USA. pp. 561-570. ASME. <https://doi.org/10.1115/GT2005-68459>.
- [83] Rosic, B., Denton, J. D. (2008). Control of shroud leakage loss by reducing circumferential mixing. ASME. Journal of Turbomachinery. Vol. 130(2): 021010. <https://doi.org/10.1115/1.2750682>
- [84] Rosic, B., Denton, J. D., Curtis, E. M., and Peterson, A. T. (2008). The influence of shroud and cavity geometry on turbine performance: an experimental and computational study – part I and II. ASME. Journal of Turbomachinery. Vol. 130(4): 041002. <https://doi.org/10.1115/1.2777202>.
- [85] Rulik, S., Wróblewski, W., Frączek, D. (2017). Metamodel-based optimization of the labyrinth seal. PAN. Archive of Mechanical Engineering. Vol. 64(1). <https://doi.org/10.1515/meceng-2017-0005>
- [86] Salehi, M., Heshmat, H., Walton, J.F., and Cruszen, S., (1999, June 20-24). The application of foil seals to a gas turbine engine. Proceedings of the 35th AIAA/ASME/SAE/ASEE Joint Propulsion Conference and Exhibit, Los Angeles, CA, USA. AIAA. Paper No. 99-2821. <https://doi.org/10.2514/6.1999-2821>
- [87] Satair. (2021, October). Are these the aircraft engines of the future? <https://blog.satair.com/are-these-the-aircraft-engines-of-the-future> (Accessed: 2023, September)
- [88] Schramm, V., Denecke J., Kim S., Wittig S. (2004). Shape optimization of a labyrinth seal applying the simulated annealing method. Hindawi. International Journal of Rotating Machinery. <https://doi.org/10.1155/S1023621X04000375>

- [89] Schramm, V., Willenborg, K., Kim, S., Wittig, S. (2000). Influence of a honeycomb facing on the flow through a stepped labyrinth seal. ASME. Journal of Engineering for Gas Turbines and Power. Vol. 124(1). pp. 140–146. <https://doi.org/10.1115/1.1403460>
- [90] Shapiro, A. H. (1953). The dynamics and thermodynamics of compressible fluid flow. ISBN: 978-0471066910. Wiley.
- [91] Speak, T. H., Sellick, R. J., Kloos, V., Jeschke, P. (2016). Dual Drive Booster for a Two-Spool Turbofan: Performance Effects and Mechanical Feasibility. ASME. J. Eng. Gas Turbines Power, 138(2): 022603. <https://doi.org/10.1115/1.4031274>.
- [92] Szymanski A., Dykas S., Wroblewski W., (2017, April 3-7). Experimental and numerical validation study of the labyrinth seal configurations. Proceedings of 12th European Conference on Turbomachinery Fluid dynamics & Thermodynamics. Stockholm, Sweden. <https://doi.org/10.29008/ETC2017-340>
- [93] Szymanski A., Wroblewski W., Dykas S. (2015, March 23-27). Flow analysis of the turbine rotor tip seal on a highly rotary test rig. Proceedings of 11th European Conference on Turbomachinery Fluid dynamics & Thermodynamics. Madrid, Spain. Paper No. ETC2015-062
- [94] Szymański, A., Dykas, S., Majkut, M., Stozik, M. (2016). The assessment of the calculation method for determining characteristics of one straight fin labyrinth seal. Transactions of the Institute of Fluid Flow Machinery. pp. 89-107. http://www.imp.gda.pl/fileadmin/files/transactions/134/134_6.pdf
- [95] Taylor, E. S. (1974). Dimensional analysis for engineers. ISBN: 978-0198561224. Oxford University Press.
- [96] TRACE User Guide: Turbulence model extensions. (2020) http://www.trace-portal.de/userguide/trace/page_turbulenceModels.html . (Accessed: 2023, September)
- [97] Traupel, W. (1977). Thermische Turbomaschinen: Erster Band Thermodynamisch-strömungstechnische Berechnung. ISBN: 978-3642963742. Springer, Berlin, Heidelberg. <https://doi.org/10.1007/978-3-642-96374-2>
- [98] Wallis, A. M., Denton, J. D., and Demargne, A. A. J. (2001). The control of shroud leakage flows to reduce aerodynamic losses in a low aspect ratio, shrouded axial flow turbine. ASME. Journal of Turbomachinery. Vol. 123(2), pp. 334–341. <https://doi.org/10.1115/1.1354143>.
- [99] Waschka W.; Wittig S.; Kim S. (1992) influence of high rotational speeds on the heat transfer and discharge coefficients in labyrinth seals. ASME. Journal of Turbomachinery. Vol. 114. pp. 462-468; <https://doi.org/10.1115/1.2929166>
- [100] Wein L., (2020). Large-Eddy-Simulation von Deckbandlabyrinthdichtungen [Doctoral dissertation, Leibniz University Hannover]. <https://doi.org/10.15488/10202>.

- [101] Wein, L., Kluge, T., Seume, J. R. , Hain, R., Fuchs, T., Kahler, C., Schmierer, R., Herbst, F. (2020, September 21–25) Validation of RANS turbulence models for labyrinth seal flows by means of Particle Image Velocimetry. Proceedings of the ASME 2020 Turbo Expo 2020. Vol. 10A. Virtual, Online. ASME. <https://doi.org/10.1115/GT2020-14885>
- [102] Wein, L., Seume, J. R., Herbst, F., (2017, June 26-30). Improved prediction of labyrinth seal performance through scale adaptive simulation and stream aligned grids, Proceedings of ASME 2017 Turbo Expo. Charlotte, NC, USA. ASME. <https://doi.org/10.1115/GT2017-64257>.
- [103] Wilcox, D.C. (1998). Turbulence modeling for CFD. Ed. 2nd. ISBN: 978-1928729105. DCW Industries
- [104] Willenborg, K., Kim, S., Wittig, S. (2001). Effects of Reynolds number and pressure ratio on leakage loss and heat transfer in a stepped labyrinth seal. ASME. Journal of Turbomachinery. Vol. 123(4). pp. 815–822. <https://doi.org/10.1115/1.1397304>
- [105] Wittig, S. L. K., Dorr, L., and Kim, S. (1983). Scaling effects on leakage losses in labyrinth seals. ASME. Journal of Engineering for Gas Turbines and Power. Vol. 105. pp. 305-309. <https://doi.org/10.1115/1.3227416>
- [106] Wróblewski, W., Bochon, K., Borzecki, T. (2017). What-if analysis of the labyrinth seal of the gas turbine rotor tip. Transactions of the Institute of Fluid-Flow Machinery. Vol. 136(2017). pp. 3-21. https://www.imp.gda.pl/files/transactions/136/136_1.pdf
- [107] Yan, X., Li, J., Song, L., and Feng, Z. (2009). Investigations on the discharge and total temperature increase characteristics of the labyrinth seals with honeycomb and smooth lands. ASME. Journal of Turbomachinery. Vol. 131(4): 041009. <https://doi.org/10.1115/1.3068320>
- [108] Yang, H., Nuernberger, D., and Kersken, H. (2006). Toward excellence in turbomachinery computational fluid dynamics: A hybrid structured-unstructured Reynolds-Averaged Navier-Stokes solver." ASME. Journal of Turbomachinery. Vol. 128(2). pp. 390–402. <https://doi.org/10.1115/1.2162182>
- [109] Yaras, M. I., Sjolander, S. A. (1992). Prediction of tip-leakage losses in axial turbines. ASME. Journal of Turbomachinery. Vol. 114(1). pp. 204–210. <https://doi.org/10.1115/1.2927987>
- [110] Zimmermann, H, Wolff, KH. (1998, June 2–5). Air system correlations: Part 1 – labyrinth seals. Proceedings of the ASME 1998 International Gas Turbine and Aeroengine Congress and Exhibition. ASME. <https://doi.org/10.1115/98-GT-206>.

List of figures

| | |
|--|----|
| Figure 1.1 Distribution of efficiency along channel height for typical LPT. | 7 |
| Figure 1.2 Scheme of the dissertation and technical roadmap in a course of development and evaluation of new solutions for LPT OAS | 11 |
| Figure 2.1 Schematic representation of a state-of-the-art Outer Air Seal of LPT [44] | 14 |
| Figure 2.2 Different types of brush seals: typical [23] configuration, advanced design [6], and brush seal integrated within a labyrinth seal [58]..... | 15 |
| Figure 2.3 Different types of sealing solutions: finger seal [64], leaf seal [78], foil seal [86], brush seal with a pad [41] | 16 |
| Figure 2.4 Aircraft turbine with two ACC systems dedicated separately to HPT and LPT [8] | 17 |
| Figure 2.5 Turning devices in the rear OAS cavity of the shrouded steam HPT [83] | 18 |
| Figure 2.6 Inverse fins configuration [57]. Hybrid solution of conventional fins combined with inverse configuration with additional static fin in a rear cavity [44]. Additional features for improvement of OAS rear cavities [84] | 19 |
| Figure 2.7 Secondary flow suppression structure concept. Shaping of stator leading edge [27]..... | 20 |
| Figure 2.8 Devices for additional sealing between rotor and stator of turbine [40], [20] | 20 |
| Figure 2.9 Comparison of steady numerical prediction with PIV at rear cavity and static pressure distribution at the casing for shrouded outer air seal test rig [101] | 24 |
| Figure 2.10 Flow structures resulting from the OAS leakage. Negative incidence at shroud of subsequent stator and resulting separation. [29]..... | 26 |
| Figure 2.11 Flow structures developing at the stator behind LPT OAS [39]..... | 27 |
| Figure 2.12 Comparison of the primary flow structures between conventional and inverse fins arrangements [57]..... | 28 |
| Figure 2.13 Sources of losses for LPT associated with OAS presence..... | 29 |
| Figure 2.14 Fraction of losses due to shroud sealing at different gaps obtained with cascade testing acc. Yaras and Sjolander [109]..... | 30 |
| Figure 2.15 Entropy production due to LPT air seals and their impact on next stator [3] | 31 |
| Figure 3.1 Scheme of preselection of the ideas and matrix of concepts for multidisciplinary evaluation of the solutions..... | 36 |
| Figure 3.2 Geometry of the main gas path with inner and outer cavities of baseline 3-stage LPT...39 | |
| Figure 3.3 Geometry of the channel and outer cavities of the baseline three-stage LPT | 39 |
| Figure 3.4 Baseline LPT mainstream and cavity meshes..... | 40 |
| Figure 3.5 CFD model and TRACE Boundary Conditions of the reference LPT | 42 |
| Figure 3.6 CFD model of 1.5-stage part of the baseline LPT in CFX | 42 |
| Figure 3.7 CFD modeling of the Front Deflector..... | 43 |
| Figure 3.8 Comparison of the meshes for different Front Deflector configurations. From the left: reference cavity, Front Deflector without static fin and Front Deflector with static fin. | 44 |
| Figure 3.9 VBH channel geometry and its researched variations | 45 |

| | |
|---|----|
| Figure 3.10 Different types of VBH channel meshes used for analyses | 45 |
| Figure 3.11 Impact of different VBH mesh on mass flow and efficiency of 1.5-stage LPT part | 46 |
| Figure 3.12 Simplified modeling of VBH with mass outlet and mass intake. | 47 |
| Figure 3.13 Detailed modeling of VBH in TRACE and CFX. | 48 |
| Figure 4.1 Approach for confirming increase in efficiency from developed solutions by validated CFD analyses of the reference LPT | 51 |
| Figure 4.2 CFD prediction in comparison to experimental data of relative efficiency of the reference 3-stage LPT over relative channel height..... | 52 |
| Figure 4.3 Circumferentially averaged profiles of normalized total pressure and circumferential velocity angle behind rotating blade and Outer Air Seal [47]..... | 54 |
| Figure 4.4 Airfoil loading at 80%, 85%, 90% and 95% span of the downstream stator [46] | 55 |
| Figure 4.5 Normalized total pressure and circumferential velocity angle at LPT outlet [46] | 56 |
| Figure 4.6 Transfer of Outer Air Seal geometry from 1.5-stage TFD turbine to the RLP [48] | 57 |
| Figure 4.7 Seal geometries with smooth wall and honeycomb researched in RLP | 57 |
| Figure 4.8 Primary instrumentation available at RLP | 58 |
| Figure 4.9 Boundary conditions applied to RLP with the smooth wall and the honeycomb | 59 |
| Figure 4.10 RLP with smooth wall – sensitivity to sector size and unsteadiness | 59 |
| Figure 4.11 Different meshes for numerical analyses of RLP with smooth wall and honeycomb ... | 60 |
| Figure 4.12 Sensitivity of the mass flow to the mesh of RLP with smooth wall | 61 |
| Figure 4.13 Sensitivity of the mass flow to the mesh of RLP with honeycomb | 61 |
| Figure 4.14 Cross-sectional view to the axial flow velocity at the first fin of RLP with smooth wall and honeycomb for different mesh refinements..... | 62 |
| Figure 4.15 Relative mass flow with variation of pressure ratio and rotational speed in RLP with smooth wall above the fins..... | 63 |
| Figure 4.16 Distribution of the static pressure along and total pressure at the outlet of RLP with smooth wall above the fins..... | 64 |
| Figure 4.17 Relative mass flow with variation of pressure ratio and rotational speed in RLP with honeycomb above the fins..... | 65 |
| Figure 4.18 Distribution of the static pressure along and total pressure at the outlet of RLP with honeycomb above the fins..... | 65 |
| Figure 5.1 Dependency of relative mass flow and axial velocity on radial clearance at OAS | 67 |
| Figure 5.2 Schematic visualization of the flow at outer channel of LPT. | 68 |
| Figure 5.3 Mixing in vicinity of LPT OAS with marked flow features described in the Table 5-1 .. | 68 |
| Figure 5.4 Impact of interactions between mainstream and front and rear parts of OAS cavity | 70 |
| Figure 5.5 Quantities meaningful for flow through Outer Air Seals [70] | 71 |
| Figure 5.6 Dependency of axial Reynolds number on pressure ratio, relative clearance, circumferential Mach number and inlet swirl ratio | 73 |
| Figure 5.7 Influence of the ratio $pt, in / N\mu$ on axial Reynolds number..... | 73 |
| Figure 5.8 Dependency of outlet swirl ratio on pressure ratio, relative clearance and circumferential Mach number..... | 74 |

| | |
|---|-----|
| Figure 5.9 Dependency of outlet swirl ratio on circumferential Mach number and inlet swirl | 75 |
| Figure 5.10 Influence of the ratio $pt, in / N\mu$ on outlet swirl ratio | 76 |
| Figure 5.11 Dependency of heating on axial Reynolds, pressure ratio and relative clearance | 76 |
| Figure 5.12 Dependency of windage heating circumferential Mach number and inlet swirl | 77 |
| Figure 5.13 Dependency of windage heating on the change in the swirl ratio across the seal at different circumferential Mach numbers and inlet swirl ratios | 77 |
| Figure 5.14 Influence of the ratio $pt, in / N\mu$ on windage heating | 78 |
| Figure 6.1 Summary of new ideas developed for improvement of LPT OAS | 81 |
| Figure 6.2 Schematic representation of state-of-the-art Outer Air Seal of LPT EP3561228B1 [44] | 84 |
| Figure 6.3 Schematic representation of the FD concept. Reference patent EP19209602A1 [68] ... | 85 |
| Figure 6.4 Preliminary multidisciplinary rating of the Front Deflector concept..... | 85 |
| Figure 6.5 Schematic representation of the VBH concept. Reference patent EP4123124A1 [69] ... | 86 |
| Figure 6.6 Preliminary multidisciplinary rating of the Vane Bleed Holes concept | 87 |
| Figure 6.7 Schematic representation of the most promising solution of LPT OAS – Front Deflector combined with Vane Bleed Holes. Reference patents – EP19209602A1 [69], EP4123124A1 [68] | 88 |
| Figure 7.1 Main aerodynamic benefits from Front Deflector | 89 |
| Figure 7.2 Investigated designs cases of front cavity reduction with FD without static fin | 90 |
| Figure 7.3 LPT Efficiency benefit from front cavity reduction with FD without static fin | 91 |
| Figure 7.4 Relative Circumferential Velocity and streamlines for investigated cases of Front Deflector without static fin in different configurations | 91 |
| Figure 7.5 Relative Turbulent Kinetic Energy and streamlines for investigated cases of Front Deflector without static fin in different configurations | 92 |
| Figure 7.6 Comparison of characteristic numbers for OAS with Front Deflector without static fin in different configurations for one of the OAS..... | 92 |
| Figure 7.7 Breakdown of LPT efficiency benefit due to front volume reduction | 93 |
| Figure 7.8 Investigated designs cases of front cavity reduction with Front Deflector with static fin | 93 |
| Figure 7.9 Relative Turbulent Kinetic Energy and streamlines for investigated cases of Front Deflector with static fin in different configurations | 94 |
| Figure 7.10 Comparison of characteristic numbers for OAS with Front Deflector with static fin in different configurations | 95 |
| Figure 7.11 LPT Efficiency benefit from front cavity reduction mounted on all stages..... | 95 |
| Figure 7.12 Main benefits resulting from Vane Bleed Holes..... | 96 |
| Figure 7.13 Flow field and development of the secondary flows for the Reference vane and vane equipped with VBH. Main flow features are marked with letters..... | 97 |
| Figure 7.14 Quantities meaningful for flow through VBH | 98 |
| Figure 7.15 Sensitivity to Mach at VBH outlet. Results obtained with simplified modeling | 100 |
| Figure 7.16 Sensitivity to fraction of OAS leakage mass flow. Results with simplified modeling | 102 |
| Figure 7.17 Sensitivity to VBH outlet location. Results obtained with simplified modeling | 103 |
| Figure 7.18 VBH sensitivity to circumferential velocity angle at the VBH outlet | 104 |

Figure 7.19 Sensitivity to radial velocity angle at outlet. Results with simplified modeling 105

Figure 7.20 Efficiency benefit resulting from VBH with respect to leakage mass flow fraction obtained with detailed 3D model of VBH on a 1.5-stage part of reference LPT 107

Figure 7.21 Visualization of exemplary scenarios for two different VBH flows as a fraction of the OAS leakage obtained with detailed model of VBH 108

Figure 7.22 Circumferentially averaged relative Turbulent Kinetic Energy for different ratios of OAS leakage and flow through VBH flow. 109

Figure 7.23 Efficiency benefit from VBH with respect to mass flow transferred through VBH for different inlet configurations. Results obtained with detailed 3D model of VBH on a 1.5-stage part of the reference LPT..... 110

Figure 7.24 Efficiency benefit resulting from VBH with respect to leakage mass flow fraction obtained with detailed 3D model of VBH on a 1.5-stage part of reference LPT 111

Figure 7.25 Contours of pressure ratio between inlet and outlet of VBH and circumferential velocity angle in the vicinity of the vane shroud 112

Figure 7.26 Efficiency benefit resulting from VBH with respect to outlet configuration obtained with detailed 3D model of VBH on a 1.5-stage part of reference LPT 113

Figure 7.27 Efficiency benefit resulting from VBH with respect to outlet position obtained with detailed 3D model of VBH on a 1.5-stage part of reference LPT 115

Figure 7.28 Circumferentially averaged relative entropy plots of the vane domain when reintroducing VBH flow with different circumferential velocity angle at the most promising investigated VBH outlet position. Results obtained with detailed 3D VBH on a 1.5-stage part of reference LPT..... 117

Figure 7.29 Circumferentially averaged relative entropy plots of the vane domain when reintroducing VBH flow with different circumferential velocity angle at the most downstream investigated VBH outlet position. Results obtained with 3D model of VBH on 1.5-stage part of reference LPT 117

Figure 7.30 Reference 3-stage LPT with and without implemented VBH 119

Figure 7.31 Final improvement in efficiency resulting from application of the most promising aerodynamically VBH design. Results obtained with detailed 3D model of VBH on a full geometry model of researched 3-stage LPT..... 119

Figure 7.32 Relative TKE circumferentially averaged with and without VBH. Results obtained with detailed 3D model of VBH on a full geometry model of researched 3-stage LPT 120

Figure 7.33 Overall benefit from the Front Deflector and Vane Bleed Holes solutions to the 3-stage high speed LPT..... 122

List of tables

| | |
|--|-----|
| Table 5-1 Flow situation and sources of mixing losses at OAS. Letter markings as in Figure 5.3. | 69 |
| Table 5-2 Selection of the quantities applied for Dimensional Analysis of OAS | 71 |
| Table 7-3 Selection of quantities applied for Dimensional Analysis of VBH | 98 |
| Table 7-4 Parameters of the simplified model for studies over Mach number | 99 |
| Table 7-5 Parameters of the simplified model for studies over VBH mass flow fraction | 101 |
| Table 7-6 Parameters of the simplified model for studies over VBH outlet location | 102 |
| Table 7-7 Parameters of the simplified model for studies over VBH mass flow fraction | 104 |
| Table 7-8 Parameters of the simplified model for studies over VBH mass flow fraction | 105 |
| Table 7-9 Geometrical variations of VBH for flow amount study | 107 |
| Table 7-10 Geometrical variations of VBH for inlet configuration study | 109 |
| Table 7-11 Geometrical variations of VBH for studies over radial angle at the VBH outlet | 111 |
| Table 7-12 Geometrical variations of VBH for studies over outlet inclination | 113 |
| Table 7-13 Geometrical variations of VBH for studies over outlet position and circumferential velocity angle | 114 |